

Modelling and Assessment of Biomass-PV Tradeoff within the Framework of the Food-Energy-Water Nexus

A DISSERTATION

Approved by the Faculty of Economics and Management Science,
Leipzig University,

for Obtaining the Academic Degree

Doktor-Ingenieur
Dr.-Ing.

Presented

by M.Sc., Keyu Bao

born on 19.06.1993 in Fujian, China

Reviewers: Daniela Thrän, Prof. Dr.
Bastian Schröter, Prof. Dr.

Date of conferral: 26 April 2023

Bibliographic description

Bao, Keyu

Modelling and Assessment of Biomass-PV Tradeoff within the Framework of the Food-Energy-Water Nexus

Leipzig University, dissertation

XVI+233 pp., 496 ref., 65 figures, 59 tab., 12 annexes

Presentation:

Food, water and energy are three essential resources for human well-being, poverty reduction and sustainable development. These resources are very much linked to one another, meaning that the actions in any one particular area often can have effects in one or both of the other areas. At the same time, an economy's shift towards climate neutrality requires a massive expansion of energy production from renewable sources. Among these ground-mounted photovoltaic (PV) and biomass will be expanded massively to meet the clean energy generation goal, simultaneously influence regional water and food availability and supply security. It is crucial to understand Food-Water-Energy Nexus (FWE) nexus during the energy transition. However, current studies have limitation both methodically (qualitative assessments) and spatially (aggregated data on a national level is more available).

Firstly, a consistent share input data set in geographical format was created with the resolution of building/field. An energy simulation platform (SimStadt) was then extended with new workflows on biomass potential, ground-mounted PV potential, food demand/potential, and urban water demand. Combining with existing workflows on urban building heating/electricity demand and roof PV potential, the dissertation created a complete simulation environmental covering most-relating FWE topics in energy transition with consistent input and output structures at a fine resolution.

Secondly, the most representative inter-linkage between ground-mounted PV and biomass on hinterland is investigated in details with the new tools. The output data of each field from ground-mounted PV and biomass workflows are linked and ranked according to the scenarios emphasizing PV yield, feasibility, profit, or biomass. The assessment and scenarios are applied at three representative German counties with distinguished land-use structures and geometries as case studies. Results show that current policies does not guarantee the technically efficient allocation of fields. The optimal technical strategy is to follow the individual market profit drive, which is very likely, at the same time for the social good, to achieve high PV yields with limited biomass losses and more significant crop water-saving effects. The local food, water, and energy demands are also included as a metric for resource allocation on the potential side.

Besides focusing on the biomass-PV tradeoff simulation and analysis, pioneer works have also been done to test the transferability of the method in cases outside Germany, and the complement of urban solid waste to agricultural biomass is explored to achieve energy autarky.

Keywords: Food-Water-Energy Nexus, Simulation platform, GIS, Ground-mounted PV, Biomass

Declaration of academic integrity

I hereby declare that I have composed this dissertation myself and without inadmissible outside help, in particular without the help of a doctoral consultant (Promotionsberater). I have used no other sources and aids than those stated. I have indicated all text passages that are incorporated, verbatim or in substance, from published or unpublished writings. I have indicated all data or information that is based on oral communication. All material or services provided by other persons are indicated as such.

Stuttgart, 2 May 2023



Keyu Bao

Summary

Food, water and energy are three essential resources for human well-being, poverty reduction and sustainable development. The food-water-energy nexus (FWE) concept, proposed in recent years, represents the interconnected production, distribution, and consumption processes of food, water, and energy (1). The core principle is that it is impossible to produce, distribute, and consume one (food, water, or energy) without producing, distributing, or consuming the other two (2). The FWE framework has been used in various contexts at many spatial levels, e.g., resources at the global level (3), energy at the national level (4), and water management at the regional level (5), for management and planning. In terms of resolution, currently, nexus issues are only assessed on a high level - both methodically (qualitative assessments) and spatially (aggregated data on a national level is more available). The reasons lie in (i) a missing consistent share input data set with high spatial resolution, and (ii) simulation tools addressing different FWE issues, and generating comparable results for nexus analysis.

At the same time, greenhouse gas emissions from natural systems and human activities cause climate change, and it is widely agreed that greenhouse gas emissions need to be reduced. Germany aims to become greenhouse gas neutral by 2045. The German economy's shift towards climate neutrality requires a massive expansion of renewable energy production. Next to wind, ground-mounted photovoltaic (PV) and biomass will be key renewable resources for energy generation in most regions in Germany. Both PV and energy biomass have their strengths: PV has a higher energy yield factor of 5 compared with biomass (6) and biomass is crucial in the transportation and heating sector (7). Beyond the energy scope, PV and biomass have distinguished impacts on other resources, i.e., water and food. Both PV and energy crop fields eliminate the food supply potential if the fields are agricultural fields for food. In the operation phase, ground-mounted PV does not require water input. On the contrary, irrigation is a boundary condition for biomass production in dry or future dry regions. So biomass and PV can not be substituted equally as the same good

Summary

without evaluating the impacts on the environment. It is natural and logical to analyze biomass-PV tradeoffs under FWE nexus framework. On agricultural fields, where ground-mounted PV and biomass are competing, the FWE framework has been adopted to optimize food security, water security and minimize carbon emissions in terms of topic.

To study the biomass-PV inter-linkage on open fields under FWE framework, several studies (8; 9; 10) applied the concept of agro-photovoltaics (APV) to avoid conflicts with food again. APV combines biomass production and solar power production on the same land area, e.g., by installing PV panels vertically and allowing enough space for agricultural machines to be deployed between module rows. However, APV is in most cases still in a pilot phase (8; 9; 10). To solve the urgency of ground-mounted PV expansion on existing agricultural lands with the matured solution in the short-term future, the exclusive tradeoff between biomass/food and PV is still missing. Furthermore, the biomass-PV inter-linkage on open fields indicates a system boundary of a region including urban areas and hinterlands.

Therefore, the work aims to develop new simulation workflows on various FWE aspects during energy transition. The new workflows should enable scenario analysis not at the aggregated level anymore but provide technical decision-making guidance at a single-field level for local authorities but for an area size of a county. Then the new workflows should be applied to analyze the biomass and PV nexus intensively, in both city and hinterland under scenarios, as one of the application cases. The proposed scenarios should include economic, social, political, and environmental concerns and situations.

This dissertation is especially valuable for the target groups, which require regional high resolution information on renewable energy expansion, i.e., county governments, that need to approve the new ground-mounted PV project or governmental decision-makers/consulting companies, that design land-use strategies. The national-level studies have focused on the aggregated values without details on each land field. Compared to studies focusing on the national level, this regional-focused work thus helps the target groups to find a land use equilibrium between energy production and biomass by taking into account potential PV and bioenergy gains, amounts of saved irrigation and food loss for each desired field.

To reach the research goal, the first step is to create a data model that covers the whole area within the system boundary (region) and has the basic element size of a single field. The dissertation extended the geo-informatics map data model, CityGML, with new attributes by overlaying several maps. The shared input

data set includes a spatial geographical map of land use, food production, soil, temporal climate data, and socioeconomic factors. The spatial input dataset has the resolution of single-field, which provides the scalability to any lower detail level, i.e., regional or national, for the bottom-up simulation tools.

An energy simulation platform (SimStadt) was extended with new workflows on biomass, ground-mounted PV, food, and water to address these research gaps. The workflows simulate the ground-mounted PV and biomass energy potential, crop water demand, food calorie potential, food calorie demand, urban water demand, and urban roof PV energy potential on green roofs. The maximal technical ground-mounted PV potentials are 1,202, 1,125, and 1,415 GWh/yr in county Ludwigsburg, Ilm-Kreis, and Dithmarschen respectively. Total biomass potentials are 652, 140, and 1,276 GWh/yr in three counties. Without converting any areas to energy technologies (ground-mounted PV and biomass), the total food potentials were 393, 352, and 679 Gkcal/yr.

In the second step, two most representative inter-linkages were investigated in details with the new tools: ground-mounted PV and biomass in hinterland, and green roofs with roof PV in city.

In hinterland the key workflows directly concerning the biomass-PV nexus are the ground-mounted PV workflow and biomass/food potential workflow. The output data of each field from these workflows are linked and ranked according to the scenarios emphasizing PV yield, feasibility, profit, or biomass. The scenarios also respond to new policy measures and highlight goals and trends concerning economic, social, and environmental issues. The assessment and scenarios are applied at three representative German counties (Ludwigsburg, Ilm-Kreis, and Dithmarschen) with distinguished land-use structures, geometries, and climate as case studies.

The base scenario that strictly follows the ease of regulation feasibility has indifferent marginal PV gain (2-4 GWh/ha), biomass loss (0.1 GWh/ha), and crop water-saving effects (5-15 $10^3 m^3/ha$) when expanding the ground-mounted PV. The base scenario addressing does not guarantee the technically efficient allocation of fields. Scenario PV maximizes the PV electricity generation by 1.2 to 3.7 times with 45% to 65% less biomass loss and up to 31% crop water-saving potential than the base scenario. By maximizing the land use profit of landowners, scenario profit increases the PV electricity production 1.2 to 2.7 times with around 63% to 79% of less biomass loss than based scenario. The substitution rate between PV and biomass alone shows up to 80% per unit biomass loss for each additional unit PV production can be avoided if the PV facilities are appropriately located. Scenario biomass does protect biomass loss between 61% to

Summary

86%, which is not significantly larger than other scenarios, however with up to 40% PV yield loss.

In conclusion, the optimal technical strategy is to follow the individual market profit drive, which is very likely, at the same time for the social good, to achieve high PV yields with limited biomass losses and more significant crop water-saving effects. The scenario 'Pro Profit' is the most ideal and optimal among the four scenarios proposed in this dissertation. Even more optimal scenarios may exist.

In contrast to hinterland, the example of the biomass-PV nexus on urban areas shows a less significant synergy in the pure energy aspect: less than 0.3% of PV yield increment on green roofs, and less than 0.7% of building heating saving potential in buildings refurbished with green roof. Bigger benefits lie in storm-water mitigation. There is no loss, but only synergy, when combining roof PV and green roofs. However, looking at the bigger picture of energy system, electricity production from roof PV can relieve the land requirement for energy in hinterland.

The local food, water, and energy demands are also included as a metric for resource allocation on the potential side. For example, there is a higher emergency in Ludwigsburg, where the electricity consumption concentrates, to promote ground-mounted PV on lands currently in the restriction to meet the regional energy autarky. Moreover, the demand-potential also reveals that regional biomass and food resources heavily rely on imports in county Ludwigsburg and Ilm-Kreis, and the loss of biomass and food is rather insignificant. The demand values do not change the prioritization list of the tradeoff but rather suggest the number of total county areas for tradeoff and main drives locally, e.g., counties with higher energy demand and energy autarky goal should consider implementing more ground-mounted PV, like in county Ludwigsburg.

Besides focusing on the biomass-PV tradeoff simulation and analysis, pioneer works have also been done. The possibility of applying the developed methods to a broader context, i.e., transferability of the method, is tested in cases outside Germany (Austria and La Réunion), and the complement of urban solid waste to agricultural biomass is explored to achieve energy autarky in a insolated island.

Acknowledgements

First of all, I would like to thank Daniela Thrän and Bastian Schröter for giving me the chance, trust, freedom, and support from the beginning to the end. I am grateful that you somehow saw my potential during the interview at HFT or reading my email asking for an external PhD opportunity. Thank you for your patience and guidance all the way, especially in the beginning. You two are the ideal combination of supervisors for me and one of the reasons I could work on my PhD in a very efficient way.

I would also like to thank my colleagues at HFT in no particular order: Eric Duminil, Matthias Betz, Sally Köhler, Verena Weiler and Chris Kesnar for the SimStadt model; Rushikesh Padsala and Joe Thunyathap Santhanavanich for the geoinformatic support; Ursula Pietzsch, Barbara Smetschka and Ernst Gebetsroither-Geringer for all the help during project IN-SOURCE; Tobias Erhart and Oliver Matrakovic for the IT support; Charitha Buddhika Heendeniya for sharing the job offer at HFT in REM group; Uta Bronner, Carolin Lahode, Jin-Suk Alexander Lee, Patrick Wuerstle, Sarah Ann Sutter and Tom Kwakman at TV3 M4_Lab; Lisa Botero for her language support; also SENCE students Lisa Bieber, Sandra Kürpick and Louis Kalisch for their great work for the papers; and everybody I forgot.



Keyu Bao

Stuttgart, 8 April 2022

List of Publications

This thesis is based on the following appended papers:

- I **Bao, K.**; Padsala, R.; Coors, V.; Thrän, D.; Schröter, B. *A Method for Assessing Regional Bioenergy Potentials Based on GIS Data and a Dynamic Yield Simulation Model*. *Energies* 2020, 13, 6488. <https://doi.org/10.3390/en13246488>
- II **Bao, K.**; Padsala, R.; Thrän, D.; Schröter, B. *Urban Water Demand Simulation in Residential and Non-Residential Buildings Based on a CityGML Data Model*. *ISPRS Int. J. Geo-Inf.* 2020, 9, 642. <https://doi.org/10.3390/ijgi91106428>
- III **Bao, K.**; Thrän, D.; Schröter, B. *Simulation and Analysis of Urban Green Roofs with Photovoltaic in the Framework of Water-Energy Nexus*. *Proceedings of REAL CORP 2021, 26th International Conference on Urban Development, Regional Planning and Information Society*. 2021, pp. 671-680. ISSN 2521-3938
- IV **Bao, K.**; Padsala, R.; Coors, V.; Thrän, D.; Schröter, B. *A GIS-Based Simulation Method for Regional Food Potential and Demand*. *Land* 2021, 10, 880. <https://doi.org/10.3390/land10080880>
- V **Bao, K.**; Kalisch, L.; Santhanavanich, T.; Thrän, D.; Schröter, B. *A bottom-up GIS-based method for simulation of ground-mounted PV potentials at regional scale*. *Energy Reports* 2022, 8, 5053. <https://doi.org/10.1016/j.egy.2022.03.187>
- VI **Bao, K.**; Thrän, D.; Schröter, B. *Land Resource Allocation between Biomass and Ground-Mounted PV under consideration of the Food-Water-Energy Nexus Framework at Regional Scale*. Submitted to *Renewable Energy*. 2022.

Work related to this thesis has also been presented in the following publications:

- VII **Bao, K.**; Padsala, R.; Coors, V.; Thrän, D.; Schröter, B. *GIS-Based Assessment of Regional Biomass Potentials at the Example of Two Counties in Germany*. *Proceedings of 28th European Biomass Conference and Exhibition*. 2020, pp 77-85. DOI: 10.5071/28thEUBCE2020-1CV.4.15

List of Publications

- VIII **Bao, K.**; Schröter, B. SimStadt. In *Urbane Energiesysteme und Ressourceneffizienz – ENsource*; Coors, V. Eds.; Fraunhofer Verlag: Stuttgart, 2021; pp 15-21.
- IX Pietzsch, U.; **Bao, K.**; Padsala, R.; Gebetsroither-Geringer, E.; Smetschka, B.; Raven, J.; Coors, V. *Stakeholder-supported Research on the Food-Water-Energy Nexus with three International Case Studies*. Proceedings of REAL CORP 2021, 26th International Conference on Urban Development, Regional Planning and Information Society. 2021, pp. 1225-1231. ISSN 2521-3938
- X Padsala, R.; Gebetsroither-Geringer, E.; **Bao, K.**; Coors, V. *The Application of CityGML Food Water Energy ADE to Estimate the Biomass Potential for a Land Use Scenario*. Proceedings of REAL CORP 2021, 26th International Conference on Urban Development, Regional Planning and Information Society. 2021, pp. 851-861. ISSN 2521-3938
- XI **Bao, K.**; Bieber, L.; Kürpick, S.; Radanielina, M.H.; Padsala, R.; Thrän, D.; Schröter, B. *Bottom-Up Assessment of Local Agriculture, Forestry and Urban Waste Potentials Towards Energy Autonomy of Isolated Regions: Example of La Réunion*. *Energy for Sustainable Development* 2022, 66, 125. DOI: 10.1016/j.esd.2021.12.002

List of Acronyms

ADE Application Domain Extension

APV Agrophotovoltaics

BUND Federation for the Environment and Nature Conservation Germany

CHP Combined heat and power

EEC European Economic Community

EEG Renewable Energy Sources Act

FAO Food and Agriculture Organization of the United Nations

FWE Food-Water-Energy

LFA Less-favoured are

MSW Municipal solid waste

NABU Nature Conservation Association Germany

PV Photovoltaic

RED European Union Renewable Energy Directive 2009/28/EC

RED II European Union Renewable Energy Directive 2018/2001

Contents

Summary	v
Acknowledgements	ix
List of Publications	xi
List of Acronyms	xiii
I Introductory chapters	xvii
1 Backgrounds	1
1.1 Food-Water-Energy Nexus dilemma	1
1.2 Transition towards an emission-free energy system	2
1.3 Biomass and PV in FWE Nexus	4
1.4 Research gap, research question, and goal	6
2 Materials and Methods	9
2.1 Input data and simulation model	11
2.2 Biomass-PV nexus as key application case	13
3 Results and discussion	17
3.1 Potential and spatial distribution of FWE resources	18
3.2 Substitution between biomass and PV	20
3.3 The marginal loss and gain of ground-mounted PV expansion	21
3.4 FWE self-sufficiency	24
4 Conclusion and Outlook	27
4.1 Conclusion	27
4.2 Beyond the nexus and future research	29

Contents

Bibliography	31
Contribution to Appended Papers	41
Curriculum Vitae	45
II Appended papers	47
1 A Method for Assessing Regional Bioenergy Potentials Based on GIS Data and a Dynamic Yield Simulation Model.	49
2 Urban Water Demand Simulation in Residential and Non-Residential Buildings Based on a CityGML Data Model	75
3 Simulation and Analysis of Urban Green Roofs with Photovoltaic in the Framework of Water-Energy Nexus	95
4 A GIS-Based Simulation Method for Regional Food Potential and Demand	107
5 A bottom-up GIS-based method for simulation of ground-mounted PV potentials at regional scale	127
6 Land Resource Allocation between Biomass and Ground-Mounted PV under consideration of the Food-Water-Energy Nexus Framework at Regional Scale	143
7 GIS-Based Assessment of Regional Biomass Potentials at the Example of Two Counties in Germany	177
8 Urbane Energiesysteme und Ressourceneffizienz – ENsource	187
9 Stakeholder-supported Research on the Food-Water-Energy Nexus with three International Case Studies	199
10 The Application of CityGML Food Water Energy ADE to Estimate the Biomass Potential for a Land Use Scenario	207
11 Bottom-Up Assessment of Local Agriculture, Forestry and Urban Waste Potentials Towards Energy Autonomy of Isolated Regions: Example of La Réunion	219

Part I

Introductory chapters

Chapter 1

Backgrounds

1.1 Food-Water-Energy Nexus dilemma

Water, energy, and food are essential resources for human development. Besides productions and demands for energy, human demands for the consumption of food and water are forecast to continue rising in the coming decades (11). The challenge will be to meet these increasing demands sustainably (12).

In terms of food, studies showed that the long-term nutrition state was improving, and food consumption patterns moved from low to higher calorie diets (13). With socio-economic development, population growth rates decreased, and diets changed: typically, consumption of animal protein, vegetable oils, fruits, and vegetables increased, while starchy staples became less important (14). For example, the Food and Agriculture Organization of the United Nations (FAO) estimates that 60% must increase the overall food production globally to meet the food demand. The growing food production requires 40% more water and 50% more energy (15).

Water plays a fundamental role in sustaining human life and the earth's ecosystems. Almost 80% of the world's population is exposed to a high-level threat of water security (16). Water stress increases between today and the 2050s in around 70% of the world's river basins (17). Precise modeling of urban water demands, covering residential and non-residential areas, can help local governments better design local water supply infrastructures and improve management of local resource potentials, if a large amount of water is required for food/biomass production.

1. Backgrounds

The expansion of renewable energy production, especially ground-mounted PV and biomass production, has significant impacts on local water demand and food production, i.e., less available arable land for crop production but energy crops.

These three resources interact in synergetic or opposing ways in most world regions. The food-water-energy nexus (FWE) concept, proposed in recent years, represents the interconnected production, distribution, and consumption processes of food, water, and energy (1). The core principle is that it is impossible to produce, distribute, and consume one (food, water, or energy) without producing, distributing, or consuming the other two (2).

To address the nexus issue regardless of the specific context, Hoff et al. introduced an initial guidance on how to solve the FWE nexus, including increasing efficiency, reducing trade-offs, building synergies, and improving governance across sectors (18). For assessing the interdependencies between FWE, two main approaches are widely adopted: bottom-up and top-down approaches (19). The bottom-up method quantifies the resource footprints of individual products or technologies crucial to reducing the products' footprints, e.g., how water-saving appliances also contribute to energy-saving (20). To notice, the bottom-up optimization approach does not necessarily guarantee the potential analysis is executed at a fine spatial resolution but rather shows the linkages between elements (21; 22; 23; 24; 25; 26).

1.2 Transition towards an emission-free energy system

Greenhouse gas emissions from natural systems and human activities cause climate change, which is related to 315 cases of natural disasters in 2018 globally (27). It is widely agreed that greenhouse gas emissions need to be reduced. Germany aims to become greenhouse gas neutral by 2045. It has set the primary targets of cutting emissions by at least 65% by 2030 compared to 1990 levels, and 88% by 2040 (28). Climate neutrality is to be achieved through energy savings, through the efficient provision, conversion, use, and storage of energy, through the selection of the most climate-friendly modes of transport, in particular, through the efficient use of renewable energy sources (28). The electrification in the mobility and heating sector (29) results in rising electricity demands by a factor of 2-2.5 until 2045 compared to the 2020 level (30). Therefore, the German energy system pathway simulation till 2045 shows that renewable energy

1.2 Transition towards an emission-free energy system

generation capacities need to be expanded dramatically to meet the emission neutrality goal,

One option is solar photovoltaic: to meet the emission neutrality goal, solar energy increases by 400% reaching around 1 TWh, and wind power increases by up to 1,500% compared to the status in 2020 (31). There are two leading solar photovoltaic (PV) concepts to generate electricity: rooftop and ground-mounted. In contrast to fossil electricity generation, solar PV produces electricity not at a few individual locations but distributed throughout the country. Solar PV also has significantly less energy density per area than fossil generation units (32). Rooftop solar PV infrastructures have limited potential and higher cost than ground-mounted PV (33). Additionally, rooftop solar PV does not have sufficient capacity to fulfill the sustainable energy generation target (34). Expanding the ground-mounted PV plants is inevitable to overcome the current political obstacles to reach the climate neutrality goal (35). The expansion would eliminate the original land use pattern, i.e., agricultural or biomass, resulting in land-use conflicts.

Meanwhile, for medium- and especially low-temperature industrial heat generation, biomass can be a vital part of possible decarbonization pathways providing a quarter of total heating demand (36). In today's energy mix, biomass, defined as plant-based material used as fuel to produce heat or electricity, exists in wood and wood residues, energy crops, agricultural residues, and waste from industry, farms, and households. This dissertation only considers biomass from forests, energy crops, and agricultural residues. Urban or industrial wastes are not included. The use of biomass for energy generation also has the potential to contribute to climate change mitigation, i.e., the urgent need to reduce fossil-born CO_2 in the atmosphere (37). The European Union Directive on the promotion of the use of energy from renewable sources (RED) includes a binding target of a 20% share of renewable energy in energy consumption in EU by 2020 (38). The total volume of biomass from agriculture in Germany for 2015 equals 117 million tDM (dry matter), among which around 68% of biomass is used for food and feed, while 19% for energy. The largest energetic biomass carrier for electricity generation is biogas with a electricity generation of 27.9 TWh (7). Bioethanol and biodiesel crops such as rapeseed and cereals are in second place with approximately 3.8 MM tDM potential and used in the transport sector. Biofuels are blended with diesel fuel or petrol by the petroleum industry under quota obligations till the foreseeable short-term future (7).

1. Backgrounds

1.3 Biomass and PV in FWE Nexus

There are many inter-linkages concerning energy system transition that can be analyzed under FWE nexus framework, e.g., biogas generation at waste water treatment plant. As mentioned in section 1.2 the most present and land-impacting inter-linkage is between biomass and PV¹, which is emphasized in this dissertation.

On the open field outside urban area, the nexus is between ground-mounted PV and biomass for energy. Both ground-mounted PV and energy biomass are their strengths: ground-mounted PV has a higher energy yield factor of 5 compared with biomass, where energy crops grow, (6) and biomass is crucial in the transportation and heating sector (7). Beyond the energy scope, PV and biomass have a distinguished impact on other resources, i.e., water and food. Both PV and energy crop fields eliminate the food supply potential if the fields are agricultural fields for food. In the operation phase, ground-mounted PV does not require water input. On the contrary, irrigation is a boundary condition for biomass production in dry or future dry regions. So biomass and PV can not be substituted equally as the same good without evaluating the impacts on the environment.

The original idea of applying FWE Nexus in biomass-PV-tradeoff context is inspired by project IN-SOURCE, on which this dissertation builds. IN-SOURCE project intends to develop and combine tools addressing different FWE fields and analyze the FWE issues in three international case regions with different densities. Appended paper IX introduces the scientific background, related tools, and case studies of the IN-SOURCE project.

Currently, some policies limit and regulate the land for ground-mounted PV, energy crops, and food.

1. With the Renewable Energy Directive 2018/2001 (RED II), adopted in December 2018, the EU is continuing the political framework for the use of renewable energy sources for the period from 2021 to 2030. The first-generation bioethanol, i.e., ethanol from crops, will be phased out until 2030 (39). Only the secondary generation biomass, i.e., residues, and first-generation biogas from current energy maize, can be further used for en-

¹ Besides biomass and PV, onshore wind is another critical energy source contributing to the emission-free goal on land surfaces. However, due to the relatively smaller land footprint of onshore wind and the scope of the paper, energy-use land tradeoffs are limited to biomass and PV in this paper.

1.3 Biomass and PV in FWE Nexus

ergy purposes. In this paper, the tradeoff between food and energy crops only happens on the current energy maize field.

2. To avoid conflicts between ground-mounted PV, other forms of land use, and ecological interests, the German government has outlined regulations in the National Renewable Energy Sources Act (German 'EEG'). The EEG thus restricts the land areas eligible for ground-mounted PV plants benefiting from feed-in tariffs (40). The eligible areas include the conversion areas² and agricultural less-favored-areas³.
3. To ensure enough renewable electricity production, a minimum area target of 2 percent of the state's surface area for onshore wind plants and PV plants was agreed in the coalition agreement in the federal state Baden-Württemberg, Germany (41). The 2% goal is not bonding in Germany's other federal states but serves as a base metric.

As subsidy-free PV plants become economically feasible, the land-use restrictions in the current EEG and municipal council are becoming more and more obsolete (42). Additionally, the Federation for the Environment and Nature Conservation Germany (German 'BUND') and the Nature Conservation Association Germany (German 'NABU') are appealing to ease the regulations placed by the EEG to accelerate the scale-up of renewable energies, pointing out that conventional monocultural agriculture has higher ecological impacts on land than ground-mounted PV (43). Additionally, the regulations only specify the feasible areas but do not prioritize fields for biomass, PV, or food. If the trend of PV expansion is inevitable, how can we choose the more promising lands simultaneously to reduce the impact on other resources loss? Another uncertainty in applying the regulations on a regional scale is the inequality of energy demand and geographical situation among regions with the national rules. Due to the decentralized nature of renewable energy production, PV is favored to install close to the demand to reduce the transportation cost. It is economically and technically initiated on regions with higher demand and PV potential to expand ground-mounted PV on current agricultural lands.

The decentralized idea is also applied for biomass. The logistical costs for collection and transport of straw and stalks strongly limit the economical transportation distances of less than 16 km to biomass logistic centers (44). Biomass

² Areas along highways or railroads within 200 m of the outer edge of the paved roadway. A corridor located along the roadway or railway of at least 15 meters wide is kept clear. Furthermore, it also includes areas which were formerly used for economic, traffic, housing or military purposes, sealed areas, designated commercial areas, and other built facilities.

³ Arable and grasslands that are located in a less-favored area (LFA) (Council Directive 86/465/EEC)

1. Backgrounds

combined heat and power (CHP) plants are more suitable for the development of biomass energy in village and town systems in cold regions. The transmission cost increases exponentially as the population density increases. Therefore, biomass CHP plants can achieve higher efficiency in transmission costs when biomass fields are close to small consumption centers (45).

In urban areas the biomass exist in urban green infrastructure, i.e., parks, trees, lawns, and green roofs. Large amounts of residual grass originating from the management of landscape and natural areas are produced. This material, which is not competing for land use like energy crops, and is only partially recovered for animal feeding, can be profitably used for sustainable bioenergy production (46). However, the specific biomass-PV inter-linkage is rather limited to roof PV installation on green roofs. This topic is rather minor compared with the ground-mounted PV and biomass inter-linkage on hinterland.

1.4 Research gap, research question, and goal

The FWE framework has been used in various contexts at many spatial levels, e.g., resources at the global level (3), energy at the national level (4), and water management at the regional level (5), for management and planning. The resolution of previous studies is only one node the same as the system boundary, i.e., the tradeoffs are at aggregated regional level but without further information on each land field.

To the author's knowledge, there are so far no analysis work and tool at the regional level addressing the FWE nexus, especially biomass-PV tradeoff, at a fine spatial resolution at the regional scale. There are significant gaps in tools and data. Firstly, there are no standalone methods and tools for practicing and implementing the nexus approach. Therefore, a nexus methodology should be developed by combining multiple methods and tools, including qualitative and quantitative, and natural and social science mixed methods (47). Secondly, it is challenging to geographically generalize and transfer the nexus methodologies, methods, and tools. Tools that can be replicated and/or adjusted at different sites and scales (48) and/or new methods/tools can be constructed as specific case studies (49; 47; 50) are not available. Thirdly, utilization of robust datasets from multiple sources is still lacking (51).

Several studies (8; 9; 10) attempt to expand ground-mounted PV on agricultural areas with the concept of agro-photovoltaics (APV) to avoid conflicts with food again. APV combines biomass production and solar power production on the

1.4 Research gap, research question, and goal

same land area, e.g., by installing PV panels vertically and allowing enough space for agricultural machines to be deployed between module rows. However, APV is in most cases still in a pilot phase (8; 9; 10).

To solve the urgency of ground-mounted PV expansion on existing agricultural lands with the matured solution in the short term, the exclusive tradeoff between biomass/food and PV is still missing. The challenges to managing water, energy, and food resources simultaneously while meeting potentially conflicting objectives without compromising the resource base of any sector are urgent. They need to be addressed, for instance, when ground-mounted PV shall be expanded in a region by causing as limited negative impact as possible on biomass and water resources (51). This challenge demands an integrated approach, considering economic, social, political, and environmental dimensions (47).

Based on the research gaps, the following two research questions need to be answered:

1. How can a consistent modelling framework assess various FWE issues, especially biomass x PV, with high spatial resolution within a system boundary of a region? How can this process execute with one consistent input data model and generate comparable outputs?
2. What land fields are preferred for ground-mounted PV or biomass considering the impacts on other resources, i.e., water and food, under scenarios including economic, political, and environmental factors?

Therefore, the work aims to develop new simulation workflows covering FWE issues, especially on biomass and ground-mounted PV potential, with a high spatial resolution nature. The simulation tools should enable scenario analysis not at the aggregated level anymore but provide technical decision-making guidance at a single-field level for local authorities for individual cases. The proposed scenarios should include economic, social, political, and environmental concerns and situations.

This dissertation is especially valuable for those target groups, which require regional high-resolution information on renewable energy expansion, i.e., county governments which need to approve the new ground-mounted PV projects, or governmental decision-makers/consulting companies that design land-use strategies. The national-level studies have focused on the aggregated values without details on each land field. Compared to studies focusing on the national level, this regional-focused work thus helps the target groups to find a land use equilibrium between energy production and biomass by considering potential

1. Backgrounds

PV and bioenergy gains, amounts of saved irrigation, and food loss for each desired field.

Chapter 2

Materials and Methods

The first step of the dissertation is to 1) build a shared consistent data model and 2) extend an existing energy-focused simulation platform, SimStadt, with new established main workflows covering ground-mounted PV potential, biomass, as well as optional workflows including urban water demand, green roof, and food demand/potential. SimStadt comprises modular workflow management, with each workflow serving a specific purpose, and multiple workflows sharing the same input data. Before this dissertation, SimStadt initially focused on urban energy demands (heating and electricity), energy potentials (roof PV), and GHG emissions from heating. The newly-established workflows perfectly fill the research gaps in missing tools for the biomass-PV tradeoff.

The research questions define the system's spatial boundary (regional/sub-regional). The system boundary is German county ('Landkreis') in this dissertation, as 1. each county has a clear administrative boundary, 2. counties usually determine the land-use change decisions, 3. for later supply-demand analysis, the surrounding suburban lands can be seen as the energy hinterland for cities in the same county. The analysis of the PV-biomass tradeoff in this paper takes place in the suburban area covering agricultural and grasslands, which are referred to as hinterland in the following dissertation. Besides the system boundary, the first research question also defines the resolution of the work as a single land field. A land field refers to an area of open land, especially one planted with crops or pasture, typically bounded by hedges, roads, or fences.

The section [2.1](#) introduced the input data and the development of SimStadt for the problem setting. The related methodology papers **I-V** and **VII-VIII** show each new workflows.

2. Materials and Methods

After the first step, SimStadt and its input can simulate many FWE issues separately but with consistent results for nexus analysis. The second step of the dissertation is to combine the results of newly-established workflows in an interactive way to investigate the hinterland biomass-PV nexus issue stated before as an example (section 2.2).

The field characteristics, i.e., energy potential or demands on other resources, from simulation workflows are constant. The nexus analysis lies in the comparison and interpretation of the results from workflows in the real situations, that should not only strictly follow the current regulation but also explore the feasible expansion case in the short-term future. Therefore, four scenarios, that reflect current economic, environmental, and political regulation, are set up.

The critical difference between scenarios is the priority to utilize fields for different purposes, i.e., ground-mounted PV, biomass, or no change. With the defined scenarios, the next step is to translate the simulation results of workflows to comparable indicators so that the field can be ranked and prioritized to scenarios, respectively. Many direct results can not be used directly in the predefined scenarios, as they can not convey the idea of the scenarios. For example, workflows do not have economic outputs to show the economic advantages of each field. This simulation and analysis workflow proposed above is tested in three German case studies, county Ludwigsburg, Ilm-Kreis, and Dithmarschen. The three case studies represent distinguished land-use structures, solar irradiance, and geometries.

The detailed information on the biomass and ground-mounted PV application case is shown in appended paper VI.

On the contrary to hinterlands, the climate mitigation technologies in urban areas have the goal to generate renewable energy on-site and contribute to livable urban surroundings. The dissertation has the first attempt to include a representative biomass-PV nexus technology in urban areas, i.e., roof PV systems on green roofs as an side minor example. Green roofs are defined as the building roofs which are entirely or partially covered with vegetation and growth medium (52). The appended paper III extended the roof PV potential workflow introduced in (53) with a response to ambient temperature drop on green roofs.

Besides answering the research questions on biomass-PV nexus, experimental works (appended paper IX-XI) has been conducted to explore the transferability, interaction with urban waste to achieve energy autarky, and new standard application domain extension (ADE) of input data. The outlooks are shown in section 4.

2.1 Input data and simulation model

One of the critical reasons why SimStadt was chosen is its geographical nature. The simulation of SimStadt usually starts from analyzing the geometry of building in a collective CityGML file that includes all the required buildings. The dissertation extended the CityGML input with land field objects with attributes by overlaying several maps as a shared input data set. The shared input data set includes a spatial geographical map of land use, food production, soil, temporal climate data, and socioeconomic factors. The spatial input data set has the resolution of fields, which provides the scalability to any lower detail level, i.e., regional or national, for the bottom-up simulation tools. The shared data input ensures the data consistency and comparability of the results for tradeoffs. SimStadt has a modular structure, i.e., each step serves a purpose and can be shared between workflows. Table 2.1 shows the inputs, their resolutions, and sources used in this dissertation.

Table 2.1: The data inputs, their resolutions and sources used in this dissertation.

Data	Spatial Resolution	Source
DLM land use	1:10,000/1:25,000 of the topographic objects; ± 3 m for linear objects	AdV
Crop type	30 m	Griffiths, Nendel et al. (2019)
Soil distribution	1:100,000 (1 km)	BGR
Reference food calorie potential	5 arc minutes (around 6 km in Germany)	Pradhan et al. (2013)
Climate (precipitation and temperature)	One representing point per region	Meteonorm

SimStadt has been developed at HFT Stuttgart for years, and many works have been done to develop, validate, complete and apply the SimStadt platform. Another key advantage of SimStadt is the modular structure hosting various workflows. Therefore, SimStadt is reliable and has extension potential. Until the dissertation, SimStadt had a strong focus on energy issues, i.e., energy demand (heating (54) and electricity (55)), energy potential (roof PV (53)), and emission based on heating consumption (56). Appended paper VIII describes the energy functions of SimStadt model till this dissertation.

2. Materials and Methods

Nevertheless, the FWE related workflows were still missing. New simulation workflow steps, i.e., ground-mounted PV potential processor, biomass processor, yield generator, and water+food demand processor, were programmed to simulate the identified FWE issues. Figure 2.1 shows the geographical and socio-economic inputs (table 2.1), workflows, also the scenarios and analysis methods.

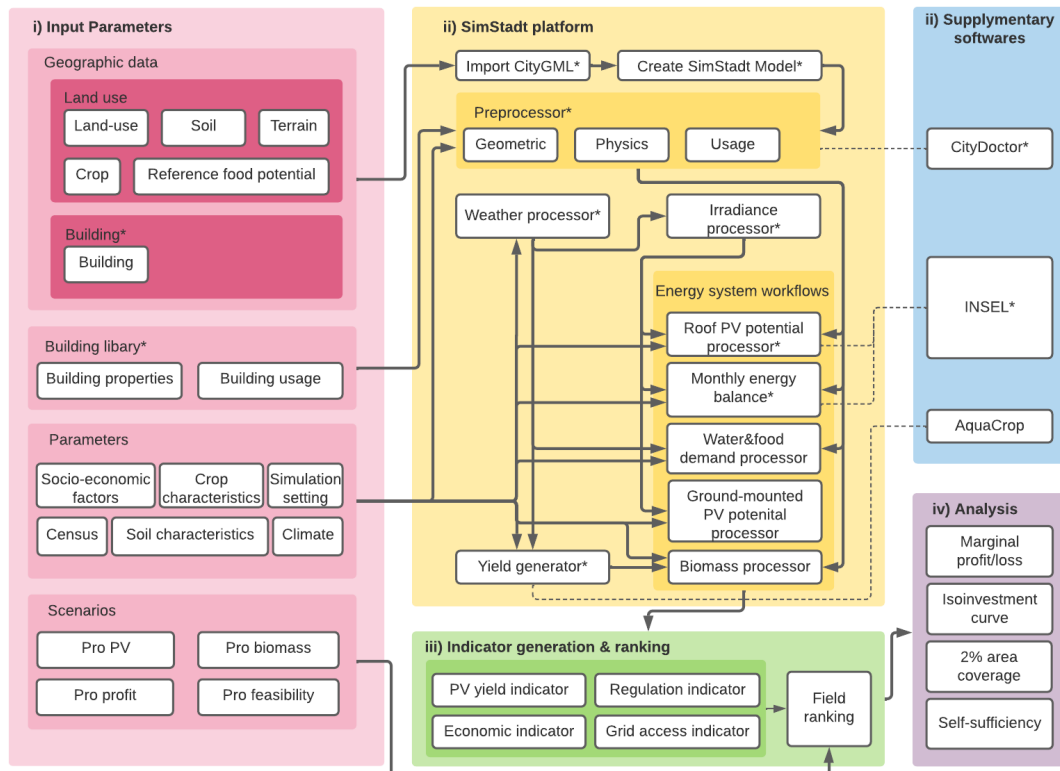


Figure 2.1: The model structure as well as inputs, scenarios, indicator and analysis methods. The existing and unchanged steps are marked with *.

The most dramatic landscape change toward climate neutrality is on hinterlands with technologies like ground-mounted PV and biomass. On the hinterlands, the biomass workflow simulates the annual crop yield, transpiration/irrigation demand, and bioenergy carrier potential (appended paper I, VII). The food potential workflow extends the biomass workflow with animal and vegetal food products' annual calorie potential (appended paper IV). The last topic on the hinterland is ground-mounted PV. The ground-mounted PV potential workflow simulates the capacity and annual electricity yield of each field based on terrain,

2.2 Biomass-PV nexus as key application case

orientation, and the solar irradiance from (53). The method to simulate ground-mounted PV potential is introduced in appended paper V.

Till here, all the required workflows to simulate tradeoff at the potential side are completed. To have the whole picture, demand values can also be critical. The demand side is a driving factor to tradeoff decisions towards specific directions, i.e., the urgency for local energy production might release the restriction for food production. Some demand values at the regional level are not statistically available. Two workflows were developed to overcome the barriers. Simulation workflows on urban food calorie demand and residential/non-residential water demand were set up shown in appended paper IV and II respectively.

2.2 Biomass-PV nexus as key application case

It is not very likely this dissertation addresses all inter-linkages of FWE nexus. A deep dive of inter-linkage between ground-mounted PV and biomass is the key application case. The above mentioned workflows on ground-mounted PV potential and biomass/food potential are the two essential tools.

In total four scenarios are set up, shown in table 2.2, that do not only strictly follow the current regulation but also explore the feasible expansion case in the short-term future. The scenario 'Pro PV' only excludes fields with hard land protection restriction, i.e., natural protection sites, and looks for fields with the highest PV potential $GW h_{electricity}/yr$. Scenario 'Pro feasibility' does not only consider hard land protection restrictions regarded as the 'no-go' areas for ground-mounted PV. It also includes the soft restrictions, i.e., conversion areas, agricultural-less-productive lands, grasslands, and the distance to medium voltage power lines. The 'Pro profit' scenario includes the financial initiative for landowners in the decision-making process: the land-leasing price to PV contractors in EUR/yr is compared with the revenue by growing crops also in EUR/yr . The 'Pro biomass' scenario intends to protect energy crop and biomass production under RED II regulation, which restricts the energy crop production only to biogas maize.

2. Materials and Methods

Table 2.2: Scenarios at potential side addressed in the dissertation.

Scenario	Description
Pro PV	The land fields with high PV potential are preferred.
Pro feasibility	Ground-mounted PV plants are install in the land fields with high technical and political feasibility.
Pro profit	The land fields with high payback ratio between PV and agricultural production are preferred.
Pro biomass	The maize fields for biogas are less favoured for PV, as well as field with high bioenergy potential.

The indicators presented in table [2.3](#) translate the simulation results into numeric values that can be compared among land use fields for scenarios. In each scenario all fields are targeted with different indicator values. Fields with higher indicator values are prioritized to install PV. Each scenario employs one or more than one indicators: (i) scenario 'Pro PV' scenario: PV yield indicator, (ii) scenario 'Pro feasibility': grid access indicator and scenario-indicator, (iii) scenario 'Pro profit': an economic indicator . (iv) 'Pro biomass' scenario does not require additional indicator but directly reads the crop type and biomass yield.

Three case study regions (German 'Landkreise' or counties) are chosen for this study out of a total of 400 counties, because, firstly, county-wide land use data are available; secondly, they differ concerning their land use structure; thirdly, they are located in different parts of Germany, with different climatic conditions. This allows a more holistic view of regional PV potentials and their national ramifications. The case studies allow to test the accuracy and functionality of the established tools from [2.1](#) in the regional level.

1. Sub-urban: Ludwigsburg, Baden-Wuerttemberg, Southern Germany
2. Forest dominant, semi-urban: Ilm-Kreis, Thuringia, Mid-Eastern Germany
3. Agriculture dominant: Dithmarschen, Schleswig-Holstein, Northern Germany

The choice of these counties thus reflects the diversity of Germany and to some extent more broadly typical northern and central European landscapes. Table [2.4](#) provides key characteristics for each county.

2.2 Biomass-PV nexus as key application case

Table 2.3: Assessment indicators, its target, and definition for land use decision making at FWE framework.

Indicator	Target	Definition
PV yield	The electricity generation efficiency of PV.	The GCR, i.e., PV panel area compared with total field area, range from 0 to 1. 1 means the full coverage of PV.
Economic	The investment pay-back comparison for land-owners	The ratio between the land leasing income for PV to the income of growing crops. The ratio then is divided by the maximal ratio over scenarios to make sure it is between 0 and 1.
Regulation	The difficulty of converting land for PV from agriculture	1: conversion area or non-vegetal area, 0.75: disadvantage area, 0.5: grassland, 0.25: agricultural arable area, 0: Non-eligible land for PV, i.e., forest, orchard and vineyard).
Grid access	The difficulty to connect PV with grid.	1: the polygon lies within 1 km radius of medium voltage grid (≥ 1 and < 72.5 kV). Otherwise 0.

Table 2.4: Relevant socio-economic, geographic and energetic data of the case study regions.

Parameter	Unit	Ludwigs-Ilm- burg	Kreis	Dithmar- schen
Area ¹	km ²	687	805	1,428
Population Density ¹	pers./km ²	794	132	93
Agricultural land cover rate ²	%	55	47	76
Forest land cover rate ²	%	18	45	4
Electricity demand ^{3,4,5}	GWh/yr	1,795	428	841

¹(57); ²(58); ³(59); ⁴(60); ⁵(61)

The urban nexus between roof PV and green roofs does not require new workflows, but a further analysis of the result from the existing workflow 'Roof PV potential'. The electricity yield is adjusted due to the decrease of ambient temperature. The appended paper III introduces this urban PV-biomass example with focus of energy-water nexus.

Chapter 3

Results and discussion

The first research question demands simulation workflows covering most relating FWE issues. For this dissertation, the platform SimStadt determines relating attributes, i.e., technical bioenergy potential, ground-mounted PV potential, crop water consumption, food calorie potential/demand, urban water demand, roof PV potential of each field and building. The direct output of these workflows are the demand and potential in a certain region with a fine spatial resolution. Due to the geographical input with field polygon/building resolution, the results can be listed as CSV sheets and be visualized and analyzed on maps with exact coordinates and shapes. Section [3.1](#) shows the potential/demand spatial distribution results of biomass, PV, water, and food.

In this section, detailed results on the ground-mounted PV-biomass nexus are presented. Similar detailed analysis can also be conducted for, e.g., PV-food nexus. The technical energy yield in $GWh/ha/yr$ can be directly compared between biomass and PV even they represent different energy carriers, i.e., biofuel and electricity. As the total land area in a region is constant, and biomass and PV are competitors in terms of land, by increasing the share of land for one technology, the overall energy outcome of the technology will increase, the other technology will yield a lower energy outcome. For tradeoff between biomass and PV for energy, the substitution rates are various between scenarios (the deployment strategy of PV/biomass) illustrated in section [3.2](#)

Another critical response to the second research question is the marginal gain or the loss of PV, biomass, and water if a certain amount of agricultural area is converted to PV. In this paper, APV is neglected due to the technical variability and application uncertainty. Therefore, with the increase of lands for PV plants,

3. Results and discussion

original vegetation (crop, forest, grove, and orchard) will be removed. Section 3.3 shows the specific gain/loss in $GWh/ha/yr$ under different scenarios.

Although this result section focuses on tradeoffs between biomass and ground-mounted PV on the potential side, side analysis efforts of comparing resource demand and potential are also presented in section 3.4. The demand values do not change the prioritization relation of fields for tradeoff but rather suggest the number of total county areas and main resourcing-application drives locally, e.g., a county with higher energy demand and energy autarky goal should consider implementing more ground-mounted PV. The urban roof PV potential, including yield increment benefits brought by green roofs, i.e., PV-biomass nexus in urban area, is seen as demand-side management.

3.1 Potential and spatial distribution of FWE resources

Appended paper I and VII simulate the technical biomass potentials in the forms of energy carrier, i.e., biogas, biofuel, and solid fuel, are simulated for each eligible field. However, besides agricultural land-use, biomass potential exists on forests and groves as energy wood or residue. The solid residue contributes to the most significant share, up to 73% of available biomass potential in each region. Biogas maize reminds the most energy crop. 32% of total biomass potential in Dithmarschen, where maize plantation areas are higher, is biogas from maize, compared with 18% in Ludwigsburg. Due to increasing forecasted rainfall and ambient temperature, the biomass yield is expected to increase 0.2% to 4%. In general, Germany has the ideal climate for crops. Relative biomass⁴ is higher than 93% for most crops in all regions, i.e., applying irrigation could improve the biomass potential by around 2% in Ilm-Kreis compared with less than 1% in other regions at the expense of between 58 and 680 $m^2/ha/yr$ of irrigation water.

Paper V shows the detailed results of ground-mounted potential PV at a resolution of a single field in all three case studies. For all three counties, conversion areas make up 2.0 % to 2.6 % of the total land area. The LFA in Ludwigsburg accounts for around 0.4% of the overall land area, which reflects the high agricultural productivity due to better soil conditions. On the contrary, Dithmarschen and Ilm-Kreis have a larger share of LFA of 33% and 36%, respectively. This means that current regulation promotes ground-mounted PV installation in re-

⁴ Relative biomass is the ratio between actual biomass amount and the reference (no water, no soil fertility, no soil salinity stress, no weed infestation)

3.1 Potential and spatial distribution of FWE resources

gions with low soil quality. The specific solar PV yield varies between 0.53 *GWh/ha/yr* to 0.68 *GWh/ha/yr*. Higher yield is expected in the southern region, e.g., Ludwigsburg, due to higher solar irradiance and hilly topology with south-facing slopes.

The food potential has the same trend responding to climate change and irrigation with biomass potential since they share the same yield simulation result. Restricting land used exclusively for energy crop production, which RED II regulates from 2030, is the most effective way to increase annual food production potentials by 15%. The detailed results of food potential analysis can be found in paper IV.

The results of urban food and water demands are also per building base, i.e., each building has its demands according to its geometry and volume. The method to simulate the food calorie demand with diet pattern change has been introduced in appended paper IV. Urban water demand of residential and non-residential buildings can be simulated by water demand workflow only with a 3D building model (appended paper II). The water and food demand workflows conquered the data limitation to generate demand values at any scale for residential and non-residential buildings, which are usually not available to the public.

The results mentioned above are aggregated from all field polygons. A 3D viewer was established to illustrate the attributes of each field and building at the example of Ludwigsburg⁵. Besides the biomass and food potential of each field polygon mentioned before, the food, water, and heating demand, rooftop PV potential are also visualized. The figure 3.1 illustrates a visualization screenshot at an example of Affalterbach, Ludwigsburg. The users can visualize per building demand and per field potential simultaneously.

⁵ <https://transfer.hft-stuttgart.de/pages/in-source/lkrludwigsburg3d/>

3. Results and discussion



Figure 3.1: Visualization screenshot of food demand (per building) and food potential (per field polygon around settlement areas) in Affalterbach, Ludwigsburg.

3.2 Substitution between biomass and PV

The PV and biomass are competing with each other for fields due to their exclusive natures. Increasing the production of one technology would damage the production of the other considering the limitation of field areas. An isoinvestment curve in the context of this paper, i.e., a function $z(x, y) = C$, connects all optimal combinations of PV and biomass with the same technical energy potential on fields. The technical energy potential represents the maximal amount of energy generated on the fields regardless of the energy carrier forms. The figure [3.2](#) shows isoinvestment curves as functions of biomass abatement and PV increment, which are the two leading area-intensive energy technologies compared with onshore PV. The x-axis represents the PV yield divided by the total county area, and the y-axis is the biomass yield of the whole case study county divided by the total county area. The gradient dy/dx of an isoinvestment curve $y(x)$ is the marginal rate of substitution between one GWh of increased PV yield and one GWh of biomass yield. A higher gradient absolute value means an immense sacrifice of biomass yield when substituting an agricultural field with PV.

3.3 The marginal loss and gain of ground-mounted PV expansion

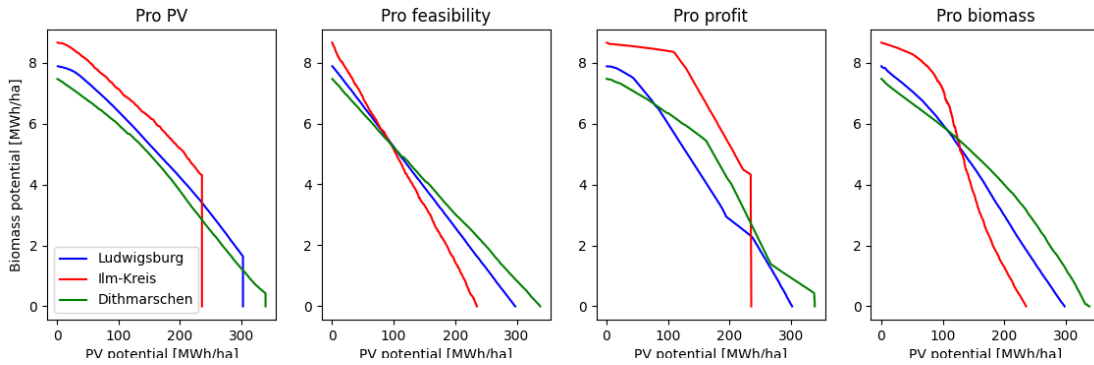


Figure 3.2: The insoinvestment curves between PV and biomass.

Scenario 'Pro PV' has the specific loss of biomass yield of GWh/ha is the highest among all case studies. Due to the more considerable gain of PV yield, the biomass yield loss compared with PV yield gain in all three case studies is not the highest. The absolute gradient of figure 3.2 is between 30% and 60% as the gradients in scenario 'Pro feasibility', i.e., the loss of biomass is 40 to 70% less when every GWh ground-mounted PV is installed comparing with current scenario ('Pro feasibility'). The second scenario 'Pro feasibility' has the constant substitution rate between biomass and PV, i.e., the loss of biomass of GWh/ha is indifferent if one more hectare of land is converted into PV following the current regulation. The absolute value of gradient, however, varies between case studies from -0.027 to $-0.032 \text{ GWh}_{Biomass}/\text{GWh}_{PV}$. Ilm-Kreis has the highest gradient of $-0.044 \text{ GWh}_{Biomass}/\text{GWh}_{PV}$ due to relatively lower PV specific yield. The scenario 'Pro profit' and 'Pro biomass' both avoid high biomass loss, i.e., smaller gradient values of $-0.002 \text{ GWh}_{Biomass}/\text{GWh}_{PV}$ in Ilm-Kreis, when the first 5,000 GWh of PV yield are realized. The lower gradient indicates the lower per-unit biomass potential loss when each GWh PV facility is built. It only shows the relative ratio between biomass loss and PV gain per energy unit, but not guarantee the low absolute biomass loss for a certain area, since it is possible that the absolute PV gain is high.

The detailed result is presented in paper VI.

3.3 The marginal loss and gain of ground-mounted PV expansion

Figure 3.3 illustrates the change of marginal PV yield, crop water demand, and biomass yield. The PV land cover ratio is the sensitivity variable. The

3. Results and discussion

four scenarios show distinguished trends of these parameters. In the marginal gain/loss context, we are looking for scenarios with high PV gain (left column), low biomass loss (middle column), and high crop water saving potential (right column).

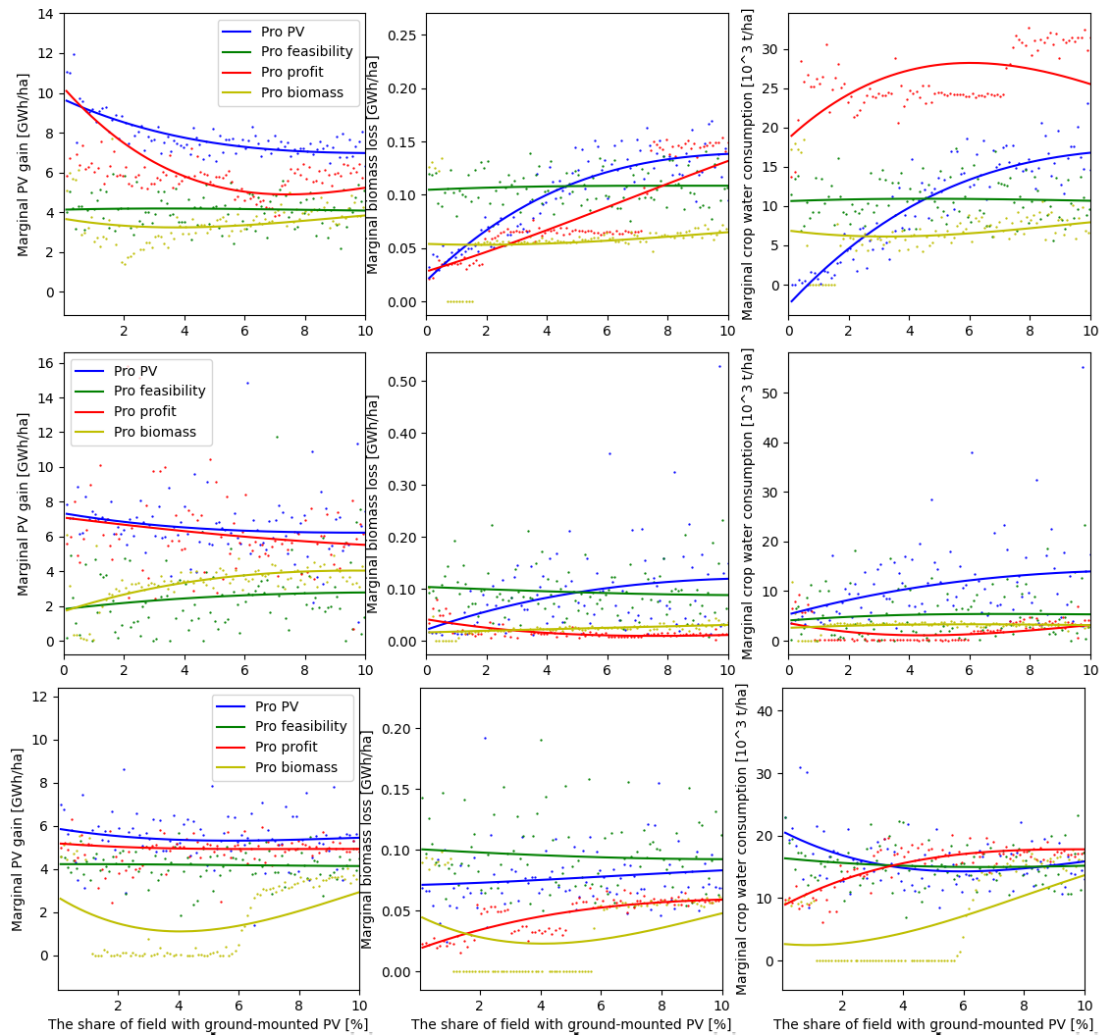


Figure 3.3: The marginal gain and loss of PV yield, biomass yield, crop water consumption in relation with the share of fields as PV farms. The share of fields for PV varies between 0% to 10% of the overall land area with a step of 0.1%. Forth degree polynomial function is used as the fitting function. Upper row: Ludwigsburg, Middle row: Ilm-Kreis, Lower row: Dithmarschen

3.3 The marginal loss and gain of ground-mounted PV expansion

In scenario 'Pro PV' around 12 GWh/ha of electricity can be generated if the first 0.1% of fields are converted into PV farms in Ludwigsburg. The marginal PV yield decreases if more fields are included. Despite the decreasing trend, the marginal PV yield gain is still above the 10 GWh/ha when PV covers 10% fields. In Ilm-Kreis and Dithmarschen, 'Pro PV' scenario has also the highest marginal PV gain all the time. However, the absolute marginal values are lower than Ludwigsburg (around 7 GWh/ha in Ilm-Kreis and 6 GWh/ha in Dithmarschen) due to the lower solar irradiance values in more northern part of Germany. Additionally the marginal PV gain curves are more flat and they are more close to each other, indicating the more flat geometry in the county.

The scenario 'Pro feasibility' excludes the technical advantages of fields for PV, resulting in constant fitting curves, i.e., the locations of PV plants are indifferent. This scenario shows the average marginal gain/loss of PV yield (5-10 GWh/ha), biomass yield (0.05-0.1 GWh/ha), and crop water demand (5,000-11,000 t/ha). In scenario 'Pro profit', the marginal PV yield is second highest after 'Pro PV'. As this scenario promotes land-owner's land-use income and PV plants' leasing income is higher than agricultural production, fields with above-average PV specific yield are usually included first. Between 2% and 7% PV land cover ratios, where grassland is the major crop type, the marginal biomass yield and crop water consumption are almost constant at 0.05 GWh/ha and 2,400 t/yr. The 'Pro biomass' scenario has the lowest biomass loss of 0.05 GWh/ha and the lowest PV yield gain of 4 GWh/ha among all scenarios. An increasing trend is observed at marginal PV yield, biomass loss, and crop water consumption.

The marginal biomass yield loss increases from 0.03 GWh/ha to 0.2 GWh/ha in all case studies across all scenarios. The marginal biomass curves always have either constant or increasing development trend, i.e., the stakeholders have always the chance to employ ground-mounted PV on field with less biomass loss and more than average PV gain. As the fields with high PV potential are usually not covered by crops, but vineyards and orchards, whose energy biomass yields are low and water demand are not considered. When more arable fields are included, the marginal biomass yield loss and water demand increase. Usually the higher biomass production, the more water is required. This trend can also be observed among all regions. However, there are few exceptions due to the specific crop types: the 'Pro profit' scenario avoided highest water consumption and at the same time maintain the biomass loss at a relative low level comparing with other scenarios.

I would argue that based on optimal scenario criteria mentioned in the beginning of this section, the 'Pro feasibility' scenario has constantly the advantages, thus

3. Results and discussion

the ideal scenario solution for ground-mounted PV expansion strategy among all proposed scenarios. The detailed result is presented in paper VI.

3.4 FWE self-sufficiency

Self-sufficiency is the ratio between potential and demand. The self-sufficiency rate represents the supply-demand situation in the region rather than absolute potential values, assuming local demand is fulfilled by the local supply first. Higher self-sufficiency indicates the relative richness of the resources within the region compared with the demand. For example, the lack of water resources in a region sets the priority of tasks to implant water-saving technologies, other than focusing on increasing energy supply. The analysis in this section compares the supply and demand values in three counties and brings discussions qualitatively.

Table 3.1: Summary of potentials and demands on rooftop and ground-mounted PV, biomass, water and food if 2% of area is covered by ground-mounted PV in three case study.

	Ludwigsburg	Ilm-Kreis	Dithmarschen
PV [<i>GWh/yr</i>]			
Rooftop potential (Green roofs)	1061 (1064)	337 (338)	781 (783)
Ground-mounted potential	511-1,202	320-1125	715-1415
End energy demand	4273	515	679
Biomass [<i>GWh/yr</i>]			
Loss	8.5-9.2	7-8.1	15.8-17.7
Remained potential	636-652	123-140	1,051-1,276
Demand	1,399	486	850
Food [<i>Mcal/yr</i>]			
Potential loss (RED II)	7,243 (5,385)	5,632 (3,221)	12,671 (9,259)
Demand	556,004	90,985	128,437
Water [$10^3t/yr$]			
Urban water demand	56,641	4,726	7,763
Rainwater potential	50,082	48,461	112,955
Reduced crop water demand	219-838	397-983	1,352-4,681
Reduced irrigation	38-91	1,018-3,345	0-1,961

The urban water demand is simulated by method from append paper II; urban roof PV potential as demand-side management by method from paper III; urban food demand by method from append paper IV; Energy demand for PV and biomass is taken directly from (31). Table 3.1 shows the changes of potential and self-sufficiency rate of PV, biomass, food and water, if 2% guideline is effect. In the guideline onshore wind power is also included. Due to relative smaller land footprint, in this dissertation I assumed 2% of the total county area is covered only by ground-mounted PV.

The spatial context directly decides the relevance of food security. The discussion on food security/self-sufficiency lies at the national, continental, or global level (62). At the EU level, the food system is self-sufficient, i.e., producing beyond the own demand (63). Food security is not a relevant topic at the regional level, at least in Germany, as the required food variety can not be grown all locally. However, for regions that rely on the agricultural industry, the loss of food calorie potential by converting agricultural lands into PV farms is a factor in the decision-making process. Total food potential loss is expected on average 3,221 Mkal/yr to 12,671 Mkal/yr. By introducing RED II, the food loss is reduced by 26% to 43% by restricting energy crops. Higher loss is observed in Dithmarschen due to a higher share of arable land. Compared with the local demands shown in (64), the food loss by PV expansion needs to be highlighted in Dithmarschen, where the ratio between food loss and demand is around 10%. Indeed not all location food is consumed in the same counties. However, it reflects the dependence and interest on agriculture.

Regional energy, i.e., PV and biomass, self-sufficiency, is more in the current discussion than food and water. As the land transition and planning is a long-term process facing the future, the energy demands from the planned energy system scenarios are favored to be taken. The expected improved insulation of the German building structure by refurbishment, market penetration of electric vehicles, more efficient electric applications, and the reshaping of the industry landscape also contribute to less end energy demand. On the other hand, the electrification of different sectors plays a key role, which is reflected in increasing electricity production. The end energy demand forecast of biomass and PV in 2045 by Bartholdsen et al. is taken as the base (31).

By installing rooftop PV on all eligible roofs⁶, the annual maximal electricity potentials are 1061 GWh, 337 GWh and 781 GWh in Ludwigsburg, Ilm-Kreis and Dithmarschen, respectively. Based on the method introduced in appended paper III, the annual PV yield increases 0.27%, 0.3%, and 0.33% in Ilm-Kreis, Dithmarschen, and Ludwigsburg, respectively, assuming rooftop PV panels are

⁶ Roof area > 25 m², roof insolation > 900 kWh/(m²yr)

3. Results and discussion

installed on green roofs. The warmer the climate, the greater the cooling effect of green roofs. The potential gains are less than 0.3% compared with PV's total electricity demand. Therefore, combining green roofs with PV can not make a fundamental difference on the supply side in Germany.

Compared with the maximal rooftop PV potential, installing ground-mounted PV plants on conversion areas alone yield annual electricity up to 1,400 GWh. It can be concluded that rooftop PV alone can not meet the PV demand in most cases. Converting fields to ground-mounted PV is inevitable to meet the sustainable goal. The importance and urgency of adopting ground-mounted PV depend on the local demand and rooftop PV potential. For example, in Ludwigsburg, it is foreseeable that by 2045 around 4300 GWh/yr electricity demand needs to be either generated in the county or imported from the same federal state. The PV potential on roofs and 2% of fields combined (max. 2,300 GWh/yr) is not sufficient for desired PV demand. Therefore, there is a higher emergency in Ludwigsburg, where the consumption concentrates, to promote ground-mounted PV on lands currently in the restriction. On the contrary, in Ilm-Kreis and Dithmarschen, PV end energy demands are around 15% of the demand in Ludwigsburg. The maximal PV potential from roofs and conversion areas covers all annual demands with more than 200% redundancy.

Chapter 4

Conclusion and Outlook

4.1 Conclusion

This dissertation established and integrated novel FWE simulation workflows with a shared geometrical data input on the same platform. The main relevant FWE workflows reveal each field's resource potential and demand (biomass, ground-mounted PV, food, water, and irrigation) in hinterlands and urban areas. The workflows simulate FWE issues individually without dependency on other workflows. Due to the bottom-up and high spatial natures the workflows generate results with high accuracy and reliability.

The nexus between PV and biomass on hinterland was investigated intensively as an application case - how several workflows integrate. The high-resolution outputs enable tradeoff and synergy scenario analysis between biomass and ground-mounted PV not at the aggregated level anymore but provide technical decision-making guidance at a single-field level for local authorities in individual cases. The scenario analysis answers the long-lasting question in the short-term future, when APV is not technically mature enough: which field should be converted to ground-mounted PV first with optimal substitution of other resources, e.g., biomass, food, and water. The technical inefficiency of the current ground-mounted PV policy should be improved with a systematic a more optimal PV allocation strategy under the FWE content.

First of all, the investigations show that geography has a strong power over the potential and competitiveness of biomass and ground-mounted PV. Due to higher irradiance in southern Germany, the specific PV yield can theoretically reach around 5 to 10 GWh/ha, as Ludwigsburg is a mild hilly area with

4. Conclusion and Outlook

south-facing slopes. Additionally, 3.2% of the county area is vineyards, usually located on the slopes with high PV yield. It is less feasible that vineyards can be eliminated but replaced with PV due to the highest economic revenue (4,000 €/ha/yr) of all crop types and cultural importance. The other two regions have a lower marginal PV yield gain of around 5 GWh/ha/yr due to the lower solar irradiance and flat geometry.

The cost of biomass loss is another debatable point. Focusing on land energy production tradeoff, the substitution rate between biomass and PV shows the incremental gain of one resource at the cost of the other resource loss. A higher gradient absolute value means an immense sacrifice of biomass yield when substituting an agricultural field with PV. Scenario 'Pro feasibility' has the highest gradient of substitution ($0.03 \text{ GWh}_{Biomass}/\text{GWh}_{PV}$), followed by scenario 'Pro PV' ($0.015 \text{ GWh}_{Biomass}/\text{GWh}_{PV}$), then 'Prof biomass' ($0.012 \text{ GWh}_{Biomass}/\text{GWh}_{PV}$), in the end 'Pro feasibility' ($0.007 \text{ GWh}_{Biomass}/\text{GWh}_{PV}$).

After building up new FWE simulation workflows with consistent inputs, the next step is to apply the results to find a strategy/scenario that locates ground-mounted PV on most PV-yield valuable land with low biomass loss and high crop water-saving potential. Additionally, the absolute substitution rate should be low when comparing biomass and PV alone to avoid crucial biomass loss. Based on these criteria, the ideal scenario identified by this work is scenario 'Pro profit'. Scenario 'Pro profit' combines two main factors: field output of PV and agriculture biomass loss. High land leasing price indicates the high PV yield, and low agriculture revenue indicates the low importance of the crop types. It is reasonable that this scenario achieves a less specific PV yield than scenario 'Pro PV'. However, the biomass loss is less than 26% compared with the technical maximal. Continuing current regulations (scenario 'Pro feasibility') obstructs high electricity production from PV and does not save biomass due to the imprecise and broad definition of LFA with low agricultural productivity. Even more optimal scenarios may exist than the four scenarios proposed in this dissertation.

Scenario 'Pro biomass' avoids biomass mass loss by 50% to 90%. The average biomass loss is between 0.03 to 0.15 GWh/ha/yr by expanding PV. Biomass loss is the loss of agricultural residue waste for energy purposes. Therefore, the biomass loss is relatively low than the PV yield gain (2.5 to 10 GWh/ha/yr). However, biomass can be utilized by a wide variety of combustion and gasification technologies producing heat, power, or fuels for transportation (65). PV is 30 folds more efficient than biomass in specific energy output. The biomass mass yield loses 1.4% to 5.8% if 2% of the county area is PV. Energy crop becomes less significant if RED II is enforced, as only biogas maize will be allowed to grow

and biogas maize only takes 7% of maize cultivation area (66). The biogas maize fields can be easily avoided during PV expansion under the 2% guideline.

In all case studies, grasslands have low-profit payback rates. It has been proved that prioritizing PV on south-facing grasslands is the optimal solution compromising PV yield and biomass loss.

La

4.2 Beyond the nexus and future research

Besides focusing on the biomass-PV tradeoff simulation and analysis, pioneer works were also done to explore the possibility of applying the developed methods to a broader context. The transferability and the accuracy of the result rely on the quality of geometrical input (CityGML data model), as the simulating methods and principles are universally applicable and well-proven. Besides three representative case studies in Germany shown in this dissertation, the method can be transferred and scaled to complete flexibility in Germany. Because the required raw maps with high resolution (DLM land use, crop type, and soil type) are available for all of Germany. Regardless of the data obstacles, pilot works have been done to transfer the method to other regions, e.g., Vienna (appended paper X) and La Réunion (appended paper XI). However, a tremendous amount of pre-proceeding work is required to generate an integrated map for SimStadt case by case. This process has not been fully standardized and automatized. For future study, a standardized geometric processing process or a database with ready-to-use maps with high resolution worldwide would be desired.

Municipal solid waste (MSW) includes residential, commercial, institutional, industrial, and municipal sources. MSW is another source of biomass that has not been included in this dissertation. The amount and streams of MSW are heterogeneous among regions. In the appended paper XI MSW potential data was collected from the local report. Depending on the scenario, biomass and MSW could cover between 19% and 22% of 2019 electricity demand compared to an actual value of 6%. Furthermore, prioritizing the production of secondary energy carriers allows to meet 8% of 2019 energy demand in the transport sector.

Onshore wind is another energy generation technology with biomass and ground-mounted PV on the hinterland. Wind power and solar PV can compensate each other to achieve a more stable generation curve better corresponding to demands. The appended paper V indicates that installing a more significant capacity of ground-mounted PV does not guarantee a higher temporal self-

4. Conclusion and Outlook

sufficiency rate, i.e., peak generation concentrating around noon time needs to be either stored or exported. Onshore wind generation might affect the ground-mounted PV installation capacity, eventually other FWE resources. Future works on onshore wind potential simulation are helpful for FWE simulation. Onshore wind power workflow is under development at HFT.

The giant leap of the dissertation work is to bring the FWE analysis to a new high spatial resolution. Extending the current work to a higher temporal resolution is also worthwhile. The biomass potential simulation is at annual temporal resolution and the food and water demand. The ground-mounted PV simulation can be further disaggregated to hourly resolution, but this dissertation's current annual resolution is sufficient. If wind power is included, the hourly interaction between PV and wind is interesting to address as another decision-making criterion.

Lastly, this work applied a simulation method, although it gave the optimized prioritization list of fields under scenarios. Furthermore, an ideal scenario is indeed identified in this dissertation. Even the preferred land use is assigned for each field, it is questionable that the fields follow the desired use due to different ownership of the fields. Each region's heterogeneous political, energetic, and geographical situations require different object functions, e.g., regions with energy autarky goals would set an object function to minimize the energy import. Therefore, a simulation methodology was adopted rather than an optimization methodology when planning the dissertation early.

Bibliography

- [1] D. J. Garcia, F. You, [The water-energy-food nexus and process systems engineering: A new focus](https://doi.org/10.1016/j.compchemeng.2016.03.003), *Computers Chemical Engineering* 91 (2016) 49–67, 12th International Symposium on Process Systems Engineering 25th European Symposium of Computer Aided Process Engineering (PSE-2015/ESCAPE-25), 31 May - 4 June 2015, Copenhagen, Denmark. doi:<https://doi.org/10.1016/j.compchemeng.2016.03.003>. URL <https://www.sciencedirect.com/science/article/pii/S0098135416300552>
- [2] D. Garcia, F. You, [Systems engineering opportunities for agricultural and organic waste management in the food–water–energy nexus](https://doi.org/10.1016/j.coche.2017.08.004), *Current Opinion in Chemical Engineering* 18 (2017) 23–31, biotechnology and bioprocess engineering / Process systems engineering. doi:<https://doi.org/10.1016/j.coche.2017.08.004>. URL <https://www.sciencedirect.com/science/article/pii/S2211339817300230>
- [3] P. Andrews-Speed, R. Bleischwitz, T. Boersma, C. Johnson, G. Kemp, S. D. VanDeveer, The global resource nexus: The struggles for land, energy, food, water, and minerals.

-
- [4] A. Flammini, M. Puri, L. Pluschke, O. Dubois, [Walking the nexus talk: assessing the water-energy-food nexus in the context of the sustainable energy for all initiative](#), Environment and Natural Resources Management. Working Paper (FAO) eng no. 58 (2014).
URL <https://agris.fao.org/agris-search/search.do?recordID=XF2015001455>
- [5] E. Ramos, D. Kofinas, C. Papadopoulou, M. Papadopoulou, F. Gardumi, F. Brouwer, M. Fournier, E. Lluís, X. Domingo, L. Vamvakieridou-Lyroudia, [D1.5: Framework for the assessment of the nexus](#).
URL www.sim4nexus.eu
- [6] M. E. Leirpoll, J. S. Næss, O. Cavalett, M. Dorber, X. Hu, F. Cherubini, [Optimal combination of bioenergy and solar photovoltaic for renewable energy production on abandoned cropland](#), Renewable Energy 168 (2021) 45–56. [doi:10.1016/j.renene.2020.11.159](https://doi.org/10.1016/j.renene.2020.11.159).
URL <https://www.sciencedirect.com/science/article/pii/S0960148120319236>
- [7] N. Szarka, H. Haufe, N. Lange, F. Schier, H. Weimar, M. Banse, V. Sturm, L. Dammer, S. Piotrowski, D. Thrän, [Biomass flow in bioeconomy: Overview for germany](#), Renewable and Sustainable Energy Reviews 150 (2021) 111449. [doi:10.1016/j.rser.2021.111449](https://doi.org/10.1016/j.rser.2021.111449).
URL <https://www.sciencedirect.com/science/article/pii/S1364032121007322>
- [8] D. Ketzler, N. Weinberger, C. Rösch, S. B. Seitz, Land use conflicts between biomass and power production – citizens’ participation in the technology development of agrophotovoltaics, Journal of Responsible Innovation 7 (2) (2020) 193–216. [doi:10.1080/23299460.2019.1647085](https://doi.org/10.1080/23299460.2019.1647085).
- [9] G. Barron-Gafford, A. Salazar, Phelps-Garcia, L. V., IV, L. Lopez, I. Barnett-Moreno, W. Cooke, M. S. Thompson, R. L. Minor, P. Murphy, M. Pavao-Zuckerman, J. Macknick, Co-locating agriculture and solar power renewables (agrivoltaics) to create a more sustainable food, energy, and water future, AGU Fall Meeting Abstracts 2019 (2019) B41B–01.
- [10] G. A. Barron-Gafford, M. A. Pavao-Zuckerman, R. L. Minor, L. F. Sutter, I. Barnett-Moreno, D. T. Blackett, M. Thompson, K. Dimond, A. K. Gerlak, G. P. Nabhan, J. E. Macknick, [Agrivoltaics provide mutual benefits across the food–energy–water nexus in drylands](#), Nature Sustainability 2 (9) (2019) 848–855. [doi:10.1038/s41893-019-0364-5](https://doi.org/10.1038/s41893-019-0364-5).
URL <https://www.nature.com/articles/s41893-019-0364-5>

-
- [11] G. Rasul, [Managing the food, water, and energy nexus for achieving the sustainable development goals in south asia](#), *Environmental Development* 18 (2016) 14–25. [doi:10.1016/j.envdev.2015.12.001](#).
URL <https://www.sciencedirect.com/science/article/pii/S2211464515300646>
- [12] M. Obersteiner, B. Walsh, S. Frank, P. Havlík, M. Cantele, J. Liu, A. Palazzo, M. Herrero, Y. Lu, A. Mosnier, H. Valin, K. Riahi, F. Kraxner, S. Fritz, D. van Vuuren, [Assessing the land resource-food price nexus of the sustainable development goals](#), *Science Advances* 2 (9) (2016) e1501499. [doi:10.1126/sciadv.1501499](#).
- [13] T. Kastner, M. J. I. Rivas, W. Koch, S. Nonhebel, [Global changes in diets and the consequences for land requirements for food](#), *Proceedings of the National Academy of Sciences of the United States of America* 109 (18) (2012) 6868–6872. [doi:10.1073/pnas.1117054109](#).
URL <https://www.pnas.org/content/109/18/6868/#ref-8>
- [14] P. Pradhan, D. E. Reusser, J. P. Kropp, [Embodied greenhouse gas emissions in diets](#), *PloS one* 8 (5) (2013) e62228. [doi:10.1371/journal.pone.0062228](#).
URL <https://journals.plos.org/plosone/article?id=10.1371/journal.pone.0062228>
- [15] FAO, *The future of food and agriculture: Alternative pathways to 2050*, Rome, 2018.
- [16] C. J. Vörösmarty, P. B. McIntyre, M. O. Gessner, D. Dudgeon, A. Prusevich, P. Green, S. Glidden, S. E. Bunn, C. A. Sullivan, C. R. Liermann, P. M. Davies, [Global threats to human water security and river biodiversity](#), *Nature* 467 (7315) (2010) 555–561. [doi:10.1038/nature09440](#).
- [17] J. ALCAMO, M. FLÖRKE, M. MÄRKER, [Future long-term changes in global water resources driven by socio-economic and climatic changes](#), *Hydrological Sciences Journal* 52 (2) (2007) 247–275. [doi:10.1623/hysj.52.2.247](#).
- [18] H. Hoff (Ed.), [Understanding the Nexus: Background paper for the Bonn2011 Nexus Conference](#), Stockholm Environment Institute, 2011.
URL https://publications.pik-potsdam.de/pubman/faces/viewitemfullpage.jsp?itemid=item_17278_1&view=export
- [19] C. Böhringer, T. F. Rutherford, [Combining bottom-up and top-down](#), *Energy Economics* 30 (2) (2008) 574–596. [doi:10.1016/](#)

- [j.eneco.2007.03.004](https://www.sciencedirect.com/science/article/pii/S014098830700059X).
URL <https://www.sciencedirect.com/science/article/pii/S014098830700059X>
- [20] W. A. Hussien, F. A. Memon, D. A. Savic, [An integrated model to evaluate water-energy-food nexus at a household scale](https://doi.org/10.1016/j.envsoft.2017.03.034), *Environmental Modelling Software* 93 (2017) 366–380. doi:<https://doi.org/10.1016/j.envsoft.2017.03.034>.
URL <https://www.sciencedirect.com/science/article/pii/S1364815216306594>
- [21] Z. Chamas, M. Abou Najm, M. Al-Hindi, A. Yassine, R. Khat-
tar, [Sustainable resource optimization under water-energy-food-carbon nexus](https://doi.org/10.1016/j.jclepro.2020.123894), *Journal of Cleaner Production* 278 (2021) 123894. doi:[10.1016/j.jclepro.2020.123894](https://doi.org/10.1016/j.jclepro.2020.123894).
URL <https://www.sciencedirect.com/science/article/pii/S0959652620339391>
- [22] Charalampos Avraam, Ying Zhang, Sriram Sankaranarayanan, Benjamin Zaitchik, Emma Moynihan, Prathibha Juturu, Roni Neff, Sauleh Siddiqui, [Optimization-based systems modeling for the food-energy-water nexus](https://doi.org/10.1007/s40518-020-00161-5), *Current Sustainable/Renewable Energy Reports* 8 (1) (2021) 4–16. doi:[10.1007/s40518-020-00161-5](https://doi.org/10.1007/s40518-020-00161-5).
URL <https://link.springer.com/article/10.1007/s40518-020-00161-5>
- [23] L. Ji, B. Zhang, G. Huang, Y. Lu, [Multi-stage stochastic fuzzy random programming for food-water-energy nexus management under uncertainties](https://doi.org/10.1016/j.resconrec.2019.104665), *Resources, Conservation and Recycling* 155 (2020) 104665. doi:[10.1016/j.resconrec.2019.104665](https://doi.org/10.1016/j.resconrec.2019.104665).
URL <https://www.sciencedirect.com/science/article/pii/S0921344919305713>
- [24] J. Liu, Y. Li, X. Li, [Identifying optimal security management policy for water–energy–food nexus system under stochastic and fuzzy conditions](https://doi.org/10.3390/w12113268), *Water* 12 (11) (2020) 3268. doi:[10.3390/w12113268](https://doi.org/10.3390/w12113268).
URL <https://www.mdpi.com/2073-4441/12/11/3268>
- [25] M. Li, V. P. Singh, Q. Fu, D. Liu, T. Li, Y. Zhou, [Optimization of agricultural water–food–energy nexus in a random environment: an integrated modelling approach](https://doi.org/10.1007/s00477-019-01672-4), *Stochastic Environmental Research and Risk Assessment* 35 (1) (2021) 3–19. doi:[10.1007/s00477-019-01672-4](https://doi.org/10.1007/s00477-019-01672-4).

-
- URL <https://link.springer.com/article/10.1007%2Fs00477-019-01672-4>
- [26] L. Wu, A. Elshorbagy, S. Pande, La Zhuo, [Trade-offs and synergies in the water-energy-food nexus: The case of saskatchewan, canada](#), *Resources, Conservation and Recycling* 164 (2021) 105192. doi:10.1016/j.resconrec.2020.105192.
URL <https://www.sciencedirect.com/science/article/pii/S0921344920305097>
- [27] S. Fawzy, A. I. Osman, J. Doran, D. W. Rooney, [Strategies for mitigation of climate change: a review](#), *Environmental Chemistry Letters* 18 (6) (2020) 2069–2094. doi:10.1007/s10311-020-01059-w.
URL <https://link.springer.com/article/10.1007/s10311-020-01059-w#Sec32>
- [28] [Federal climate change act](#) (2019).
URL https://www.gesetze-im-internet.de/englisch_ksg/englisch_ksg.html
- [29] IEA, *World Energy Outlook 2019*, International Energy Agency, Paris, 2019, <https://www.iea.org/reports/world-energy-outlook-2019>.
- [30] H. Wirth, S. Bächle, [Wie wir mit Sonnenenergie einen Wirtschaftsboom entfesseln und das Klima schützen](#), <https://www.ise.fraunhofer.de/de/presse-und-medien/presseinformationen/2021/wie-wir-mit-sonnenenergie-einen-wirtschaftsboom-entfesseln-und-das-klima-schuetzen.html>, (Accessed: 2021-09-15) (Jun. 2021).
- [31] H.-K. Bartholdsen, A. Eidens, K. Löffler, F. Seehaus, F. Wejda, T. Burandt, P.-Y. Oei, C. Kemfert, C. v. Hirschhausen, [Pathways for germany’s low-carbon energy transformation towards 2050](#), *Energies* 12 (15) (2019) 2988. doi:10.3390/en12152988.
- [32] B. Ristic, M. Mahlooji, L. Gaudard, K. Madani, [The relative aggregate footprint of electricity generation technologies in the european union \(eu\): A system of systems approach](#), *Resources, Conservation and Recycling* 143 (2019) 282–290. doi:10.1016/j.resconrec.2018.12.010.
URL <https://www.sciencedirect.com/science/article/pii/S0921344918304658>
- [33] P. Ruiz, W. Nijs, D. Tarvydas, A. Sgobbi, A. Zucker, R. Pilli, R. Jonsson, A. Camia, C. Thiel, C. Hoyer-Klick, F. Dalla Longa, T. Kober, J. Badger, P. Volker, B. S. Elbersen, A. Brosowski, D. Thrän, [Enspreso - an](#)

- open, eu-28 wide, transparent and coherent database of wind, solar and biomass energy potentials, *Energy Strategy Reviews* 26 (2019) 100379. doi:10.1016/j.esr.2019.100379.
URL <https://www.sciencedirect.com/science/article/pii/S2211467X19300720>
- [34] C. Mikovits, T. Schauppenlehner, P. Scherhauser, J. Schmidt, L. Schmalzl, V. Dworzak, N. Hampl, R. G. Sposato, *A spatially highly resolved ground mounted and rooftop potential analysis for photovoltaics in Austria*, *ISPRS International Journal of Geo-Information* 10 (6) (2021) 418. doi:10.3390/ijgi10060418.
URL <https://www.mdpi.com/2220-9964/10/6/418/html#B7-ijgi-10-00418>
- [35] T. Bründlinger, J. E. König, O. Frank, D. Gründig, C. Jugel, P. Kraft, O. Krieger, S. Mischinger, P. Prein, H. Seidl, et al., *dena-leitstudie integrierte energiewende: Impulse für die Gestaltung des Energiesystems bis 2050*, Deutsche Energie-Agentur GmbH (dena), ewi Energy Research & Scenarios gGmbH: Berlin/Köln, Germany (2018).
- [36] N. Szarka, V. Lenz, D. Thrän, *The crucial role of biomass-based heat in a climate-friendly Germany—a scenario analysis*, *Energy* 186 (2019) 115859. doi:10.1016/j.energy.2019.115859.
URL <https://www.sciencedirect.com/science/article/pii/S0360544219315312>
- [37] N. D. Jablonowski, S. D. Schrey, *Bioenergy crops: Current status and future prospects*, *Agronomy* 11 (2) (2021) 316. doi:10.3390/agronomy11020316.
URL <https://www.mdpi.com/2073-4395/11/2/316/html>
- [38] N. Scarlat, J.-F. Dallemand, M. Banja, *Possible impact of 2020 bioenergy targets on European Union land use. A scenario-based assessment from national renewable energy action plans proposals*, *Renewable and Sustainable Energy Reviews* 18 (2013) 595–606. doi:https://doi.org/10.1016/j.rser.2012.10.040.
URL <https://www.sciencedirect.com/science/article/pii/S1364032112005916>
- [39] K. Meisel, M. Millinger, K. Naumann, F. Müller-Langer, S. Majer, D. Thrän, *Future renewable fuel mixes in transport in Germany under Red II and climate protection targets*, *Energies* 13 (7) (2020) 1712. doi:10.3390/



en13071712.

URL <https://www.mdpi.com/1996-1073/13/7/1712>

- [40] BMVI, Räumlich differenzierte Flächenpotentiale für erneuerbare Energien in Deutschland, BMVI-Online-Publikation, Federal Ministry of Transport and Digital Infrastructure, Berlin, https://www.bbsr.bund.de/BBSR/DE/veroeffentlichungen/ministerien/bmvi/bmvi-online/2015/BMVI_Online_08_15.html (Aug. 2015).
- [41] Ministerium für Umwelt, Klima und Energiewirtschaft Baden-Württemberg, [Freiflächensolaranlagen: Handlungsleitfaden](https://um.baden-wuerttemberg.de/fileadmin/redaktion/m-um/intern/Dateien/Dokumente/2_Presse_und_Service/Publikationen/Energie/Handlungsleitfaden_Freiflaechensolaranlagen.pdf), URL https://um.baden-wuerttemberg.de/fileadmin/redaktion/m-um/intern/Dateien/Dokumente/2_Presse_und_Service/Publikationen/Energie/Handlungsleitfaden_Freiflaechensolaranlagen.pdf
- [42] H. Wirth, Aktuelle Fakten zur Photovoltaik in Deutschland, Tech. rep., Fraunhofer ISE, <https://www.ise.fraunhofer.de/de/veroeffentlichungen/studien/aktuelle-fakten-zur-photovoltaik-in-deutschland.html> (May 2021).
- [43] BUND, NABU, Positionspapier zur Solarenergie von BUND und NABU, Tech. rep., <https://www.bund-bawue.de/service/publikationen/detail/publication/positionspapier-zur-solarenergie-von-bund-und-nabu/> (Jul. 2021).
- [44] A. Suardi, S. Bergonzoli, V. Alfano, A. Scarfone, L. Pari, [Economic distance to gather agricultural residues from the field to the integrated biomass logistic centre: A spanish case-study](https://doi.org/10.3390/en12163086), *Energies* 12 (16) (2019) 3086. doi: [10.3390/en12163086](https://doi.org/10.3390/en12163086). URL <https://www.mdpi.com/1996-1073/12/16/3086>
- [45] Y. Zhang, C. Qin, Y. Liu, [Effects of population density of a village and town system on the transportation cost for a biomass combined heat and power plant](https://doi.org/10.1016/j.jenvman.2018.06.071), *Journal of environmental management* 223 (2018) 444–451. doi: [10.1016/j.jenvman.2018.06.071](https://doi.org/10.1016/j.jenvman.2018.06.071). URL <https://www.sciencedirect.com/science/article/pii/S0301479718307230>
- [46] A. Mattioli, D. Boscaro, F. Dalla Venezia, F. Correale Santacroce, A. Pezuolo, L. Sartori, D. Bolzonella, Biogas from residual grass: A territorial approach for sustainable bioenergy production, *Waste and biomass valorization* 8 (8) (2017) 2747–2756.

-
- [47] A. Endo, M. Yamada, Y. Miyashita, R. Sugimoto, A. Ishii, J. Nishijima, M. Fujii, T. Kato, H. Hamamoto, M. Kimura, T. Kumazawa, J. Qi, [Dynamics of water–energy–food nexus methodology, methods, and tools](#), *Current Opinion in Environmental Science & Health* 13 (2020) 46–60. doi:10.1016/j.coesh.2019.10.004. URL <https://www.sciencedirect.com/science/article/pii/S246858441930056X>
- [48] L. Yung, E. Louder, L. A. Gallagher, K. Jones, C. Wyborn, [How methods for navigating uncertainty connect science and policy at the water-energy-food nexus](#), *Frontiers in Environmental Science* 7 (2019) 37. doi:10.3389/fenvs.2019.00037. URL <https://www.frontiersin.org/articles/10.3389/fenvs.2019.00037/full>
- [49] M. Kurian, [The water-energy-food nexus: Trade-offs, thresholds and transdisciplinary approaches to sustainable development](#), *Environmental Science & Policy* 68 (2017) 97–106. doi:10.1016/j.envsci.2016.11.006. URL <https://www.sciencedirect.com/science/article/pii/S1462901116305184>
- [50] M.-C. Hu, C. Fan, T. Huang, C.-F. Wang, Y.-H. Chen, [Urban metabolic analysis of a food-water-energy system for sustainable resources management](#), *International Journal of Environmental Research and Public Health* 16 (1) (2019) 90. doi:10.3390/ijerph16010090. URL <https://www.mdpi.com/1660-4601/16/1/90/htm>
- [51] A. Purwanto, J. Sušnik, F. X. Suryadi, C. de Fraiture, [Water-energy-food nexus: Critical review, practical applications, and prospects for future research](#), *Sustainability* 13 (4) (2021) 1919. doi:10.3390/su13041919. URL <https://www.mdpi.com/2071-1050/13/4/1919/htm>
- [52] F. Abass, L. H. Ismail, I. A. Wahab, A. A. Elgadi, [A review of green roof: Definition, history, evolution and functions](#), *IOP Conference Series: Materials Science and Engineering* 713 (1) (2020) 012048. doi:10.1088/1757-899X/713/1/012048. URL https://iopscience.iop.org/article/10.1088/1757-899X/713/1/012048/meta#fnref-MSE_713_1_012048bib9
- [53] L. Rodríguez, E. Duminil, J. Sánchez Ramos, U. Eicker, [Assessment of the photovoltaic potential at urban level based on 3d city models: A case study and new methodological approach](#), *Solar Energy* 146 (2017) 264–275. doi:10.1016/j.solener.2017.02.043.

-
- URL <https://www.sciencedirect.com/science/article/pii/S0038092X17301445>
- [54] M. Zirak, V. Weiler, M. Hein, U. Eicker, [Urban models enrichment for energy applications: Challenges in energy simulation using different data sources for building age information](#), *Energy* 190 (2020) 116292. doi:10.1016/j.energy.2019.116292.
URL <https://www.sciencedirect.com/science/article/pii/S0360544219319875>
- [55] S. Köhler, M. Betz, U. Eicker (Eds.), *Stochastic Generation of Household Electricity Load Profiles in 15-minute Resolution on Building Level for Whole City Quarters*, 2019.
- [56] V. Weiler, H. Harter, U. Eicker, [Life cycle assessment of buildings and city quarters comparing demolition and reconstruction with refurbishment](#), *Energy and Buildings* 134 (2017) 319–328. doi:10.1016/j.enbuild.2016.11.004.
URL <https://www.sciencedirect.com/science/article/pii/S0378778816314141>
- [57] DESTATIS, *Daten aus dem Gemeindeverzeichnis: Kreisfreie Städte und Landkreise nach Fläche, Bevölkerung und Bevölkerungsdichte am 31.12.2020*, <https://www.destatis.de/DE/Themen/Laender-Regionen/Regionales/Gemeindeverzeichnis/Administrativ/04-kreise.html>, (Accessed: 2021-09-19) (Sep. 2021).
- [58] Federal and state statistical offices, *Regionaldatenbank Deutschland: Bodenfläche nach Art der tatsächlichen Nutzung - Kreise und kreisfreie Städte (Stichtag 31.12.2015)*, <https://www.regionalstatistik.de/genesis/online?operation=abruftabelleBearbeiten&levelindex=1&levelid=1632081112969&auswahloperation=abruftabelleAuspraegungAuswaehlen&auswahlverzeichnis=ordnungsstruktur&auswahlziel=werteabruf&code=33111-01-01-4&auswahltext=&werteabruf=Werteabruf#abreadcrumb>, (Accessed: 2021-09-19) (Sep. 2021).
- [59] G. Grassl, C. Blach, U. Eicker, V. Coors, N. Bartke, M. Müller, S. Roth, D. Schreyer, A. Wenninger, M. Herrmann, S. Weyland, F. Gericke, S. Anker, E. Klenert, *Landkreis Ludwigsburg - Integriertes Klimaschutzkonzept. Abschlussbericht Band 1*, Tech. rep. (Oct. 2015).

-
- [60] EUT, Klimaschutzprogramm Ilm-Kreis 2005-2015, Tech. rep., Energie- und Umweltpark Thüringen e.V. (2013).
- [61] R. Bottenbruch, E. Wamboldt, L. Winter, M. Pöhler, M. Wangelin, Integriertes Klimaschutzkonzept für den Kreis Dithmarschen, Tech. rep. (2013).
- [62] F. Humpenöder, A. Popp, B. L. Bodirsky, I. Weindl, A. Biewald, H. Lotze-Campen, J. P. Dietrich, Klein. David, U. Kreidenweis, C. Müller, S. Rolinski, M. Stevanovic, [Large-scale bioenergy production: how to resolve sustainability trade-offs?](#), *Environmental Research Letters* 13 (2) (2018) 024011. doi:10.1088/1748-9326/aa9e3b.
URL <https://iopscience.iop.org/article/10.1088/1748-9326/aa9e3b>
- [63] A. Sadowski, A. Baer-Nawrocka, [Food self-sufficiency of the european union countries - energetic approach](#), *Journal of Agribusiness and Rural Development* 40 (2) (2016) 407–414. doi:10.17306/JARD.2016.44.
URL <http://ww1.up.poznan.pl/jard/index.php/jard/article/view/255>
- [64] K. Bao, R. Padsala, V. Coors, D. Thrän, B. Schröter, [A gis-based simulation method for regional food potential and demand](#), *Land* 10 (8) (2021) 880. doi:10.3390/land10080880.
URL <https://www.mdpi.com/2073-445X/10/8/880>
- [65] V. Dornburg, A. P. Faaij, [Efficiency and economy of wood-fired biomass energy systems in relation to scale regarding heat and power generation using combustion and gasification technologies](#), *Biomass and Bioenergy* 21 (2) (2001) 91–108. doi:10.1016/S0961-9534(01)00030-7.
URL <https://www.sciencedirect.com/science/article/pii/S0961953401000307>
- [66] FNR, [Bioenergy in germany: Facts and figures 2020](#).
URL https://www.fnr.de/fileadmin/allgemein/pdf/broschueren/broschuere_basisdaten_bioenergie_2020_engl_web.pdf

Contribution to Appended Papers

The authors' contribution to the work reported in the appended papers were as follows:

- I **Bao, K.;** Padsala, R.; Coors, V.; Thrän, D.; Schröter, B. *A Method for Assessing Regional Bioenergy Potentials Based on GIS Data and a Dynamic Yield Simulation Model*. *Energies* 2020, 13, 6488. <https://doi.org/10.3390/en13246488>

Bao, Schröter and Thrän developed the idea. Bao established the new workflow in Java, validated the workflow, defined scenarios, conducted simulation, and wrote the paper. Padsala created GIS input data model. Thrän and Schröter provided expert guidance and feedbacks on simulation principle, and reviewed the paper. Coors is the supervisor of Padsala.

- II **Bao, K.;** Padsala, R.; Thrän, D.; Schröter, B. *Urban Water Demand Simulation in Residential and Non-Residential Buildings Based on a CityGML Data Model*. *ISPRS Int. J. Geo-Inf.* 2020, 9, 642. <https://doi.org/10.3390/ijgi91106428>

Bao, Schröter and Thrän developed the idea. Bao established the new workflow in Java, validated the workflow, defined scenarios, conducted simulation, and wrote the paper. Padsala adapted GIS data in the case study regions and visualized the results. Thrän and Schröter provided expert guidance and feedbacks, and reviewed the paper.

- III **Bao, K.;** Thrän, D.; Schröter, B. *Simulation and Analysis of Urban Green Roofs with Photovoltaic in the Framework of Water-Energy Nexus*. *Proceedings of REAL CORP 2021, 26th International Conference on Urban Development, Regional Planning and Information Society*. 2021, pp. 671-680. ISSN 2521-3938

Bao, Schröter and Thrän developed the idea. Bao extended workflow, validated the workflow, defined scenarios, conducted simulation, and wrote the paper. Thrän and Schröter provided expert guidance and feedbacks, and reviewed the paper.

Contribution to Appended Papers

- IV **Bao, K.;** Padsala, R.; Coors, V.; Thrän, D.; Schröter, B. *A GIS-Based Simulation Method for Regional Food Potential and Demand*. Land 2021, 10, 880. <https://doi.org/10.3390/land10080880>

Bao, Schröter and Thrän developed the idea. Bao established workflow in Java and Python, validated the workflow, defined scenarios, conducted simulation, visualized the results, and wrote the paper. Thrän and Schröter provided expert guidance and feedbacks, and reviewed the paper. Padsala created GIS input data model. Coors is the supervisor of Padsala.

- V **Bao, K.;** Kalisch, L.; Santhanavanich, T.; Thrän, D.; Schröter, B. *A bottom-up GIS-based method for simulation of ground-mounted PV potentials at regional scale*. Energy Reports 2022, 8, 5053. <https://doi.org/10.1016/j.egy.2022.03.187>

Bao, Schröter, Kalisch developed the idea. Bao established workflow in Python, conducted the simulation, visualized the results. Bao and Kalisch together validated the workflow, defined scenarios, and wrote the paper. Thrän and Schröter provided expert guidance and feedbacks, and reviewed the paper. Santhanavanich created GIS input data model.

- VI **Bao, K.;** Thrän, D.; Schröter, B. *Land Resource Allocation between Biomass and Ground-Mounted PV under consideration of the Food-Water-Energy Nexus Framework at Regional Scale*. Submitted to Renewable Energy. 2022.

Bao, Schröter and Thrän developed the idea. Bao integrated existing workflows, validated the workflow, defined scenarios, conducted the simulation, visualized the results, and wrote the paper. Thrän and Schröter provided expert guidance and feedbacks, and reviewed the paper.

- VII **Bao, K.;** Padsala, R.; Coors, V.; Thrän, D.; Schröter, B. *GIS-Based Assessment of Regional Biomass Potentials at the Example of Two Counties in Germany*. Proceedings of 28th European Biomass Conference and Exhibition. 2020, pp 77-85. DOI: 10.5071/28thEUBCE2020-1CV.4.15

Bao, Schröter and Thrän developed the idea. Bao established the new workflow in Java, conducted the simulation, validated the workflow, defined scenarios, conducted simulation, and wrote the paper. Padsala created GIS input data model and visualized the results. Thrän and Schröter provided expert guidance and feedbacks, and reviewed the paper. Coors is the supervisor of Padsala.

- VIII **Bao, K.;** Schröter, B. *SimStadt*. In *Urbane Energiesysteme und Ressourceneffizienz – ENsource*; Coors, V. Eds.; Fraunhofer Verlag: Stuttgart, 2021; pp 15-21.

Bao and Schröter wrote the book chapter together.

- IX Pietzsch, U.; **Bao, K.**; Padsala, R.; Gebetsroither-Geringer, E.; Smetschka, B.; Raven, J.; Coors, V. *Stakeholder-supported Research on the Food-Water-Energy Nexus with three International Case Studies*. Proceedings of REAL CORP 2021, 26th International Conference on Urban Development, Regional Planning and Information Society. 2021, pp. 1225-1231. ISSN 2521-3938

Pietzsch, Bao and Padsala wrote most the paper on the project. Gebetsroither-Geringer, Smetschka, Raven and Coors extended and reviewed the paper.

- X Padsala, R.; Gebetsroither-Geringer, E.; **Bao, K.**; Coors, V. *The Application of CityGML Food Water Energy ADE to Estimate the Biomass Potential for a Land Use Scenario*. Proceedings of REAL CORP 2021, 26th International Conference on Urban Development, Regional Planning and Information Society. 2021, pp. 851-861. ISSN 2521-3938

Padsala developed the idea and shared data model. Gebetsroither-Geringer simulated the land-use change in the future. Bao extended the biomass workflow to adapt Vienna case study. Padsala, Gebetsroither-Geringer and Bao wrote the paper together. Coors provided technical guidance to Padsala and reviewed the paper.

- XI **Bao, K.**; Bieber, L.; Kürpick, S.; Radanielina, M.H.; Padsala, R.; Thrän, D.; Schröter, B. *Bottom-Up Assessment of Local Agriculture, Forestry and Urban Waste Potentials Towards Energy Autonomy of Isolated Regions: Example of La Réunion*. *Energy for Sustainable Development* 2022, 66, 125. DOI: 10.1016/j.esd.2021.12.002

Bao, Bieber, Kürpick, Radanielina and Schröter developed the idea. Bao extended the biomass workflow to adapt La Réunion case study, run the simulation and visualized the results. Bieber and Kürpick collected and process the data. Bieber, Kürpick, Bao and Schröter defined the scenario. Bieber, Kürpick and Bao analysed the results and wrote the paper. Radanielina provided guidance on local urban waste potential data. Thrän and Schröter provided expert guidance and feedbacks, and reviewed the paper.

Curriculum Vitae

Keyu Bao

Born: 19.06.1993

Nationality: PR China with permanent residency in Germany

Experience

Since 03.2021	Helmholtz-Zentrum für Umweltforschung, Leipzig Guest researcher
Since 01.2020	Hochschule für Technik Stuttgart, Stuttgart Helmholtz-Zentrum für Umweltforschung, Leipzig Universität Leipzig Doctoral candidate
Since 06.2019	Hochschule für Technik Stuttgart, Stuttgart Research assistant
11.2018 – 05.2019	Fraunhofer-Institut für Solare Energiesysteme, Freiburg Research assistant
03.2018 – 10.2018	Fraunhofer-Institut für Solare Energiesysteme, Freiburg Master thesis 'System Simulation and Efficiency Improvement Strategies of a Home PV-Battery System'
11.2017 – 03.2018	Albert-Ludwigs-Universität Freiburg Student assistant
08.2017 – 10.2017	TÜV SÜD Battery Testing, München Internship
03.2017 – 04.2017	TÜV SÜD Battery Testing, München Internship

Curriculum Vitae

Education

Since 03.2020	University of Leipzig PhD: Sustainable Development
10.2016 – 10.2018	Albert-Ludwigs-Universität Freiburg Master of Science: Renewable Energy Engineering and Management
07.2016	St.Petersburg Polytechnic University Summer school, Sustainable Civil Engineering
10.2014 – 02.2015	Technische Universität München Exchange semester
09.2012 – 07.2016	Harbin Institute of Technology Bachelor of Engineering: Energy Engineering, Building Environment and Facility Engineering

Stuttgart, 8 April 2022



Keyu Bao

Part II

Appended papers

Chapter 1

A Method for Assessing Regional Bioenergy Potentials Based on GIS Data and a Dynamic Yield Simulation Model.

Bao, K.; Padsala, R.; Coors, V.; Thrän, D.; Schröter, B.

Energies 2020, 13, 6488. <https://doi.org/10.3390/en13246488>

Article

A Method for Assessing Regional Bioenergy Potentials Based on GIS Data and a Dynamic Yield Simulation Model

Keyu Bao ^{1,*}, Rushikesh Padsala ² , Volker Coors ², Daniela Thraen ^{3,4,5} and Bastian Schröter ¹ 

¹ Center for Sustainable Energy Technology, Hochschule für Technik Stuttgart, Schellingstraße 24, D-70174 Stuttgart, Germany; bastian.schroeter@hft-stuttgart.de

² Center for Geodesy and Geoinformatics, Hochschule für Technik Stuttgart, Schellingstraße 24, D-70174 Stuttgart, Germany; rushikesh.padsala@hft-stuttgart.de (R.P.); volker.coors@hft-stuttgart.de (V.C.)

³ Department of Bioenergy, Helmholtz Center for Environmental Research, Torgauer Strasse 116, D-04247 Leipzig, Germany; daniela.thraen@ufz.de or thraen@wifa.uni-leipzig.de or daniela.thraen@dbfz.de

⁴ Chair of Bioenergy System, Faculty of Economic Sciences, University of Leipzig, Grimmaische Straße 12, D-04109 Leipzig, Germany

⁵ Unit Bioenergy System, Deutsches Biomasseforschungszentrum GmbH, Torgauer Strasse 116, D-04347 Leipzig, Germany

* Correspondence: keyu.bao@hft-stuttgart.de

Received: 16 November 2020; Accepted: 2 December 2020; Published: 8 December 2020



Abstract: The assessment of regional bioenergy potentials from different types of natural land cover is an integral part of simulation tools that aim to assess local renewable energy systems. This work introduces a new workflow, which evaluates regional bioenergy potentials and its impact on water demand based on geographical information system (GIS)-based land use data, satellite maps on local crop types and soil types, and conversion factors from biomass to bioenergy. The actual annual biomass yield of crops is assessed through an automated process considering the factors of local climate, crop type, soil, and irrigation. The crop biomass yields are validated with historic statistical data, with deviation less than 7% in most cases. Additionally, the resulting bioenergy potentials yield between 10.7 and 12.0 GWh/ha compared with 13.3 GWh/ha from other studies. The potential contribution from bioenergy on the energy demand were investigated in the two case studies, representing the agricultural-dominant rural area in North Germany and suburban region in South Germany: Simulation of the future bioenergy potential for 2050 shows only smaller effects from climate change (less than 4%) and irrigation (below 3%), but the potential to cover up to 21% of the transport fuels demand in scenario supporting biodiesel and bioethanol for transportation.

Keywords: potential analysis; geographical information system (GIS); bioenergy; AquaCrop

1. Introduction

Although the metabolism of industrial societies strongly relies on minerals and fossilized biomass, annually harvested biomass from vegetation contributes about 10% to primary energy use in the European Union [1]. Biomass can be derived from different resources, e.g., agricultural land or forest, and transferred into different forms of bioenergy, e.g., biogas, liquid, and solid fuel. In decentralized and renewable energy systems, bioenergy can play important roles in fueling the parts of the transport sector that cannot be easily electrified, or in securing controllable electricity supply that can counteract fluctuations of intermittent wind and photovoltaic power sources [2]. It is therefore important to assess regional biomass potentials and to understand the possible variables that might influence the potential in order to help local governments and planning authorities to make informed choices regarding

the potentials and trade-offs between different renewable energy sources (RESs) on a strategic level, especially improve understanding of future energy supply systems with high shares of renewables. The resource focused assessment is adapted in this paper, which takes the form of inventories of potential bioenergy sources, with an evaluation of possibilities to utilize the sources for energy purpose [3]. The method thus needs to be reasonably accurate in the context of local energy systems and build upon a similar data structure as the methods already implemented, such as assessments of rooftop photovoltaic (PV) potentials [4] or the energy demand for heating on the city quarter level [5], but it does not need to be able to compete with specialized tools that focus for example solely on assessing local potentials of one RES.

Biomass potential assessments so far are widely used for either specific types of land use and biomass, e.g., forests [6], or highly aggregated scenarios, since their focus lies on providing data on a national or supranational level [7]. For the first, e.g., D. Lauka et al. introduced a model that is able to assess low-quality biomass resources, e.g., solid fuel directly for burning, and potential, but without taking biogas or bioethanol potentials into account [8], while the technical potential for power production from forest biomass was assessed in [6]. For the second, biomass potentials in various scenarios on a national level are evaluated for example in [7].

Moreover, methods based on GIS are widely applied to assess biomass potentials [9–12]. Ref. [9,10] both focus on residue potential; [11] analyzed forest biomass potential; and [12] assesses the suitable power plant location based on biomass potential. They typically overlay various layers of data (such as forest, agriculture, urban, slope, and road) in order to define suitable areas with biomass potentials. However, typically only a statistical crop distribution is applied to aggregated feasible lands because of a lack of crop distribution maps. Those methods are thus limited in their degree of accuracy and simplicity.

To the authors' knowledge, there are a lack of models that combine biomass potential assessments with other RES sources, most importantly solar photovoltaics and wind, on the regional level in one aggregated modeling and simulation environment. Such an approach is of great benefit if the goal is to assess local synergies, potential conflicts, economic merit orders, or summed potentials of RES sources and contrast these with local demands.

This paper introduces a newly established bioenergy assessment method that fills this gap. The accuracy of the method is brought by applying (i) high-resolution soil and crop distribution GIS maps. (Section 2.1) (ii) Dynamic yield simulation model that takes environmental factors, crop species, and soil texture into consideration (Sections 2.2 and 2.3). This workflow adapts the resource-focused assessments (Section 2.4), which take the form of inventories of potential bioenergy sources, with an evaluation of possibilities to utilize the sources for energy purposes. The versatility of this method is brought by extending an existing local energy system simulation platform that can assess heat and power demands in residential areas [13] and rooftop photovoltaic potentials [14] on a single-building level (Section 2.5). The method is validated through the examples of three counties with different land cover characteristics in Germany (Section 2.6). Scenarios concerning climate change, transportation fuel, and irrigation are illustrated demonstrating the possible applications of the method (Sections 2.7 and 2.8). As followed, the results of scenarios analysis are summarized in Section 3. Section 4 discusses the result and the advantage and limitation of the method. In the end Section 5 conclude the novelty of the method as a feasible tool for regional bioenergy analysis under the framework of Food-Water-Energy (FWE) nexus.

2. Materials and Methods

2.1. Input Data

The primary input data for the newly established workflow consists of the digital landscape model (DLM) data in the shapefile data format provided by Germany's Official Real Property Cadastre Information System (ALKIS) [15]. ALKIS was developed by the Working Group of the Surveying

Authorities of the sixteen states of Germany (AdV). The DLM map consists of several object layers, including buildings, water bodies, vegetation, transportation, etc. Since the land area dedicated to transportation is stored as line geometry, a buffer with road width is created in the transportation layer and overlapped with the vegetation layer. The intersected part of the vegetation layer is cropped out to avoid its inflation. For each polygon in the vegetation layer of the DLM map information on vegetation land use type, land area in meter and polygon boundary coordinates were included. DLM data is derived from the topographic map with a resolution of 1:10,000/1:25,000 and for linear features resolution of ± 3 m.

DLM data accurately indicate the boundary and land use of each polygon. However, the specific crop type for agricultural polygons is missing. To fill this gap, the DLM data was combined with satellite data on crop types from [16]. There, Griffiths et al. derive a map of crop types and land cover from satellite data, and compare their results to agricultural reference data from three (German) states and to the results of a national agricultural census. The resulting raster map captured the crop type distribution across Germany at 30 m resolution and achieved 81% overall accuracy for 12 classes in the three states. For several crops, notably cereals, maize, and rapeseed, mapped acreages compared very well with the official census data, with differences of 11%, 2%, and 3%, respectively. Other classes (grapevine and forest classes) performed less well, likely because the available reference data did not fully capture the variability of these classes across Germany. The land use and crop types differentiated in [16] are shown in Table 1.

Table 1. Land use and crop category used in this study. Data adapted from [15,16].

Crop Type Only Specified in Satellite Map	Crop Type Specified in Both DLM and Satellite Map	Crop Type Only Specified DLM Map
Winter cereals	Grassland	Short Rotation Coppice
Spring cereals	Grapevine	Fruit orchard
Maize	Deciduous mix forest	Fruit orchard in grassland
Winter rapeseed	Coniferous forest	Fruit orchard in farming land
Sugar beet	Built-up	Grove
Potato	Water	

Conflicts between maps from different sources are common, since they were derived with different methods and were based on different primary sources. Generally, the DLM data has a high level of accuracy and reliability in terms of overall land use type, e.g., farming land, vineyard, or built-up area, when compared with satellite data, e.g., from Google Maps. Therefore, the polygons from this source serve as the basic unit when merging the two sources [15]. In the case of a conflict regarding overall land use, DLM data is prioritized. Crop information [16] is then attached to each DLM polygon as an additional attribute. In case multiple crop types from [16] exist on the same DLM polygon, which for agricultural land mostly refers to individual fields, the land use type with the largest area share is assigned to this polygon. Generally, only areas classified as agricultural in the DLM map are attached with additional crop type information from [16].

Plant–soil relationships in the surface soil layer affect crop productivity [17]. For example, yields of *Miscanthus* range from 5 to 13 t/(ha a) on poor soil or marginal land, while from 7 to 44 t/(ha a) on arable land with higher-quality soils [18]. Therefore, local soil types should be considered to achieve a more accurate biomass or bioenergy yield simulation. For this, a map showing the distribution of typical soil types (soil texture) in the top soils of Germany (resolution 1:100,000) from the Federal Institute for Geosciences and Natural Resources [19] was overlaid with the enriched DLM map. Considering the large heterogeneity in the data and the resulting uncertainty in the precision for a given site, the depiction of the obtained soil texture is presented at the level of the soil types group, according to the German soil classification system (KA5) [19] and as shown in Appendix A.

Figure 1 shows the original DLM, crop data, soil data, and the superimposed data at the example of the city of Marbach, Ludwigsburg county, in the south-western state of Baden-Württemberg. It is

transformed into the open CityGML data format [20], in order to use the combined map data within the structure of our existing modeling environment [21].

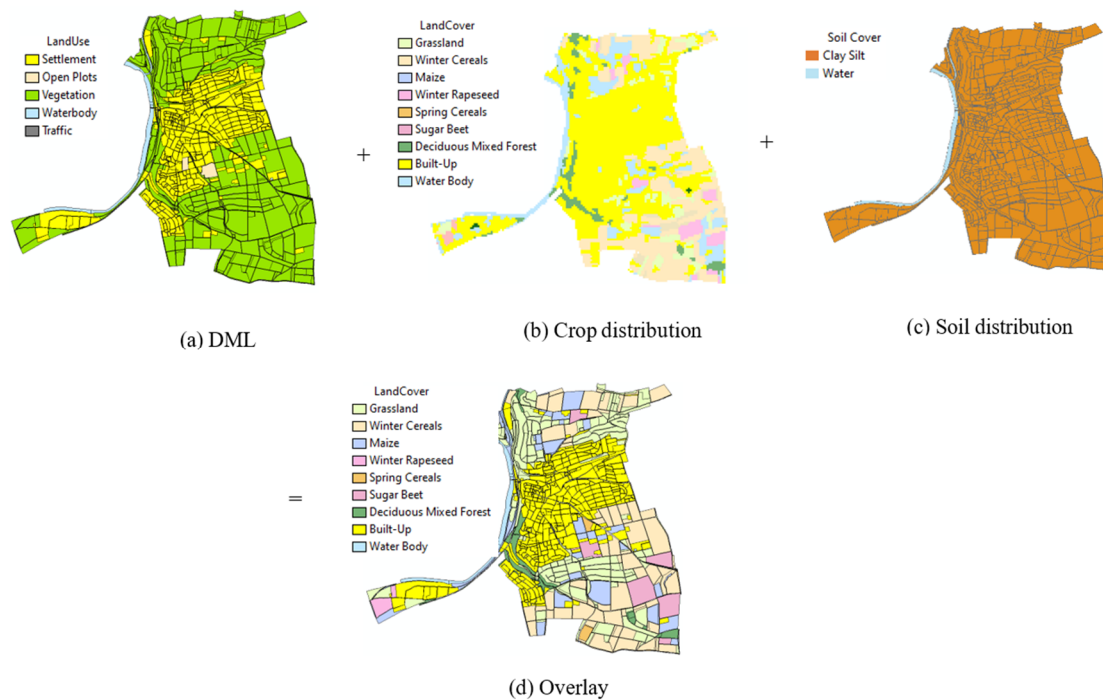


Figure 1. Set of input and resulting maps for Marbach, Ludwigsburg county, Baden-Württemberg. (a) Digital landscape model (DLM) map in polygons with land use; (b) satellite map in raster with crop type; (c) soil map; and (d) overlay of (a) and (b).

The accuracy of the thus created CityGML data set was validated by comparing it to statistical data for Ludwigsburg county. The county's total land area, classified into the main forms of land use, was compared with the total land area from the state's 2018 land use report [22]. As Table 2 shows, the total area dedicated to agriculture and forest differed by only 3.2%, and the farming area by less than 7%. Grassland and garden areas show larger differences between, with possible reasons being (i) that the DLM dataset only counted polygons with areas of more than one hectare, with smaller fields not included in the dataset in the first place and (ii) that the DLM dataset contained more categories than the state land use report. For instance, orchard meadows, tree nurseries, and fruit plantations are part of the created GML map, but not the land use report. Since orchard meadow could for example be regarded as grassland with fruit trees, combining both categories yield a sum (8210 ha) that is closer to the grass land area from the land use report (7967 ha). Similarly, adding nurseries and fruit plantations to the garden category reduced this initial difference.

2.2. Assessment Method for Local Biomass Potential

Biomass potentials can be distinguished between theoretical, technical, economic, exploitable, and sustainable potentials.

The theoretical potential describes the potential that exists in a given region within a certain time period of physically usable energy supply, e.g., the energy stored in the entire plant mass. It is determined by physical limits and marks the upper limit of bioenergy's theoretically realizable contribution to energy supply. Due to insurmountable technical, ecological, economic, and administrative barriers, this potential can generally only be tapped to a limited extent. It therefore has no practical relevance for assessing the actual usability of biomass [23].

The technical potential describes that part of the theoretical potential that can be used after taking into account technical restrictions, e.g., salvage rate, storage losses, and conversion losses.

In addition, existing structural and ecological restrictions and other legal requirements and possible social restrictions are taken into account, as they represent barriers to the use of bioenergy similar to technically induced restrictions [23]. In the following, the technical bioenergy potential is the potential after processing (e.g., pelletizing, pyrolysis, and methanization) in the form of secondary energy carriers (biomethane, biodiesel, bioethanol, and burning fuel) or primary energy carriers (energy wood and residues) destined for combustion.

Table 2. Ludwigsburg county: comparison of the summed value of land area in the created CityGML file and in the state’s 2018 land use report. Statistical land area data is adapted from [22].

		Area, Land Use Report [22]	Area, GML Map	Difference
		(ha)	(ha)	(%)
Agriculture		37,704	36,493	3.2
	Farming	26,990	25,150	6.8
	Grass	7967	3417	57.1
	Orchard meadow	-	4793	-
	Sum of grass and orchard meadow	7967	8210	3.1
Of which	Garden	549	234	57.4
	Tree nursery	-	137	-
	Fruit plantation	-	467	-
	Vineyard	2198	2292	4.3
	Brown land	0	0	0.0
Forest		12,362	11,997	3.0

In order to calculate the biomass yield considering climate, soil situation, land management, and irrigation patterns, an external crop yield and water demand model, AquaCrop, was integrated into our energy simulation environment (see also the next section). The amount of biomass produced over the course of a growing season on a given area is given as one of the outputs of AquaCrop, which can be considered as the yield of the crop and starting point for assessing bioenergy potentials [24]. By applying conversion factors to theoretical and technical energy yields, the energy potential at these two levels can be calculated and given as the output of the energy simulation model.

It has to be noted that the dynamic yield modeling only applies to field crops, grass, and short rotation coppice, while not to forests and fruit plantations, as the AquaCrop’s model does not apply to tree-based biomass creation. Moreover, woody biomass as residue is collected only under the situations of the clearing of fields and of irregular intervals, when trees are felled because of excessive age, diseases, and/or storm damage [23]. The woody biomass from these sources is accumulated through several years. In this paper harvesting of energy crops were simulated at the annual base. Therefore, in this simulation the yield of vineyard, bushes, fruit plantation, and orchard meadow have the static raw biomass yield from the literature [23]. The potentials calculated in this paper as well as their calculation methods are summarized in Table 3.

2.3. Dynamic Yield Model

AquaCrop is a model that describes the interactions between the plant, atmospheric factors, and the soil. From the root zone, the plant extracts water and nutrients. Calculation scheme of AquaCrop is affected by water stress and temperature stress [24]. The accumulation of biomass and transpiration of crop are influenced by crop type, atmospheric temperature, rainfall, irradiation, CO₂ concentration, irrigation, ground water level, and fertilization. In this study the ground water level and fertilization are not included in the yield model. With the help of the dynamic yield model a more accurate biomass yield can be retrieved for the further simulation. The local climate, soil texture, or even irrigation can result in very different yield values than the typical statistical values.

The aim of the new bioenergy potential workflow is to extract the amount of above-ground biomass indicated, which is the starting point for further bioenergy conversion processes. The biomass

produced is proportional to the cumulative amount of crop transpiration (ΣTr), with the biomass water productivity (WP) in dry mass as the proportionality factor. Normalization for climatic conditions yields normalized biomass water productivity (WP*), valid for diverse locations, seasons, and CO₂ concentrations [24]. Water in the soil that is easily extracted by the plant is called readily available water (RAW). Hereby, water stress is defined as the percentage of RAW in the root zone, with 0% meaning the soil water is at field capacity, which is ideal for crop growing, and 100% representing the threshold of stomatal closure.

Table 3. Calculation approach to biomass potentials for different crops and types of biomass.

Land Cover Type	Calculable Potentials			Method Used
	Theoretical	Technical, Excluding Residues	Technical Only, Including Residues	
Winter cereals	x	x	x	AquaCrop
Spring cereals	x	x	x	AquaCrop
Maize	x	x	x	AquaCrop
Winter rapeseed	x	x	x	AquaCrop
Sugar beet	x	x	x	AquaCrop
Potato	x	x	x	AquaCrop
Short Rotation Coppice (SRC)	x	x	x	AquaCrop
Grassland	x	x	x	AquaCrop
Grapevine			x	Static
Bushes and hedges			x	Static
Deciduous and mix forest	x			Static
Coniferous forest	x			Static
Built-up				
Water				
Fruit orchard			x	Static
Fruit orchard in grassland			x	Static
Fruit orchard in farming land			x	Static

2.4. Calculation of Bioenergy Potentials

The calculation of theoretical potential is required for the calculation of technical potentials in a next step. The theoretical energy potential of a certain form of biomass can be described by its heating value, multiplied with its dry mass production yield and its water content percentage, with production yields calculated by taking environmental factors including temperature, precipitation, irradiation, soil texture, and irrigation into account (as discussed in Section 3.3).

As explained in Section 3.2, the technical potential of crops and grass can be derived from the theoretical potential by applying conversion coefficients including conversion losses, and the percentage that are used for energetic purposes. As a first step, the distribution between energy and food is defined for specific crops. Secondly, for the part that is used energetically, in most cases more than one type of secondary (bio-)energy carrier can be obtained per crop, so the respective shares need to be determined. Thus, multiplying bioenergy conversion coefficients with the amount of available biomass allows one to calculate the technical potential of a certain crop in a certain form of bioenergy. Here, the solid bioenergy potential is set equal to the theoretical potential of any crop type. This process is pursued for each land field, each crop type, and each possible form of bioenergy. It has to be noted that the thus calculated technical potential is the potential of the crop used for energetic purposes only. Regardless of whether the crop is used for food purpose or energy purpose, its byproducts, e.g., grain straw or leaf mass, are always considered to have technical energy potential of residue.

Of the harvested forest wood, around 26% are utilized for an energetic purpose in Germany [25], making it an important contributor to local bioenergy potentials, especially in rural and mountainous regions. However, given that the growth of forest biomass is also dependent on other factors than soil, climate, and temperature, notably groundwater levels [26], it is much more difficult to model dynamically. Therefore, a static value for the annual technical potential of forest-based bioenergy (in the form of energy wood) is assumed in the following.

Similar to forest, we used literature values of the biomass yield potential of orchard, vineyard, and bushes/hedges. A limited share of the biomass from annual pruning in landscape conservation areas is used as solid residue, since its collection is often complex and expensive.

Finally, all formulas and related parameters for the calculation of biomass and bioenergy potentials for the most widely spread crops in Germany are given in Appendix B.

2.5. Simulation Environment and Interface

As mentioned earlier, the assessment of biomass potentials is to be included in an existing modeling environment in order to compare different RES potentials and contrast these with energetic demands in a given region (Figure 2). The modeling environment SimStadt developed at HFT Stuttgart allows one to assess electricity, cooling and heat demands, and renewable energy potentials (photovoltaic) on a single-building level using 3D city models (in the CityGML format [21]). SimStadt provides a modular workflow management for various, primarily energetic, system analysis purposes. Each workflow serves a specific purpose, e.g., heating demand of buildings or photovoltaic potential, while certain modules are shared between workflows, e.g., importing data or data preprocessing [27].

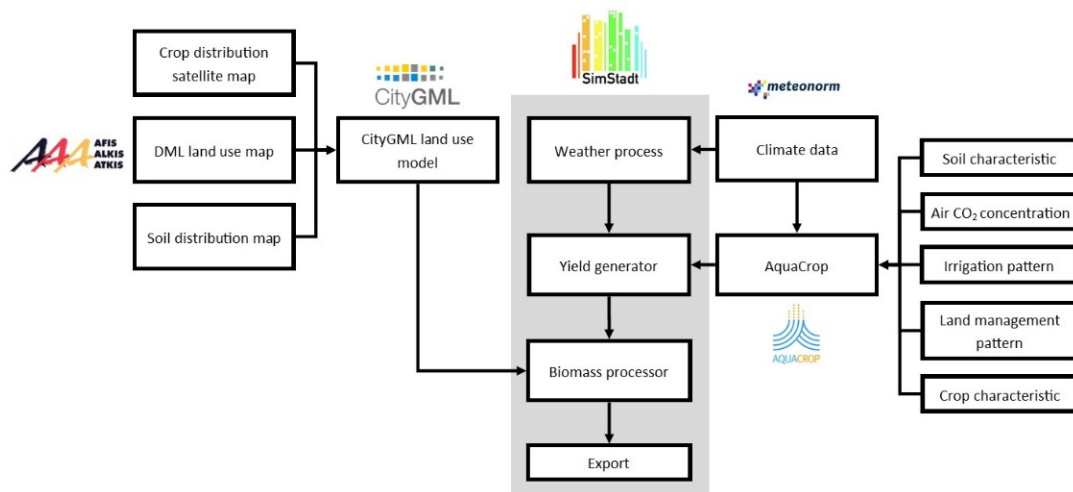


Figure 2. Flow chart of the newly established SimStadt bioenergy workflow.

For the newly established workflow on regional bioenergy potentials, most of the predefined modules are not applicable due to the fact that the input data is land use polygons instead of building geometries, the exception being the import module that can read CityGML files regardless of the type of objects (building or land use polygon) and the weather model that imports the meteorological data in TMY3 format generated by Meteororm for the specific region in hourly or monthly resolution. The meteorological data are stored in SimStadt and can be called in later steps.

To model bioenergy potentials more accurately than by using static values for all crops, a new module “YieldGenerator” was developed. Firstly, climate data, including daily precipitation and temperature data from the step “WeatherProcessor” is read, converted, and saved in a form that AquaCrop can process. Secondly, the crop reference evapotranspiration (ET_o) is determined from meteorological data, including latitude, longitude, altitude, temperature, relative humidity, wind speed, and cloud shading. The FAO Penman–Monteith method [28] was used for the computation of ET_o from meteorological data. These meteorological data were called and calculated according to the Penman–Monteith method on a daily basis over a whole year. Thirdly, irrigation patterns are assigned to crops. In this paper we were interested in the net water demand of a crop to determine the amount of potential irrigation required, on top of precipitation, in a given environment. Net irrigation requirement was calculated by adding a certain amount of water to the soil profile each day in case the local soil water content itself was not sufficient for a given crop type. Fourthly, project files for each crop on all

possible soil types in a given region were generated by the workflow, which serve as the main input to the AquaCrop model; all required crop parameters are listed in Appendix C. To limit the complexity of the model, we assumed the soil profile of each soil type was deep (>1.5 m) and uniform, regardless of the possibility that soils could have several layers with different characteristics. Fifthly, the AquaCrop Plug-In was called from SimStadt; as output, the annual biomass incremental yield in t/(ha a) and water demand, including potential irrigation demands, in millimeters of all crops on all soil types were stored in an XML configuration file extending other input settings, e.g., the conversion pathways to different bioenergy forms per relevant crop, static default biomass yields, or bioenergy conversion factors from raw biomass.

Another module, “BiomassProcessor” then processes all land use polygons. Users can modify parameters, such as the annual forest wood energetic use rate, the share of energy crops such as corn and rapeseed that are actually used for energetic purposes, or the grass land energy usage rate. The default variables values are shown in Appendix D where data are collected and adapted from [23,25,29–31]. Further input parameters can also be imported from an XML configuration file step. The module analyses each land field polygon, tagged with a certain type of vegetation and soil. Therefore, the module was able to find the corresponding biomass yield of the crop on the soil, the possible bioenergy usages and bioenergy conversion coefficient from the XML configuration file. It then calculated the corresponding technical bioenergy energy potential, with the output being exported to a CSV file.

2.6. Approach to Data Validation

The biomass yield results of AquaCrop for various crop and soil types were validated by comparison to statistical data. The biomass yield given by AquaCrop is the above-ground value in dry mass (DM), whereas statistical values are typically given in fresh mass, i.e., including average water contents [23,32] and thus requiring conversion into dry mass values. In SimStadt, yields were simulated for three German counties with different climate patterns, under no specific field management, no irrigation, and no shallow ground water available.

The county of Ludwigsburg is located in the centre of Baden-Württemberg, in Germany’s south-western corner. It covers an area of 687 km², with a population of about 550,000 inhabitants. 55% of the county’s land area is agricultural land, and 18% forest [33]. The county of Dithmarschen in the state of Schleswig-Holstein is bordering the North Sea. Its population of 133,000 is spread over an area of 1428 km², with 78% of the county’s land area being agricultural land, and 3% forest [34]. The county of Ilm-Kreis has the land area of 805 km², among which 43% is agricultural land and 42% is forest [35]. The total population in year 2019 is about 106,000 [35].

Thus, Ludwigsburg represents a suburban and densely populated county in Germany’s south, whereas Dithmarschen represents a rural county in Germany’s north with low forest cover and high agriculture cover, and Ilm-Kreis represents a neither very rural nor (sub)urban county in Germany’s hilly and relatively densely forested center. However, both counties use a sizeable share of their land for agriculture and should thus have meaningful bioenergy potentials

Table 4 shows the comparison of yield simulation results with actual yields for selected crops in and the three German counties of Ludwigsburg (south-west), Dithmarschen (north), and Ilm-Kreis (mid-eastern Germany). Only yields on soil types that actually exist in the respective county are compared. As yields vary between location due to a difference in climate, a location-dependent actual yield was introduced to better validate yields in different locations. Actual crop yield data were obtained from the global yield gap atlas (GYGA) [36]. GYGA provides robust estimates of untapped crop production potential on existing farmland, based on current climate data and available soil and water resources globally [37]. In Germany, crop yield data is only available for wheat, maize, and barley. Since barley did not feature in the crop category in Table 1, only yields of rainfed wheat and maize could be compared with modeling results. The actual yield only considered the yield of the harvestable organ, e.g., grain of wheat and maize. Harvest index values, i.e., the ratio between weight of

harvestable organ and the weight of the whole plant, of 52% and 47% for maize and wheat respectively were retrieved from [38,39]. Furthermore, it has to be noted that GYGA did not differentiate between spring and winter cereals. The climate data used for validation was the average climate between year 2000 and 2010.

As Table 4 shows, all modeling results lay within the yield range given by GYGA. The difference between yields on different soils of the same crop was highest for winter cereals, with 5.2 $t_{DM}/(ha\ a)$, while for most crops the yield difference between soils was in the order of 1 $t_{DM}/(ha\ a)$. In Ludwigsburg county, the actual yield of spring cereal was 15.3 $t_{DM}/(ha\ a)$, compared with 15.5 $t_{DM}/(ha\ a)$ based on our model, i.e., a deviation of 1.3%. The modeled yield of spring cereals was even closer to the actual yield for IIm-Kreis with 16.0 and 16.1 $t_{DM}/(ha\ a)$, respectively, i.e., a difference of 0.1 $t_{DM}/(ha\ a)$ or 0.6%. Larger deviations occurred for winter cereal in Ludwigsburg and in IIm-Kreis, and maize in IIm-Kreis. The modeled yield of maize in IIm-Kreis had the largest deviation of 7.4 $t_{DM}/(ha\ a)$, or 35%, compared with statistical yield of 21 $t_{DM}/(ha\ a)$. Deviation can be explained by the deviation of crop harvest rates and low spatial resolution. No yield data of maize in Dithmarschen was available based on GYGA data, even though [15] shows maize being grown in Dithmarschen.

Table 4. Result of simulated biomass yield in dry mass (DM) on different soils and different climates, and comparison to actual yields for the German counties of Ludwigsburg, IIm-Kreis, and Dithmarschen. Unit: $t_{DM}/(ha\ a)$.

Crop Type	Minimal Yield	Maximal Yield	Actual Yield	Simulated Yield			Average Simulated Yield	Deviation
				Silty Clay	Loamy Silt	Clayish Silt		
County Ludwigsburg								
Spring Cereal	6.3	20.4	15.3	15.5	15.5	15.5	15.5	1.3%
Winter Cereal	8.4	22.8	15.3	23.2	25.4	25.3	25.3	65.4%
Maize	3.3	26.4	17.0	17.2	17.7	17.6	17.5	2.9%
County Dithmarschen								
Spring Cereal	6.3	20.4	18.9	16.8	16.3	16.8	16.6	-12.2%
Winter Cereal	8.4	22.8	18.9	20.1	25.1	23.4	20.2	6.9%
Maize	3.3	26.4	-	11.2	12.1	12.0	11.8	-
County IIm-Kreis								
Spring Cereal	6.3	20.4	16.0	16.1	16.1	16.1	16.1	0.6%
Winter Cereal	8.4	22.8	16.0	24.4	25.2	25.2	25.2	57.5%
Maize	3.3	26.4	21.0	13.6	13.7	13.7	13.7	34.8%

Differences between simulated and actual yields can furthermore be explained by the biomass modeling process: while simulated yields were the accumulated yields over the growing periods, including all the parts above ground and without land management and fertilization, any form of land management to remove, e.g., unwanted parts of plants during the growing period would change the actual yield.

A validation of modeled bioenergy potentials on a subnational and substrate level with actual bioenergy usage levels was inherently limited, since for example information on in/exports of bioenergy as primary or secondary energy carriers into and out of a (in our case) county is typically not available, and technical potentials are rarely fully exploited for a variety of reasons. On a national level in Germany, few studies have assessed aggregated bioenergy potentials in long-term scenarios [30,40,41]. Generally, bioenergy potentials vary depending on natural protection regulation, which impacts the available land area for energy crops, yielding for example values from 543, without consideration of energy crops, to 1425 PJ/a in a “highest probability” scenario, to 1900 PJ/a under an “optimal land use” scenario [41]. As the model presented here considered the total natural land use area, the total natural vegetation cover area of Germany, 298,065 ha, would be applied to derive energy yields on a national level. Given that, the average technical bioenergy yield should be between 5.1 and 17.7 MWh/(ha a) based on above-mentioned potentials [41], with the energy yield of 13.3 MWh/(ha a) as the most realistic considering the constrains. As Table 5 shows, the model in this paper yielded the total bioenergy

technical potentials between 10.7 and 12.0 GWh/ha in all three counties, which fit the result of other studies quite well.

Table 5. Technical bioenergy potential yield in three counties in Germany.

Parameter	Unit	Ludwigsburg	Dithmarschen	Ilm-Kreis
Total area	(ha)	50,302	124,108	74,451
Total bioenergy potential	(GWh)	647	1346	796
Bioenergy energy yield	(GWh/ha)	12.0	10.8	10.7

2.7. Scenarios Setting

For each of the counties of Ludwigsburg and Dithmarschen, one base case and three sensitivity scenarios were defined to quantify the influence of (i) climate change, (ii) priority setting on the forms of bioenergy produced from the available biomass resources, and (iii) use of irrigation on energy yields. Hereby, the aim is not to come up with comprehensive and realistic future scenarios, but rather to test whether the proposed modeling approach reacts reasonably to parameter changes.

Table 6 gives an overview of the four scenarios. Here, only changes with regards to the base case are listed, with all other parameters remaining the same as in the base case (Table A5). The values from Table A5 were applied in the base case while Table A6 gives the share of various secondary energy carriers produced from the most important energy crops in the base case scenario (Germany, 2018 data) [29]. Table 7 gives the key parameters of climate at current state (average between 2000 and 2010) and in forecasted case 2050. It has to be noted that beyond the crops listed in Table A6, it is possible to for example produce bioethanol from plants rich in starch, e.g., potato. However almost all the potato for non-food use goes to material production for industrial starch [29]. Furthermore, residue of energy crops is mostly directly used as solid fuel, without any further conversion, while about 40% of maize silage residue is used for biogas production [29,31] (the other maize residue products are assumed to become solid fuel).

Table 6. Base case and sensitivity scenarios.

Scenario Name	Explanation
Base case	Values of Tables A5 and A6 in Appendix D applied [23]
Climate 2050	Climate forecast data in 2050 including temperature, precipitation, and CO ₂ concentration change. The key parameters of climate situation in both counties are listed in Table 7.
Optimization for fuel consumption	If an energy crop can be a source for biodiesel and bioethanol, all of its yield will be used to this end. If the crop cannot be used for the production of this biofuel carrier, it would follow the same distribution as given in Table A6
Water-energy nexus	The impact of different irrigation levels on bioenergy potential. Water stress is set at different levels in percentage to simulate water demand under different irrigation conditions. The irrigation water demand is the minimum amount of water that has to remain in the root zone throughout the growing cycle, and as such the water stress that is allowed in the season.

2.8. Ludwigsburg and Dithmarschen Test Cases

Land coverages and populations data for Ludwigsburg and Dithmarschen were already introduced in Section 2.6.

As for Ludwigsburg, it has set itself a goal (in 2013) of reducing greenhouse gas emissions by 90% until 2050 through increased energy efficiency and increasing the share renewable energy sources, e.g., through using biomass for local heat and power generation [43]. The extrapolated 2018 end energy demand (electricity, heating, gasoline, and diesel) in Ludwigsburg is 8506 GWh, with diesel and gasoline accounting for 106 GWh and 58 GWh, respectively [43,44]. The extrapolated end energy

demand in Dithmarschen in 2018 was 5714 GWh. Among this, end energy demand for transport was 971 GWh, or 11% of the total for diesel and 6% for petrol [45,46].

Table 7. Temperature, precipitation, and CO₂ concentration levels in the three counties, average climate between 2000 and 2010 and 2050. The climate data is generated by Meteonorm [42].

Climate	Unit	Ludwigsburg		Dithmarschen	
		2000–2010	2050	2000–2010	2050
Yearly average temperature [42]	(°C)	10.1	10.8	9.5	10.1
Precipitation [42]	(mm/a)	729	716	794	839
CO ₂ concentration [24]	(ppm)	409	469	Same as Ludwigsburg	

3. Results

3.1. The Impact of Climate Change

Changes in ambient temperature, precipitation, and atmospheric CO₂ concentration (see Table 7), allow one to assess the impact of climate change on crop and by this bioenergy yields. Climate change will increase average temperatures in all three regions, by about 0.5 °C until 2050 compared to the average value between 2000 and 2010, while the change in precipitation patterns was mixed: yearly precipitation levels were expected to increase from 794 to 839 mm in Dithmarschen, and from 570 to 590 mm in Ilm-Kreis, while they were expected to fall from 729 to 716 mm in Ludwigsburg.

Figure 3 shows how various crops react to changes in these parameters as indicated in Table 6 for Ludwigsburg and Dithmarschen. The spans of black lines indicate different yields on different soil types, while the points show the median value of crops yield under the average climate between 2000 and 2010 and climate in 2050. These developments would imply changes of ± 0.2 t_{DM}/(ha a) by 2050 for most crops compared with current yields, except for maize, with around 1.5 t_{DM}/(ha a) higher yields in Dithmarschen. In fact, only the change in climate until 2050 might make maize cultivation economically attractive in Dithmarschen. Taking these temperature and precipitation changes into account, our model still gives plausible results. In both counties, the yield of rapeseed increased between 11% and 13%. The specific yield of maize in Dithmarschen shows an increase of 35%, as the region moved into a climatic zone favorable to maize cultivation; however, in Ludwigsburg, maize yields decreased by 12%. Opposite to that, grass would produce 21% less biomass in Dithmarschen but 8% more in Ludwigsburg. This can be explained by grass tending to be in favor of moderate cool and humid climate. In both counties, yields of spring cereal, winter cereal, sugar beet, and potato changed by less than $\pm 3\%$ until 2050.

As Appendix E shows, the total bioenergy potential increased by only 0.2%, from 646 to 648 GWh/a, due to climate change in Ludwigsburg. Therein, bioethanol and solid fuel potentials do not change at all, while the biodiesel potential increased by 13%, from 1.5 to 1.7 GWh/a, which could be explained by the fact that the yield of rapeseed, being the main source for biodiesel (see Table A6), was positively affected by a temperature increase from 10.1 to 10.8 °C as expected for Ludwigsburg until 2050. In Dithmarschen, the technical energy potential changed by 4%, from 1327 to 1381 GWh/a by 4%. Half of the increase could be explained by the increase in the yield of maize, leading to higher biogas yields. Additionally, higher yields of SRC resulted in higher solid fuel potentials. In both regions, the potentials of energy wood from forest are generally limited as (i) less than 4% of forest biomass can be harvested annually (see Table A5), (ii) only about 25% (see Table A5) of harvested wood biomass was directed to energetic uses, and (iii) forests were not the dominant type of land cover type in both regions, with shares of 33% and 3% in Ludwigsburg and Dithmarschen, respectively.

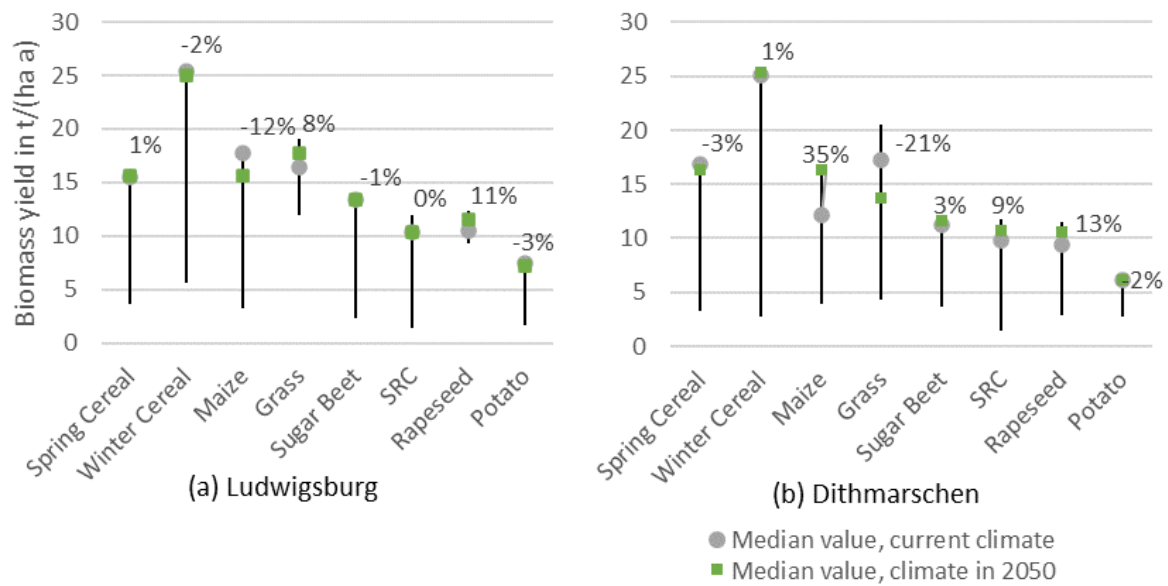


Figure 3. Above-ground biomass yields and their changes in percentage of crops from simulation result under current climate and forecasted climate in 2050 in (a) Ludwigsburg and in (b) Dithmarschen (right). The minus represents the decrement of median value between two climate scenarios.

3.2. Optimizing Biofuel for Transportation Sector

Biofuels have been required to account for at least 2% of the total transportation fuels used in EU member states since 2005. With the Renewable Energy Directive 2018/2001 (RED II), adopted in December 2018, the EU is continuing the political framework for the use of renewable energy sources in the transport sector for the period from 2021 to 2030 [47], while first-generation bioethanol, i.e., ethanol from agricultural crops, will be phased out until 2030. According to [48], sugarcane ethanol will no longer appear in the mix from 2025, as straw ethanol is considered the most attractive unrestricted non-food and non-feed-based option for gasoline. In Germany, the additional introduction of a biofuel quota in 2007 required oil companies to ensure that 4.4% of diesel sales are made of biodiesel. In addition, they needed to ensure that 1.2% (from 2008, 2%; from 2009, 2.8%; and from 2010, 3.6%) of the sales of motor fuel originate from biofuels [49]. In a scenario that optimizes biofuels for transportation, all energy crops that can be converted into biofuels (biodiesel and bioethanol) were used to 100% for that purpose. In this scenario, 1st generation bioethanol is still considered as a source for transportation in the short term and can be produced from grains, maize, sugar beet, potato, and SRC, while biodiesel is produced from rapeseed. The climate data is unchanged as in the base case with average climate between 2000 and 2010.

As Figure 4 shows, bioethanol potentials increased from 48.1 to 98.5 GWh/a, i.e., by 105%, in Ludwigsburg. Since crops used for bioethanol could alternatively be used for biogas production, biogas potentials decreased by 62%. Similarly, in Dithmarschen the amount of bioethanol potential increased by 100%. However, the technical potential of biodiesel in both counties stayed unchanged.

Differences in total technical bioenergy potentials stem from different conversion efficiencies from biomass to biogas and bioethanol, respectively, as indicated in Table 8: for instance, for cereals, maize and SRC, a conversion to biogas yields 4–18 percentage points higher energy in the secondary energy carrier than in the case of bioethanol. The actual use of maize as an energy crop (see Table A6) also prioritizes for bioethanol production, regardless of the fact that biogas production would be more effective. In case of being used as food feedstock, however, maize silage is used for biogas production [29].

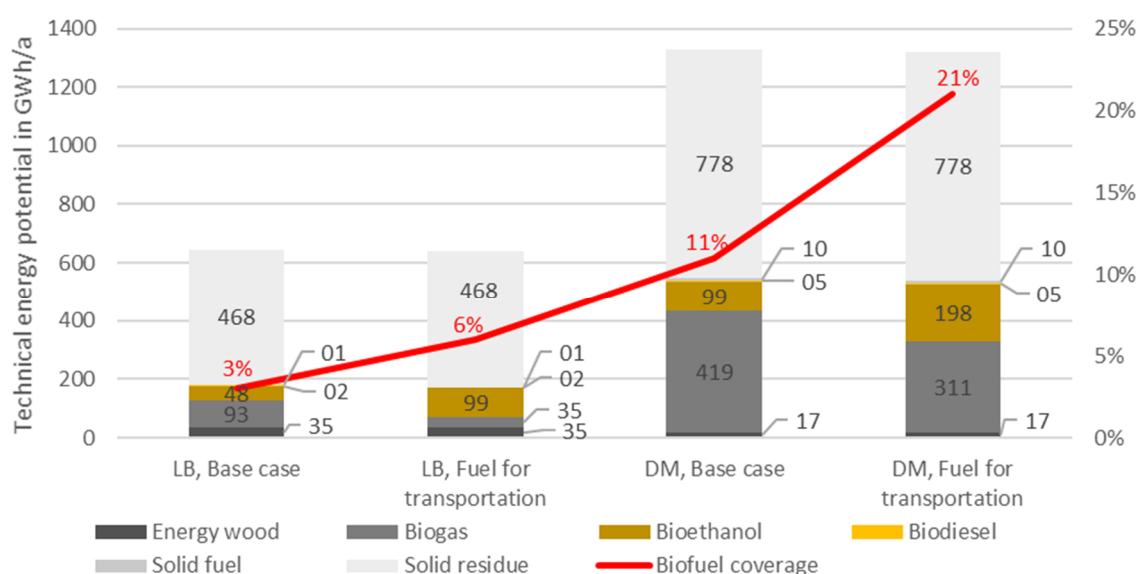


Figure 4. Technical biofuel potential and the transportation fuel demand covered by biofuel of base case and biofuel preferred case in Ludwigsburg and Dithmarschen.

Table 8. Typical conversion efficiency to bioethanol and biogas of crops.

Crop	Conversion Efficiency to Biogas ^{1,2}	Conversion Efficiency to Bioethanol ³
Cereal	54%	46%
Maize	62%	44%
Sugar Beet	68%	75%
Short Rotation Coppice	48%	44%
Potato	58%	60%

Data collected and adapted from ¹ Faustzahlen für die Landwirtschaft, pp. 938–940; ² Bayerisches Staatsministerium für Ernährung, Landwirtschaft und Forsten, Biogasausbeuten-Datenbank; ³ Flaig, Holger, and Hans Mohr, eds. Energie aus Biomasse, p. 337.

Next to conversion efficiencies, a decisive factor is the demand for certain types of biofuel. In 2018, Ludwigsburg county used 1722 GWh of diesel and 997 GWh of gasoline for transportation [43]. In the base case, if all bioethanol and biodiesel had been used for transportation, biofuels would have covered 3% of the total fuel demand, while biofuels could have covered 6% of the fuel consumption in the scenario prioritizing biodiesel and bioethanol production. In Dithmarschen 106 GWh of diesel and 58 GWh of gasoline were consumed in 2017. Being more rural than Ludwigsburg, bioethanol and biodiesel could have covered 11% of the total fuel demand in the base case and 21% in the scenario prioritizing biodiesel and bioethanol production.

3.3. The Impact of Irrigation

In a fourth scenario, external irrigation is applied in addition to natural precipitation. A crop's irrigation demand is determined by the minimal amount of external water that has to remain in the root zone throughout the growing cycle, so that the given water stress is maintained in the growing season. Water stress levels from 10% to 90%, in 10% steps, and from 92% to 98% in 2% steps, were set to simulate water demand under different irrigation conditions. The higher the water stress level, the less water is allowed to stay in the soil. Adequate or more water in the soil (lower actual water stress level than set value) brought by natural rainfall is allowed. In this case no external irrigation is needed.

Figure 5 shows the relation between relative technical bioenergy yield and the amount of irrigation. The relative technical bioenergy yield is defined as the total technical bioenergy yield under current water stress level with the total technical bioenergy yield at a water stress level of 0% (adequate water during growing period). As Figure 4 shows, irrigation led to a technical bioenergy potential increased

4. Discussion

This paper proposed a new workflow that allows one to assess technical bioenergy potentials at the regional level in high resolution, considering local climates and soil conditions, and crop distributions. It builds on commonly available input data such as digital landscape models. In the newly established workflow the advantages of two tools are combined: SimStadt assesses regional energy potentials and demands primarily based on geoinformatic data, and AquaCrop simulates biomass yields and water demands based on soil types, crop types, and climate situations [50]. Integrating AquaCrop enables more accurate bioenergy potential calculations than merely applying average statistical yields that disregard local environmental parameters such as climate and soil.

Yield modeling results were compared with actual yield from GYGA, with deviations of usually less than 1.3%. On the aggregated level, bioenergy potential studies for Germany have shown average biomass technical energy yields of between 5.1 and 17.7 MWh/(ha a), with most realistic yields of 13.3 MWh/(ha a) considering existing constraints. The newly established workflow yields values between 10.7 and 12.0 MWh/(ha a), thus in line with [20,40,41]. For the case studies of Ludwigsburg and Dithmarschen, technical bioenergy potentials were calculated as 465 GWh/a and 1327 GWh/a respectively, which would be 5% and 23% of the total extrapolated 2018 and 2017 end energy demands. As a comparison around 3.9% of electricity is covered by biomass in county Ludwigsburg in 2014 [43]; while 6.6% of the thermal energy demand is covered by biomass in Dithmarschen in 2010 [45]. It has to be noticed that the biomass in the reports [43,45] does not necessarily come from local sources. The results show that at least for the case of Dithmarschen, the more rural county of the two, there might still be a substantial untapped potential in local biomass utilization.

Climate change will lead to a 0.2% increase in the technical bioenergy potential in Ludwigsburg until 2050, and a 4% increase in Dithmarschen according to the result of this paper. For Dithmarschen, the increment of temperature from climate condition favors the maize; in Ludwigsburg a very slight increase of biomass potential is driven by two opposing effects: the temperature increment is favorable however reduced precipitation is detrimental to biomass yields, consistent with results in [51].

By directing bioenergy production to bioethanol and biodiesel for transportation, bioethanol productions could almost double in both regions covering 6% and 21% of the total transportation energy consumption in Ludwigsburg and in Dithmarschen respectively. Under the current application case, solid fuel or biogas could be used in a combined heat and power unit (CHP), while bioethanol and biodiesel play a more important role in transportation until 2030. However, with the introduction of act RED II, bioethanol and biodiesel production from crop is not allowed beyond 2030. While biogas is expected to be the dominant fuel for non-electric transportation until 2050 [52]. Thus, the local energy planner should also consider the policy restraints to make policies to direct biomass use.

With regards to irrigation, our model shows that yield gains were at best modest for the most important relevant crops in the studied regions: in Ludwigsburg 128 m³/ha of irrigation water only brought the total technical energy potential increment of less than 1% (See Figure 5). The benefits seemed more significant in Dithmarschen—a 4% total technical energy potential increment with 441 m³/ha irrigation (see Figure 5). Different amounts of external irrigation to keep the water stress level between 10% and 98% did not bring significant gain among them. Most crops had close to 100% relative biomass rate in both regions, which means crop yields could not be improved through additional irrigation. This is in accordance to the presented simulation results showing limited benefits from irrigation. Irrigation should thus only be applied selectively, e.g., on SRC on silty clay in Ludwigsburg, where the relative biomass rate could be increased by 52%.

There are limitations to the method in this paper: (i) The availability of reasonably detailed soil and crop maps determined the applicability, even though the method itself is generic and globally applicable. So far, the bioenergy potential in any region only in Germany can be assessed. (ii) For forests and orchards, static biomass yield values from the literature were assigned, rather than the in-depth modeling applied to crops such as cereals or maize. As forest growing cycles span multiple years and yields also depend on groundwater levels, rather than merely on precipitation. A model that assesses

forest similar to crops would be much more complex. Therefore, the influence from precipitation and irrigation is only restricted to crop. (iii) The secondary energy carriers that might be produced do not (yet) include hydrogen from biomass. Even though it is now widely recognized that considerable amounts of hydrogen can be produced from renewable sources through biological processes such as bacterial hydrogen fermentation, at the present stage of development of hydrogen fermentation technology has not been applied at the industrial-scale with economic advantage [53]. Nevertheless, the presented method can and should be extended to cover hydrogen potential analysis in order to confront with the biofuel development trend.

5. Conclusions

The methodology and workflow presented in this paper present a novel, generic method to evaluate bioenergy potentials for any region with good accuracy, by simultaneously considering constraints of water availability, climate, and soil. Furthermore, these bioenergy potentials can compare other RES to potentials and local heating, cooling, or electricity demands within one simulation platform based on a consistent set of input data that is moreover relatively accessible for many regions. The new method does not, however, aim to provide a highly accurate assessment of regional bioenergy potentials based on customized data for a specific region.

In the context of the water-energy nexus, our research extends an energy-centric modeling environment to water-related aspects, namely crop transpiration and potential irrigation benefits or requirements. A combination with the urban residential and non-residential water demand simulation workflow presented in [54], which also bases on similar input data, allows one to study the nexus between bioenergy, crop irrigation, and urban water consumption in the regional context. With the newly established biomass, roof PV, electricity, and heating demand workflow [27] in place, the modeling environment SimStadt can now assess regional renewable energy balances with the constraint of water and climate in regions without rich wind, ground-based PV, or hydro potentials. As the next steps, (i) a workflow similar to the presented bioenergy one will be developed for wind power. (ii) The nexus will be extended to food-energy nexus, by, e.g., (a) assessing local balances between food-use and energy-use of crops to fulfill local demands and to meet strategic goals of emission reduction by regionalization of food supply [55]. (b) Investigating the impact of diet change, e.g., more plant-based diets, on local food and energy potentials will be carried out.

Author Contributions: Conceptualization: K.B.; Data curation: K.B., R.P.; Investigation: K.B.; Methodology: K.B.; Software: K.B.; Validation: K.B.; Formal analysis: K.B.; Visualization: R.P., K.B.; Supervision: B.S., D.T., V.C.; Writing—original draft: K.B.; Writing—review and editing: B.S., D.T., R.P. All authors have read and agreed to the published version of the manuscript.

Funding: This paper is part of the project IN-SOURCE (INtegrated analysis and modeling for the management of sustainable urban FEW ResSOURCES). This research was funded from the European Union’s Horizon 2020 research and innovation program under grant agreement No 730254.

Acknowledgments: This paper extends the paper “GIS-Based Assessment of Regional Biomass Potentials at the Example of Two Counties in Germany” published in the e-EUBCE 2020 conference proceeding. Food and Agriculture Organization of the United Nations (FAO) is the source and copyright holder of the biomass yield and water simulation software AquaCrop. The CityGML maps of Dithmarschen and Ilm-Kreis are required in the project EnSys-LE (03ET4061B) funded by Federal Ministry for Economic Affairs and Energy.

Conflicts of Interest: The authors declare no conflict of interest.

Abbreviations

Abbreviations	Explanation
GIS	Geographic information system
RES	Renewable energy sources
FWE	Food-Water-Energy
DLM	Digital Landscape Model
ALKIS	Germany’s Official Real Property Cadastre Information System

AdV	Working Group of the Surveying Authorities of the sixteen states of Germany
KA5	German soil classification system
SRC	Short Rotation Coppice
Σ Tr	Crop transpiration
WP	Water productivity
WP*	Normalized water productivity
CO ₂	Carbon dioxide
RAW	Readily Available Water
CityGML	City Geography Markup Language
FAO	Food and Agriculture Organization of the United Nations
ET _o	Crop reference evapotranspiration
XML	Extensible Markup Language
GYGA	Global Yield Gap Atlas
DM	Dry mass
RED II	Renewable Energy Directive 2018/2001
LB	County Ludwigsburg
DM	County Dithmarschen
PV	Photovoltaic

Appendix A

Table A1. Soil type group according to German soil classification system [19].

Soil Surface not Sealed	Soil Surface Sealed
Pure sands Silty sands	City center areas (surface > 70 % sealed)
Normal clays Loamy silt	Anthropogenically embossed surfaces (surface 30–70% sealed)
Silt clays Loamy sands	Technogenic ally designed areas, including mining areas
Sand Loams Clay Loams Clay silt Moors Tidal flats	

Appendix B

$$P_{theoretical} = \sum A_{vegetation,i} \cdot Y_{vegetation,i} \cdot H_{u,i}, \quad (A1)$$

$P_{theoretical}$ is the theoretical energy potential of a specific land field in GJ/ha·a. i is the crop type. $A_{vegetation}$ is the area in ha of the vegetation type. $Y_{vegetation}$ is the dry matter production yield of a specific vegetation type in t/(ha·a). H_u is the calorific value in gigajoules per tonne [GJ/t_{lntro}].

$$P_{wood} = \sum A_{forest,i} \cdot Efm_i \cdot Efm \cdot n_{f,energy,i} \cdot n_{f,cf,i} \cdot p_i \cdot H_{u,i}, \quad (A2)$$

where P_{wood} is the forest fuel potential in gigajoules per year [GJ/a]. A_{forest} stands for the area of the individual forest type (broad-leaf, coniferous forest, the mix of both) in hectares (ha). Efm is the harvest cubic metres per hectare per year [m³/ha/a]. One harvest cubic metre of wood is equivalent to one cubic metre of solid wood stored without gaps in the stratification. $n_{f,cf}$ is the harvest share. $n_{f,energy}$ is

the share of energetic uses. p is the conversion factor for firewood [t_{lutro}/m^3]. H_u is the calorific value in gigajoules per tonne [GJ/t_{lutro}].

$$P_{biogas, GL/OM} = \sum A_i \cdot E_{crop,i} \cdot TS_i \cdot oTS_i \cdot E_{CH_4,i} \cdot n_{energy,i} \cdot H_{u,i}, \quad (A3)$$

where $P_{biogas, \frac{GL}{OM}}$ is the annual biogas fuel potential [GJ/a]. i is the crop type. A_i is the area of the crop that can be as the source of biogas production in hectares (ha), E_{crop} is the crop harvest yield of fresh mass of each crops [$kg/ha \cdot a$], TS and oTS are its dry mass rate and organic dry mass rate, and $E_{CH_4,i}$ is its methane yield [$l/kg \ oTS$]. $n_{energy,i}$ is the share of actual energetic use per crop, and H_u is the calorific value of methane in gigajoules per tonne [$GJ/l \ CH_4$].

$$P_{biodiesel} = \sum A_{biodiesel,i} \cdot P_{theoretical,i} \cdot C_{biodiesel,i}, \quad (A4)$$

where P_{VO} is the fuel potential from rapeseed cultivation for vegetable oil production [GJ/a]. $A_{biodiesel}$ is the area of the area of biodiesel production crops (rapeseed). $P_{Primary}$ is the theoretical yield of the crop in $GJ/(ha \ a)$, $C_{biodiesel}$ is the conversion efficiency from dry raw mass to biodiesel.

$$P_{ethanol} = \sum A_{ethanol,i} \cdot P_{theoretical,i} \cdot C_{ethanol,i}, \quad (A5)$$

where $P_{ethanol}$ is the fuel potential from energy crops for ethanol production [GJ/a], $A_{ethanol}$ is the area of the area of bioethanol production crops (sugar beet, grain maize and cereals), and C_{energy} is the ethanol conversion factor from dry raw mass. $P_{Primary}$ is the theoretical yield of the crop in $GJ/(ha \ a)$.

$$P_{residue} = \sum A_i \cdot Y_i \cdot C_{residue,i} \cdot TS_i \cdot n_{energy,i} \cdot H_{u,i}, \quad (A6)$$

where $P_{residue}$ is the fuel potential of residues as solid fuels in gigajoules per year in GJ/a , A is the area of individual object types in ha, Y is the dry matter production yield of a specific vegetation type in $t/(ha \cdot a)$, $C_{residue}$ is the residue yield in wet mass per total yield in wet mass, TS is the dry mass rate, n_{energy} is the percentage of energy usage of residue, and H_u is the heat value in gigajoule per kilogram.

Table A2. Biomass potential yield factors of most relevant types of vegetation in Germany.

Potential	Parameter	Unit	Winter Cereal	Spring Cereal	Maize	Grass
Theoretical potential	Wet mass range ⁶	t/ha a	9.5–20	8.0–17	10.0–22.0	9.0–18.8
	Water content ⁶	%	15	15	67	15
	Heating value ^{4,5,8}	MJ/kg	17.1	17.1	17.1	16.5
	Primary biomass yield factor	GJ/(ha t ha)	14.5	14.5	5.6	14.0
Biogas	oTS Organic dry mass of dry mass ⁷	%	94	95	95	88
	Biogas yield ⁷	$l_N/kg \ oTS$	520	520	600	560
	Methan content ^{7,8}	%	52.0	52.0	52.0	54.0
	biogas coefficient per fresh mass yield	GJ/(t FM ha a)	7.8	7.9	3.5	8.1
Bioethanol Biodiesel	Conversion efficiency ³	GJ/GJ_Primary	0.5	0.5	0.4	-
	Conversion efficiency ³	GJ/GJ_Primary				
Residue	Yield range ^{1,2}	t FM/(ha a)	3.5–9.4	3.5–9.4	4.2–10	4.2–26
	Residue yield factor	$t_{residue \ FM}/t_{biomass \ FM}$	0.4	0.4	0.4	1.0
	Water content	%	14	14	14	50
	Heat value	GJ/kg	0.0143	0.0143	0.0143	0.0143
	Residue factor	GJ/t FM biomass	5.2	5.5	5.0	7.2

Table A2. Cont.

Potential	Parameter	Unit	Sugar Beet	SRC	Rapeseed	Potato
Theoretical potential	Wet mass range ⁶	t/ha a	40–85	4–18	8.5–13.5	33–50
	Water content ⁶	%	76	29	12	76
	Heating value ^{4,5,8}	MJ/kg	17.4	18.5	18.0	18.0
	Primary biomass yield factor	GJ/(ha t ha)	4.2	13.1	15.8	4.3
Biogas	oTS Organic dry mass of dry mass ⁷	%	92	91	85	90
	Biogas yield ⁷	L _N /kg oTS	700	516	630	640
	Methan content ^{7,8}	%	51	52.2	55.3	50
	biogas coefficient per fresh mass yield	GJ/(t FM ha a)	2.8	6.3	9.4	2.5
Bioethanol Biodiesel	Conversion efficiency ³	GJ/GJ_Primary	0.8	0.4	-	0.6
	Conversion efficiency ³	GJ/GJ_Primary	-	-	0.3	-
Residue	Yield range ^{1,2}	t FM/(ha a)	10.0–32.0	2.5–4	4.2–10	10–32
	Residue yield factor	t _{residue FM} /t _{biomass FM}	0.3	0.3	0.6	0.5
	Water content	%	66	66	14	66
	Heat value	GJ/kg	0.0143	0.0143	0.0143	0.0143
	Residue factor	GJ/t FM biomass	1.5	1.6	7.3	2.3

^{1,2,3,4} Flaig, Holger, and Hans Mohr, eds. Energie aus Biomasse, pp. 280–281,275,337,609; ^{5,6,7} Faustzahlen für die Landwirtschaft, pp. 917,299–300,913,938–940; ⁸ Bayerisches Staatsministerium für Ernährung, Landwirtschaft und Forsten (StMELF), Biogasausbeuten-Datenbank; ⁹ Heat value of sugar beet, silphy, orchard meadow are not give, average value 17.8 MJ/kg taken.

Appendix C

Table A3. Key parameters of crops for biomass yield simulation.

Parameter	Winter Cereal	Spring Cereal	Maize	Sugar Beet	Potato	SRC
Base temperature °C	5	0	8	5	2	0
Upper temperature °C	35	26	30	30	26	25
Plant density (Plants per ha)	2,000,000	4,500,000	75,000	100,000	40,000	266,667
Plant to emergence (GDD)	88	150	80	23	200	0
Planting to maximum rooting depth (GDD)	720	864	1409	408	1079	3080
Planting to start senescence (GDD)	819	1700	1400	1704	984	2410
Planting to maturity (GDD)	2162	2400	1700	2203	1276	3080
Planting to flowering (GDD)	754	1250	880	865	550	0
Maximum rooting depth (m)	1.2	1.5	2.3	1	1.5	0.8
Maximum canopy cover in fraction soil cover	0.91	0.96	0.96	0.98	0.92	0.96
Water productivity normalized for ET ₀ and CO ₂ (g/m ²)	15	15	33.7	17	18	10.4
Canopy growth coefficient (CGC) (fraction soil cover per day) (GDD)	0.02833	0.005001	0.012494	0.010541	0.01615	0.003543
Canopy decline coefficient (CDC): decrease in canopy cover (in fraction per day) (GDD)	0.0668	0.004	0.01	0.003857	0.002	0.00383
Soil water depletion factor for canopy expansion, upper limit	0.25	0.2	0.14	0.2	0.2	0.25
Soil water depletion factor for canopy expansion, lower limit	0.55	0.65	0.72	0.6	0.6	0.55
Shape factor for water stress coefficient for canopy expansion	4	5	2.9	3	3	0
Soil water depletion factor for pollination (p-pol), upper threshold	0.9	0.85	0.8	0.8	0.8	0.9
Shape factor for water stress coefficient for stomatal closure	3	2.5	6	3	3	0
Shape factor for water stress coefficient for canopy senescence	3	2.5	2.7	3	3	0

Table A4. Continued table: Key parameters of crops for biomass yield simulation.

Parameter	Winter Cereal	Spring Cereal
Base temperature °C	5	0
Upper temperature °C	30	30
Plant density (Plants per ha)	60,000	440,000
Plant to emergence (Calendar Days)	11	7
Planting to maximum rooting depth (Calendar Days)	124	70
Planting to start senescence (Calendar Days)	209	120
Planting to maturity (Calendar Days)	244	206
Planting to flowering (Calendar Days)	0	87
Maximum rooting depth (m)	0.7	0.3
Maximum canopy cover in fraction soil cover	0.75	0.8
Water productivity normalized for ET ₀ and CO ₂ (g/m ²)	14	18.6
Canopy growth coefficient (CGC) (fraction soil cover per day) (Calendar Days)	0.04626	0.09713
Canopy decline coefficient (CDC): decrease in canopy cover (in fraction per day) (Calendar Days)	0.17	0.052

Table A4. *Cont.*

Parameter	Winter Cereal	Spring Cereal
Soil water depletion factor for canopy expansion, upper limit	0	0.2
Soil water depletion factor for canopy expansion, lower limit	0.35	0.55
Shape factor for water stress coefficient for canopy expansion	2.5	3.5
Soil water depletion factor for pollination (p-pol), upper threshold	0.9	0.9
Shape factor for water stress coefficient for stomatal closure	2	5
Shape factor for water stress coefficient for canopy senescence	2	3

Appendix D

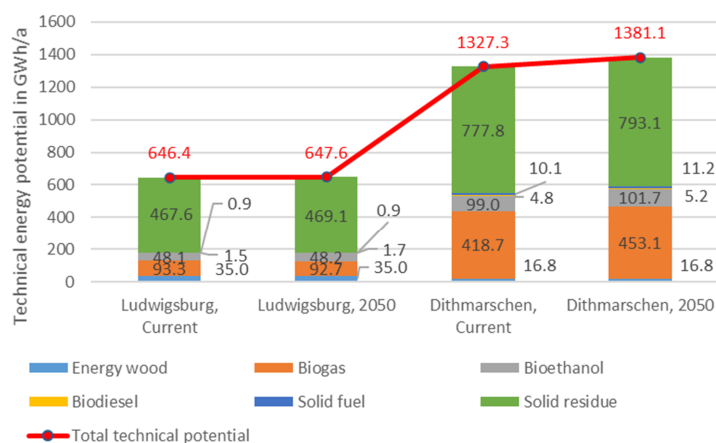
Table A5. Default parameter values used in modelling local bioenergy potentials.

Parameter	Default Value	Explanation
Conifer trees harvest rate	4.5% [23]	The percentage in volume of conifer trees harvested annually out of all conifer trees
Deciduous trees harvest rate	3.0% [23]	The percentage in volume of deciduous trees harvested annually out of all deciduous trees
Forest energy usage rate	25.6% [25]	The percentage in volume of solid forest wood with diameters > 7 cm that is used for energy purposes
Energy crop rate	14.0% [29]	The percentage of farmland area used for energy crop cultivation (e.g., rapeseed, maize). Energy crops are used exclusively for energetic purposes. Since no data source gives information on the end product of a crop (energy or food) per field, we assume, in line with statistical data, that 14% of each field's area is used for energetic purposes.
Residue energy usage rate	62.0% [30]	The percentage of residue by-products which are used for energetic purposes.
Rate of maize residue for Biogas production	39.4% [29,31]	The percentage of maize residue (silage) for biogas production. The rest of maize residue of maize is used as solid fuel.

Table A6. Distribution of energy crop yields among different forms of possible secondary energy carriers. Source: FNR [23].

Crop	Biogas	Bioethanol	Vegetable Oil	Solid Fuel
Cereal	57%	43%	–	–
Maize	–	100%	–	–
Short-rotation coppice (SRC)	–	–	–	100%
Sugar beet	42%	58%	–	–
Rapeseed	–	–	100%	–
Grass	98%	–	0%	2%

Appendix E

**Figure A1.** Technical bioenergy potential in current climate and in year 2050 in Ludwigsburg and Dithmarschen.

References

1. Scarlat, N.; Dallemand, J.F.; Taylor, N.; Banja, M.; Sanchez Lopez, J.; Avraamides, M. *Brief on Biomass for Energy in the European Union*; Publications Office of the European Union: Luxembourg, 2019; ISBN 927977235X.
2. German National Academy of Sciences Leopoldina; acatech—National Academy of Science and Engineering; Union of the German Academies of Sciences and Humanities. *Biomass: Striking a Balance between Energy and Climate Policies. Strategies for Sustainable Bioenergy Use*; acatech—National Academy of Science and Engineering: Munich, Germany; German National Academy of Sciences Leopoldina: Schweinfurt, Germany; Union of the German Academies of Sciences and Humanities: Munich, Germany, 2019; ISBN 978-3-8047-3929-1.
3. Berndes, G.; Hoogwijk, M.; van den Broek, R. The contribution of biomass in the future global energy supply: A review of 17 studies. *Biomass Bioenergy* **2003**, *25*, 1–28. [\[CrossRef\]](#)
4. Mittelstädt, A.; Köhler, S.; Sihombing, R.; Duminil, E.; Coors, V.; Eicker, U.; Schröter, B. (Eds.) *A Multi-Scale, Web-Based Interface for Strategic Planning of Low-Carbon City Quarters, Proceedings of the Second International Conference on Urban Informatics, Hong Kong, China, 24–26 June 2019*; The Hong Kong Polytechnic University: Hong Kong, China, 2019.
5. Braun, R.; Weiler, V.; Zirak, M.; Dobisch, L.; Coors, V.; Eicker, U. Using 3D CityGML Models for Building Simulation Applications at District Level. In *Proceedings of the 2018 IEEE International Conference on Engineering, Technology and Innovation (ICE/ITMC)*, Stuttgart, Germany, 17–20 June 2018; pp. 1–8.
6. Bouchard, S.; Landry, M.; Gagnon, Y. Methodology for the large scale assessment of the technical power potential of forest biomass: Application to the province of New Brunswick, Canada. *Biomass Bioenergy* **2013**, *54*, 1–17. [\[CrossRef\]](#)
7. Ericsson, K.; Nilsson, L.J. Assessment of the potential biomass supply in Europe using a resource-focused approach. *Biomass Bioenergy* **2006**, *30*, 1–15. [\[CrossRef\]](#)
8. Lauka, D.; Barisa, A.; Blumberga, D. Assessment of the availability and utilization potential of low-quality biomass in Latvia. *Energy Procedia* **2018**, *147*, 518–524. [\[CrossRef\]](#)

9. Haase, M.; Rösch, C.; Ketzer, D. GIS-based assessment of sustainable crop residue potentials in European regions. *Biomass Bioenergy* **2016**, *86*, 156–171. [[CrossRef](#)]
10. Lozano-García, D.F.; Santibañez-Aguilar, J.E.; Lozano, F.J.; Flores-Tlacuahuac, A. GIS-based modeling of residual biomass availability for energy and production in Mexico. *Renew. Sustain. Energy Rev.* **2020**, *120*, 109610. [[CrossRef](#)]
11. Quinta-Nova, L.; Fernandez, P.; Pedro, N. GIS-Based Suitability Model for Assessment of Forest Biomass Energy Potential in a Region of Portugal. *IOP Conf. Ser. Earth Environ. Sci.* **2017**, *95*, 42059. [[CrossRef](#)]
12. Voivontas, D.; Assimacopoulos, D.; Koukios, E.G. Assessment of biomass potential for power production: A GIS based method. *Biomass Bioenergy* **2001**, *20*, 101–112. [[CrossRef](#)]
13. Padsala, R.; Coors, V. Conceptualizing, Managing and Developing: A Web Based 3D City Information Model for Urban Energy Demand Simulation. 2307-8251. 2015. [[CrossRef](#)]
14. Rodríguez, L.R.; Duminil, E.; Ramos, J.S.; Eicker, U. Assessment of the photovoltaic potential at urban level based on 3D city models: A case study and new methodological approach. *Solar Energy* **2017**, *146*, 264–275. [[CrossRef](#)]
15. Arbeitsgemeinschaft der Vermessungsverwaltungen der Länder der Bundesrepublik Deutschland. Digitales Basis-Landschaftsmodell (Basis-DLM). Available online: <http://www.adv-online.de/AdV-Produkte/Geotopographie/Digitale-Landschaftsmodelle/Basis-DLM/> (accessed on 10 November 2020).
16. Griffiths, P.; Nendel, C.; Hostert, P. Intra-annual reflectance composites from Sentinel-2 and Landsat for national-scale crop and land cover mapping. *Remote Sens. Environ.* **2019**, *220*, 135–151. [[CrossRef](#)]
17. Wyland, L.J.; Jackson, L.E.; Chaney, W.E.; Klonsky, K.; Koike, S.T.; Kimple, B. Winter cover crops in a vegetable cropping system: Impacts on nitrate leaching, soil water, crop yield, pests and management costs. *Agric. Ecosyst. Environ.* **1996**, *59*, 1–17. [[CrossRef](#)]
18. Searle, S.Y.; Malins, C.J. Will energy crop yields meet expectations? *Biomass Bioenergy* **2014**, *65*, 3–12. [[CrossRef](#)]
19. Bundesanstalt für Geowissenschaften und Rohstoffe. Karte der Bodenarten in Oberböden 1:1.000.000 (BOART1000OB). Available online: https://www.bgr.bund.de/DE/Themen/Boden/Informationsgrundlagen/Bodenkundliche_Karten_Datenbanken/Themenkarten/BOART1000OB/boart1000ob_node.html (accessed on 24 September 2020).
20. Kolbe, T.H.; Gröger, G.; Plümer, L. CityGML: Interoperable Access to 3D City Models. In *Geo-Information for Disaster Management*; Fendel, E.M., van Oosterom, P., Zlatanova, S., Eds.; Springer: Berlin/Heidelberg, Germany, 2005; pp. 883–899. ISBN 978-3-540-27468-1.
21. Nouvel, R.; Brassel, K.-H.; Bruse, M.; Duminil, E.; Coors, V.; Eicker, U. SimStadt, a New Workflow-Driven Urban Energy Simulation Platform for CityGML City Models. In Proceedings of the International Conference CISBAT 2015 Future Buildings and Districts Sustainability from Nano to Urban Scale. No. CONF. LESO-PB, EPFL, Lausanne, Switzerland, 9–11 September 2015.
22. Statistisches Landesamt Baden-Württemberg. Flächenerhebung nach Art der tatsächlichen Nutzung 2015. Available online: https://www.statistischebibliothek.de/mir/servlets/MCRFileNodeServlet/BWHeft_derivate_00008321/3336_15001.pdf (accessed on 2 December 2020).
23. Martin, K.; Hans, H.; Hermann, H. *Energie aus Biomasse: Grundlagen, Techniken und Verfahren*; Springer: Berlin/Heidelberg, Germany, 2001.
24. Food and Agriculture Organization of the United Nations. Introductin AquaCrop. Available online: <http://www.fao.org/aquacrop/en> (accessed on 26 October 2020).
25. Mantau, U.; Döring, P.; Weimar, H.; Glasenapp, S.; Jochem, D.; Zimmermann, K. *Rohstoffmonitoring Holz: Erwartungen und Möglichkeiten*; Fachagentur Nachwachsende Rohstoffe e. V. (FNR): Gülzow-Prüzen, Germany, 2018.
26. Kath, J.; Reardon-Smith, K.; Le Brocque, A.F.; Dyer, F.J.; Dafny, E.; Fritz, L.; Batterham, M. Groundwater decline and tree change in floodplain landscapes: Identifying non-linear threshold responses in canopy condition. *Glob. Ecol. Conserv.* **2014**, *2*, 148–160. [[CrossRef](#)]
27. Weiler, V.; Stave, J.; Eicker, U. Renewable Energy Generation Scenarios Using 3D Urban Modeling Tools—Methodology for Heat Pump and Co-Generation Systems with Case Study Application. *Energies* **2019**, *12*, 403. [[CrossRef](#)]
28. Allen, R.G. *Crop Evapotranspiration—Guidelines for Computing Crop Water Requirements*; FAO: Rome, Italy, 1998; ISBN 9251042195.

29. Rohstoffe, F.N. Anbau und Verwendung nachwachsender Rohstoffe in Deutschland 2019. Available online: <https://www.weltagrarbericht.de/fileadmin/files/weltagrarbericht/Weltagrarbericht/16AgrarspritBioenergie/FNR2019.pdf> (accessed on 26 October 2020).
30. Nitsch, J.; Pregger, T.; Naegler, T.; Heide, D.; Luca de Tena, D.; Trieb, F.; Scholz, Y.; Nienhaus, K.; Gerhardt, N.; Sterner, M.; et al. *Langfristszenarien und Strategien für den Ausbau der Erneuerbaren Energien in Deutschland bei Berücksichtigung der Entwicklung in Europa und Global*; Federal Ministry for the Environment, Nature Conservation and Nuclear Safety: Berlin, Germany, 2012.
31. Statistisches Bundesamt. Anbauflächen, Hektarerträge und Erntemengen ausgewählter Anbaukulturen im Zeitvergleich. Available online: <https://www.destatis.de/DE/Themen/Branchen-Unternehmen/Landwirtschaft-Forstwirtschaft-Fischerei/Feldfruechte-Gruenland/Tabellen/liste-feldfruechte-zeitreihe.html> (accessed on 1 October 2020).
32. Döhler, H. (Ed.) *Faustzahlen für die Landwirtschaft*; völlig neu bearb; Kuratorium für Technik und Bauwesen in der Landwirtschaft e.V.(KTBL): Darmstadt, Germany, 2005; ISBN 3784321941.
33. Statistisches Landesamt Baden-Württemberg. Flächen für Landwirtschaft in den Kreisen Baden-Württembergs. *Statistisches Monatsheft Baden-Württemberg 9/2018* **2018**, 55–59.
34. Ulich, E.; Geruhn, A.; Demmer, H.; Frank, K. Regionalprofil 2006 des Kreises Dithmarschen. Einschließlich Stärken- und Schwächen-Analyse. Available online: https://www.dithmarschen.de/media/custom/647_2783_1.PDF (accessed on 26 May 2020).
35. Thüringer Landesamt für Statistik. Available online: <https://statistik.thueringen.de/startseite.asp> (accessed on 20 August 2020).
36. Global Yield Gap Atlas. Available online: <http://www.yieldgap.org/home> (accessed on 5 October 2020).
37. Actual Yield Determination—Global Yield Gap Atlas. Available online: <http://www.yieldgap.org/web/guest/methods-actual-yield> (accessed on 5 October 2020).
38. Xiying, Z.; Suying, C.; Hongyong, S.; Dong, P.; Yanmei, W. Dry matter, harvest index, grain yield and water use efficiency as affected by water supply in winter wheat. *Irrig. Sci.* **2008**, *27*, 1–10. [[CrossRef](#)]
39. Echarte, L.; Andrade, F.H. Harvest index stability of Argentinean maize hybrids released between 1965 and 1993. *Field Crops Res.* **2003**, *82*, 1–12. [[CrossRef](#)]
40. Öko-Institut. Modell Deutschland. Klimaschutz bis 2050: Vom Ziel her Denken. Available online: https://www.wwf.de/fileadmin/fm-wwf/Publikationen-PDF/WWF_Modell_Deutschland_Endbericht.pdf (accessed on 2 December 2020).
41. Nitsch, J.; Krewitt, W.; Nast, M.; Viebahn, P.; Gärtner, S.; Pehnt, M.; Reinhardt, G.; Schmidt, R.; Uihlein, A.; Barthel, C.; et al. Ökologisch Optimierter Ausbau der Nutzung Erneuerbarer Energie in Deutschland. 2004. Available online: <https://www.ise.fraunhofer.de/content/dam/ise/en/documents/publications/studies/recent-facts-about-photovoltaics-in-germany.pdf> (accessed on 2 December 2020).
42. Meteonorm. Available online: <https://meteonorm.com/en/> (accessed on 12 August 2020).
43. Landratsamt Ludwigsburg. Klimaschutzkonzept Ludwigsburg Kurzbericht. 2015. Available online: https://www.landkreis-ludwigsburg.de/fileadmin/user_upload/seiteninhalte/natur-umwelt/umwelt/klimaschutz/20151007_endbericht_band1_klimaschutzkonzept.pdf (accessed on 5 October 2020).
44. Statistisches Landesamt Baden-Württemberg. Struktur und Entwicklung des Energieverbrauchs nach Verbrauchsart und Verbrauchergruppen. Available online: <https://www.statistik-bw.de/Energie/Energiebilanz/LRt1002.jsp> (accessed on 24 June 2020).
45. Kreis Dithmarschen. Integriertes Klimaschutzkonzept für den Kreis Dithmarschen. Available online: https://www.dithmarschen.de/media/custom/647_8081_1.PDF (accessed on 20 October 2020).
46. Statistisches Amt für Hamburg und Schleswig-Holstein. Energie- und CO₂-Bilanzen für Schleswig-Holstein—Statistikamt Nord. Available online: <https://www.statistik-nord.de/zahlen-fakten/umwelt-energie/energie/dokumentenansicht/product/6207/energie-und-co2-bilanzen-fuer-schleswig-holstein-360?cHash=653b32db13abf009ce4a187a9911a9fa> (accessed on 20 October 2020).
47. Directive (EU) 2018/2001 on the Promotion of the Use of Energy from Renewable Sources. European PARLIAMENT and of the Council. 2018. Available online: https://eur-lex.europa.eu/legal-content/EN/LSU/?uri=uriserv:OJ.L_.2018.328.01.0082.01.ENG (accessed on 2 December 2020).
48. Meisel, K.; Millinger, M.; Naumann, K.; Müller-Langer, F.; Majer, S.; Thrän, D. Future Renewable Fuel Mixes in Transport in Germany under RED II and Climate Protection Targets. *Energies* **2020**, *13*, 1712. [[CrossRef](#)]

49. Biofuel Chain Development in Germany: Organisation, Opportunities, and Challenges. Available online: <https://www.sciencedirect.com/science/article/pii/S0301421507003436> (accessed on 8 October 2020).
50. Bao, K.; Padsala, R.; Coors, V.; Thrän, D.; Schröter, B. GIS-Based Assessment of Regional Biomass Potentials at the Example of Two Counties in Germany. *Eur. Biomass Conf. Exhib. Proc.* **2020**, *77*–85. [[CrossRef](#)]
51. Verón, S.R.; De Abelleira, D.; Lobell, D.B. Impacts of precipitation and temperature on crop yields in the Pampas. *Clim. Chang.* **2015**, *130*, 235–245. [[CrossRef](#)]
52. Millinger, M.; Meisel, K.; Thrän, D. Greenhouse gas abatement optimal deployment of biofuels from crops in Germany. *Transp. Res. Part D: Transp. Environ.* **2019**, *69*, 265–275. [[CrossRef](#)]
53. Bao, K.; Padsala, R.; Thrän, D.; Schröter, B. Urban Water Demand Simulation in Residential and Non-Residential Buildings Based on a CityGML Data Model. *ISPRS Int. J. Geo-Inf.* **2020**, *9*, 642. [[CrossRef](#)]
54. Robledo, C.B.; Oldenbroek, V.; Abbruzzese, F.; van Wijk, A.J.M. Integrating a hydrogen fuel cell electric vehicle with vehicle-to-grid technology, photovoltaic power and a residential building. *Appl. Energy* **2018**, *215*, 615–629. [[CrossRef](#)]
55. Pradhan, P.; Kriewald, S.; Costa, L.; Rybski, D.; Benton, T.G.; Fischer, G.; Kropp, J.P. Urban Food Systems: How Regionalization Can Contribute to Climate Change Mitigation. *Environ. Sci. Technol.* **2020**, *54*, 10551–10560. [[CrossRef](#)]

Publisher's Note: MDPI stays neutral with regard to jurisdictional claims in published maps and institutional affiliations.



© 2020 by the authors. Licensee MDPI, Basel, Switzerland. This article is an open access article distributed under the terms and conditions of the Creative Commons Attribution (CC BY) license (<http://creativecommons.org/licenses/by/4.0/>).

Chapter 2

Urban Water Demand Simulation in Residential and Non-Residential Buildings Based on a CityGML Data Model

Bao, K.; Padsala, R.; Thrän, D.; Schröter, B.

ISPRS Int. J. Geo-Inf. 2020, 9, 642. <https://doi.org/10.3390/ijgi91106428>

Article

Urban Water Demand Simulation in Residential and Non-Residential Buildings Based on a CityGML Data Model

Keyu Bao ^{1,*}, Rushikesh Padsala ² , Daniela Thraen ^{3,4,5}  and Bastian Schröter ¹

¹ Center for Sustainable Energy Technology, Hochschule für Technik Stuttgart, 70174 Stuttgart, Germany; bastian.schroeter@hft-stuttgart.de

² Center for Geodesy and Geoinformatics, Hochschule für Technik Stuttgart, 70174 Stuttgart, Germany; rushikesh.padsala@hft-stuttgart.de

³ Department of Bioenergy, Helmholtz Center for Environmental Research, 04247 Leipzig, Germany; daniela.thraen@ufz.de

⁴ Chair of Bioenergy System, Faculty of Economic Sciences, University of Leipzig, 04109 Leipzig, Germany

⁵ Unit Bioenergy System, Deutsches Biomasseforschungszentrum GmbH, 04347 Leipzig, Germany

* Correspondence: keyu.bao@hft-stuttgart.de

Received: 20 September 2020; Accepted: 23 October 2020; Published: 28 October 2020



Abstract: Humans' activities in urban areas put a strain on local water resources. This paper introduces a method to accurately simulate the stress urban water demand in Germany puts on local resources on a single-building level, and scalable to regional levels without loss of detail. The method integrates building geometry, building physics, census, socio-economy and meteorological information to provide a general approach to assessing water demands that also overcome obstacles on data aggregation and processing imposed by data privacy guidelines. Three German counties were used as validation cases to prove the feasibility of the presented approach: on average, per capita water demand and aggregated water demand deviates by less than 7% from real demand data. Scenarios applied to a case region Ludwigsburg in Germany, which takes the increment of water price, aging of the population and the climate change into account, show that the residential water demand has the change of -2% , $+7\%$ and -0.4% respectively. The industrial water demand increases by 46% due to the development of economy indicated by GDP per capita. The rise of precipitation and temperature raise the water demand in non-residential buildings (excluding industry) of 1%.

Keywords: CityGML (Geography Markup Language); occupant estimation; urban water demand; urban energy and water system modelling

1. Introduction

Water plays a fundamental role in sustaining human life and the Earth's ecosystems. However, almost 80% of the world's population face a high-level threat of water security [1], and there is growing evidence that human activities are placing unsustainable stress on water resources. The water stress will increase between today and the 2050s in around 70% of the world's river basins [2]. A precise modeling of urban water demands, covering residential and non-residential areas, can help local governments to better design local water supply infrastructures and improve management of local resource potentials. Water demand simulation is heavily focused on the residential sector with limited function on non-residential buildings. The simulation approach is usually top-down with aggregated occupant number and empirical water demand assumption. The research gaps and innovation part are further addressed in Section 2.

The objective of this paper is to develop an approach to assess the water demand on urban areas based on a building model in Geography Markup Language (CityGML) with 3D building geometry data, including all building types (i.e., residential and non-residential). The urban building model in CityGML is applied as the main input to estimate the water demand at building/household level, overcoming this limit also imposed by data privacy rules. The same CityGML will also be the input to the assessment of other renewable energy resources, e.g., photovoltaic on roofs, and energy demand of the same simulation platform [3]. Therefore, the regional energy system can be simulated with the same level of detail and based on same data to avoid error and complexity. The structure of the simulation platform is introduced in Section 3.1.

Based on building geometry and census data, a building's heated area, its number of households and number of occupants per household are assessed. For residential buildings, specific water demand per capita in relation to local climate, type of housing (e.g., single or multi-family home), household size, income, water price, age of occupants and potential availability of on-site wells is assessed. For non-residential buildings, specific water demand is calculated based on specific water demand per area, influenced by building use (e.g., office, retail) and local climatic conditions. The method and approach are addressed in Section 3.2, Section 3.3, Section 3.4.

The newly established workflow is validated with three German counties, which differ in geographic location as well as socio-economic and population density conditions and urban structures (Section 3.5). Furthermore, scenarios that assess changes in water demand due to changing climatic situations, an ageing society and increasing water prices are studied on the level of a single-village, Rainau in South-Western Germany, for which highly accurate CityGML and other data are available (Section 3.6).

2. Research State-of-Art and Gap

Residential water demand has been an important research topic. There are many variables that affect water demand, including water price, income, or household composition [4,5]. Detailed studies exist on water demand, including domestic hot water and cold water, in residential buildings [6]. Since domestic hot water accounts for about 20% of heat or electricity demand in buildings [7–9], hourly usage profiles of domestic hot water are available [10,11]. Furthermore, modeling tools exist that examine water demand patterns for different types of residential dwellings and areas [12].

In contrast, water demand of non-residential buildings has not been studied in the same level of detail yet. Water demand in hotels, swimming pools, washing shops, shopping centers, food processing plants and drink manufacturers including detailed information about peak demand and duration curves were studied in [6]. Office water demand was estimated by main end-uses in monthly resolution and then compared with measured data in [13]. Another study quantified the mean potable cold water demand in 19 hospitals in Germany, with the annual cold water demand being in accordance with the hospital's geographic location, heating-degree-days per year, cold-degree-days per year, hospital category depending on the number of beds, floor area and number of workers [14]. However, the water demand in sport halls, exhibition halls and industrial facilities in general, has not been well researched yet to the knowledge of the authors.

A range of tools and models apply various methods to assess urban water demand, thereby mostly focusing on residential buildings [15]. Many models [16–21] work on municipal level, highly aggregating spatial data instead of assessing micro level data (e.g., on household level). On the other hand, models which consider census block scale [22–24] face the challenges (1) that water utility service areas do not necessarily match administrative boundaries (e.g., census blocks), (2) that data usually must be aggregated to protect customer privacy and (3) of limited consistency in water demand data collection between water utilities. In cases where models assess individual water demand data and aggregate to census tract scale, the availability of geo-tagged data is typically limited and assessed building types are restricted to single-family houses [25,26].

In terms of scenario planning, to give one example, URBANICA is a tool which enables the user to analyze the impacts of spatial planning scenarios and resulting water demand of all land use types,

including residential, industrial and agricultural area [27]. However, its algorithm is based on average water demands per land area, which lacks 3D building information details, e.g., that urban areas with multi-story buildings have higher water demands than low-rise areas, even though they share the same footprint area.

To the knowledge of the authors, there is no tool yet that allows one to simulate water demand for all building types (i.e., residential, office, school, industry, etc.), based on CityGML. With this method it is possible to simulate the water demand at different scales, e.g., city quarter, city or county, with a flexible boundary, e.g., nearby houses in different administration districts can be simulated together. Instead of applying average residential water demand per capita value from higher scales, e.g., federal state, this method determines per capita residential water demand value from local climate and socio-economic factors. By applying CityGML it is able to distinguish residential and non-residential buildings and simulate their water demand, respectively, with corresponding methods and values.

3. Materials and Methods

The water demand assessment method is based on a geoinformatics CityGML model with individual buildings as the base element to calculate the water demand of each household/building. The respective datasets, including CityGML building models, and the simulation environment used are introduced in Section 3.1. Besides using the same CityGML data as input, water demands of buildings with different functions, e.g., residential buildings, hospitals and hotels, are assessed with different methods, e.g., using a log-log model or taking a literature value. For building functions such as retail, where water demand per square meter is available, the building floor area is extracted from the CityGML model. Next, the specific water demand per area is applied, based on a log-log model. The approach to assess a building's volume and its floor area is shown in Section 3.2. Water demand in residential buildings is simulated by a newly developed method which is introduced in Section 3.3, while Section 3.4 shows how water demands are assessed in non-residential buildings, mostly based on the approach presented in Section 3.2. Section 3.5 presents the validation process of the model. The scenario set up for a case study is introduced in Section 3.6.

3.1. Datasets and Simulation Environment

The water demand workflow is implemented within the simulation platform *SimStadt*, a platform under constant development at HFT Stuttgart [28]. Figure 1 shows inputs and calculation steps of the water demand workflow on a high-level step.

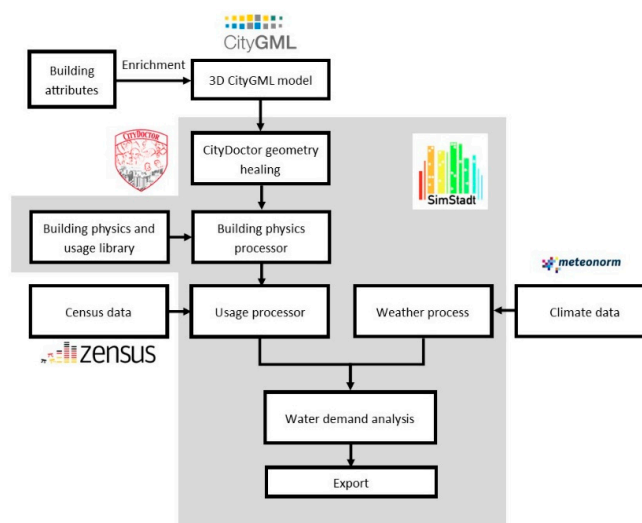


Figure 1. Water analysis workflow in a SimStadt simulation environment with dataset sources. The blocks lying in gray background are included in SimStadt Water Demand Workflow.

The CityGML data format that serves as basic inputs can depict existing environments such as buildings, roads and landscape. Building models are available in five *Levels of Detail* (LoD), with LoD 0 relating to a planar shape, LoD1 to data where buildings are represented as building blocks with average building height and a flat roof, LoD2 which has more detailed information about building heights and roof shapes, LoD3 introducing windows and LoD4 featuring information on ground plans and wall thicknesses [3]. The building function, e.g., residential, office etc., and year of construction is attached with CityGML as the basic input for the simulation. Building function decides in which calculation process the building should be directed to. Year of construction of residential determines the distribution of household sizes in terms of flat area and family size from census data.

The CityGML model is quality-checked by the tool CityDoctor [29], which can repair possible geometrical errors, e.g., open polygons, which prevent the buildings from being recognized properly. The model can then be stored in the CityGML 3D City Database (3DCityDB) geodata server or directly used for simulation in SimStadt [3].

The building physics library classifies buildings according to their type and year of construction. For each building type and period, there exists a typical building with its respective wall, roof and window properties. These properties are then applied to the actual building geometry for further calculation [30].

The usage library is based on several German norms and standards, focusing on heating set point temperatures, occupancy schedules and internal gains that are different according to the usage (residential, office, retail, etc.) of each building. To estimate the occupants in residential buildings, the usage library was extended with information on household size and number of occupants per household for all types of residential buildings based on the latest available German Census from the year 2011. The occupant numbers and the type of residential buildings (single family house or multi-family house) determines the water demand per capita as well as the total water demand.

The weather processor retrieves weather data of the geospatial location of the building model and creates synthetic hourly values for temperature and precipitation from monthly means in case only monthly data are available. Precipitation and temperature can have an impact on the water demand in residential buildings as well as some non-residential buildings [5,6]. The climate data are provided by Meteonorm, which generates representative typical years for any place on earth, including precipitation, temperature, irradiation etc., in hourly resolution [31]. The precipitation and temperature have impacts on water demand in residential buildings (Chapter 2.3), offices (Chapter 2.4.1) and hotels (Chapter 2.4.3).

The information flow of Figure 2 shows the input data and data generated in intermediate steps, which are necessary for water demand calculation. Beside the information mentioned above, other necessary parameters are also included in the simulation, which are shown on the right side in the Figure 2. All the inputs generated and processed from the above-mentioned steps are passed on to the newly established water demand processor to estimating the water demand per building in the chosen region.

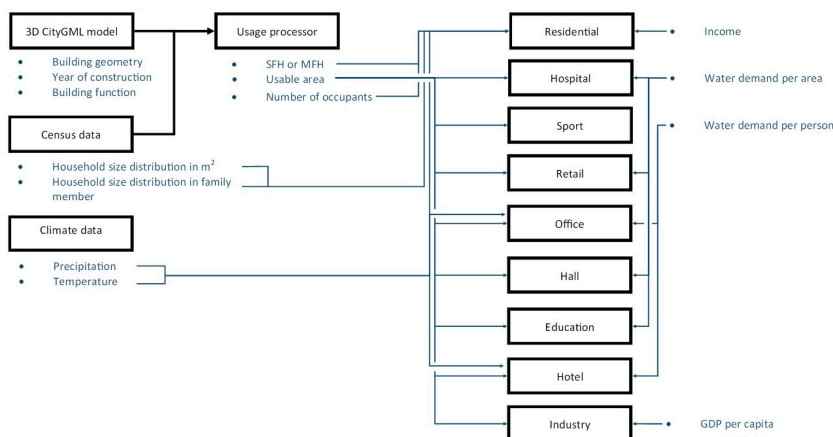


Figure 2. Information flow of inputs from CityGML, other sources and intermediate result to the water demand simulation of each building function. Information needed for calculations is marked in blue.

3.2. Building Volume and Heated Area Estimation

Given its wide and standardized availability, building geometric data are taken as one key input for the new workflow.

A building's volume allows one to determine the number of residents or users. To determine the building volume, at least an LoD1, preferably LoD2, model is required. An LoD2 model has more details, e.g., attic, which increases the accuracy of the simulation. Each polygon of the building geometry is defined by a sequence of points in counterclockwise order. Volume calculation is integrated as part of a geometry processor in SimStadt [29]. If the data model is LoD2 or LoD3 (there is no information about internal structure of the building), it is assumed that the building has one thermal zone per story, internal ceilings are added to the model and the air volume is reduced by the volume occupied by these surfaces. Information related to cellar can be externally provided: if the cellar exists and, in that case, if it is conditioned or not. If this information is not provided, it is assumed that there is no cellar and, therefore, the floor is in contact with the ground. The attic is assumed to be ventilated but not heated unless other information is externally provided [32].

As the building volume calculation process mentioned before only calculates the heated area, the area is derived from the heated volume is heat area. The heat area is calculated according to Equation (1). Traffic areas such as entrance areas, stairwells, elevators and corridors are assumed to be heated. Technical areas (heating room, machine rooms, technical operating rooms), cellar and unheated attic are not included. The building heated area A^N in m^2 is calculated in residential buildings as below:

$$A^N = 0.32 \frac{1}{m} V_e \quad (1)$$

where V_e is the calculated building volume in m^3 .

If the average story height of a residential building, measured from the surface of the floor to the surface of the floor of the story above, is more than 3 m or less than 2.5 m, the useful floor area of the building shall be determined as Equation (2), notwithstanding the formula above:

$$A^N = \left(\frac{1}{h^G} - 0.04 \frac{1}{m} \right) V_e \quad (2)$$

where h^G is the story height in meters [33].

3.3. Occupant Number Estimation and Water Demand in Residential Buildings

The water demand of residential buildings is usually given as the value per occupant [10,14,23,26]. To assess the occupant number, this paper uses a method for linking CityGML building models with 2011 census data [34] to obtain information on household size and number of occupants per household for all types of residential buildings. Based on the floor area described in Section 3.2, this step assesses the number of occupants and households in buildings for the next analysis. The information related includes: (1) single-family houses only have one household with its number of occupants; (2) the occupant numbers per household/dwelling in all multi-family houses. The latter method is subject to ongoing research and an upcoming publication [35].

Sleich et al. [5] econometrically analyze the impact of several economic, environmental and social determinants on per capita water demand in about 600 water supply areas in Germany. Besides price, income and household size, the effect of population age, the share of houses with wells, house type, precipitation and temperature are considered.

Household water demand is a composite of the direct demand for drinking purposes and demand for activities such as cooking, cleaning, washing, personal hygiene and gardening [36]. The extent to which water demand responds to changes in prices depends on whether water is used for necessities (e.g., to cook) or non-necessities (e.g., to wash cars).

In this research we take the method from Schleich et al. [5] to estimate water demand in residential buildings. Among all the influencing factors, few factors more related to this paper are chosen, including the price for fresh water and sewage (EUR/m³), average net income per capita (EUR), number of household members, house type (single family house (SFH) or multi-family house (MFH)), number of days with rainfall > 1 mm in summer months and average temperature in summer month into consideration. Only share the households with wells is not relevant to this paper and for individual household/building the statistical data of having wells is not available.

A log-log model, where all parameters enter the regression equation in logarithmic form, is used. The unit and definition of each parameter are shown in Table 1. The log-log model allows parameter estimates to be directly interpreted as elasticities of demand. However, one drawback is that the model it presumes these elasticities to be constant over the entire range of the variables. The regression equation for the water demand per capita and day in a log-log model is then given as:

$$water = \beta_1 price + \beta_2 income + \beta_4 size + \beta_5 age + \beta_6 wells + \beta_7 onefam + \beta_8 raindays + \beta_9 temp + State_i + constant + \mu_0, \quad (3)$$

Table 1. Parameters impacting water demand and mean, minimum and maximum values for Germany on county level. Source: [5].

Variable	Definition	Unit	Mean	Min.	Max.
WATER	Average water demand per capita per day	[Liters]	128.47	67.90	228.70
PRICE	Price for fresh water and sewage	[€/m ³]	3.79	1.99	7.10
INCOME	Average net income per capita	[€]	16,541	12,735	21,893
SIZE	Average number of household members	[Number of persons]	2.03	1.49	3.66
AGE	Average age of population	[Years]	42.19	36.40	47.40
WELLS	Share of households with wells	[%]	1	0	20
ONEFAM	Share of single-family houses	[%]	51	26	91
RAINDAYS	Average number of days with rainfall > 1 mm in summer months ¹	[Number of days]	7.90	5.00	10.80
TEMP	Average temperature in summer months ¹	[Celsius]	16.72	13.10	19.80

¹ Summer months: April to September.

Lower case letters indicate that variables are in natural logarithmic form. $State_i$ is associated with federal states (of Germany), which is also relevant here: Germany's five "new" eastern states, excluding Berlin, have average demand of 95 liter per capita per day and by this around 20% less water demand per capita and day than the "old" western states [5,37]. To reflect this difference, a correction value for each federal state is applied. Furthermore, μ_0 is the error component which is not given in the result. Values for β_i and μ_0 in (3) are assessed by Ordinary Least Squares (OLS) to find the best fit for the data input, which contains 592 samples in Germany. The result is shown in Table 2.

Table 2. Estimation results for water demand for the log-log model with the sample size of 592. Source: [5].

Variable	Elasticity β	Standard Error
Price	-0.242	0.058
Income	0.355	12.724
Size	-0.436	0.179
Age	0.603	0.329
Wells	-0.014	0.006
Onefam	0.073	0.065
Raindays	-0.147	0.088
Temp	-0.047	0.164
Constant	-146.83	62.121

Since our method accesses water demand of each building, whereas the parameter "ONEFAM" represents the percentage of single-family houses among all the residential buildings statistically in

an area, the parameter “ONEFAM” should be simplified to a binary variable, with one value for a single-family house and one for a multi-family house. In the case water demands for multi-family house are to be assessed, it is assumed that the area under consideration consists only of multi-family house, with “ONEFAM” equal to 0. Since logarithms do not allow for 0 as value, the maximal and minimal values of the component $\beta_{7onefam}$ based on the maximal and minimal value of ONEFAM are calculated and then extrapolated linearly to the case {ONEFAM = 0; ONEFAM = 1}. The values of $\beta_{7onefam}$ in both extreme cases are listed in Table 3. As the parameters indicate, single-family houses can be expected to have higher water demands than multi-family houses, which is plausible, given the presence of gardens and their occasional irrigation in summer months.

Table 3. Estimation results for per capita daily water demand for the log-log model.

Value of ONEFAM	Method	Value of $\beta_{7onefam}$
1	Linear extension	0.00250929
0.91 (Max. in the real data)	Direct logarithmic calculation	−0.00298998
0.26 (Min. in the real data)	Direct logarithmic calculation	−0.04270695
0	Linear extension	−0.05859373

Thus, the formulas for calculating the daily per capita water demands in residential buildings in single-family house (SFH) and multi-family house (MFH), respectively, are:

$$water_{SFH,O} = 0.054932 - 0.242price + 0.355income - 0.436size + 0.603age - 0.014wells - 0.147raindays - 0.047temp + State, \quad (4)$$

$$water_{MFH,O} = -0.0857 - 0.242price + 0.355income - 0.436size + 0.603age - 0.014wells - 0.147raindays - 0.047temp + State, \quad (5)$$

3.4. Water Demand in Non-Residential Buildings

The water demand simulation in non-residential buildings takes the floor area as the main building attribute. Literature data for area-specific water demand are available for hospital, sport halls, retail and educational buildings [6,14,38,39]. For offices and hotels, occupant numbers for a certain floor area serve as basis for assessing water demands. Regarding the limits of a generic method on water demand modelling for exhibition halls and industry, area specific water demand values are derived from the total amount of water demand in Germany or single states and their total floor area, respectively. The water demand values per square meter in hospitals, sport facilities, retails, halls and education facilities are directly taken from literature, indicated in Table 4.

Table 4. Key parameters of water demand assessment in non-residential buildings.

Building Type	Floor Area per Occupant	Daily Water Demand per Occupant	Annual Water Demand
Unit	[m ² /p]	[liter/person]	[m ³ /(m ² a)]
Hospital			$1.01 + \frac{7.693}{\text{Floor Area}}$ [14]
Sport			0.279 [38]
Retail			1.1315 [6]
Office and Administration	14 [39]	96 (per working day) [6]	1.7
Hall			0.05 [40]
Education			3 [41]
Hotel	19 [42]	323 [6]	1.9
Industry			96 [43–45]

3.4.1. Water Demand in Offices

For offices, a workplace typically requires 8 to 10 m², including furniture and a proportionate amount of traffic space, according to existing guidelines. For open-plan offices, in view of the greater

need for traffic space and possibly greater disruptive effects (e.g., acoustic, visual), a space requirement of 12 to 15 m² per workplace is to be assumed [39]. Water demand per occupant per working day is 96 liters [6], with a typical assumption of 250 working days per year.

As Figure 3 indicates, water demand (including water for cooling) increases in summer with higher temperatures, with demand of drinking and process water for WC flushing decreasing, which dampens the total increase. The increase in water demand with rising daytime temperatures by up to 40% can be attributed to air conditioning systems [39].

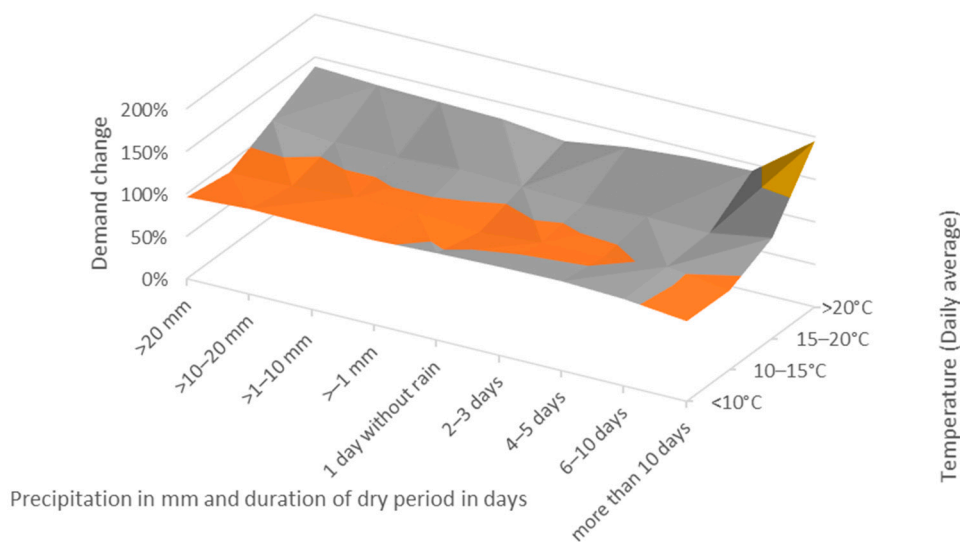


Figure 3. Office water demand change (Total demand without irrigation) depending on temperature and precipitation. Source: [6].

3.4.2. Water Demand in Educational Buildings

Educational buildings are specified as a separate building category in the CityGML data. In the following Table 5, a water demand assumption of 3 m³/m² a is assigned for educational buildings.

Table 5. Water demand per square meter and year in buildings for educational purposes. Source: [41].

Building Type	Unit	Water Demand
Social sciences	[m ³ /(m ² a)]	0.5–0.8
Nature sciences with medium amount of technical facilities (e.g., physics, electrical engineering)	[m ³ /(m ² a)]	2.0–4.0
Natural sciences with high amount of technical facilities (chemistry, biology)	[m ³ /(m ² a)]	4.0–7.0

3.4.3. Water Demand in Hotels

Hotel facilities usually consist of guest rooms, a lobby, breakfast/restaurant room, spa/wellness room, administration rooms and more. Differences in floor area, especially with regards to the guest rooms, exist between hotel categories. For a mid-tier hotel, for example, 25 m² usable floor space incl. bathroom is a reference value per room. Adding to this the proportional share for lobby, conference facilities etc. result in total floor space per room. For example, the above-mentioned hotel with a room size of 25 m² would have a total floor space of about 37.5 m² if corrected for public space. Generally, the resulting net floor area can be roughly achieved by an area surcharge of about 1/3 [42]. In the following, we use the net floor area of the middle-class hotel as the standard case.

The average hotel occupancy rate in western Europe was 63.6% in 2019, which was still unaffected by the COVID-19 crisis [46]. We assume all hotel rooms are double rooms with two occupants, with a water demand per day of 345 liters [6]. The climatic situation, especially with regards to precipitation and temperature, which influence water demands, is considered. The impact by precipitation and temperature to water demand in hotels is shown in Figure 4.

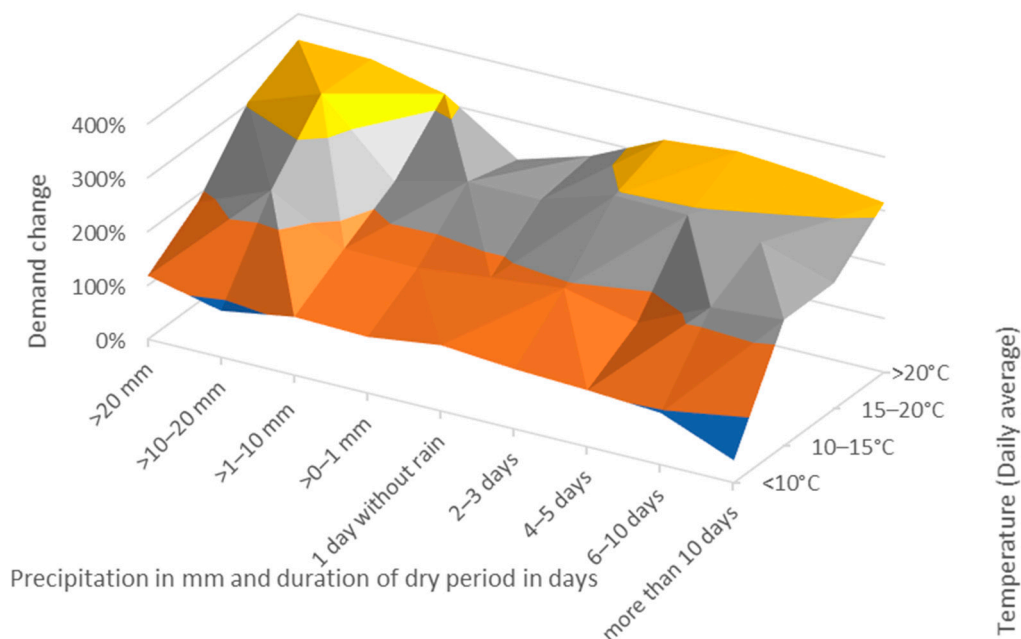


Figure 4. Hotel water demand change (total demand without irrigation) with temperature and precipitation. Source: [6].

Total hotel water demand increases with average daily temperatures, due to the fact that occupancy rates increase in summer. Furthermore, water demand also increases with rising precipitation levels, potentially due to an increased use of wellness/spa facilities under rainy weather. Likewise, an increase in demand can be observed in connection with persistent dryness, especially on the warmer days. Here, an increasing irrigation of outdoor facilities may be of importance.

3.4.4. Water Demand in Industry

Overall water demand and yearly water demand patterns in industry of course differ very much with the type of industry under consideration—to give just one example, a warehouse will have a much lower water demand in almost all circumstances than a brewery or food processing plant. However, CityGML data do not specify which type of industry an individual industrial building belongs to. Regarding water intensity, cross-temporal and cross-regional data suggest that as GDP per capita increases, many countries follow a pattern of decreasing water demand per industrial value add [47]. This finding suggests that industrial water demand can be linked to local economic conditions as indicated by GDP per capita, available through census data (Figure 5). Therefore, the overall water demand in industry, GDP per capita and ground area used by industry in the three federal counties assessed here, located in the states of North-Rhine-Westphalia, Baden-Württemberg, Thuringia, were analyzed. Data were obtained from each State Bureau of Statistics [48–50]. As data on industrial floor area at state level are not available, industrial ground area is taken as an approximation. Performing a regression analysis, the Pearson’s correlation coefficient between GDP per capita and industrial water demand is 0.62, a moderate strength of relationship (strong > 0.7, moderate 0.4–0.6, weak < 0.4 [51]). Of course, industrial water demand is defined by many other factors than GDP, most importantly the type of industry. Given the level of information contained in CityGML, a correlation with per capita GDP is, however, widely applicable.

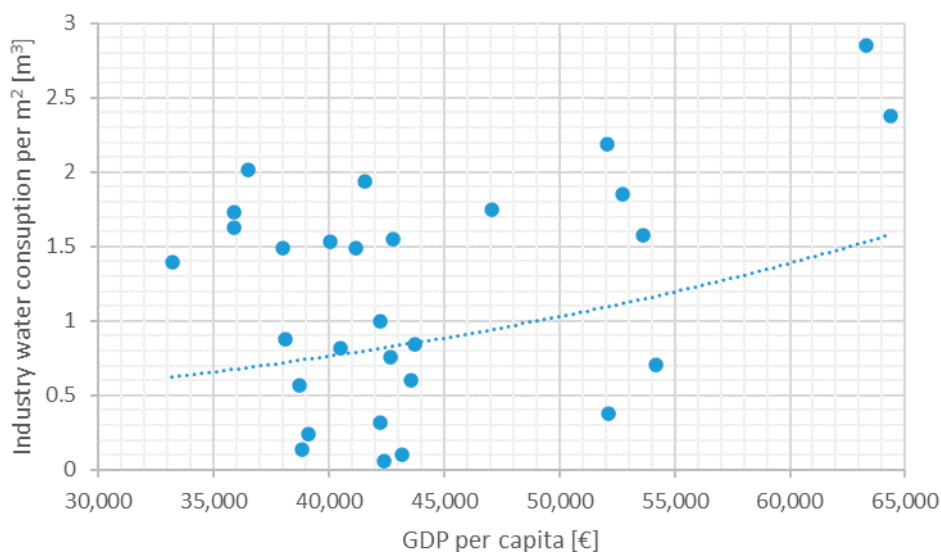


Figure 5. Water demand in industry per m² of ground area in log scale in relation to GDP per capita. The trend line is required by the regression analysis. Expansional correlation is $y = 0.2315 \cdot \exp(3^{-5} \cdot x)$.

3.5. Validation

As mentioned earlier, three German counties with different climatic and socio-economic conditions were used to validate the feasibility, accuracy and resilience of the established water demand workflow. The city of Cologne (North-Rhine-Westphalia) represents a densely populated urban area, while the county of Ludwigsburg (Baden-Württemberg) represents a typical southern suburban area and the county of Ilm-Kreis (Thuringia) a more rural region that is in many dimensions close to the average German county outside of large metropolitan areas. Key socio-economic and climatic data for the tree counties between 1995 to 2015 are listed in Table 6.

Table 6. Socio-economic and climatic data of the three German counties used for validation.

Parameter	Unit	Ludwigsburg	Ilm-Kreis	Cologne
Average age [52]	[Years]	42.1	45.6	42.4
Annual net income [53,54]	[€/person]	17,244	13,847	15,984
Water price	[€/m ³]	5.37 [55]	4.03 [56]	3.16 [57,58]
Longitude	[°]	9.150	10.948	6.958
Latitude	[°]	48.900	50.757	50.937
Average altitude	[m]	302	421	57
Yearly average temperature	[°C]	10.1	8.7	12.0
Precipitation	[mm/a]	729	602	811
Percentage of flats in buildings with living space less than 40 m ² [59]	[%]	4.1	6.1	10.2
Residential floor area per capita	[m ²]	43 [60]	46 [61]	39 [62]
Population density [33]	[Person/km ²]	792	136	2168

Table 7 shows the results of the newly established water demand workflow, including household and occupant number as well as water demands per different sectors for the three aforementioned counties. Comparing the estimation result with the statistical number from German Census 2011 data [63,64], the model yields differences (to statistical data) from 15% to 40% for the number of households, and 11% to 31% for the number of residents. Since the household estimation model introduced in Section 3.3 uses average German household floor areas and an average number of occupants per household, our modeling results are more accurate in areas with a mid-sized population

density such as Ludwigsburg, which are close the German average value. In rural areas, e.g., IIm-Kreis, a house with relatively large floor areas is usually occupied by fewer occupants than on average (in Germany), leading to an overestimate of the number of households and their population. Similarly, in densely populated cities, such as Cologne, the floor area per household is typically smaller and at the same time the number of occupants per dwelling is higher than indicated based on German average statistical data (Table 6). Thus, our workflow simulation yields around 19% less households and 31% fewer resident number.

Table 7. Key validation results.

Variable	Unit	Ludwigsburg			IIm-Kreis			Cologne		
		Si ¹	St ¹	Di ¹	Si ¹	St ¹	Di ¹	Si ¹	St ¹	Di ¹
Water demand of residential buildings	[1000 m ³ /a]	16,619	14,176	17%	5360	3607	49%	39,573	60,301	−34%
Water demand per capita	[L/(dp)]	113	114	−1%	97	90	7%	147	154	−5%
Water demand of non-residential buildings, excluding industry	[1000 m ³ /a]	3278	3116	5%	682	1604	−57%	12,106	11,920	2%
Water demand of industry	[1000 m ³ /a]	36,744	-	-	88	361	−76%	145,349	56,377	158%
Industry building area	[ha]	-	-	-	133	1233	−89%	36,835	15,378	140%
Water demand of residential buildings after scaling	[1000 m ³ /a]	14,982	14,176	6%	3848	3607	7%	57,342	60,301	−5%
Households	[1000-]	174	152	15%	77	55	40%	418	515	−19%
Residents	[1000-]	392	353	11%	152	109	39%	738	1070	−31%
Residential floor area	[ha]	-	-	-	666	489	36%	2873	3809	−25%

¹ Simulation (Si); Statistic (St); Difference (Di).

In terms of water demand per capita in residential buildings, numbers calculated by the newly established workflow deviate by between 1% and 7% from the statistical value. It has to be noted that the residential water demand given by North-Rhine Westphalia's statistical office for Cologne includes small business units, which explains higher values than the simulation result. At a county and city level, the result of residential water demand per capita tends to be accurate compared with statistical data. If the error is eliminated by scaling the aggregated residential water demand in each region with the same ratio resident number difference, the gap between simulation result and statistical value narrows to between 5% and 7%.

Statistically, the value for water demand in non-residential buildings is the difference between the total public water supply to end users and water supply to households. As more detailed data on water demand per building category, e.g., retail, school and etc. are not available, validating the accuracy of the water demand output of individual building types in the newly established workflow against statistical data is difficult. We assume that the building types including office, hospital, retail, sport facility, hall, education and hotel, source all their water from the water utility, i.e., self-extraction is assumed to be zero. In that case, water demands in Ludwigsburg and Cologne deviate by 5% and 2%, respectively, from derived statistical data, shown in Table 7.

Larger differences in water demand in industry in the studied counties result from errors in building function assignment in the CityGML. For example, 1100 ha out of a total of 1233 ha of industrial area are missing for IIm-Kreis, whereas the industrial floor area in Cologne seems to be overestimated by 35,000 ha, which in reality seem to be residential areas. On top of this, water demand in industry differs from region to region as mentioned Section 3.4.4. However, water demand per floor area is estimated in all regions at the same magnitude according based on regression analysis.

It can thus be seen that the accuracy and quality of the CityGML data plays an important role in the accuracy of water demand assessments, with missing building functions and errors in building geometries yielding up to 36% in difference in residential building floor area estimations, and missing buildings in the data model resulting in lower water demand than statistically assessed.

3.6. Scenarios and Location Setting

As stated in the end of last section, a well-validated CityGML data file of the village of Rainau (Baden-Württemberg) is used for a scenario study [65]. It has a population of 3318 and a land area of 2547 ha. Of this, 75 ha are used for residential living and 23 ha for industry [66].

Table 8 indicates the three parameters used for creating different scenarios, which are related to the parameters stated in Table 1: climate, average age, water price. Average historic climate data for 2000–2010 and predicted climate data in 2030 were taken from Meteonorm (precipitation and ambient temperature). Age represents the average age of the population, which is 38.9 in Rainau compared with the German average of 43.3. The water price includes fresh water supply as well as wastewater disposal and treatment cost per cubic meter.

Table 8. Scenarios setting for Rainau, Baden-Württemberg, Germany.

Scenario	Climate	Average Age [Years] [67]	Water Price [€] [68]
1	Average history data in year 2000–2010	38.9	4.89
2			5.42
3		43.3	4.89
4			5.42
5	Predicted in year 2030	38.9	4.89
6			5.42
7		43.3	4.89
8			5.42

4. Results of Scenario Analysis

Table 9 shows the water demand simulation result of all eight scenarios in Rainau as defined in Table 8. The result is based on the assumptions that (1) The total number of inhabitants is constant across these eight scenarios since the same CityGML file is given and the distribution function of occupant estimation algorithm is not changed; (2) the water demand pattern is based on the data collected in the past. The change of water demand pattern in the future is not forecasted in this study.

Table 9. Simulation results of case study Rainau.

Scenario	Residential Water Demand	Residential Water Demand per Capita	Non-Residential (Excluding Industry) Water Demand	Industrial Water Demand
Unit	[1000 m ³ /a]	[L/p d]	[1000 m ³ /a]	[1000 m ³ /a]
1	174.2	102.6	192	397
2	169.9	100.1	192	397
3	185.8	109.5	192	397
4	181.2	106.8	192	397
5	173.5	102.3	194	579
6	169.3	99.8	194	579
7	185.1	109.1	194	579
8	180.6	106.4	194	579

As with the nature of Equations (2) and (3), the higher the average number of days with rainfall exceeding 1 mm in the summer, the lower the water demand, due to reduced water demand for gardening [5]. In contrast, increasing summer temperatures is statistically a less significant influencing factor on water demand, since the absolute value of elasticity is the lowest of all (see Table 2).

Comparing scenarios 1–4 against scenarios 5–8 residential water demand in 2030 decreases by around 700 m³/a, or 0.4%, compared with demand based on the current climate. Table 10 shows the climate in Rainau, in terms of precipitation and temperature in summer months. As in Equation (3), only the summer climate and precipitation have an impact on residential water demand. The climate is shown in two cases—the historical average between year 2000 and 2010 and the forecast value in year

2030. While in April, May and June, average temperatures in Rainau will increase by 0.7 °C (indicated in Table 10), the weather data predict more rainfall in the summer in this region, which overcompensates additional water demands due to rising temperatures.

Table 10. Climate in summer months (April to September) during 2000–2010 and 2030 in Rainau.

Month	Ambient Temperature [°C]		Precipitation [mm]	
	2000–2010	2030	2000–2010	2030
Apr	10.0	9.8	43.0	56.0
Mai	14.7	14.4	82.0	77.0
Jun	18.1	17.4	79.0	90.0
Jul	19.1	19.5	88.0	88.0
Aug	19.0	19.2	78.0	82.0
Sep	14.6	15.8	58.0	62.0
Annual average	10.1	10.5	247.0	248.0

Furthermore, the results show an ageing society can lead to higher residential water demand. If the average age increases by 4.4 years, as indicated in Table 8, per capita water demand increases by about 6 liters per day. Water demand may increase with age because retired people spend more time at home and gardening [5]. The data from a recent survey of energy use patterns from more than 20,000 households in Germany and show that older people take fewer showers and more baths, corroborating our findings [69].

Lastly, increasing the water price from EUR 4.89 to EUR 5.42 per m³, per capita water demand in the residential sector drops by between two and three liters per day. Combining the influences brought by climate in 2030 and aging of the population, residential water demand per capita will increase from 102.6 L/d to in scenario 1 to 109.1 L/d in scenario 7. Scenario 7 is the most likely situation in the future. In order to limit the residential water demand, the possible solution would be to increase the water and wastewater price. By raising the water price from EUR 4.89 to EUR 5.42 per m³, the per capita water demand in the most likely scenario in the future will go down to 106.4 L/d in scenario 8 from 109.1 L/d in scenario 7.

The water demand calculation in non-residential sector, excluding industry, lacks the linkage with the socio-economic parameters; only changes in climate data have an influence on non-residential water demand in the scenarios presented in Table 8 (excluding industry). Considering an annual average temperature increase of 0.4 °C, and annual precipitation remaining (almost) constant, non-residential water demand (excluding industry) increasing from 192 m³/a to 194 m³/a.

In the workflow, industrial water demand is only related to the local economic situation, represented by GDP per capita. According to the forecast of the German Federal Ministry of Transport and Digital Infrastructure, GDP per capita will grow by 14% between 2020 (EUR 42,709 per person) and 2030 (EUR 48,689 per person) [70]. By this, Rainau's industrial water demand increases by 200 m³/a in Rainau 46% between 2020 and 2030.

The above-mentioned results were combined with CityGML data for visualization in the web framework CesiumJS, using 3D Tiles. Figure 6 shows the total water demand of each building in Rainau of the default scenario: buildings in blue have water demands of less than 500 m³ per year, with most single-family houses belonging to this category. Buildings in green are mostly multi-family houses, a few single-family houses and office buildings with annual water demand between 500 and 1000 m³. Most office buildings, all sport halls and schools belong to the yellow and orange category with annual water demand between 1000 and 10,000 m³. Industrial buildings with the highest water demand per buildings, above 10,000 m³, are colored in red.

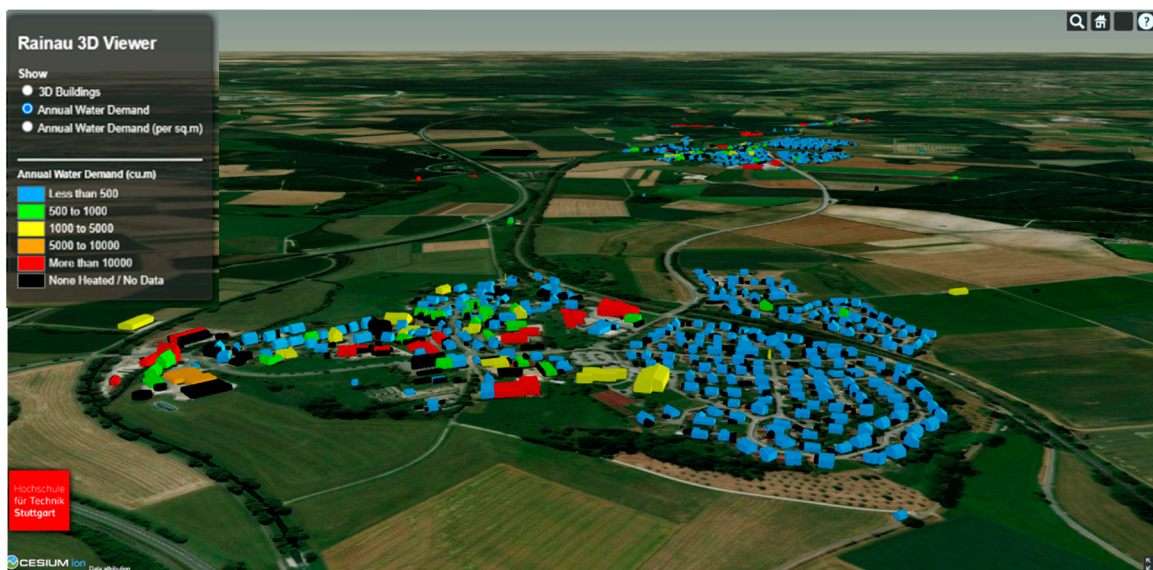


Figure 6. Visualization of water demand per building in m^3 in Rainau with CityGML and satellite map.

Figure 7 does not give the total water demand, but water demand per floor area. Residential buildings have water demands per square meter below $1.5 \text{ m}^3/\text{m}^2$ and year (in blue, green and yellow), with a few single-family houses in blue having values per m^2 below $0.5 \text{ m}^3/\text{m}^2$. As occupants in single-family houses have more living space per person, even though they consume more water per person the water demand per area in SFH is in the lowest category. In Figure 5 the sports hall located in the middle part in yellow has one of the highest absolute water demands ($1455 \text{ m}^3/\text{a}$); however, per square meter demand is among the lowest and below $0.5 \text{ m}^3/\text{m}^2$. Due to lower values of floor area per resident than in single-family houses, multi-family houses have the highest water demand per square meter among residential buildings, peaking with some yielding more than $1.5 \text{ m}^3/\text{m}^2$. Office buildings have the second-highest water demand category in orange between 1.5 and $2 \text{ m}^3/\text{m}^2$ behind industrial building with values above $2 \text{ m}^3/\text{m}^2$ in red. There is no difference between industrial buildings in term of water demand per area, as the identical specific water is applied to all industrial buildings in the same region.

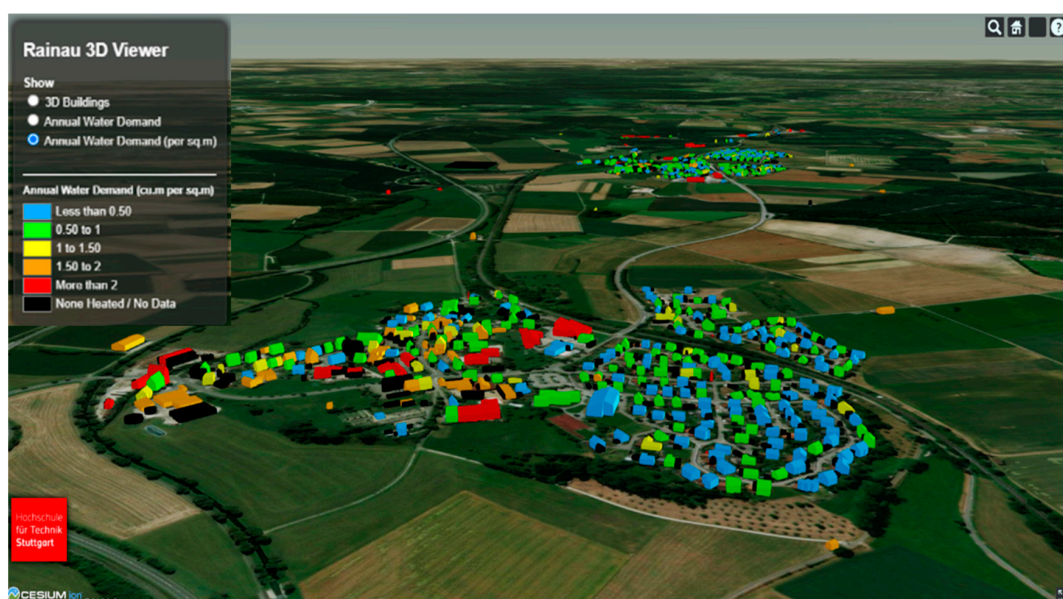


Figure 7. Visualization of water demand per square meter per building in m^3/m^2 in Rainau with CityGML and satellite map.

5. Discussion

A newly established workflow with the function of water demand modelling in Germany was introduced to an existing urban energy simulation platform based on widely available CityGML models and standard statistical data as its key inputs. Next to being based on these data types, the uniqueness of the new workflow is to allow a resolution down to the single building, whereas existing water demand models focus more on the municipal (or even higher) levels. The annual water demand of individual residential households and non-residential buildings can be modeled and visualized in 3D.

The method fills the gap of assessing an individual building or city quarter's water data based on CityGML, thus allowing assessments to be performed with a limited set of input data. In residential buildings, the workflow models water demand per occupant had a deviation from 1% to 7% from the statistic values for three German counties. With enough confidence, we argue that the simulation tool is reliable in terms of calculating per capita water demand and total water demand in residential buildings with the correct CityGML input data model. There is more uncertainty of water demand simulation in non-residential buildings. However, the magnitude of demand value is at the same level. This accuracy is realized by considering local climate and some socio-economic factors. More importantly, the modelling process is fully automated, at least for Germany, but can be easily applied to other world regions, provided CityGML models and statistical data are available.

The workflow thus completes a gap in the analysis of regional food-water-energy nexus issues. For instance, a combination of its results with water demands from agriculture and local water availabilities allows us to assess the level of regional water stress and to define improved strategies for crop cultivation or water conservation in urban and rural areas. Such assessments can greatly help local governments to make strategical decisions on existing and new-built areas either in the current situation or in the future.

Because of the highly aggregated inputs, using values at country level, which might not always match the local situation, a certain level of uncertainty in the modelling results is added, e.g., using average German household size and occupancy rates. As a next step, local census data on key parameters should replace German average values, so that local resident number can be estimated more accurately, e.g., in dense urban areas.

The inaccuracy of building function can be eliminated by cross-checking CityGML with OpenStreetMap as OpenStreetMap is more frequently maintained by private users. Adding building function sub-classes of non-residential buildings can also improve the simulation accuracy, e.g., water demand in elementary school and university are distinctive, even though they are both classified under "education" in standard CityGML. Generally, limited statistical data are available on water demand of non-residential buildings. As a result, empirical values of water demand per area have to be taken from literature and studies focusing on the German national level. Adding on the German residential water demand method, the water demand simulation model is only restricted for the application in any city in Germany. Moreover, lacking water demand data in non-residential buildings makes the accurate validation of water demand in specific facilities difficult. This decreases the accuracy of the model. Here, a next step might be the gathering of relevant information from other sources to further improve modelling quality.

Author Contributions: Data curation: Keyu Bao, Rushikesh Padsala; Formal analysis: Keyu Bao; Investigation: Keyu Bao; Methodology: Keyu Bao; Software: Keyu Bao; Validation: Keyu Bao; Visualization: Rushikesh Padsala; Supervision: Bastian Schröter, Daniela Thrän; Writing—original draft: Keyu Bao; Writing—review and editing: Keyu Bao, Rushikesh Padsala, Bastian Schröter, Daniela Thrän. All authors have read and agreed to the published version of the manuscript.

Funding: This paper is part of the project IN-SOURCE (INtegrated analysis and modeling for the management of sustainable urban FEW ResSOURCES). This research was funded from the European Union's Horizon 2020 research and innovation program under grant agreement No 730254.

Acknowledgments: The authors would like to thank Matthias Betz for his support in Java programming, Sally Köhler for reviewing the paper as well as her precious advice. The 3D model, its extension and its

visualization are based on the data provided by the State Agency for Spatial Information and Rural Development Baden-Württemberg (LVG BY) (www.lgl-bw.de). The 3D map of case study Rainau is funded by project ENsource. The ENsource project (www.ensource.de) is funded by the Ministry of Science, Research and the Arts Baden-Württemberg and the European Regional Development Fund (ERDF). Reference number: CELEBR_ZAFH_1248932.

Conflicts of Interest: The authors declare no conflict of interest.

References

1. Vörösmarty, C.J.; McIntyre, P.B.; Gessner, M.O.; Dudgeon, D.; Prusevich, A.; Green, P.; Glidden, S.; Bunn, S.E.; Sullivan, C.A.; Liermann, C.R.; et al. Global threats to human water security and river biodiversity. *Nature* **2010**, *467*, 555–561. [[CrossRef](#)]
2. Alcamo, J.; Flörke, M.; Märker, M. Future long-term changes in global water resources driven by socio-economic and climatic changes. *Hydrol. Sci. J.* **2007**, *52*, 247–275. [[CrossRef](#)]
3. Weiler, V.; Stave, J.; Eicker, U. Renewable Energy Generation Scenarios Using 3D Urban Modeling Tools—Methodology for Heat Pump and Co-Generation Systems with Case Study Application. *Energies* **2019**, *12*, 403. [[CrossRef](#)]
4. Arbués, F.; García-Valiñas, M.Á.; Martínez-Espiñeira, R. Estimation of residential water demand: A state-of-the-art review. *J. Socio Econ.* **2003**, *32*, 81–102. [[CrossRef](#)]
5. Schleich, J.; Hillenbrand, T. Determinants of residential water demand in Germany. *Ecol. Econ.* **2009**, *68*, 1756–1769. [[CrossRef](#)]
6. Neunteufel, R.; Richard, L.; Perfler, R.; Tuschel, S.; Böhm, K.; Haas, E. Wasserverbrauch und Wasserbedarf. Auswertung Empirischer Daten zum Wasserverbrauch. Available online: <https://www.messe.de/files/000-fs5/media/downloads/deutsche-messe-nachhaltigkeitsbericht-2.pdf> (accessed on 11 August 2020).
7. Vine, E.; Diamond, R.; Szydlowski, R. Domestic hot water consumption in four low-income apartment buildings. *Energy* **1987**, *12*, 459–467. [[CrossRef](#)]
8. Kõiv, T.-A.; Toode, A. Trends in domestic hot water consumption in Estonian apartment buildings. *Proc. Est. Acad. Sci. Eng.* **2006**, *12*, 72–80.
9. Yao, R.; Steemers, K. A method of formulating energy load profile for domestic buildings in the UK. *Energy Build.* **2005**, *37*, 663–671. [[CrossRef](#)]
10. Fuentes, E.; Arce, L.; Salom, J. A review of domestic hot water consumption profiles for application in systems and buildings energy performance analysis. *Renew. Sustain. Energy Rev.* **2018**, *81*, 1530–1547. [[CrossRef](#)]
11. Ahmed, K.; Pylsy, P.; Kurnitski, J. Hourly consumption profiles of domestic hot water for different occupant groups in dwellings. *Sol. Energy* **2016**, *137*, 516–530. [[CrossRef](#)]
12. Troy, P.; Holloway, D. The use of residential water consumption as an urban planning tool: A pilot study in Adelaide. *J. Environ. Plan. Manag.* **2004**, *47*, 97–114. [[CrossRef](#)]
13. Proença, L.C.; Ghisi, E. Water end-uses in Brazilian office buildings. *Resour. Conserv. Recycl.* **2010**, *54*, 489–500. [[CrossRef](#)]
14. González, A.; García-Sanz-Calcedo, J.; Salgado, D. Quantitative Determination of Potable Cold Water Consumption in German Hospitals. *Sustainability* **2018**, *10*, 932. [[CrossRef](#)]
15. House-Peters, L.A.; Chang, H. Urban water demand modeling: Review of concepts, methods, and organizing principles. *Water Resour. Res.* **2011**, *47*. [[CrossRef](#)]
16. Maidment, D.R.; Miaou, S.-P.; Crawford, M.M. Transfer Function Models of Daily Urban Water Use. *Water Resour. Res.* **1985**, *21*, 425–432. [[CrossRef](#)]
17. Maidment, D.R.; Miaou, S.-P. Daily Water Use in Nine Cities. *Water Resour. Res.* **1986**, *22*, 845–851. [[CrossRef](#)]
18. Gato, S.; Jayasuriya, N.; Roberts, P. Temperature and rainfall thresholds for base use urban water demand modelling. *J. Hydrol.* **2007**, *337*, 364–376. [[CrossRef](#)]
19. Adamowski, J.F. Peak Daily Water Demand Forecast Modeling Using Artificial Neural Networks. *J. Water Resour. Plan. Manag.* **2008**, *134*, 119–128. [[CrossRef](#)]
20. Praskievicz, S.; Chang, H. Identifying the Relationships Between Urban Water Consumption and Weather Variables in Seoul, Korea. *Phys. Geogr.* **2009**, *30*, 324–337. [[CrossRef](#)]
21. Wong, J.S.; Zhang, Q.; Chen, Y.D. Statistical modeling of daily urban water consumption in Hong Kong: Trend, changing patterns, and forecast. *Water Resour. Res.* **2010**, *46*. [[CrossRef](#)]

22. Kaschub, T.; Jochem, P.; Fichtner, W. Solar energy storage in German households: Profitability, load changes and flexibility. *Energy Policy* **2016**, *98*, 520–532. [[CrossRef](#)]
23. House-Peters, L.; Pratt, B.; Chang, H. Effects of Urban Spatial Structure, Sociodemographics, and Climate on Residential Water Consumption in Hillsboro, Oregon. *JAWRA J. Am. Water Resour. Assoc.* **2010**, *46*, 461–472. [[CrossRef](#)]
24. Shandas, V.; Parandvash, G.H. Integrating Urban Form and Demographics in Water-Demand Management: An Empirical Case Study of Portland, Oregon. *Environ. Plan. B Plan. Des.* **2010**, *37*, 112–128. [[CrossRef](#)]
25. Wentz, E.A.; Gober, P. Determinants of Small-Area Water Consumption for the City of Phoenix, Arizona. *Water Resour. Manag.* **2007**, *21*, 1849–1863. [[CrossRef](#)]
26. Lee, S.-J.; Wentz, E.A.; Gober, P. Space–time forecasting using soft geostatistics: A case study in forecasting municipal water demand for Phoenix, Arizona. *Stoch. Environ. Res. Risk Assess.* **2009**, *24*, 283–295. [[CrossRef](#)]
27. Stollnberger, R.; Gebetsroither-Geringer, E.; Magerl, U. *Integrated Qualitative and Quantitative Analysis of Causal Urban Food-Water-Energy Relations towards More Climate-Resilient Cities*; REAL CORP: Aachen, Germany, 2020.
28. Nouvel, R.; Brassel, K.-H.; Bruse, M.; Duminil, E.; Coors, V.; Eicker, U. SimStadt, a New Workflow-Driven Urban Energy Simulation Platform for CityGML City Models. In Proceedings of the International Conference CISBAT 2015 Future Buildings and Districts Sustainability from Nano to Urban Scale, Lausanne, Switzerland, 9–11 September 2015.
29. Coors, V.; Betz, M.; Duminil, E. A Concept of Quality Management of 3D City Models Supporting Application-Specific Requirements. *PGF* **2020**, *88*, 3–14. [[CrossRef](#)]
30. Institut Wohnen und Umwelt GmbH. Institut Wohnen und Umwelt (IWU): Gebäudetypologie und Gebäudebestand. Available online: <https://www.iwu.de/publikationen/fachinformationen/gebaudetypologie/> (accessed on 12 August 2020).
31. Meteonorm. Meteonorm. Available online: <https://meteonorm.com/en/> (accessed on 12 August 2020).
32. Monsalvete Alvarez de Urribari, P.; Coors, V. A Dynamic Model for District-Scale Building Demand Simulation. In Proceedings of the Dynastee Symposium: The Building as the Cornerstone of our Future Energy Infrastructure, Bilbao, Spain, 10–11 April 2019.
33. Verordnung über Energiesparenden Wärmeschutz und Energiesparende Anlagentechnik bei Gebäuden (EnEV). Available online: https://www.gesetze-im-internet.de/enev_2007/ (accessed on 7 September 2020).
34. ZENSUS2011—Homepage. Available online: https://www.zensus2011.de/EN/Home/home_node.html (accessed on 11 August 2020).
35. Köhler, S.; Betz, M.; Bao, K.; Weiler, V. Determination of Household Size and Number of Occupants for Residential Buildings Based on Census Data and 3D-CityGML Building Models at Urban Scale in Germany. In Proceedings of the Building Simulation 2021 Conference, Bruges, Belgium, 1–3 September 2021; submitted.
36. Höglund, L. Household demand for water in sweden with implications of a potential tax on water use. *Water Resour. Res.* **1999**, *35*, 3853–3863. [[CrossRef](#)]
37. Pro-Kopf-Verbrauch von Wasser in Deutschland nach Bundesland 2016|Statista. Available online: <https://de.statista.com/statistik/daten/studie/249427/umfrage/wasserverbrauch-nach-bundesland/> (accessed on 18 August 2020).
38. Kitzerow, H.-G.; Magyar, P. Energiekonzept für die Sporthalle Süd. Available online: https://www.baua.de/DE/Angebote/Rechtstexte-und-Technische-Regeln/Regelwerk/ASR/pdf/ASR-A1-2.pdf?__blob=publicationFile (accessed on 11 August 2020).
39. Technischen Regeln für Arbeitsstätten. ASR A1.2 Raumabmessungen und Bewegungsflächen. Available online: https://www.baua.de/DE/Angebote/Rechtstexte-und-Technische-Regeln/Regelwerk/ASR/pdf/ASR-A1-2.pdf?__blob=publicationFile (accessed on 22 July 2020).
40. Deutschen Messe, A.G. *Bericht zur Nachhaltigkeit*; Deutsche Messe: Hannover, Germany, 2020.
41. Ministerium für Umwelt, Klima und Energiewirtschaft Baden-Württemberg und Statistisches Landesamt Baden-Württemberg. In *Energiebericht Baden-Württemberg 1985–1990. Wasser-Verbrauchskennwert Staatlicher Gebäude*; Statistisches Landesamt Baden-Württemberg: Stuttgart, Germany, 2018.
42. Pauen, W.; Piller, V. Hotelbewertungen: Flächen. Available online: https://www.reguvis.de/xaver/wertermittlerportal/start.xav?start=%2F%2F%5B%40attr_id%3D%27wertermittlerportal_2321513867%27%5D#__wertermittlerportal__%2F%2F%5B%40attr_id%3D%27wertermittlerportal_22494510091%27%5D__1595431618670 (accessed on 11 August 2020).

43. Statistisches Landesamt Baden-Württemberg. Öffentliche Wasserversorgung seit 2004 im Landesvergleich. Available online: https://www.statistik-bw.de/Service/Veroeff/Statistik_AKTUELL/803409006.pdf (accessed on 22 July 2020).
44. Statistisches Landesamt Baden-Württemberg. Wasserversorgung in Baden-Württemberg. 2009. Available online: https://www.statistik-bw.de/Service/Veroeff/Statistik_AKTUELL/803409006.pdf (accessed on 22 July 2020).
45. Ellwanger & Geiger. *Industrie- und Logistikflächenumsatz in der Region Stuttgart in den Jahren von 2010 bis 2018 (in Quadratmeter)*; Statista Research Department: New York, NY, USA, 2009.
46. STR. *Global Hotel Review (Media Version)—Constant Currency Edition. Industry Performance for the Month of December 2019*; STR Global: London, UK, 2020.
47. Bijl, D.L.; Bogaart, P.W.; Kram, T.; de Vries, B.J.M.; van Vuuren, D.P. Long-term water demand for electricity, industry and households. *Environ. Sci. Policy* **2016**, *55*, 75–86. [CrossRef]
48. Information und Technik Nordrhein-Westfalen Statistisches Landesamt. Landesdatenbank NRW. Available online: <https://www.landesdatenbank.nrw.de/ldbnrw/online> (accessed on 1 October 2020).
49. Thüringer Landesamt für Statistik. Thüringer Daten-Tabellen und Übersichten. Available online: <https://statistik.thueringen.de/datenbank/default2.asp> (accessed on 22 July 2020).
50. Bayerische Landesanstalt für Statistik. GENESIS-Online Datenbank. Available online: <https://www.statistikdaten.bayern.de/genesis/online/> (accessed on 22 July 2020).
51. Barnston, A.G. Correspondence among the Correlation, RMSE, and Heidke Forecast Verification Measures; Refinement of the Heidke Score. *Weather Forecast.* **1992**, *7*, 699–709. [CrossRef]
52. Census Database—Population, Households and Families-Key Figures. Available online: https://ergebnisse.zensus2011.de/?locale=en#StaticContent:16070,BEV_11_14,m,table (accessed on 11 August 2020).
53. Durchschnittliche Anzahl der Haushaltsmitglieder in Deutschland nach Bundesländern 2019|Statista. Available online: <https://de.statista.com/statistik/daten/studie/200374/umfrage/anzahl-der-haushalte-in-deutschland-im-jahr-2010-nach-bundeslaendern/> (accessed on 11 August 2020).
54. Nettoeinkommen—Bundesländer|Statista. Available online: <https://de.statista.com/statistik/daten/studie/5758/umfrage/verfuegbares-nettoeinkommen-nach-bundeslaendern/> (accessed on 11 August 2020).
55. Trink- und Abwasserpreise in Baden-Württemberg. Available online: <https://www.statistik-bw.de/Umwelt/Wasser/Trink-Abwasserpreise.jsp> (accessed on 12 August 2020).
56. Zweckverband Wasser und Abwasser Suhl. Gebühren und Beiträge-ZWAS Zweckverband Wasser und Abwasser Suhl. Available online: https://www.zwas.de/gebuehren_und_beitraege.php (accessed on 12 August 2020).
57. Statistisches Bundesamt. Entgelt für die Trink-Wasser-Versorgung in Tarifgebieten nach Tariftypen. Available online: <https://www.destatis.de/DE/Themen/Gesellschaft-Umwelt/Umwelt/Wasserwirtschaft/Tabellen/tw-07-entgelt-trinkwasserversorgung-tarifgeb-nach-tariftypen-2017-2019-land-bund.html> (accessed on 12 August 2020).
58. Abwassergebühren. Available online: <https://www.steb-koeln.de/abwasser-und-entwaesserung/abwassergebuehren/abwassergebuehren.jsp> (accessed on 12 August 2020).
59. Zensusdatenbank. Ludwigsburg—Fläche der Wohnung (20 m²-Intervalle). Available online: https://ergebnisse.zensus2011.de/#StaticContent:08118,WOHNFLAECHE_20S,m (accessed on 20 August 2020).
60. Statistisches Landesamt. *Baden-Württemberg. Entwicklung der Wohnflächenversorgung in den Städten und Gemeinden Baden-Württembergs*; Statistisches Landesamt: Stuttgart, Germany, 2020.
61. Thüringer Landesamt für Statistik. Bestand an Wohnungen in Wohn- und Nichtwohngebäuden am 31. Dezember nach Kreisen—Fortschreibung auf Basis der endgültigen Ergebnisse der Gebäude- und Wohnungszählung 2011 in Thüringen. Available online: <https://statistik.thueringen.de/datenbank/TabAnzeige.asp?tabelle=kr000716%7C%7C> (accessed on 20 August 2020).
62. Landesdatenbank Nordrhein-Westfalen. Fortschr. Wohngebäude- u. Wohnungsbestand GWZ2011 Wohngebäude, Wohnungen und Wohnfläche nach Anzahl der Wohnungen—Gemeinden—Stichtag. Available online: https://www.statistik-bw.de/Service/Veroeff/Monatshefte/PDF/Beitrag10_01_03.pdf (accessed on 20 August 2020).
63. Zensusdatenbank—Deutschland—Größe des privaten Haushalts. Available online: https://ergebnisse.zensus2011.de/#StaticContent:00,HHGROESS_KLASS,m (accessed on 20 August 2020).
64. Zensusdatenbank Deutschland. Einwohnerzahlen. Available online: <https://ergebnisse.zensus2011.de/#StaticContent:00,EINWOHNERZAHLEN,m> (accessed on 20 August 2020).
65. Zirak, M.; Weiler, V.; Hein, M.; Eicker, U. Urban models enrichment for energy applications: Challenges in energy simulation using different data sources for building age information. *Energy* **2020**, *190*, 116292. [CrossRef]

66. Statistisches Landesamt Baden-Württemberg. Fläche in Rainau nach Art der tatsächlichen Nutzung. Available online: <https://www.statistik-bw.de/BevoelkGebiet/GebietFlaeche/990160xx.tab?R=GS136089> (accessed on 26 August 2020).
67. Statistisches Landesamt Baden-Württemberg. Durchschnittsalter und Altersgruppen nach Geschlecht in Rainau. Available online: <https://www.statistik-bw.de/BevoelkGebiet/Bevoelkerung/01035100.tab?R=GS136089> (accessed on 7 September 2020).
68. Statistisches Landesamt Baden-Württemberg. Trink- und Abwasserpreise Rainau. Available online: <https://www.statistik-bw.de/Umwelt/Wasser/22025050.tab?R=GS136089> (accessed on 7 September 2020).
69. Schlomann, B.; Gruber, E.; Eichhammer, W.; Diekmann, J.; Ziesing, H.-J.; Rieke, H.; Wittke, F.; Herzog, T.; Barbosa, M.; Lutz, S.; et al. *Energieverbrauch der privaten Haushalte und des Sektors Gewerbe, Handel, Dienstleistungen. Bericht für das Bundesministerium für Wirtschaft und Arbeit*; Bundesministerium für Wirtschaft und Arbeit: Karlsruhe/Berlin/Nürnberg/Leipzig/München, Germany, April 2004.
70. BMVI. Strukturdatenprognose 2030. Available online: <https://www.bmvi.de/SharedDocs/DE/Artikel/G/strukturdatenprognose-2030.html> (accessed on 21 August 2020).

Publisher's Note: MDPI stays neutral with regard to jurisdictional claims in published maps and institutional affiliations.



© 2020 by the authors. Licensee MDPI, Basel, Switzerland. This article is an open access article distributed under the terms and conditions of the Creative Commons Attribution (CC BY) license (<http://creativecommons.org/licenses/by/4.0/>).

Chapter 3

Simulation and Analysis of Urban Green Roofs with Photovoltaic in the Framework of Water-Energy Nexus

Bao, K.; Thrän, D.; Schröter, B.

Proceedings of REAL CORP 2021, 26th International Conference on Urban Development, Regional Planning and Information Society. 2021, pp. 671-680. ISSN 2521-3938

Simulation and Analysis of Urban Green Roofs with Photovoltaic in the Framework of Water-Energy Nexus

Keyu Bao, Daniela Thrän, Bastian Schröter

(MSc.Keyu Bao, Center for Sustainable Energy Technology, Hochschule für Technik Stuttgart, Schellingstraße 24, D-70174 Stuttgart, keyu.bao@hft-stuttgart.de)

(Prof. Dr. Daniela Thrän, Department of Bioenergy, Helmholtz Center for Environmental Research, Torgauer Strasse 116, D-04247 Leipzig, daniela.thraen@ufz.de, Chair of Bioenergy System, Faculty of Economic Sciences, University of Leipzig, Grimmaische Straße 12, D-04109 Leipzig; thraen@wifa.uni-leipzig.de, Unit Bioenergy System, Deutsches Biomasseforschungszentrum GmbH, Torgauer Strasse 116, D-04347 Leipzig; daniela.thraen@dbfz.de)

(Prof. Dr. Bastian Schröter, Center for Sustainable Energy Technology, Hochschule für Technik Stuttgart, Schellingstraße 24, D-70174 Stuttgart, bastian.schroeter@hft-stuttgart.de)

1 ABSTRACT

Urban green infrastructures such as green roofs can reduce building energy demand, mitigate rainfall run-off and improve urban air quality. On the other hand, decentralized renewable energy systems such as rooftop photovoltaics (PV), are one of the key actions towards reducing a building's energy dependence and greenhouse gas emissions. This study assesses the technical and economic benefits of a combination of green roofs and PV systems and thereby considers increased PV yields, decreased building heat demands, and reduced rainwater runoff mitigation, that can stem from this combination. For this, two workflows within an urban simulation environment, SimStadt, were applied and extended for two city quarters in Stuttgart, Germany. The results show that by installing green roofs with PV systems where possible, annual PV yields increase by about 0.3%, annual space heating demands decrease by 0.1 %, and 30 % of rainwater runoff can be avoided in the case study areas. The economic cost-benefit analysis, however, shows that only around 31% of the initial investment can be recurred over the assets' lifetime.

Keywords: Simulation, Urban green infrastructure, Analysis, Water-Energy Nexus, Green roof with PV

2 INTRODUCTION

Globally, more and more people live in urban areas (Kotzeva and Brandmüller 2016). Next to its multiple benefits, increased urbanisation and densification pose problems such as pollution or urban heat island effects (McMichael 2000). Urban green infrastructure, i.e., parks, trees, lawns, and green roofs, can dampen these impacts by, for example, improving public health (Lee and Maheswaran 2011), reducing building energy demands (Castleton et al. 2010), mitigating water runoffs through water harvesting, and enhancing infiltration and evapotranspiration (Silvennoinen et al. 2017). In particular, green roofs improve stormwater management (Stovin 2007; Mentens et al. 2006), water run-off quality (Berndtsson et al. 2009), urban air quality (Yang et al. 2008), roof lifetimes (Teemusk and Mander 2009), and reduce the urban heat island effect (Doug et al. 2005) as well as building energy consumption (Lamnatou and Chemisana 2015; Movahhed et al. 2019; Wong et al. 2003) through reduced heat fluxes, increased solar reflectivity (Gaffin 2005) and increased building thermal masses (Niachou et al. 2001). Furthermore, the building's architectural interest and its rooftop biodiversity increase (Koehler 2003).

There are two types of green roofs, extensive and intensive, defined by the depth of the substrate layer (Speak et al. 2013). Extensive green roofs have a thin substrate layer (less than 150 mm) with low-level planting, typically sedum or lawn, and can be comparably lightweight in structure. Intensive roofs have a deeper substrate layer to allow deeper-rooting plants such as shrubs and trees to survive. Extensive green roofs are relatively maintenance-free and readily survive in European climates (Castleton et al. 2010). However, in regions with hot arid climates (annual temperature $\geq 18^\circ\text{C}$; annual precipitation $\geq 5 \times$ threshold for dryness as defined by (Peel et al. 2007)), irrigation of up to 9 mm per day (drip irrigation) can be required (van Mechelen et al. 2015).

On the other hand, the implementation of energy systems that produce heat and electricity from renewable energy sources is one of the key actions towards reducing a building's energy dependence and greenhouse gas emissions. Electricity production from photovoltaic (PV) panels is one option of utilising a building's roof. To maximise electricity output, PV module efficiency should be as high as possible. It is generally characterised by material limitation and decreases with increasing ambient temperature. Furthermore, PV cells exhibit long-term degradation if their surface temperature exceeds a certain limit (Rahman et al. 2015). Green roofs can reduce this effect since the evapotranspiration of the plants reduces ambient air

temperatures. Simulations and experimental works show that there is a relative increase in annual PV output on green surfaces that ranges from 0.08% (Witmer 2010) to 8.3% (Hui and Chan 2011).

The benefits of a combination of PV and a green roof on a single building have been studied before (Baumgartner et al. 2016; Silvennoinen et al. 2017; Hui and Chan 2011; Movahhed et al. 2019). The work of Carter and Keeler (2008), for example, conducted a cost analysis of green roofs plus PV at the urban watershed level. However, it applied average PV yield gains and heating energy cost savings across all buildings. To the knowledge of the authors, there is no existing tool that assesses a building's heating demand, rooftop PV yield, and rooftop water run-off in an integrated way, on a single-building level, with the option of scalability to city quarter or city level. To fill this gap, this study applied the urban simulation platform SimStadt that allows simulating building heating and cooling demands (Weiler et al. 2019) and rooftop PV yields (Rodríguez et al. 2017) on a single building level. The goal of the presented method is not to simulate PV yields of green roofs in very high detail as in Zheng and Weng (2020) and Scherba et al. (2011), but to contribute to research on the water-energy nexus in urban areas and provide guidance to urban planners.

The energetic impact simulation methods, including heating demand simulation workflow and roof PV simulation workflow, are introduced in section 2.1., while section 2.2 introduces the method to quantify the benefits of reduced water run-offs. The cost-benefit analysis method of green roofs plus PV is introduced in section 2.3. A case study is introduced in section 2.4, followed by results (section 3), and a discussion (section 4).

3 MATERIAL AND METHOD

3.1 Energetic impacts of PV-green roof

This work considers two aspects of the energetic impact of green roofs with PV: (i) higher PV module conversion efficiencies due to the evaporative cooling effect of rooftop green, and (ii) heating and cooling demand reductions due to lower U-values (better insulation of green roofs compared to conventional roofs).

Rooftop PV potentials and hourly yields can be simulated by the appropriate workflow in SimStadt (Rodríguez et al. 2017). It uses 3D building models in the CityGML data model as basic input (Open Geospatial Consortium 2021). Besides the CityGML model, one of the input parameters is PV module efficiency, with a value of 15% taken as a base case for non-green roofs (Rahman et al. 2015). The output of the workflow is a CSV file including PV potential in MWh/a and monthly irradiance in W/m². The PV module efficiency difference is the decisive factor in electricity yields between non-green roofs and green roofs. The efficiency changes of PV modules on green roofs are not only a result of a drop in ambient temperature but also of the reflection albedo factor of the plants, which is higher than a non-greened roof (Lamnatou and Chemisana 2015). A monthly average PV module efficiency change was applied based on previous research by Nagengast et al. (2013) to align better with the existing workflow output. Linear regression equations were used to find the relationships between ambient temperature, PV back-surface panel temperature (equation 1), and hence PV module output (equation 2) for both roof types (Nagengast et al. 2013). In this paper, the module cell temperature is equal to the back-surface panel temperature.

$$T_{module} = \beta_0 + \beta_1 T_{ambient} \quad (1)$$

$$P = \beta_2 + \beta_3 T_{module} + \beta_4 I \quad (2)$$

Where T_{module} is the PV module cell temperature in °C, $T_{ambient}$ is the ambient air temperature in °C, P is the PV output in kW, and I is the solar irradiance on PV module in W/m². The power data was collected over one year in Pittsburg, USA, of the same polycrystalline 275 W PV modules tilted at 15°. The power modules were 1.96 m by 0.99 m, mounted faced south. The coefficients for both roof types are subsumed in table 1:

Coefficient	Non-green roof	Green roofs
β_0	1.2	1.3
β_1	1.5	1.3
β_2	0.17	0.1

β_3	-2.4E-03	5.6E-04
β_4	0.013	0.013

Table 1: Regression values for non-green and green roofs(Nagengast et al. 2013).

Monthly average irradiance on PV panels from SimStadt, and monthly average ambient temperature from Meteonorm (2021) were the monthly inputs for equations 1 and 2. Multiplied by the hours per month, PV potential on two types of roofs could be calculated.

The building's heating and cooling demand with and without green roofs, driven by a decrease of the roof's U-value in the latter case, will be simulated with the heating-demand-with-refurbishment-scenarios workflow in SimStadt(Weiler et al. 2019; Zirak et al. 2020). The heating demand simulation workflow also used a CityGML file as the main input. Furthermore, buildings were classified based on their function and year of construction. A building physics library in SimStadt then applied relevant physical properties such as U-values for walls, roofs, and windows to each class of buildings. These properties were subsequently applied to the actual building geometries of a given case study [11]. Similar to a building physics library, a usage library was based on several German norms and standards, focusing on heating setpoint temperatures, occupancy schedules, and internal gains that are different according to the usage (residential, office, retail, etc.) of each building. The U-value of green roofs could be set for roof-only refurbishment scenarios in SimStadt.

According to the German Building Energy Act of 2020 ("Gebäudeenergiegesetz", GEG), the required U-value is 0.24 W/(m²K) for new buildings(GEG). Green roofs have a U-value between 0.24 to 0.34 W/(m²K)(Niachou et al. 2001). From an energy standpoint, savings were thus limited by installing a green roof on a new building. However, for non-insulated roofs, the U-value could be reduced up to 92% by applying green roofs (Niachou et al. 2001). It is assumed here that only flat roofs, i.e. with a tilt of less than 10°, can be retrofitted into green roofs.

3.2 Rainfall mitigation

In addition to energetic aspects, the reduction in rainwater runoff from green roofs was investigated. The share of rainwater runoff of total precipitation can be as high as 91% for a non-greened roof and as low as 15% for an intensive green roof. Main influencing factors include the depth of the substrate layer, rain duration, rain intensity, and the antecedent dry weather period, while the age of the green roof, slope angle, and length are not measurably correlated to yearly run-offs(Mentens et al. 2006; Garofalo et al. 2016). On a roof with solar PV panels, a green "upgrade" should be restricted to extensive or low-profile vegetation to avoid shading of the PV panels(Hui and Chan 2011). Based on the previous observations, a relationship was obtained between the runoff depth (RD) in mm, i.e., the amount of rainfall turns into the ground surface runoff, or precipitation depth (PD) in mm, and the antecedent dry weather period (ADWP), i.e. the period between two independent rainfall events in hours(Garofalo et al. 2016). The relation is shown in equation 3, which exhibits an R² of 0.99. The assumed substrate layer was 80 mm belonging to an intensive green roof:

$$RD = -0.24 + 1.01 PD - 0.27 \ln ADWP \quad (3)$$

The hourly precipitation data over a year was a part of the climate data package used in SimStadt for energetic simulation in section 2.1. Based on this information the PD and ADWP of each rainfall event in the year were identified. Combined with equation 3, the RD of the rainfall events could be calculated.

3.3 Economic analysis of green roofs

Apart from the technical benefits of PV plus green roofs, favourite economic factors are crucial to achieve relevant penetration rates. A cost-benefit analysis is widely recognised as a useful framework for assessing the positive and negative aspects of prospective actions and policies, and for making the economic implications alternatives an explicit part of the decision-making process (Kenneth J. Arrow et al. 1996). One approach to cost-benefit analysis is to use the net present value (NPV) to compare alternative approaches with possibly different lifetimes, investments, and operating costs(Carter and Keeler 2008).

The incremental green roof construction costs is 36.5€/m² to 60.0€/m² compared to non-green roofs (Carter and Keeler 2008). In the following, an average cost of 48.25 €/m² was used. For rooftop PV systems of less than 100kW_p that were put into operation before January 2021, the feed-in tariff in Germany is 8,16

€cent/kWh for 20 years (Wirth 2021). Based on the energy carrier mix in the heating sector (Eichhammer et al. 2019) and average heating cost for individual heating technologies (Verbraucherzentrale Rheinland-Pfalz e.V. 2017), the average heating cost in Germany was around 10 € cent/kWh in 2019.

The prevailing German caselaw calls for separate stormwater fees based upon estimates of the actual contribution of a parcel to the total stormwater burden (Nickel et al. 2014). Stormwater fees in Germany are based upon individual parcel assessments and are determined by the surface area which drains to the central conveyance system, with an average annual stormwater charge of 0.89€ per m² impermeable surface. Green roofs were rewarded with a discount, typically 50% (Ansel et al. 2011). The economic benefits of stormwater mitigation were thus set at 0.45 €/m² of impermeable surface annually.

The parameters for the cost-benefit analysis were summarised in table 2.

Parameters	Green roof investment cost	Green roof lifetime	Feed-in electricity price	Heating cost	Discount rate (KfW 2021)
Unit	€/m ²	Years	€/kWh	€/kWh	%
Value	48.25	60	0.086	0.098	2.3%

Table 2: Cost and benefit of integrated PV green roof.

3.4 Case study and input data

A major part of the city center of Stuttgart, Germany, currently undergoes significant redevelopment in the context of the construction of a new underground central rail station. The two case study areas in Stuttgart's city center include an area with existing buildings that could be retrofitted with green roofs and PV systems, and an area still covered with railway tracks that will develop into a new neighborhood. The two areas are thus representative for two common situations faced by urban planners, architects, project developers, and city authorities. The developed tools can thus contribute to improving the planning of so-called technical master plans (Grassl 2013).

The area defined here as Hauptbahnhofviertel is covered with buildings (red in figure 1). As mentioned in section 2.3., a flat roof with a slope of less than 10° was assumed to be convertible into a green roof. It is thus important to have detailed knowledge of building envelopes, provided in our case by the 3D building model in the CityGML data format. Generally, building models in CityGML format are available in five Levels of Details (LoD), with LoD 0 relating to a planar shape representing a building's floor plan, LoD1 relating to buildings as blocks with average building height and a flat roof, LoD2 to models with additional information on building heights and particularly roof shapes, while LoD3 introduces windows and LoD4 information on (interior) ground plans and wall thicknesses as further information (Weiler et al. 2019). Furthermore, building functions, e.g., residential, office, etc., and year of construction (Zirak et al. 2020) can be attached. The LoD2 data model of great Hauptbahnhofviertel area was provided by the City of Stuttgart Measurement Office (Landeshauptstadt Stuttgart 2021). According to satellite images (BKG 2021), most of the existing flat roofs in the investigated area already covered with green roofs. To reduce complexity, it was assumed that 10% of flat roofs in the area still non-green roofs.



Fig. 1: Illustration of city quarter great Hauptbahnhofviertel (red) and Rosensteinviertel (blue). Source: Landeshauptstadt Stuttgart, Stadtmessungsamt

The other area studied here, Rosensteinviertel, is to date covered with railway tracks and rail-related buildings (blue in figure 1). After 2025, it will be converted into a mixed-use block with offices, retail space, and residential areas. As all the buildings in the Rosenstein quarter will be new-built, thus adhering to the latest energy efficiency standards, this part of the case study aimed to demonstrate an integrated rooftop approach, i.e. featuring green covers and PV panels, in new-built areas. For this area, a 3D building model in LoD 1 CityGML format was created based on the current state of planning (ASP ARCHITEKTEN 2019), shown in figure 2. A further assumption thus was that all newly constructed buildings will feature flat roofs, supported by the available planning material.

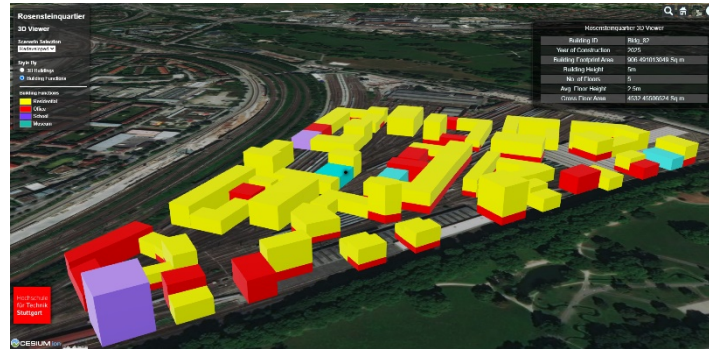


Fig. 2: LoD1 building data model of to-be-constructed buildings in Rosensteinviertel. Source: HFT Stuttgart

Besides this geoinformatics data, climate data (precipitation, temperature, irradiation, etc) of the last 10 years as well as for 2030, 2040, and 2050 in Stuttgart was sourced from Meteonorm (Meteonorm 2021).

4 RESULTS

4.1 Energetic benefits

Table 2 shows the energetic benefits, including electricity generation potential and heating demand, for the two case study quarters.

In the great Hauptbahnhofviertel area (red in figure 1), electricity generation potentials from rooftop PV systems were 180 GWh/a, including 2,7 MWh from angled roofs. Due to better thermal insulation, the buildings with green roofs had lower heating demands. For LoD1 buildings without roof details, the decrement amount of heating demand is 0.1%; while all LoD2 buildings with flat roofs consumed 0.04% less heating energy according to simulation. This difference was brought by the missing information on the shape and its heating situation of attics of the LoD1 model (Nouvel et al. 2017). As all the buildings in Rosensteinviertel were assumed to be constructed with a U-value of 0.24 W/(m² K), there is no additional benefit in terms of heating demand savings. PV systems can nevertheless be installed, also in combination with green roofs, with a yearly PV yield increase of 0.3%.

Building model	Roof angle	Roof condition	Hauptbahnhofviertel		Rosensteinviertel	
			PV generation [MWh/a]	Heating demand [MWh/a]	PV generation [MWh/a]	Heating demand [MWh/a]
LoD1	Flat	Status Quo	768	2,450	1,734	14,933
		Green Roof	770	2,447	1,740	14,933
		Difference	0.3%	-0.1%	0.3%	0.0%
LoD2	Flat	Status Quo	14,801	160,844	0	0
		Green Roof	14,855	160,775	0	0
		Difference	0.3%	-0.04%	0	0
	Angled		2,721	27,671	0	0

Table 2: Energetic benefits, including electricity generation potential and heating demand, in Hauptbahnhofviertel and Rosensteinviertel.

Energetic benefits of green roofs were also simulated in 10-year intervals until 2050, thus integrating changing climatic conditions.¹ In 2050, PV systems on green roofs would produce on average 0.31% more electricity than on non-green roofs per year. However, heating demands regardless of the roof types experienced a more pronounced drop of 5% till 2050. Nevertheless despite the warmer climate in winter, by retrofitting them into green roofs, the heating demands of existing buildings with non-green roofs could decrease by around 0.7 %.

The annual specific PV yields of buildings with various geometries are only determined by the available roof area, as it is assumed that irradiance is constant within a city quarter. However, a building's geometry has a decisive impact on its space heating demand: the larger the ratio between a building's volume and its ground area, the less heat dissipates through the roof. Figure 3 gives an example: the slim high-rise building (blue) has a smaller footprint than the lower building (yellow) of similar volume. In this case, upgrading the roof would be more important for the yellow building.

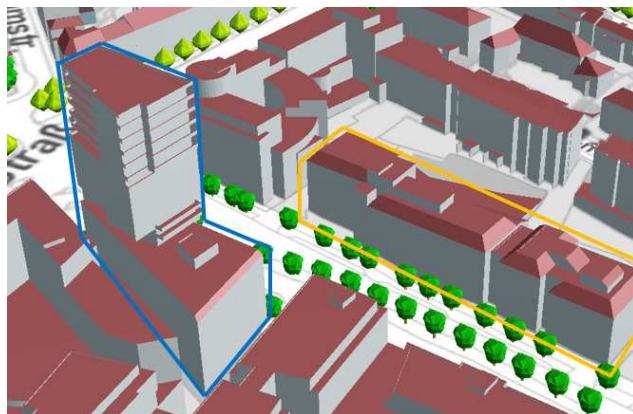


Fig. 3: Buildings from case study area of different geometry with similar volume to ground area ratio. Source: Source: LHS Stuttgart, Stadtmessungsamt

4.2 Rainfall-runoff mitigation benefit

In the Hauptbahnhofviertel, flat roofs make up 87% of the total roof area of 4.1 million m². As mentioned in section 2.4., 10% of this area had the potential to be converted into green roofs with the ability to better mitigate stormwater events and to decrease rainwater run-offs, while in Rosensteinviertel the whole roof area of 76,000 m² is assumed to be flat roofs (ASP ARCHITEKTEN 2019).

In 2020, annual precipitation in Stuttgart was 711 mm and was forecasted to increase by about 2 mm/a every 10 years until 2050. Without green roofs, the precipitation would be collected in the tank, or redirected to the garden, or go directly to the sewage system in the absence of rainwater storage systems or ground-based percolation systems (Ansel et al. 2011). Green roofs can absorb and store around 30% (table 3) of the rainfall on an annual basis according to equations 1 and 2. The study by (Uhl and Schiedt 2008) shows that the rainfall run-off of green roofs can be reduced by 32% in Münster, Germany, which shares a similar precipitation amount and pattern as in Stuttgart. The aligned results confirmed the accuracy of the method.

City quarter	Precipitation	Flat roof area	Run-off of non-green roofs	Run-off of green roofs	Difference
Unit	mm/a	1,000 m ²	1,000 m ³ /a	1,000 m ³ /a	%
Hauptbahnhof	711	359	256	179	-29.9%
Rosenstein		77	55	38	

Table 3: Total run-off on normal roofs and green roofs with precipitation amount in the year 2020.

Figure 4 shows the ratio between mitigated runoff and precipitation on green roofs in 2020 (left) and 2050 (right) in rainfall events of differing precipitation and ADWPs of differing lengths. Generally, green roofs absorbed 100% of the rainfall if the precipitation amount per event was <1 mm and ADWP >100 h. Although the total 2050 precipitation does increase by 6 mm/a from 2020 to 2050, the rainfall pattern became more extreme, with (1) increased precipitation per rainfall event, indicated by more raster blocks with precipitation

¹ According to meteorological data, average winter temperatures in Stuttgart (November to February) increase from 3.4°C to 4°C, while average summer temperatures (June to August) increase from 19.1°C to 19.9°C between 2020 and 2050.

amount to more than 5 mm, (2) a longer dry period between two rainfall events, indicated by an ADWP value of up to 300 h compared to 250 h in 2020. The positive relation between rainwater retention of green roofs and ADWP according to equation 3 roughly compensated for the reduced retention with the increased precipitation amount per rain event. Green roofs were predicted to mitigate 30.2% of annual precipitation in the year 2050 comparing with 29.9% in the year 2020.

As indicated in section 3.2, the area, tilt, and orientation of roofs have only limited impacts on rainfall runoff mitigation and are thus not included in equation 3. Therefore, the rainfall mitigation efficiency is similar between city quarters with similar rainfall patterns. The amount of mitigated rainfall should thus be similar for quarters with similar values of roof area per ground area.

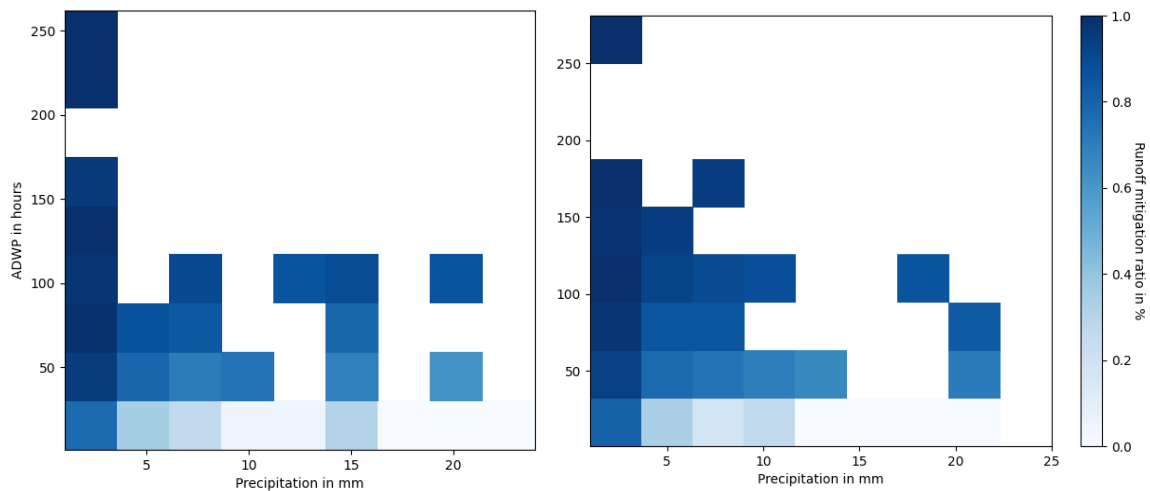


Fig. 4: Ratio between mitigated runoff in relation to ADWP (the period between two independent rainfall events) in hours, and precipitation per rainfall event in mm on green roofs in the year 2020 (left) and in the year 2050 (right).

4.3 Cost-benefit analysis

Economic benefits of green roofs were estimated for both city quarters as shown in table 4. The results are based on the assumption that (1) all green roofs were installed with PV modules; (2) 10% of all the current flat roofs were non-green roofs; (3) no stormwater management solutions were applied today, (4) the lifetime of green roofs is 60 years, (5) the annual discount rate is 2.3% (KfW 2021). The annual benefits over the lifetime were discounted to the present value in the same year with the investment. In great Hauptbahnhofviertel, a 0.3% increase of PV module efficiency increases revenues through feed-in to the grid by 0.66 million €, which compensated about 1% of the area's green roof renovation cost of 17.3 million €. The benefit of heating savings over 60 years of around 23,000 € was the least significant factor (< 0.1 million €). Mitigation of rainwater runoff brought the largest benefit, with 5.3 million €. Overall, all the benefits brought by green roof renovation were not sufficient for a positive NPV for green roof investment, as the total lifetime NPV is negative.

Similar to Europaviertel, in Rosensteinviertel the NPV of the benefits and the cost was -2.6 million €, which was not sufficient to initiate the green roof transition. The total energetic benefits accounted for 0.014 million €, which is much lower than in Hauptbahnhof, as there was no heating saving potential for new-built.

		Hauptbahnhof	Rosensteinviertel
Green roof renovation cost	10 ⁶ €	17.34	3.71
Benefits from feed-in tariff	10 ⁶ €	0.13	0.014
Benefits from heating saving	10 ⁶ €	0.023	0
Benefits from stormwater mitigation	10 ⁶ €	5.30	1.13
NPV	10 ⁶ €	-11.89	-2.60

Table 4: Comparison of green roofs' benefits in Europaviertel and Rosensteinviertel in NPV of the whole lifetime.

5 DISCUSSION

This paper applied validated energy simulation workflows in the urban energy simulation platform SimStadt to assess the energetic and stormwater mitigation benefits of green roofs. The use of one unified single input of building model data in CityGML format ensured compatibility and comparability of results between PV yields, and heating demands. Greening all roofs in the newly built Rosensteinviertel and retrofitting 10% of roofs in the Hauptbahnhofviertel quarter would increase yields by about 0.3%. In addition, heating demands in the Hauptbahnhofviertel quarter might be reduced marginally by 0.1% through retrofitting 10% of buildings without green roofs. Looking at the retrofit-demanded buildings alone, about 0.7 % of the heating demands could be saved by improving the roof thermal characteristics alone. Furthermore, about 30% of the yearly rainwater run-off could be avoided through green roofs. More importantly, runoff during extreme rainfall events of > 20 mm could be reduced by more than 50%, reducing pressure on existing sewage systems in great Hauptbahnhofviertel and reducing infrastructure costs in the new-built Rosensteinviertel. To the knowledge of the authors, the study on how rooftop PV systems affect the extensive green roof rainfall mitigation ability is still missing. For future research, it is meaningful to quantify this effect.

In terms of a cost-benefits analysis the economic benefits of green roofs, namely increased PV yields, rainwater retention, and reduced heating demands were by far not sufficient to finance initial investments: over a lifetime of 60 years, only about 30% of investments could be recovered through operational savings in both city quarters. This was in line with results from (Carter and Keeler 2008), who showed that in a conventional setup (no reduction in green roof investments, no increase of heating cost, external factors such as improved air quality not included), green roofs were 19% more expensive than the normal roofs over the lifetime. For older buildings with high heating demands, e.g., the heating demands could be saved up to 2.5% in buildings built before 1950 and this resulted in a positive NPV over the lifetime.

The increasingly milder climate brings less heating demands: in Stuttgart, Germany, annual heating demands are expected to decrease by around 1.5% every 10 years until 2050. Therefore, in regions where heating in winter is the dominant use of energy, heating energy saving through the green roof are becoming even less attractive in the future; while green roofs in regions with cooling in summer as the more important source of energy use, green roofs can play an increasingly important role in energy savings, at least as long as irrigation demands can be restrained (Lamnatou and Chemisana 2015).

The proposed method can be applied to any location in Germany. It is also possible to apply the method internationally, when a local building physics library exists or can be created, i.e., information on typical U-values of building envelope components in different construction years. Generally, city quarters are expected to show similar characteristics if they (i) share a similar share of flat roof buildings (ii) have buildings with similar building physics properties, (iii) have similar building geometries, and (iv) similar precipitation patterns.

6 CONCLUSION

This work established a workflow that quantifies the benefits of green roofs on building heating demand, rainfall run-off mitigation, and electricity yield of roof PV systems at the city quarter or regional level. The 3D building model that serves as the main input and the structured process ensure flexibility, i.e., from buildings in a pre-planning stage to existing buildings for retrofitting, scalability, i.e., from a single building to the whole region, and transferability, i.e., to any location in Germany or possibly globally. This work can thus support architects, urban planners, and city authorities in the decision-making process concerning the nexus between green roofs and PV systems and the development of technical master plans for urban planning.

7 ACKNOWLEDGEMENT

The authors would like to thank Rushikesh Padsala for providing the LoD1 map of the Rosenstein quarter as part of the project M4_Lab. This research was funded by the project M4_Lab and IN-SOURCE (INtegrated analysis and modeling for the management of sustainable urban FEW ResSOURCES). M4_Lab is part of the "Innovative University" funding initiative funded by the Federal Ministry of Education and Research (BMBF) under the number 03IHS032A. The IN-SOURCE project was funded by the European Union's Horizon 2020 research and innovation program under grant agreement No 730254.

8 REFERENCES

- Ansel, W.; Baumgarten, H.; Dickhaut, W.; Kruse, E.; Meier, R. (2011): Leitfaden Dachbegrünung für Kommunen. ASP ARCHITEKTEN (2019): International competition Rosenstein, Stuttgart. Available online at <https://www.asp-stuttgart.de/en/portfolio-items/international-competition-rosenstein-stuttgart/>.
- Baumgartner, F.; Dreisiebner, A.; Carigiet, F.; Schär, D.; Baumann, T. (2016): Performance Analysis of PV Green Roof Systems. In 32nd European Photovoltaic Solar Energy Conference and Exhibition, pp. 1618–1622. DOI: 10.4229/EUPVSEC20162016-5CO.14.3.
- Berndtsson, Justyna Czemieli; Bengtsson, Lars; Jinno, Kenji (2009): Runoff water quality from intensive and extensive vegetated roofs. In *Ecological Engineering* 35 (3), pp. 369–380. DOI: 10.1016/j.ecoleng.2008.09.020.
- BKG (2021): GeoBasis-DE / BKG.
- GEG (2020): Building Energy Act.
- Carter, Timothy; Keeler, Andrew (2008): Life-cycle cost–benefit analysis of extensive vegetated roof systems. In *Journal of environmental management* 87 (3), pp. 350–363. DOI: 10.1016/j.jenvman.2007.01.024.
- Castleton, H. F.; Stovin, V.; Beck, S.B.M.; Davison, J. B. (2010): Green roofs; building energy savings and the potential for retrofit. In *Energy and Buildings* 42 (10), pp. 1582–1591. DOI: 10.1016/j.enbuild.2010.05.004.
- Doug, Banting; Hitesh, Doshi; James, Li; Paul, Missios (2005): Report on the Environmental Benefits and Costs of Green Roof Technology for the City of Toronto. Available online at <https://mpira.ub.uni-muenchen.de/70526/>.
- Eichhammer, Wolfgang; Fritz, Markus; Pehnt, Martin; Fritz, Sarah; Nast, Michael; Steinbach, Jan et al. (2019): German Sustainable Heating Solutions - Best practices and Application in China. Fraunhofer ISI; Ifeu; IREES. Sino-German Energy Partnership, Deutsche Gesellschaft für Internationale Zusammenarbeit (GIZ). Available online at https://www.isi.fraunhofer.de/content/dam/isi/dokumente/ccx/GIZ_China_Waerme/German_Sustainable_Heating_Solutions_EN.pdf.
- Gaffin (2005): Energy balance modelling applied to a comparison of white and green roof cooling efficiency.
- Garofalo, Giuseppina; Palermo, Stefania; Principato, Francesca; Theodosiou, Theodoros; Piro, Patrizia (2016): The Influence of Hydrologic Parameters on the Hydraulic Efficiency of an Extensive Green Roof in Mediterranean Area. In *Water* 8 (2), p. 44. DOI: 10.3390/w8020044.
- Grassl, Gregor C. (Ed.) (2013): SCIM (Sustainable City Information Model): State-of-the-art planning instruments for sustainable urban districts. PLEA2013 – 29th Conference, Sustainable Architecture for a Renewable Future. Munich, 10 – 12 September.
- Hui, Sam C. M.; Chan, Sook-Chien (Eds.) (2011): Integration of green roof and solar photovoltaic systems. Joint Symposium 2011: Integrated Building Design in the New Era of Sustainability. Hong Kong, 22 November.
- Kenneth J. Arrow; Maureen L. Cropper; George C. Eads; Robert W. Hahn; Lester B. Lave; Roger G. Noll et al. (1996): Is There a Role for Benefit-Cost Analysis in Environmental, Health, and Safety Regulation? In *Science* 272 (5259), pp. 221–222. DOI: 10.1126/science.272.5259.221.
- KfW (2021): Management Report and Financial Statements 2020.
- Koehler (2003): Plant survival research and biodiversity: lessons from Europe, p. 313.
- Kotzeva, Mariana M.; Brandmüller, Theodóra (2016): Urban Europe: statistics on cities, towns and suburbs: Publications Office of the European Union.
- Lamnatou, Chr.; Chemisana, D. (2015): A critical analysis of factors affecting photovoltaic-green roof performance. In *Renewable and Sustainable Energy Reviews* 43, pp. 264–280. DOI: 10.1016/j.rser.2014.11.048.
- Landeshauptstadt Stuttgart (2021): Stadtmessungsamt. Available online at <https://www.stuttgart.de/vv/verwaltungseinheit/stadtmessungsamt.php>, updated on 3/11/2021, checked on 3/11/2021.
- Lee, A.C.K.; Maheswaran, R. (2011): The health benefits of urban green spaces: a review of the evidence. In *J Public Health (Oxf)* 33 (2), pp. 212–222. DOI: 10.1093/pubmed/fdq068.
- McMichael, Anthony J. (2000): The urban environment and health in a world of increasing globalization: issues for developing countries. In *Bull World Health Organ* 78, pp. 1117–1126. DOI: 10.1590/S0042-9686200000900007.
- Mentens, Jeroen; Raes, Dirk; Hermy, Martin (2006): Green roofs as a tool for solving the rainwater runoff problem in the urbanized 21st century? In *Landscape and Urban Planning* 77 (3), pp. 217–226. DOI: 10.1016/j.landurbplan.2005.02.010.
- Meteonorm (2021): Meteonorm. Available online at <https://meteonorm.com/en/>, updated on 8/12/2020, checked on 8/12/2020.
- Movahhed, Yasin; Safari, Amir; Motamedi, Sina; Khoshkhou, Ramin Haghighi (2019): Simultaneous use of PV system and green roof: A techno-economic study on power generation and energy consumption. In *Energy Procedia* 159, pp. 478–483. DOI: 10.1016/j.egypro.2018.12.037.
- Nagengast, Amy; Hendrickson, Chris; Scott Matthews, H. (2013): Variations in photovoltaic performance due to climate and low-slope roof choice. In *Energy and Buildings* 64, pp. 493–502. DOI: 10.1016/j.enbuild.2013.05.009.
- Niachou, A.; Papakonstantinou, K.; Santamouris, M.; Tsangrassoulis, A.; Mihalakakou, G. (2001): Analysis of the green roof thermal properties and investigation of its energy performance. In *Energy and Buildings* 33 (7), pp. 719–729. DOI: 10.1016/s0378-7788(01)00062-7.
- Nickel, Darla; Schoenfelder, Wenke; Medearis, Dale; Dolowitz, David P.; Keeley, Melissa; Shuster, William (2014): German experience in managing stormwater with green infrastructure. In *Journal of Environmental Planning and Management* 57 (3), pp. 403–423. DOI: 10.1080/09640568.2012.748652.
- Nouvel, Romain; Zirak, Maryam; Coors, Volker; Eicker, Ursula (2017): The influence of data quality on urban heating demand modeling using 3D city models. In *Computers, Environment and Urban Systems* 64, pp. 68–80. DOI: 10.1016/j.compenvurbsys.2016.12.005.
- Open Geospatial Consortium (2021): CityGML. Available online at <https://www.ogc.org/standards/citygml>, updated on 3/2/2021, checked on 3/2/2021.
- Peel, M. C.; Finlayson, B. L.; McMahon, T. A. (2007): Updated world map of the Köppen-Geiger climate classification. In *Hydrology and Earth System Sciences* 11 (5), pp. 1633–1644. DOI: 10.5194/hess-11-1633-2007.
- Rahman, M. M.; Hasanuzzaman, M.; Rahim, N. A. (2015): Effects of various parameters on PV-module power and efficiency. In *Energy Conversion and Management* 103, pp. 348–358. DOI: 10.1016/j.enconman.2015.06.067.

- Rodríguez, Laura Romero; Duminil, Eric; Ramos, José Sánchez; Eicker, Ursula (2017): Assessment of the photovoltaic potential at urban level based on 3D city models: A case study and new methodological approach. In *Solar Energy* 146, pp. 264–275.
- Scherba, Adam; Sailor, David J.; Rosenstiel, Todd N.; Wamser, Carl C. (2011): Modeling impacts of roof reflectivity, integrated photovoltaic panels and green roof systems on sensible heat flux into the urban environment. In *Building and Environment* 46 (12), pp. 2542–2551. DOI: 10.1016/j.buildenv.2011.06.012.
- Silvennoinen, Sveta; Taka, Maija; Yli-Pelkonen, Vesa; Koivusalo, Harri; Ollikainen, Markku; Setälä, Heikki (2017): Monetary value of urban green space as an ecosystem service provider: A case study of urban runoff management in Finland. In *Ecosystem Services* 28, pp. 17–27. DOI: 10.1016/j.ecoser.2017.09.013.
- Speak, A. F.; Rothwell, J. J.; Lindley, S. J.; Smith, C. L. (2013): Rainwater runoff retention on an aged intensive green roof. In *Science of The Total Environment* 461–462, pp. 28–38. DOI: 10.1016/j.scitotenv.2013.04.085.
- Stovin (2007): Green Roofs—getting sustainable drainage off the ground, p. 11.
- Teemusk, Alar; Mander, Ülo (2009): Greenroof potential to reduce temperature fluctuations of a roof membrane: A case study from Estonia. In *Building and Environment* 44 (3), pp. 643–650. DOI: 10.1016/j.buildenv.2008.05.011.
- Uhl, M.; Schiedt, L. (Eds.) (2008): Green Roof Storm Water Retention –Monitoring Results. 11th International Conference on Urban Drainage. Edinburgh, Scotland, UK. Available online at <http://citeseerx.ist.psu.edu/viewdoc/summary?doi=10.1.1.455.6031>.
- van Mechelen, Carmen; Dutoit, Thierry; Hermy, Martin (2015): Adapting green roof irrigation practices for a sustainable future: A review. In *Sustainable Cities and Society* 19, pp. 74–90. DOI: 10.1016/j.scs.2015.07.007.
- Verbraucherzentrale Rheinland-Pfalz e.V. (2017): Kosten verschiedener Heizungssysteme im Vergleich. Available online at https://www.verbraucherzentrale-rlp.de/sites/default/files/2017-11/Einleger_Kostenvergleich_Heizungen%2024_08_2017_0.pdf.
- Weiler, Verena; Stave, Jonas; Eicker, Ursula (2019): Renewable Energy Generation Scenarios Using 3D Urban Modeling Tools—Methodology for Heat Pump and Co-Generation Systems with Case Study Application †. In *Energies* 12 (3), p. 403. DOI: 10.3390/en12030403.
- Wirth, Harry (2021): Recent Facts about Photovoltaics in Germany. Fraunhofer ISE.
- Witmer, Lucas Turner (2010): Quantification of the passive cooling of Photovoltaics using a green roof. Master of Science.
- Wong, N.H.; Cheong, D.K.W.; Yan, H.; Soh, J.; Ong, C.L.; Sia, A. (2003): The effects of rooftop garden on energy consumption of a commercial building in Singapore. In *Energy and Buildings* 35 (4), pp. 353–364. DOI: 10.1016/S0378-7788(02)00108-1.
- Yang, Jun; Yu, Qian; Gong, Peng (2008): Quantifying air pollution removal by green roofs in Chicago. In *Atmospheric Environment* 42 (31), pp. 7266–7273. DOI: 10.1016/j.atmosenv.2008.07.003.
- Zheng, Yuanfan; Weng, Qihao (2020): Modeling the Effect of Green Roof Systems and Photovoltaic Panels for Building Energy Savings to Mitigate Climate Change. In *Remote Sensing* 12 (15), p. 2402. DOI: 10.3390/rs12152402.
- Zirak, Maryam; Weiler, Verena; Hein, Martin; Eicker, Ursula (2020): Urban models enrichment for energy applications: Challenges in energy simulation using different data sources for building age information. In *Energy* 190, p. 116292. DOI: 10.1016/j.energy.2019.116292.

Chapter 4

A GIS-Based Simulation Method for Regional Food Potential and Demand

Bao, K.; Padsala, R.; Coors, V.; Thrän, D.; Schröter, B. Land 2021, 10, 880.
<https://doi.org/10.3390/land10080880>

Article

A GIS-Based Simulation Method for Regional Food Potential and Demand

Keyu Bao ^{1,*} , Rushikesh Padsala ² , Volker Coors ², Daniela Thraen ^{3,4,5}  and Bastian Schröter ¹

- ¹ Center for Sustainable Energy Technology, Stuttgart University of Applied Sciences, Schellingstraße 24, D-70174 Stuttgart, Germany; bastian.schroeter@hft-stuttgart.de
- ² Center for Geodesy and Geoinformatics, Stuttgart University of Applied Sciences, Schellingstraße 24, D-70174 Stuttgart, Germany; rushikesh.padsala@hft-stuttgart.de (R.P.); volker.coors@hft-stuttgart.de (V.C.)
- ³ Department of Bioenergy, Helmholtz Center for Environmental Research, Torgauer Straße 116, D-04247 Leipzig, Germany; daniela.thraen@ufz.de
- ⁴ Bioenergy System, Faculty of Economic Sciences, University of Leipzig, Grimmaische Straße 12, D-04109 Leipzig, Germany; thraen@wifa.uni-leipzig.de
- ⁵ Unit Bioenergy System, Deutsches Biomasseforschungszentrum GmbH, Torgauer Straße 116, D-04347 Leipzig, Germany; daniela.thraen@dbfz.de
- * Correspondence: keyu.bao@hft-stuttgart.de; Tel.: +49-711-8926-2939

Abstract: A quantitative assessment of food-water-energy interactions is important to assess pathways and scenarios towards a holistically sustainable regional development. While a range of tools and methods exist that assess energetic demands and potentials on a regional scale, the same is not true for assessments of regional food demand and potential. This work introduces a new food simulation workflow to address local food potential and demand at the regional level, by extending an existing regional energy-water simulation platform. The goal of this work is to develop a GIS-based bottom-up approach to simulate regional food demand that can be linked to similarly GIS-based workflows assessing regional water demands and energetic demands and potentials. This allows us to study food-water-energy issues on a local scale. For this, a CityGML land use data model is extended with a feed and animal potential raster map as well as a soil type map to serve as the main inputs. The workflow simulates: (1) the vegetal and animal product food potentials by taking climate, crop type, soil type, organic farming, and food waste parameters into account; (2) the food demand of vegetal and animal products influenced by population change, body weight, age, human development index, and other indicators. The method is tested and validated in three German counties with various land use coverages. The results show that restricting land used exclusively for energy crop production is the most effective way to increase annual food production potential. Climate change by 2050 is expected to result in annual biomass yield changes between -4% and 2% depending on the region. The amount of animal product consumption is expected to rise by 16% by 2050, while 4% fewer vegetal products are expected to be consumed.

Keywords: bottom-up simulation; citygml; food demand; food potential; food-water-energy nexus



Citation: Bao, K.; Padsala, R.; Coors, V.; Thraen, D.; Schröter, B. A GIS-Based Simulation Method for Regional Food Potential and Demand. *Land* **2021**, *10*, 880. <https://doi.org/10.3390/land10080880>

Academic Editors: Davide Marino and Giampiero Mazzocchi

Received: 13 July 2021

Accepted: 20 August 2021

Published: 21 August 2021

Publisher's Note: MDPI stays neutral with regard to jurisdictional claims in published maps and institutional affiliations.



Copyright: © 2021 by the authors. Licensee MDPI, Basel, Switzerland. This article is an open access article distributed under the terms and conditions of the Creative Commons Attribution (CC BY) license (<https://creativecommons.org/licenses/by/4.0/>).

1. Introduction

Human demands for the consumption of food, water, and energy are forecast to continue to rise in the coming decades [1]. The challenge will be to meet these increasing demands sustainably across all dimensions [2]. Given the fact that natural resources do not operate in isolation, a detailed recognition of their influences on one another is required [3]. Therefore, a food potential simulation serves as an important element within the framework of the food-water-energy (FWE) nexus and allows us to, for example, study the impact of regional food production potentials on local bioenergy or free-field PV potential and vice versa.

Generally, a food system includes the elements of food production, harvesting, storage, processing, transportation, and consumption [4]. Due to their complexity, the understand-

ing of food system dynamics and the consequences of their rapid transformations is still limited [5]. Indicators such as food security, biodiversity, food safety, or nutrition factors that quantify the performance of energy system are chosen by countries and organizations [5]. In this paper, the consumers' food demand, which includes the minimal nutritious demand, storage, and waste for end consumers, and food production potential, which represents the calorie amount of food potential stored in biomass, are emphasized and addressed.

On the demand side, the change of diet and its impact on cropland use were studied in [6] and typical diets pattern and their projection are shown in [7]. Both studies showed that the long-term nutrition state was improving, and food consumption patterns moved from low to higher calorie diets. With socio-economic development, population growth rates decreased and diets changed: typically, consumption of animal protein, vegetable oils, fruits, and vegetables increased, while starchy staples became less important [6]. In food balance analysis, average statistical per-capita food availability values at a national level were usually used [8]. To identify the influencing factors to food intake demand, the method introduced in [9] provided the average per-capita food energy intake at the national level depending on the age, sex, country, birth rate, and population.

On the supply side, assessing yearly biomass mass potentials locally is the first step towards a regional food potential analysis. For such an analysis at the sub-country or country level, the most common way of acquiring crop production data is through statistical portals [8,10–12]. The advantage of this approach was its accuracy; however, statistical values are usually aggregated to the country or sub-country level and follow the administration boundary. Highly aggregated yield values, thus, lead to uncertainties if regional and sub-regional crop yield assessments are required, i.e., the statistical aggregated yield varies locally due to distinctly local climate and soil situations. To downscale the national yield data to a higher spatial resolution, a gridded crop yield raster map with a resolution of 5' was adopted in [13]. Still, the data was static from statistical sources without the possibility to study the influences of, e.g., climate change and irrigation. Moreover, food waste is not considered in this study. Rosenberg et al. simulated the potential changes for crops, only including wheat, rice, maize, and soybeans, caused by climate change at the global level using compatible crop models. The impacting factors included the current mix of rainfed and irrigated production, today's crop varieties, nitrogen management, and agricultural soils. However, the method was site-specific and aggregated to the national level [14].

Several studies analyzed the food inequality between food supply and consumption across countries and sub-regions adapting GIS (Geographic Information System) methods [10,15]. Merem et al. analyzed food security by presenting and comparing collected data with GIS methods at the national level. Without simulating socio-economic and natural environmental influences, the paper only presented grain food potential without distinguishing vegetable and animal food potential at the national aggregated level [15]. Khushi et al. investigated how disaggregated data on food consumption, nutrient demand, and production of major commodities on a sub-national level could be interlinked in the GIS environment to spatially analyze food consumption inequalities [10]. The food production was taken from statistical sources aggregated to the county (district) level. This restricts the approach to (i) a higher resolution, e.g., urban surroundings, and (ii) certain external environment changes, e.g., climate change. Furthermore, Beltran-Pena et al. performed an integrated, global assessment that considers a range of factors affecting future food production and demand until 2100 at the national level [11]. Driven by its scale, highly aggregated values at the national level and assumptions were used, e.g., the per-capita calorie demand is constant for all scenarios and regions, and climate change effects are considered only for certain crop types.

A regional food potential simulation tool is thus missing, which: (i) simulates the food potential using a bottom-up approach based on a dynamic biomass yield simulator for all crop types, considering impact factors including local climate, crop type distribution, or soil texture distribution; (ii) can be applied to any chosen region without strictly following

administrative boundaries at any level of scale, i.e., from community to county to federal state; (iii) builds on commonly available GIS data models for both potential and demand analysis; (iv) is integrated into an energy-water simulation platform [16], that can simulate the roof PV potential [17], heat demand [17], electricity profile [18], water demand [19], and bioenergy [20] to complete the workflow sets for assessing FWE nexus effects. This allows studies of trade-offs between local energy and food potentially on the same land areas by also considering constraints of local water resources—even more so after the workflows that assess free land PV and wind onshore potentials are finished.

The objective of this paper was to investigate regional food consumption and production potential with a high geographical resolution, building on commonly available digital landscape models as a key input on the supply side, as well as on the demand side if population data is missing. The goal was not to rival more specialized tools that focus on food demand or supply, but to extend an existing water-energy simulation platform with a reasonably accurate workflow for assessing regional food supply-demand balances and to thus be able to investigate trade-offs along the food-water-energy nexus at any regional scale. To give an example, a combination of the workflows allows us to assess the energetic benefits of applying wind onshore or free-field PV to varying degrees on different forms of land, and their impacts on irrigation water demand and local food production potential.

Regional food potential was simulated by extending an existing GIS-based biomass workflow based on food-related GIS data, e.g., crop calorie value, food waste, and animal product amounts (Section 2.1). Regional food demands are simulated by multiplying occupant numbers based on CityGML (City Geography Markup Language) 3D building objects and per-capita calorie demand considering several socio-economic indicators (Section 2.2). Three representative case study counties in Germany were chosen (Section 2.3) and used for validation (Section 2.4) and sensitivity analysis (Section 2.5).

2. Materials and Methods

Figure 1 gives an overview of the input (yellow) and output (blue) data and methods used in this study. SimStadt, which has been under constant development at HFT Stuttgart since 2012 [16], comprises a modular workflow management, with each workflow serving a specific purpose. To date, it can assess building-related demands (cooling and heating [21,22], residential electricity [18], water [19]) and renewable energy potential (rooftop photovoltaics [17] and biomass [20,23]) on a single-building or single-field level using 3D city models or digital landscape models in the CityGML format. CityGML is an open standardized data model and exchange format to store digital 3D models of cities and landscapes [24]. The biomass workflow which integrates the dynamic yield simulation tool AquaCrop [25] applies a bottom-up approach to simulate the biomass yield in weight as well as the technical bioenergy potential for each land polygon covered with biomass. This biomass workflow is used as a basis for the newly-established food potential workflow.

Table 1 shows the (spatial) resolution and the sources of the input data. The topographic inputs include land use, crop distribution, a soil distribution map, and a food calorie map. The land use map consists of Digital Landscape Model (DLM) data from Germany's Official Real Property Cadaster Information System (ALKIS) [26]. The DLM map consists of several object types, including building, waterbody, vegetation, or transportation. Since the land area dedicated to transportation purposes is stored as a line plus a buffer width, it can overlap with the vegetation layer, and the shared part of the vegetation layer needs to be cut out to avoid its inflation. DLM data accurately indicated the boundary and main usage of each land polygon. However, the specific crop type growing on polygons classified as agricultural land was missing. To fill this gap, the DLM data was combined with satellite data on crop types distribution from [27]. Plant-soil relationships in the surface soil layer affect crop productivity [28]. For this, a soil map for Germany from the Federal Institute for Geosciences and Natural Resources (BGR) was adopted. This map shows the distribution of typical soil types in the topsoils.

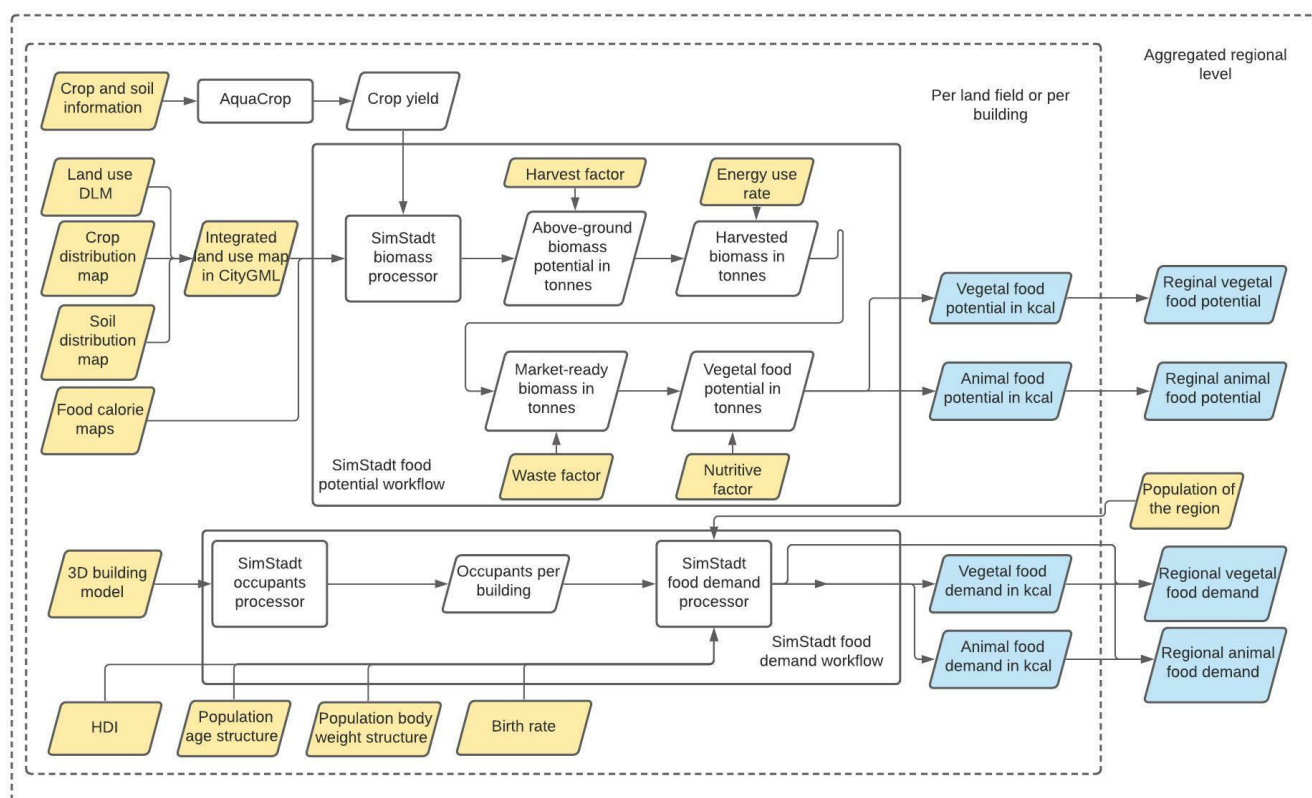


Figure 1. Flow chart diagram of inputs, models, and output of the methods presented in this paper. The data blocks with a yellow background are the inputs, and the ones with a blue background are the output.

Table 1. List of data used for this study.

Data	Spatial Resolution	Unit	Source
Nutritive factor	Per crop type	Kcal/100 g	Food and Agriculture Organization (FAO) [29]
Food waste rate	Per crop type	%	FAO [30]
DLM land use map	1:10,000/1:25,000 of the topographic objects; ± 3 m for linear objects	ha ⁻¹	AdV [26]
Crop type distribution	30 m	ha ⁻¹	Griffiths, Nendel et al. (2019) [27]
Soil distribution	1:100,000 (1 km)	ha ⁻¹	BGR [31]
Precipitation	Region	mm/a	Meteonorm [32]
Temperature	Region	°C	Meteonorm [32]
Atmospheric CO ₂ concentration	Region	ppm	FAO
Dietary pattern projection	Country	Kcal/cap/day	Kastner et al.; Pradhan et al. [6,7]
The factor of animal products out of local crop potential	5 arc min (around 6 km in southern Germany)	%	Pradhan et al. [13]

On top of these maps, climate data (precipitation, atmospheric temperature, and irradiance) for current and predicted situations were taken from Meteonorm [32]. The climatic data is available in hourly resolution for a chosen year. AquaCrop simulates the yields of all possible crops on all possible soil for biomass processors to use.

With the above-mentioned integrated land use maps, including information on land use, crop distribution, soil distribution, and climatic data, the biomass potential in weight was calculated with a single land polygon resolution. On top of this, food calorie maps

from Pradhan et al. provide information and a global gridded map on a crop's calorific production that is used as animal feedstock (FC), a crop's calorie production itself (CP), and animal calorie production (AP) [13]. Along with other additional input information, e.g., the nutritive factor that converts food weight into calorie values, the newly method assesses the annual vegetal and animal food potential in calorie values for each land polygon. This information can be aggregated to a regional level.

On the demand side, the Human Development Index (HDI), a population's age structure distribution, and the bodyweight of different age groups are the parameters that correlate strongly with current and future food calorie demand per capita [7]. If the food demand per building is required, or the study region is aligned with the administration boundary, a 3D building model containing all buildings in a given region can serve as an input for the SimStadt building occupant workflow [33] to estimate the population of the study region. However, food demand can also be assessed based on total population data, as is the case in this paper.

2.1. Food Calorie Potential

Data for animal feed, crop production, and animal production are typically provided in specific mass units, e.g., tonnes per hectare and year. Using nutritive factors [29], data were converted into calorific units, e.g., kcal per hectare and year, to be able to compare between crops and aggregate values. The crop calorie production (CP) was calculated according to Equation (1) below, using the simulated actual annual yield for a given crop (*cy*) from SimStadt biomass processor, land field area (*ha*), and nutritive factor (*nf*) (see Table S1 at Supplementary Data).

$$CP = nf \times cy \times ha \quad (1)$$

As the crop distribution map distinguished 9 food crop types (see Table 2), we only considered these 9 crop types with calorie potential, neglecting other, non-food crops. The detailed method of actual yield simulation using SimStadt and AquaCrop is presented in [20]. In [20], fruit orchards and grapevine are only considered from an energetic perspective. For this paper, static statistical fruit yields from [34] were adopted for assessing the food potential on top of the residue energy residue potential (See Table S2 in supplementary data).

Table 2. Crop categories with food and non-food use from the integrated land use map (land use [26] and crop type [27]). Only crops relevant to food production are considered in the subsequent analysis.

Crop Type for Food Use	Other Crops for Non-Food Use
Winter cereals	Grassland
Spring cereals	Grove
Maize	Deciduous mix forest
Winter rapeseed	Coniferous forest
Sugar beet	Short Rotation Coppice
Potato	
Fruit orchard	
Fruit orchard in grassland	
Fruit orchard in farming land	
Grapevine	

Pradhan et al. defined three food relevant parameters: (i) feed calorie for animals (FC) represents the amount of crop from agricultural land that serves as feedstock for animals; (ii) animal calorie production (AP) is the amount of calories of the animal products produced in the grid; (iii) crop calorie production (CP) is the amount of calories of the vegetal products produced in the grid [13]. The corresponding exemplary maps at the global scale can be found in Figures 2 and 3 in [13]. The study by Pradhan et al. generated three maps to show FC, AP, and CP individually, as well as two maps to connect these

three parameters: (i) a map showing the ratio between AP and FC, and (ii) a map showing the ratio between FC and CP. By combining these two maps, the ratio between AP and CP was obtained. Along with the CP values calculated in Equation 1, the animal food calorie potential (AP) could be determined. The two maps with food calorie information were provided in a raster grid of 5' resolution globally. We merged these two maps with the existing soil-crop-land use map. Since the soil-crop-land use map has a higher resolution, 79% of all the polygons are smaller than 30,000 m² while the two ratios are attached to each land-use polygon as extra attributes.

Furthermore, food waste rates from harvest to consumption (fw) (see Table S2 at Supplementary Data), and energetic use factors per crop (ef), i.e., the share of a crop's yield that is used purely energetically, were included to simulate the end vegetal calorie potential (EVP), i.e., the potential of market-ready vegetal products, based on Equation (2) and the end animal calorie potential (EAP), i.e., the potential of market-ready animal products, based on Equation (3). As no data is available on ef per polygon or raster cell, the same energetic use factor was applied to all polygons.

$$EVP = CP \times (1 - fw) \times (1 - ef) \times (1 - FC/CP), \quad (2)$$

$$EAP = CP \times (1 - fw) \times (1 - ef) \times AP/CP \quad (3)$$

As mentioned before, the total animal calorie potentials (AP) are linked to the crop calorie potential (CP) through the feed calorie for animals (FC) in the same grid. Grassland has no vegetal calorie potential, since only crops which can be used by humans directly were considered. Consequently, there is no animal calorie potential on grasslands. However, grass is an important feedstock for ruminant animals [35]. As all the land use polygons in the same food grid have the same AP-CP ratio and no animal calorie is excluded in the original map from [13], the animal calorie potential of grassland is distributed equally to all agricultural polygons in the same grid.

2.2. Food Calorie Demand

The two major factors determining a human's dietary energy requirements (DER) are the basal metabolic rate (BMR) and the physical activity level (PAL) [9,36]. BMR is the minimum amount of energy required for a human and depends on body weight, age, and sex [9,37], while PAL expresses a person's daily physical activity, which depends on lifestyle [9,36]. The dietary energy requirements for: (i) adults above the age of 20; (ii) infants, children, and adolescents; (iii) and pregnant women were calculated with different methods, which are shown in detail in supplementary Text S1. The method was taken from [9] without differentiating the calorie demands of different foods, i.e., it gives only one average aggregated daily calorie demand value per capita. As statistical bodyweight data from [38] is not differentiated between German federal states, the food calorie demand in this study was kept constant between states. Differences between regions stem from varying population growth [39], birth rates [40], and age distributions [41].

After a per-capita DER value was calculated, this total amount was divided into vegetal and animal calories according to statistical vegetal-animal food consumption shares from FAO [42] to align with the food calorie potential calculated in Section 2.1. It has to be noted, however, that the DER is lower than actual food consumption because of food wastage and losses in the household, for example during storage, preparation, and cooking.

Temporal Diet Pattern Change

Previous research estimated future per capita food demands on a country level until 2050 based on an exponential relationship between per capita animal product intake and the Human Development Index (HDI) [7]. Here, HDI was extrapolated with a logistic regression based on data from [43]. Logistic regression was chosen because the HDI is bounded to values between 0 and 1 (with 1 being the highest attainable score), with countries with a high HDI evolving more slowly. Further, this asymptotic behavior suggests

the existence of smooth development pathways [43]. The logistic regression formula is shown in Equation (4)

$$\text{HDI} = \frac{1}{1 + e^{-at+b}} \quad (4)$$

where t is a year, and a and b are the coefficients to fit available data. In this study, German federal states' annual HDI values between 1990 and 2017 [44] were used to derive a and b for each federal state. As an example, historical data and extrapolation values from 1990 until 2050 of the whole Germany are shown in Figure 2. For 1990 to 2017, the coefficient of determination R^2 between historical and calculated data is 0.99. The HDI of an individual federal state was interpolated to better reflect the local situation.

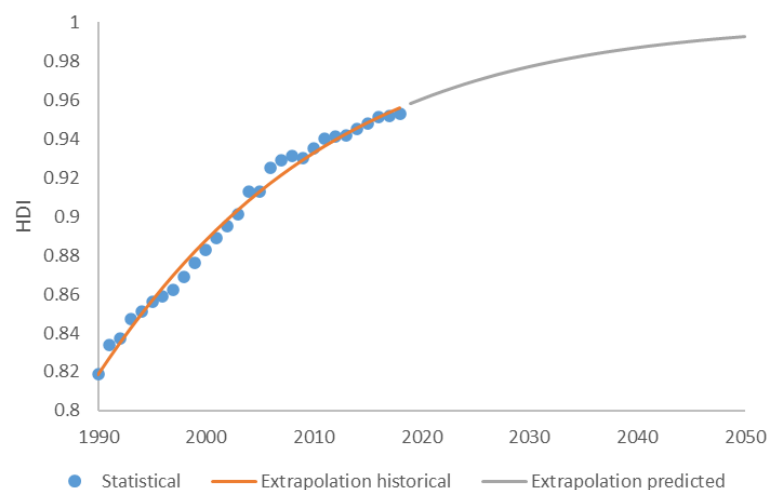


Figure 2. An example of HDI in Germany: historical data from 1990 to 2017 (blue), a fit curve of historical data (1990 to 2017, orange), and a fit and extrapolation for 2018 to 2050 (gray).

According to [5], the amount of total calorie demand, animal products, sugar-sweeteners, vegetable oils, and vegetables has an exponential relationship with HDI. The relation between c_i , the number of calories per category i [1000 kcal/cap/day], and the HDI can be expressed by Equation (5):

$$\log c_i = c_i + d_i \times \text{HDI} \quad (5)$$

where c_i and d_i are the coefficients per category, whose values are shown in Figure S6 and Table S7. The coefficient of determination R^2 between HDI and total food calorie is 0.8, and the R^2 between HDI and animal food calorie demand is 0.91 [7].

By combining Equations (4) and (5), a dietary pattern change in terms of food calorie demand for different food categories could be expressed as a function of the year. This is because the R^2 values of Equations (4) and (5) show a strong correlation between variables, a reasonably strong linkage between a given year and the food demand pattern change of the existing history. Additionally, the uncertainty of future diet pattern changes, e.g., reduced animal product consumption due to increased awareness on its impact on animal well-being or the climate, was not considered. With enough confidence, we argue that this method can be used to predict food demand change if the future diet pattern follows past developments.

Regarding the population of a given region, population numbers were taken from the statistical census portal for study regions with clear administration boundaries [41]. For regions where population data is not statistically available, e.g., randomly defined regions, the population can be simulated by a previously published method developed for SimStadt that calculates building occupant numbers for residential buildings based on high-resolution statistical census data and a 3D building model [33].

2.3. Case Study Regions

Three case study regions (German “Landkreise” or counties) were chosen for validation as well as sensitivity analysis out of a total of 400 German counties because, firstly, county-wide land use, soil, and crop distribution data are available, secondly, they differ concerning their agricultural land use, and thirdly, they are located in different parts of Germany, with differing climates.

1. Sub-urban: Ludwigsburg, Baden-Wuerttemberg, Southern Germany
2. Forest dominant: Ilm-Kreis, Thuringia, Mid-Eastern Germany
3. Agriculture dominant: Dithmarschen, Schleswig-Holstein, North Germany

The choice of these counties thus reflects the diversity of German and to some extent more broadly typical northern European landscapes. Table 3 provides key characteristics for each county and Figure 3 shows the location of the counties within Germany.

Table 3. Socio-economic and climatic data of the three German counties used for validation.

Parameter	Unit	Ludwigsburg	Ilm-Kreis	Dithmarschen
Area ¹	[km ²]	687	805	1428
Population density ²	[Pers./km ²]	794	132	93
Agricultural land cover rate ³	[%]	55	45	78
Forest cover rate ³	[%]	18	43	3

^{1,2} Federal Statistical Office of Germany [45]; ³ Federal Statistical Office of Germany [46].



Figure 3. Location of case study regions in Germany.

2.4. Validation

2.4.1. Food Demand and Consumption

Table 4 illustrates per capita food consumption and demand. As mentioned in Section 2.2, the amount of food consumption, i.e., the amount bought, is typically greater than physical food demand because of waste and storage. Data on food consumption is typically more easily available than the actual physical food demand of inhabitants [42]. Moreover, the food calorie demand method by [9] took the average PAL values of non-overweighted adults in the United States as a moderate PAL, but a PAL was not provided

for other countries. Since this paper focused on case studies in Germany, a validation process was executed to improve accuracy by eliminating the errors introduced by food waste, storage, and PAL.

Table 4. Comparison between simulated per capita food demand and statistical food consumption in the years 2005, 2009, 2013, and 2017.

Year	Mean Body Weight, in kg [38]	Simulated Physical Food Demand with Moderate PAL of the US, in kcal/capita/day	Statistical Food Consumption in, kcal/capita/day [42]	Difference in %
2005	74.9	2387	3450	31%
2009	75.6	2396	3515	32%
2013	76.3	2405	3498	31%
2017	77	2415	3542	32%

Body weight data and aggregated food demand for Germany are available for the years 2005, 2009, 2013, and 2017 [38,42]. These data were processed and listed in Table 3. As the mean body weight increases, simulated food demand increases in line, from 2387 kcal/capita/day to 2415 kcal/capita/day. Statistical data confirms this trend. However, the differences between simulated food demand and statistical food consumption are 31–32% for all years. This indicates that because of food waste and differences in PAL between Germany and the USA, actual German food consumption is about 31% higher than the simulated DER. Food consumption was thus derived from the physical food demand based on Equation (6).

$$\text{Food consumption} = \text{DER} \times 1.31 \quad (6)$$

2.4.2. Food Potential

Statistical food calorie potential and demand are only available at the national level. To validate results at a regional level, the crop calorie potentials map (CP) by Pradhan et al. with resolution of 5 arc degrees was adopted [13]. As validation reference, the gridded crop calorie potential map used downscaled data on simulated crop yields and area harvested from GAEZv3.0 for the year 2000 [47], with no more recent updates available. Therefore, GAEZv3.0 estimated crop yields and area harvested in a grid cell for the year 2000 based on FAO agricultural production statistics from the FAO.

The proposed methodology of food potential simulation was validated in the three case study counties. The crop calorie potentials simulated by SimStadt and by Pradhan and GAEZ as references are listed in Table 5. At the county level, the simulated results in our study varied from the results of Pradhan and GAEZ by −7%, 1%, and 26% in Ludwigsburg, IIm-Kreis, and Dithmarschen, respectively.

Table 5. Crop calorie potential simulated by SimStadt and by Pradhan and GAEZ.

Parameter	Unit	Ludwigsburg	IIm-Kreis	Dithmarschen
Crop calorie potential-SimStadt	[106 kcal]	583	477	1255
Crop calorie potential-GAEZ and Pradhan et al.	[106 kcal]	636	470	998
Difference		−7%	1%	26%

As mentioned in Section 2.1, the crop calorie potential map from Pradhan [13] has a resolution of 5 arc degrees (around 6 km for German latitudes), which typically covers more than 150 land use polygons from the DLM integrated land use map used for crop calorie simulation in SimStadt: as an example, Figure S6 in the supplementary data illustrates grid cells from [13] and land use polygons in Ludwigsburg county. As Figure 4 shows, 70% of the grid cells have a deviation of crop calorie potential between both approaches of −30%

and 30%. Large deviations can be due to grid cells not fully within a studied county, and the calorie potential of the grid being concentrated in the area outside the boundary, i.e., the grid cell's agricultural land lies primarily outside county boundaries and forests or urban areas can be found inside. See for example the grid cells along the left boundary in Figure S6.

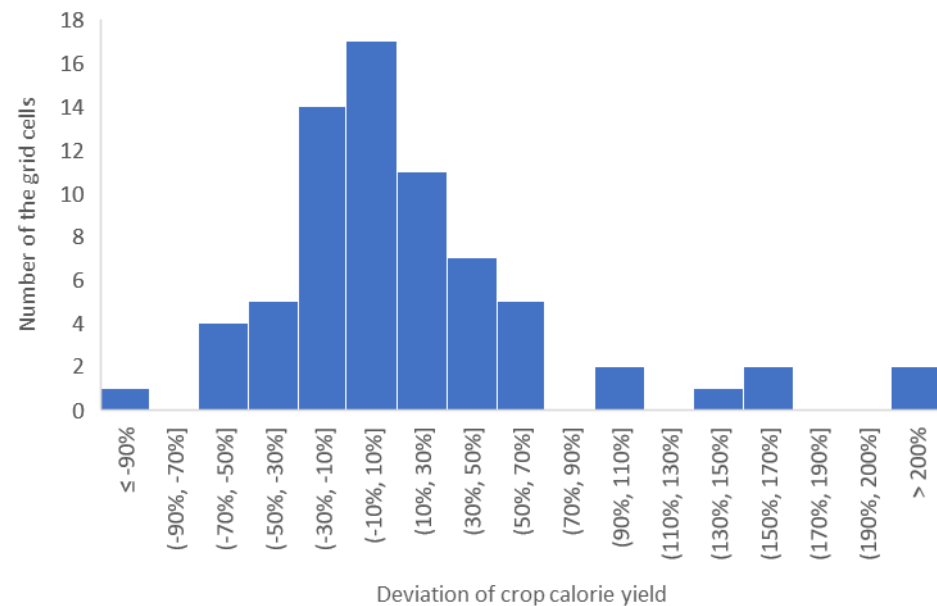


Figure 4. Histogram of deviations of results from SimStadt and GAEZ and Pradhan et al. The y -axis gives the number of grid cells within a deviation range as given on the x -axis.

2.5. Sensitivity Analysis

We defined four cases to project food production (S) and three cases to project food consumption (D) from 2020 until 2050. Case S1 is the baseline on the production side, with climate change from 2020 to 2050 as included in Meteorom data, the share of the organic farming area following historical growth rates, no artificial irrigation, and an energetic use factor of crops of zero after 2030 (Background: With the Renewable Energy Directive 2018/2001 (RED II), adopted in December 2018, the EU (European Union) is continuing to develop the political framework for the use of renewable energy sources in the transport sector for the period from 2021 to 2030 [48], while first-generation bioethanol, i.e., ethanol from crops, will be phased out until 2030). In the case of S2, RED II was not considered, allowing the energetic use of certain crops. This scenario serves as a second base case, since it allows for easier comparison of results before 2030 and afterwards.

In S1, the share of organic farmland in Germany follows historical statistical data [49] as shown in Figure S1, when the ratio increased from 1.6% in 2002 to 9.1% in 2018. In S1, we thus applied a linear fit to the historical trend. The 2050 share of the organic farming area then reaches 16.7%. Organic farming here refers to a sustainable agricultural system respecting the environment and animal welfare, but also includes all other stages of the food supply chain. To assess an organic farming yield in detail as compared to conventional methods, an extensive simulation tool that considers agricultural systems holistically would have been needed [50], which is beyond the scope of this study and the capabilities of the biomass simulation tool [20,51]. However, we examined the relative yield performance of organic and conventional farming systems globally and showed that organic farming land on average had 34% lower yields than conventional approaches in most comparable settings. Since the action plan for the development of EU organic farming aims to have at least 25% of EU agricultural land farmed organically by 2030 [52], case S3 assumed this value for 2030 and followed the same absolute increment percentage as in case S1 between 2030 and 2050. Lastly, case S4 includes artificial irrigation. A crop's

irrigation demand was determined by the minimal amount of external water that has to remain in the root zone throughout the growing cycle so that the given water stress was maintained in the growing season. The higher the water stress level, the lower the amount of water that was allowed to stay in the soil [20].

On the food demand side, D1 is the baseline case where the dietary pattern stays the same as in the year 2017, but changes in population change food demands. Population predictions were taken from [53]. In addition to population change, diet changes were considered in D2, with the changes following the extrapolating and prediction method of food demands prediction shown in Section 2.3. In D3, besides the population change and dietary demand change, a lower food waste rate was assumed: the EU and its member countries are committed to meeting the Sustainable Development Goal target to halve per capita food waste at the retail and consumer level by 2030 [54]. Sector 2.3.1 suggested a gap between food consumption, i.e., the number of calories people buy, and DER, i.e., the minimal amount of calories to maintain physical activity, of 31%. Therefore, a smaller gap of 15% was assumed in D3. All cases are summarized in Table 6.

Table 6. Scenario summaries with key parameter differences.

Case	Case Explanation
S1 (Baseline scenario for food supply)	Predicted future climate from 2020 to 2050 as provided by Meteonorm; energy crop percentage for relevant crops set to 14% from 2020 to 2030 and 0% from 2030 to 2050; share of organic farming follows the linear fitting curve based on historical data from 1994 to 2018
S2	Climate and organic farming area percentages are identical to S1, energy crop percentage stays at 14% after 2030
S3	Climate and energy crop percentage identical to S1, the organic farming area percentage set to 25% in 2030 and follows the same increment trend as in S1
S4	Climate, energy crop percentage, and organic farming area percentage identical to S3. Additional irrigation was added to keep water stress levels at 90%
D1 (Baseline scenario for food demand)	The dietary pattern stays the same as in the year 2017; population change was considered
D2	Dietary pattern changes and population changes were considered at the same time.
D3	Dietary pattern changes and population changes were considered at the same time. Half of the food waste was assumed to be avoided until 2050.

3. Results

3.1. Spatial Pattern of Food Potential

Figure 5 shows the vegetal and animal calorie potential density of each land use polygon in Ludwigsburg county. The built-up urban areas, roads, and water bodies are excluded and shown in white. The vegetal calorie potential is directly related to the land use type, as can be seen from the forested areas in the northwest, northeast, and south of the county, which have no food vegetal calorie potential. The high calorie (>15 million kcal/(ha a)) potential areas in green and blue coloring are cultivated with cereal and maize, while land areas with low to middle vegetal calorie potential (4 million kcal/(ha a) to 15 million kcal/(ha a)) are for example vineyards or fruit plantations. Polygons with a high animal potential are usually overlaid with polygons with a high vegetal potential: Figure 5 (right) shows that high animal calorie potential (>330 million kcal/(ha a)) was observed in the northwest of Ludwigsburg where grasslands and forests dominate. As animal feedstock is also imported, animal calorie potential can be higher than the vegetal calorie potential for certain polygons. But in general, the animal product calorie potential is around 10% of the vegetal calorie potential in Ludwigsburg in 2020. Similar results for county IIm-Kreis and Dithmarschen can be found in Figures S2 and S3 in supplementary data, respectively.

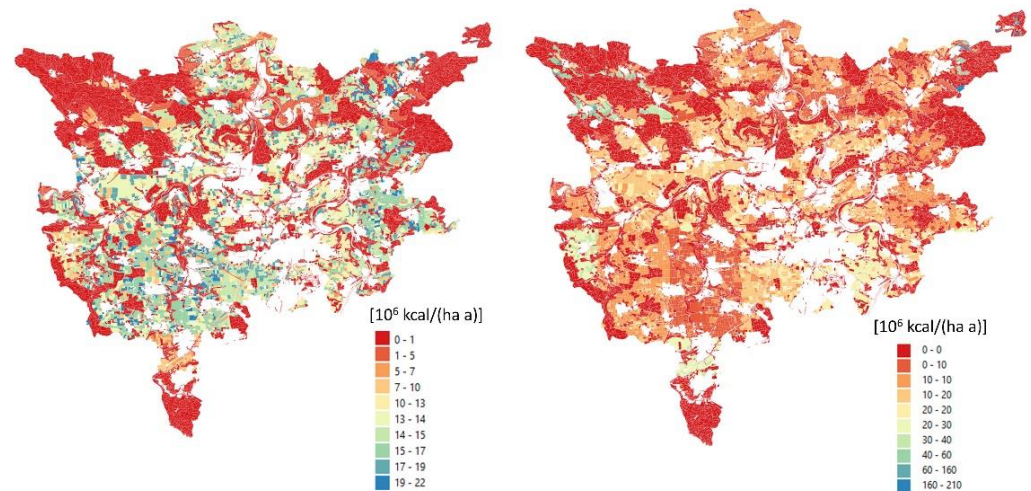


Figure 5. Vegetal (left) and animal calorie potential (right) in Ludwigsburg.

3.2. Development Food Demand until 2050

Figure 6a shows the forecast of total food calorie demands in three study regions. As case D1 only considered population development, the shape of the lines was defined by the population change. Population growth of 3% is expected in Ludwigsburg while Ilm-Kreis faces a net population decrease of 15% until 2050, with the population in Dithmarschen increasing by only 1% until 2050. In case D2, diet pattern changes are included. In our method, food demand follows the same trend as the HDI. Since HDI is expected to be steadily growing until 2050, food demand per capita increases. Compared to D1, total food calorie demand is around 3% more in D2 in 2050. In D1 and D2, a food waste rate of 30% was assumed, as was explained in Sector 2.3.1. If that rate is halved, as assumed in D3, total food demand decreases by 28% in all three case study counties.

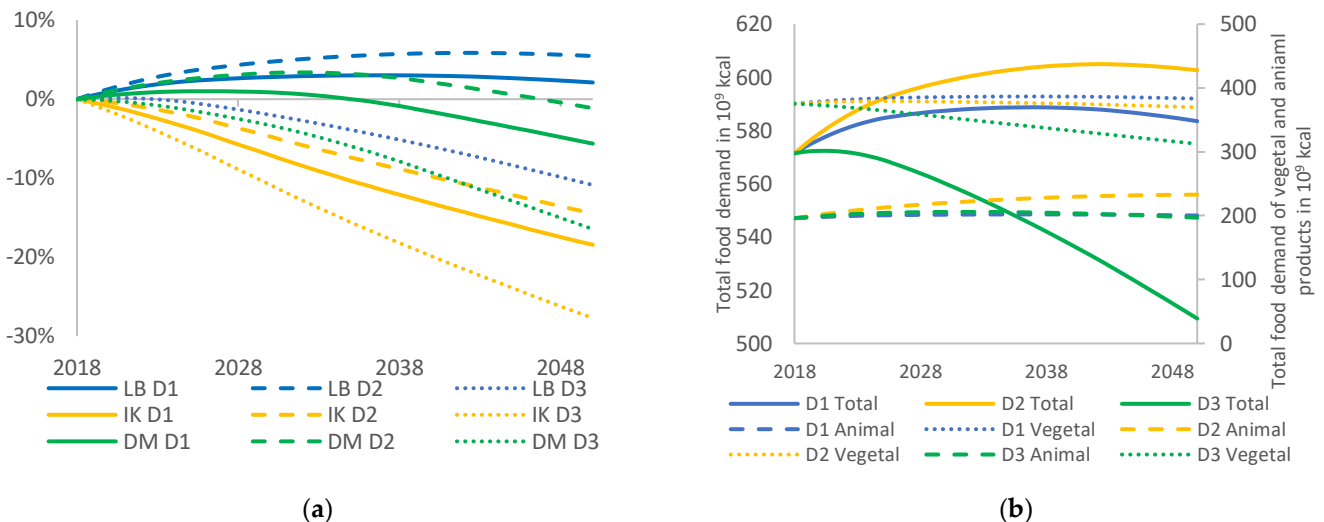


Figure 6. (a) Total food calorie demand in the three study regions for the period 2018 to 2050. The relative percentage value shows the change compared to 2018. Ludwigsburg (LB) in blue, Ilm-Kreis (IK) in orange, Dithmarschen (DM) in green; Case D1 in solid line, case D2 in dashed line, case D3 in dotted line; (b) Forecast of total food demand (solid line), vegetal food demand (dotted line), and animal food demand (dashed line) in Ludwigsburg county, 2018 to 2050.

Figure 6b shows the forecast based on our simulation of food calorie demands for Ludwigsburg. Total food demand is disaggregated into animal and vegetal food demand. In D1, the ratio between animal and vegetal food demand was kept constant based on 2018 data. The total food calorie demand for 2018 was 571 billion kcal, of which 34% was provided by animals and 66% by vegetal products. D2 indicates the impact of diet pattern

change: in 2018, a person statistically consumed 990 kcal of animal products and 1890 kcal of vegetal products per day. The amount of animal product consumption is expected to reach 1150 kcal in 2050, while 2976 kcal less vegetal products are expected to be consumed. Therefore, despite a population growth of 2.1%, 2050 demand for vegetal products in 2050 is 1.5% lower than in 2018, while animal food product demand is expected to grow by 18%. A similar trend is observed in the other two counties, shown in Figures S4 and S5 in Supplementary Data.

3.3. Temporal Development Food Potential

Annual food calorie potential for Ludwigsburg is shown in Figure 7a. Future food calorie potential was simulated for 10-year intervals from 2020 to 2050. The baseline case S1 (blue) shows a 15% increase in annual food potential, from 373 billion kcal/a in 2020 to 428 billion kcal in 2050, mostly due to RED II and its restriction on using farmland exclusively for energy production after 2030. Compared with S1, case S2 (green) assumed that about 15% of farmland can be used for energy crop cultivation [55]. In this case, climate change is the only variable: average yearly temperatures are predicted to increase from 10.2 °C in 2020 to 10.8 °C in 2050, while precipitation slightly increases from 709 mm/a to 715 mm/a. The changing climate harms crop biomass yields, thus reducing calorie yields by 1.5% until 2050 in Ludwigsburg. Case S3 (red) increases the organic farming land share to 25% in 2030, resulting in 4.5% less vegetal calorie yields compared to S1. S4 (yellow) includes artificial irrigation and shows that irrigation increases annual food calorie potential by about 1% at the expense of 4.7 to 7.1 million m³ of water demand, around 1% of Ludwigsburg's total 2020 demand [56].

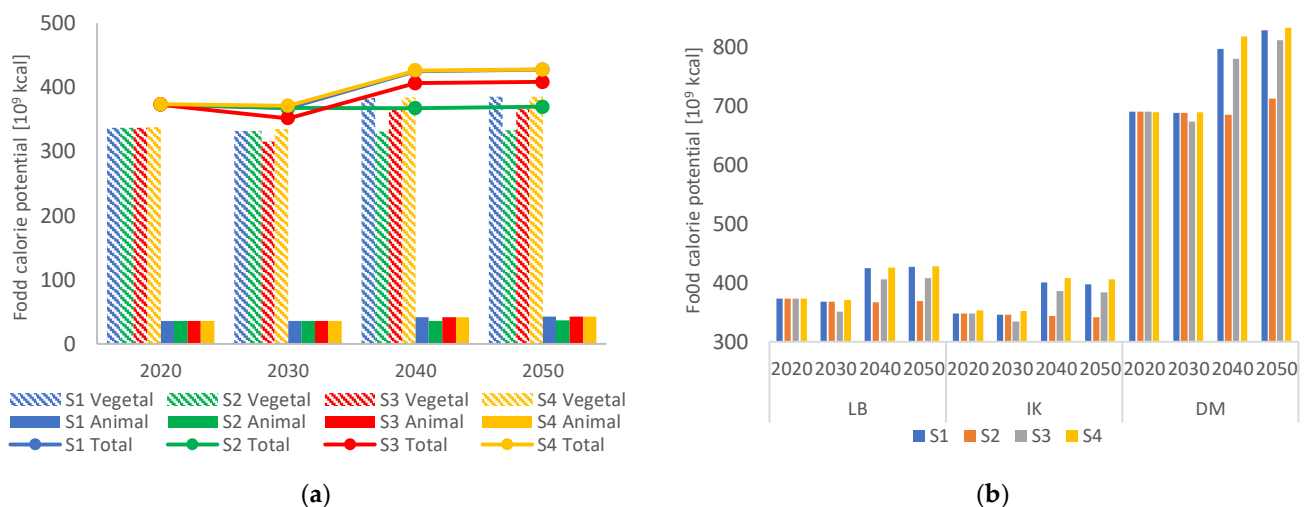


Figure 7. (a) Prediction of food calorie potential (solid lines), vegetal food potential (shaded bars), and animal food potential (solid bars) in Ludwigsburg, 2020 to 2050; (b) Prediction of total food potential in Ludwigsburg (LB), Ilm-Kreis (IK) and Dithmarschen (DM) for four cases, 2020 to 2050.

Comparing the three counties in Figure 7b shows that Dithmarschen has by far the highest annual food calorie potential of 690 billion kcal, due to having the largest agricultural land area. However, Ludwigsburg had the highest average annual yield density, of 7.4 million kcal per hectare, and Ilm-Kreis the lowest yield density of 4.7 million kcal per hectare and year in 2020. In all three regions, average annual temperatures and annual precipitation are expected to increase until 2050. Case S2 shows the food calorie potential reactions to climate change until 2050. In Ludwigsburg and Ilm-Kreis the climate change is unfavorable for crop production, resulting in a lower food calorie potential with a minor decrease of 1.6%. However, in Dithmarschen the annual food calorie potential is expected to increase by 4% between 2020 and 2050.

Comparing S1 and S4 shows that irrigation increases annual food potential by less than 2% on average. This increased potential is at the expense of between 58 and 680 m³ of irrigation water per hectare and year, as shown in Table 7. Due to its relatively dry climate, irrigation water demands in Ilm-Kreis are higher than in other regions to reach the same amount of water amount in the soil (Table S8). Therefore, applying irrigation could improve the food potential by around 2% in Ilm-Kreis compared with less than 1% in other regions. The predicted increment of rainfall reduced the additional irrigation demand from 680 tonnes per hectare (the year 2020) to 253 tonnes per hectare (the year 2050) in Ilm-Kreis. Dithmarschen required the lowest irrigation density among the three counties because it has the most humid and cool climate of all three counties.

Table 7. Irrigation water demand density to keep water stress levels in the soil at 90%, in m³ per hectare.

Year	Ludwigsburg	Ilm-Kreis	Dithmarschen
2020	95	680	53
2030	141	403	87
2040	108	189	57
2050	93	253	73

4. Discussion

The methods and tools presented in this paper provide a bottom-up method to simulate the local food potential and demand mainly based on the CityGML geoinformatics data model in one single energy-water-food simulation platform. The presented method provides reasonably accurate results in terms of local food calorie potential. Due to a lack of statistical data on this scale, the method was validated against another model and showed differences in annual food potential of between −7% and 26%. These differences between annual crop calorie potential by the SimStadt-based method presented here and the gridded crop calorie potential by Pradhan et al. and GAEZv3.0 [13] can be due to several methodical differences: (i) GAEZv3.0 took 23 major crop types both for rainfed and irrigated conditions into consideration while our method simulates all the agricultural land only with rainfed conditions; (ii) Pradhan et al. considered 19 food crop types, while only 10 food crop types are simulated in the proposed method because of limitations of applied crop distribution map by [27]. Comparing results for all cells of 5 arc minutes by 5 arc minutes, 70% of the grids had deviations between −30% and 30%.

Restricting land used exclusively for energy crop production (see the change between cases S1 and S2) is the most effective way to increase annual food production potential. Climate change (see the development between 2020 and 2050 in case S2) in contrast generally reduces annual biomass yields by about 2%. However, higher annual average temperature and precipitation in Dithmarschen increased annual food potential by around 4%. In all regions and years, irrigation provided a potential increment of less than 2% (see case S4 compared to case S1) at the expense of irrigation water requirements of between 58 to 680 m³ per hectare and year. It has to be noticed that this method only simulates 10 main crop types, which are representative in bioenergy potential calculations. In reality, local food production varieties alone cannot fulfill people's food demand, e.g., for exotic fruits. Only land-produced food potential was simulated without considering aquatic products in this study. Therefore, this method is limited to extensive food potential simulation, but its main goal is rather to simulate a relative loss of annual food production potential when using land fields more for energetic purposes, i.e., bioenergy, free land PV, or wind. With the result of this paper, low-yielded land can be identified and potentially converted into PV farms to reach more efficient land use.

The food demand assessments depend on two main parameters: the number of occupants and per capita food demand. A previous study [33] simulated the household and occupants number of each building based on the 3D building CityGML data model and census data. Even though for this study only the total number of residents per county was

relevant, it is thus also possible to simulate the food calorie potential of any neighborhood or sub-region, including across administrative boundaries or to-be-built areas where statistical values are not available. The per capita food calorie consumption, including food waste and storage, was estimated based on body weight, age distribution, PAL, and birth rate. Additionally, diet patterns were predicted according to HDI development until 2050. The simulation results show that in the Ludwigsburg region per capita, animal products demand was 990 kcal, and vegetal products demand was 1894 kcal per day in 2018. The amount of animal product consumption is expected to rise by 16% by 2050; meanwhile, 4% fewer vegetal products are expected to be consumed. The food waste by half can compensate for the increase in food demand. However, the food pattern prediction was based on historic data and behaviors. The trend of a vegetarian/vegan diet is not projected in this paper.

In Ludwigsburg, simulated local calorie potential covers 64% of simulated overall food demand, while animal calorie demand can be converted locally by less than 20% (Both with potential case S1 and demand case D2 in year 2020). In Ilm-Kreis and Dithmarschen, the respective ratios are 300/262% and 486/859%, respectively, reflecting the lower population density in Dithmarschen and the forested landscape in Ilm-Kreis. As can be seen from these numbers, and has been investigated in other works [6], a vegetal-oriented diet needs less arable land compared to an animal-oriented diet. Switching to more vegetal diets would thus open up room for higher shares of organic farming with its reduced yields but positive environmental impacts.

5. Conclusions

Every regional food system has connections and impacts other resources, notably water and energy. Due to the complexity of food systems, this study narrows down the notion of food system to food potential and demand. This study addresses the food potential and demand simulation at the regional level in high spatial resolution within a single uniformed simulation platform that already covers energy (roof photovoltaic, heating/electricity demand, bioenergy potential) and water (urban water demand of residential/non-residential buildings, crop water demand). The uniqueness of this method involves shifting the minimal result unit to land use polygon/building. This allows simulation of the food potential of each land field, which might also contain energetic potential in the form of bioenergy, free land PV, and wind. This differentiates this approach from other models and approaches that often focus on a national level. The proposed method thus helps to establish a more integrated planning of energy and water infrastructures in the context of climate change by ensuring that any repercussions in the food sphere are assessed properly. Moreover, basing the method on a generally available geoinformatics input base enables transferability to other regions in Germany and possibly globally, as well as at any regional scale from community to county to federal state.

Supplementary Materials: The following are available online at <https://www.mdpi.com/article/10.3390/land10080880/s1>.

Author Contributions: Conceptualization, K.B.; methodology, K.B.; software, K.B.; validation, K.B.; formal analysis, K.B.; investigation, K.B.; resources, B.S. and V.C.; data curation, K.B. and R.P.; writing—original draft preparation K.B.; writing—review and editing K.B., B.S. and D.T.; visualization, K.B.; supervision, B.S., D.T. and V.C. All authors have read and agreed to the published version of the manuscript.

Funding: This research was funded by the project IN-SOURCE (INtegrated analysis and modeling for the management of sustainable urban FEW ReSOURCES). This IN-SOURCE is funded by the European Union's Horizon 2020 research and innovation program under grant agreement No 730254.

Institutional Review Board Statement: Not applicable.

Informed Consent Statement: Not applicable.

Data Availability Statement: The 3D building models in different locations applied in this paper, their extension and their visualization are based on the data provided by states offices of three federal states in Germany: Ludwigsburg case: the Landesamt für Geoinformation und Landentwicklung Baden-Württemberg; Ilm-Kreis case: Thüringer Landesamt für Bodenmanagement und Geoinformation; Dithmarschen case: Federal Agency for Cartography and Geodesy (BKG). The land use DLM map of German was also provided by BKG.

Acknowledgments: The authors would like to thank Prajal Pradhan for his major support in providing GIS maps from his paper [13] on food potential, as well as information on the food waste and food energy demand of people.

Conflicts of Interest: The authors declare no conflict of interest.

Abbreviations

ALKIS	Germany's Official Real Property Cadaster Information System
AP	Animal calorie production
BCG	Federal Institute for Geosciences and Natural Resources
CP	Crop calorie production
CityGML	City Geography Markup Language
<i>cy</i>	Actual annual yield for a given crop
DLM	Digital Landscape Model
EAP	End animal calorie potential
EU	European Union
EVP	End vegetal calorie potential
FC	Animal feedstock
<i>fw</i>	Food waste rates from harvest to consumption
FWE	Food-Water-Energy
GIS	Geographic Information System
<i>ha</i>	Land field area
HDI	Human Development Index
<i>nf</i>	Nutritive factor
RED II	Renewable Energy Directive 2018/2001

References

- Rasul, G. Managing the food, water, and energy nexus for achieving the Sustainable Development Goals in South Asia. *Environ. Dev.* **2016**, *18*, 14–25. [[CrossRef](#)]
- Obersteiner, M.; Walsh, B.; Frank, S.; Havlík, P.; Cantele, M.; Liu, J.; Palazzo, A.; Herrero, M.; Lu, Y.; Mosnier, A.; et al. Assessing the land resource–food price nexus of the Sustainable Development Goals. *Sci. Adv.* **2016**, *2*, e1501499. [[CrossRef](#)]
- Ghodsvali, M.; Krishnamurthy, S.; de Vries, B. Review of transdisciplinary approaches to food-water-energy nexus: A guide towards sustainable development. *Environ. Sci. Policy* **2019**, *101*, 266–278. [[CrossRef](#)]
- Alexander, P.; Brown, C.; Arneith, A.; Finnigan, J.; Moran, D.; Rounsevell, M.D.A. Losses, inefficiencies and waste in the global food system. *Agric. Syst.* **2017**, *153*, 190–200. [[CrossRef](#)] [[PubMed](#)]
- Béné, C.; Fanzo, J.; Prager, P.D.; Harold, A.A.; Mapes, B.R.; Toro, P.A. Camila Bonilla Cedrez. Global drivers of food system (un)sustainability: A multi-country correlation analysis. *PLoS ONE* **2020**, *15*, e0231071. [[CrossRef](#)] [[PubMed](#)]
- Kastner, T.; Rivas, M.J.I.; Koch, W.; Nonhebel, S. Global changes in diets and the consequences for land requirements for food. *Proc. Natl. Acad. Sci. USA* **2012**, *109*, 6868–6872. [[CrossRef](#)] [[PubMed](#)]
- Pradhan, P.; Reusser, D.E.; Kropp, J.P. Embodied greenhouse gas emissions in diets. *PLoS ONE* **2013**, *8*, e62228. [[CrossRef](#)]
- Pradhan, P.; Kriewald, S.; Costa, L.; Rybski, D.; Benton, T.G.; Fischer, G.; Kropp, J.P. Urban Food Systems: How Regionalization Can Contribute to Climate Change Mitigation. *Environ. Sci. Technol.* **2020**, *54*, 10551–10560. [[CrossRef](#)]
- Hiç, C.; Pradhan, P.; Rybski, D.; Kropp, J.P. Food Surplus and Its Climate Burdens. *Environ. Sci. Technol.* **2016**, *50*, 4269–4277. [[CrossRef](#)]
- Khushi, S.; Ahmad, S.R.; Ashraf, A.; Imran, M. Spatially analyzing food consumption inequalities using GIS with disaggregated data from Punjab, Pakistan. *Food Sec.* **2020**, *12*, 1283–1298. [[CrossRef](#)]
- Beltran-Peña, A.; Rosa, L.; D'Odorico, P. Global food self-sufficiency in the 21st century under sustainable intensification of agriculture. *Environ. Res. Lett.* **2020**, *15*, 95004. [[CrossRef](#)]
- Haase, M.; Rösch, C.; Ketzer, D. GIS-based assessment of sustainable crop residue potentials in European regions. *Biomass Bioenergy* **2016**, *86*, 156–171. [[CrossRef](#)]

13. Pradhan, P.; Lüdeke, M.K.B.; Reusser, D.E.; Kropp, J.P. Embodied crop calories in animal products. *Environ. Res. Lett.* **2013**, *8*, 44044. [CrossRef]
14. Rosenberg, D.E.; Tarawneh, T.; Abdel-Khaleq, R.; Lund, J.R. Modeling integrated water user decisions in intermittent supply systems. *Water Resour. Res.* **2007**, *43*. [CrossRef]
15. Merem, E.C.; Twumasi, Y.; Wesley, J.; Alsarari, M.; Fageir, S.; Crisler, M.; Romorno, C.; Olagbegi, D.; Hines, A.; Ochai, G.S.; et al. Regional Assessment of the Food Security Situation in West Africa with GIS. *Food Public Health* **2019**, *9*, 60–77. [CrossRef]
16. Nouvel, R.; Brassel, K.-H.; Bruse, M.; Duminil, E.; Coors, V.; Eicker, U. SimStadt, a new workflow-driven urban energy simulation platform for CityGML city models. In Proceedings of the International Conference CISBAT 2015 Future Buildings and Districts Sustainability from Nano to Urban Scale. No. CONF. LESO-PB, EPFL, Lausanne, Switzerland, 9–11 September 2015.
17. Weiler, V.; Stave, J.; Eicker, U. Renewable Energy Generation Scenarios Using 3D Urban Modeling Tools—Methodology for Heat Pump and Co-Generation Systems with Case Study Application. *Energies* **2019**, *12*, 403. [CrossRef]
18. Köhler, S. Stochastic Generation of Household Electricity Load Profiles in 15-minute Resolution on Building Level for Whole City Quarters. In Proceedings of the 16th IAEE European Conference: Energy Challenges for the Next Decade, Ljubljana, Slovenia, 25–28 August 2019.
19. Bao, K.; Padsala, R.; Thrän, D.; Schröter, B. Urban Water Demand Simulation in Residential and Non-Residential Buildings Based on a CityGML Data Model. *ISPRS Int. J. Geo-Inf.* **2020**, *9*, 642. [CrossRef]
20. Bao, K.; Padsala, R.; Coors, V.; Thrän, D.; Schröter, B. A Method for Assessing Regional Bioenergy Potentials Based on GIS Data and a Dynamic Yield Simulation Model. *Energies* **2020**, *13*, 6488. [CrossRef]
21. Nouvel, R.; Zirak, M.; Coors, V.; Eicker, U. The influence of data quality on urban heating demand modeling using 3D city models. *Comput. Environ. Urban. Syst.* **2017**, *64*, 68–80. [CrossRef]
22. Zirak, M.; Weiler, V.; Hein, M.; Eicker, U. Urban models enrichment for energy applications: Challenges in energy simulation using different data sources for building age information. *Energy* **2020**, *190*, 116292. [CrossRef]
23. Bao, K.; Padsala, R.; Coors, V.; Thrän, D.; Schröter, B. GIS-Based Assessment of Regional Biomass Potentials at the Example of Two Counties in Germany. In Proceedings of the 28th European Biomass Conference and Exhibition Proceedings, Marseille, France, 28–30 April 2020; pp. 77–85. [CrossRef]
24. Braun, R.; Weiler, V.; Zirak, M.; Dobisch, L.; Coors, V.; Eicker, U. Using 3D CityGML Models for Building Simulation Applications at District Level. In Proceedings of the 2018 IEEE International Conference on Engineering, Technology and Innovation (ICE/ITMC), Stuttgart, Germany, 17–20 June 2018; pp. 1–8.
25. Introductin AquaCrop, Food and Agriculture Organization of the United Nations. 2016. Available online: <http://www.fao.org/3/i6321e/i6321e.pdf> (accessed on 15 January 2021).
26. Arbeitsgemeinschaft der Vermessungsverwaltungen der Länder der Bundesrepublik Deutschland. Digitales Basis-Landschaftsmodell (Basis-DLM). Available online: <http://www.adv-online.de/AdV-Produkte/Geotopographie/Digitale-Landschaftsmodelle/Basis-DLM/> (accessed on 10 November 2020).
27. Griffiths, P.; Nendel, C.; Hostert, P. Intra-annual reflectance composites from Sentinel-2 and Landsat for national-scale crop and land cover mapping. *Remote Sens. Environ.* **2019**, *220*, 135–151. [CrossRef]
28. Wyland, L.J.; Jackson, L.E.; Chaney, W.E.; Klonsky, K.; Koike, S.T.; Kimple, B. Winter cover crops in a vegetable cropping system: Impacts on nitrate leaching, soil water, crop yield, pests and management costs. *Agric. Ecosyst. Environ.* **1996**, *59*, 1–17. [CrossRef]
29. FAO. *Food Balance Sheets: A Handbook*; FAO: Rome, Italy, 2001.
30. Gustavsson, J.; Cederberg, C.; Sonesson, U.; van Otterdijk, R.; Meybeck, A. *Global Food Losses and Food Waste*; FAO: Rome, Italy, 2011.
31. Bundesanstalt für Geowissenschaften und Rohstoffe. Karte der Bodenarten in Oberböden 1:1.000.000 (BOART1000OB). Available online: https://www.bgr.bund.de/DE/Themen/Boden/Informationsgrundlagen/Bodenkundliche_Karten_Datenbanken/Themenkarten/BOART1000OB/boart1000ob_node.html (accessed on 24 September 2020).
32. Meteororm. Available online: <https://meteororm.com/en/> (accessed on 12 August 2020).
33. Köhler, S.; Betz, M.; Bao, K.; Weiler, V.; Schröter, B. Determination of household area and number of occupants for residential buildings based on census data and 3D CityGML building models for entire municipalities in Germany. In Proceedings of the Building Simulation Conference 2021, Bruges, Belgium, 1–3 September 2021.
34. Kaltschmitt, M.; Hans, H.; Hofbauer, H. *Energie aus Biomasse: Grundlagen, Techniken und Verfahren*; Springer: Berlin/Heidelberg, Germany, 2016.
35. Bouwman, A.F.; van der Hoek, K.W.; Eickhout, B.; Soenario, I. Exploring changes in world ruminant production systems. *Agric. Syst.* **2005**, *84*, 121–153. [CrossRef]
36. United Nations University; World Health Organization. Human Energy Requirements. In Proceedings of the Report of a Joint FAO/WHO/UNU Expert Consultation, Rome, Italy, 17–24 October 2001; FAO: Rome, Italy, 2004. ISBN 9251052123.
37. Schofield, W.N. Predicting basal metabolic rate, new standards and review of previous work. *Hum. Nutr. Clin. Nutr.* **1985**, *39* (Suppl. S1), 5–41. [PubMed]
38. Statistisches Bundesamt. *Mikrozensus—Fragen zur Gesundheit. 2005, 2009, 2013, 2017*. Available online: <https://www.destatis.de> (accessed on 16 January 2021).
39. Statistisches Bundesamt. Vorausberechneter Bevölkerungsstand: Bundesländer, Stichtag, Varianten der Bevölkerungsvorausberechnung. Available online: <https://www-genesis.destatis.de/genesis/online> (accessed on 15 January 2021).

40. Statista. Zusammengefasste Geburtenziffer—Anzahl der Kinder pro Frau in Deutschland nach Bundesländern. Available online: <https://de.statista.com/statistik/daten/studie/76262/umfrage/geburtenziffer---anzahl-der-kinder-pro-frau-2007-und-2008/> (accessed on 12 February 2021).
41. Statistisches Bundesamt. Population Depending on Sex and Age (Five Years Age Groups): Census from the Adjusted Stock of Registers. Available online: <https://ergebnisse.zensus2011.de/> (accessed on 13 January 2021).
42. FAO. FAOSTAT: FAO Statistical Databases: New Food Balance. Available online: <http://www.fao.org/faostat/en/> (accessed on 15 January 2021).
43. Costa, L.; Rybski, D.; Kropp, J.P. A Human Development Framework for CO₂ Reductions. *PLoS ONE* **2011**, *6*, e29262. [CrossRef]
44. HDRO (Human Development Report Office) United Nations Development Programme. Human Development Report 2018: Human Development Indices and Indicators. Available online: http://hdr.undp.org/sites/default/files/2018_human_development_statistical_update.pdf (accessed on 16 January 2021).
45. Statistisches Bundesamt. Daten aus dem Gemeindeverzeichnis: Kreisfreie Städte und Landkreise nach Fläche, Bevölkerung und Bevölkerungsdichte. Available online: <https://www.destatis.de/DE/Themen/Laender-Regionen/Regionales/Gemeindeverzeichnis/Administrativ/04-kreise.html> (accessed on 3 January 2021).
46. Statistisches Bundesamt. Anbauflächen, Hektarerträge und Erntemengen ausgewählter Anbaukulturen im Zeitvergleich: Hektarerträge ausgewählter Anbaukulturen im Zeitvergleich. Available online: <https://www.destatis.de/DE/Themen/Branchen-Unternehmen/Landwirtschaft-Forstwirtschaft-Fischerei/Feldfruechte-Gruenland/Tabellen/liste-feldfruechte-zeitreihe.html> (accessed on 16 January 2021).
47. Fischer, G.; Nachtergaele, F.O.; Prieler, S.; Teixeira, E.; Toth, G.; van Velthuizen, H.; Verelst, L.; Wiberg, D. *Global Agro-Ecological Zones (GAEZ v3.0)-Model. Documentation*; IIASA: Laxenburg, Austria; FAO: Rome, Italy, 2012.
48. *Directive (EU) 2018/2001: On the Promotion of the Use of Energy from Renewable Sources*; European Parliament and of the Council: Strasbourg, France, 2018.
49. Eurostat. Share of Organic Crop Area Out of the Total Utilised Agricultural Area (UAA). Available online: <https://ec.europa.eu/eurostat/databrowser/> (accessed on 20 January 2021).
50. Kaufmann, P.; Stagl, S.; Franks, D.W. Simulating the diffusion of organic farming practices in two New EU Member States. *Ecol. Econ.* **2009**, *68*, 2580–2593. [CrossRef]
51. Seufert, V.; Ramankutty, N.; Foley, J.A. Comparing the yields of organic and conventional agriculture. *Nature* **2012**, *485*, 229–232. [CrossRef] [PubMed]
52. European Commission. Organic Farming—Action Plan for the Development of EU Organic Production. Available online: <https://ec.europa.eu/info/law/better-regulation/have-your-say/initiatives/12555-Organic-farming-action-plan-for-the-development-of-EU-org> (accessed on 20 January 2021).
53. Eurostat. Population on 1st January by Age, Sex and Type of Projection. Available online: https://ec.europa.eu/eurostat/databrowser/view/proj_19np/ (accessed on 1 January 2021).
54. European Commission. EU Actions against Food Waste. Available online: https://ec.europa.eu/food/safety/food_waste/eu_actions_en (accessed on 26 January 2021).
55. Fachagentur Nachwachsende Rohstoffe e. V. Anbau und Verwendung Nachwachsender Rohstoffe in Deutschland. FNR. 2019. Available online: https://www.weltagrарbericht.de/fileadmin/files/weltagrарbericht/Weltagrарbericht/16_AgrarspritBioenergie/FNR2019.pdf (accessed on 4 October 2020).
56. Öffentliche Wasserversorgung—Statistisches Landesamt Baden-Württemberg. Available online: <https://www.statistik-bw.de/Umwelt/Wasser/22025035.tab?R=KR118> (accessed on 17 August 2020).

Chapter 5

A bottom-up GIS-based method for simulation of ground-mounted PV potentials at regional scale

Bao, K.; Kalisch, L.; Santhanavanich, T.; Thrän, D.; Schröter, B.

Energy Reports 2022, 8, 5053. <https://doi.org/10.1016/j.egy.2022.03.187>



Research paper

A bottom-up GIS-based method for simulation of ground-mounted PV potentials at regional scale

Keyu Bao ^{a,c,d,*}, Louis Kalisch ^{a,1}, Thunyathep Santhanavanich ^b, Daniela Thrän ^{c,d,e}, Bastian Schröter ^a

^a Center for Sustainable Energy Technology, Hochschule für Technik Stuttgart, Schellingstraße 24, 70174 Stuttgart, Germany

^b Center for Geodesy and Geoinformatics, Hochschule für Technik Stuttgart, Schellingstraße 24, 70174 Stuttgart, Germany

^c Department of Bioenergy, Helmholtz Center for Environmental Research, Torgauer Straße 116, 04247 Leipzig, Germany

^d Chair of Bioenergy System, Faculty of Economic Sciences, University of Leipzig, Grimmaische Straße 12, 04109 Leipzig, Germany

^e Unit Bioenergy System, The German Biomass Research Centre (DBFZ), Torgauer Straße 116, 04347 Leipzig, Germany



ARTICLE INFO

Article history:

Received 28 January 2022

Received in revised form 12 March 2022

Accepted 26 March 2022

Available online xxxx

Keywords:

Photovoltaic

Ground-mounted PV

Bottom-up simulation

Geographic Information System (GIS)

Food–water–energy nexus

Potential simulation

ABSTRACT

Solar photovoltaic (PV) is a key technology for any renewable energy system. As subsidy-free PV becomes more and more economically feasible, region-specific planning tools that define areas suitable for ground-mounted PV are needed. While many top-down studies have assessed suitable areas at a national scale, an accurate scalable bottom-up assessment of regional ground-mounted PV potentials in high spatial and temporal resolution that goes further than a mere identification of appropriate land areas is missing. This work introduces such a method based on digital landscape models that consider terrain slope, orientation, location-specific irradiation, and land use type, and combines this geoinformational information with a PV yield model that allows to assess hourly PV generation potential on suitable areas. The method is validated with three existing ground-mounted PV plants in Germany, where a comparison of real and simulated annual electricity yields shows average deviations of 5%. Subsequently, ground-mounted PV potentials in three German counties with varying settlement structures as well as topographic and weather patterns are assessed and a comparison of yearly and hourly simulated generation potentials with regional electricity demand is performed. While the yearly analysis demonstrates the substantial overall potentials of local ground mounted-PV in all regions, with demand coverages ranging from 80% to hypothetically more than 40 times of current electricity demand according to current regulations, the hourly autarky ratio, defined as the share of hours of a year where ground-mounted PV can satisfy demand, ranges from 25% to 40%, without consideration of storage or demand side management. A subsequent investigation of the ability to export excess electricity generation from ground-mounted PV shows that the two regions with highest ground-mounted PV potentials have less-developed grid infrastructures, thus restricting excess electricity generation export potentials.

© 2022 The Author(s). Published by Elsevier Ltd. This is an open access article under the CC BY-NC-ND license (<http://creativecommons.org/licenses/by-nc-nd/4.0/>).

1. Introduction

To decarbonize the energy system, countries worldwide are emphasizing the replacement of fossil fuel-based energy supply by renewable energy (RE) plants. To date, solar photovoltaic (PV) is the cheapest renewable, even in many parts of the world, the

most inexpensive power generation technology in absolute terms. PV will thus play a significant role in a 100% renewable energy system also in Germany (Badelt et al., 2020, p. 1). At the same time, many countries face rising electricity demands, driven by the electrification in the mobility and heating sector (IEA, 2019, p. 258). Projections for Germany see an increase of electricity demand by a factor of up to 2–2.5 until 2045, compared to 2020 levels (Wirth and Bächle, 2021). In their recently published coalition agreement, the new German government set a target of an increase of installed PV power from 54 GW in 2020 (Wirth, 2021) to 200 GW by 2030 (SPD et al., 2021). This production capacity cannot be reached by rooftop PV plants alone, but also requires an upscaling of ground-mounted PV plants.

Ground-mounted PV plants are rows of PV panels installed on frames, typically connected to the ground via metal foundations.

* Corresponding author at: Center for Sustainable Energy Technology, Hochschule für Technik Stuttgart, Schellingstraße 24, 70174 Stuttgart, Germany.

E-mail addresses: keyu.bao@hft-stuttgart.de (K. Bao),

02kalo1mse@hft-stuttgart.de (L. Kalisch),

thunyathep.santhanavanich@hft-stuttgart.de (T. Santhanavanich),

daniela.thraen@ufz.de, thraen@wifa.uni-leipzig.de, daniela.thraen@dbfz.de

(D. Thrän), bastian.schroeter@hft-stuttgart.de (B. Schröter).

¹ These authors contribute equally to the paper.

In most cases, the frames are fixed, i.e., they do not track the sun, and panels face south in the northern hemisphere. For German latitudes of about 50° N, a tilt of 20° to the horizontal plane optimizes yearly electricity production. Compared to rooftop PV installations, ground-mounted PV plants can achieve installed capacities of many MW, thus benefit from economies of scale and achieve lower levelized cost of electricity (Kost et al., 2021). In Germany, the average size of ground-mounted PV plants is 1.4 MW_{peak}, based on plants built in 2019 and 2020 (BNetzA, 2021). In 2017, the share of ground-mounted PV plants in Germany was 28% of the overall installed PV fleet and was expected to be rising due to their higher cost-efficiency compared to rooftop PV (Kelm et al., 2019, p. 13). However, ground-mounted PV has a high level of land consumption compared to rooftop PV or conventional power plants and thus competes with other forms of land use, especially agriculture (BMVI, 2015, p. 9). To limit conflicts between ground-mounted PV and other land-use forms, the German government has outlined regulations in the National Renewable Energy Sources Act (German EEG) to restrict areas for PV plants eligible for feed-in tariffs (BMVI, 2015, p. 9). As PV plants are becoming economically feasible also outside the feed-in tariff scheme, EEG-based land use restrictions are becoming less important (Wirth, 2021, p. 7).

This dynamic calls for tools that investigate the potentials of ground-mounted PV plants on different land-use forms on a regional scale, since municipal entities usually give approvals for non-subsidized PV plants. Ideally, these region-specific plans are aligned with regional electricity demand characteristics to guarantee an efficient transformation process towards an all-renewable power system (Alanne and Saari, 2006). As Charabi et al. demonstrated in their study, land topography strongly influences possible ground-mounted PV panel installation density (Charabi et al., 2016) and hence local yields per area. Therefore, any regional analysis should incorporate detailed terrain data.

Several studies have analyzed areas eligible for ground-mounted PV and installable potential in various contexts and scenarios. At European Union (EU) level, Castillo et al. worked out a suitability map for ground-mounted PV across the EU. A multicriteria assessment (MCA) including irradiance, socio-economic and topographic characteristics helped achieve a high spatial resolution of the suitability categorization. However, capacity or yield calculations were not performed, and electricity demands were not considered (Perpiña Castillo et al., 2016). At a German level, the Federal Ministry of Transport and Digital Infrastructure commissioned a study in 2015 investigating potential areas suitable for ground-mounted PV. It yielded a technical potential of 316,400 ha of restriction-free land area, which accounts for 0.9% of the total surface area of Germany. Regarding the potential yield, an assumption of 0.45 MW_{peak}/ha was used, resulting in a technical potential of 143 GW_{peak} (BMVI, 2015, p. 112). Furthermore, Kelm et al. examined scenarios for land use regulations for ground-mounted PV in Germany. The study concluded that nationally, up to 229,350 ha of potential surface area was available. However, yield calculations were not performed (Kelm et al., 2019, p. 22). Charabi et al. have elaborated an approach to calculate the layout and potential of PV plants on south-facing terrains (Charabi et al., 2016), it neglects the case of modules on non-south-facing terrains.

The studies mentioned above have all assessed ground-mounted PV potentials. However, research gaps exist as results were primarily expressed in suitable areas and missed one or more of the four aspects: (1) Since the study focuses on a global or national level, spatial resolution is too coarse. (2) Specific terrain data such as slope is not considered. (3) Electricity yields on available areas are calculated using static conversion factors rather than a physical model considering, e.g., hourly solar

altitudes. (4) A comparison of potential electricity yields from local ground-mounted PV and regional demand is lacking.

To fill the research gaps the work presents a method to calculate the ground-mounted PV potential at a regional scale, considering terrain data, i.e., slope and orientation, and solar irradiance data to calculate detailed yield potentials at the single-field level. With the resulting high-resolution data, different land-use scenarios are compared for specific case study regions, three German counties. Additionally, resulting yield potentials are compared to the counties' electricity demands. In combination with a method to examine regional biomass and bioenergy potentials (Bao et al., 2021), ground-mounted PV potentials can be used for a more holistic analysis of the food–water–energy (FME) nexus of the studied regions.

2. Materials and methods

As mentioned in Section 1, the presented method combines Geographic Information System (GIS) data with solar irradiance data to calculate electric yield potentials for ground-mounted PV. The relevant inputs, outputs, and processes of this workflow are visualized in Fig. 1.

After the definition of land-use scenarios in Section 2.1, relevant GIS data are assessed for the study regions to generate a list of potential land polygons suitable for ground-mounted PV plants. This process is derived from Ministry of the Environment, Climate Protection and Energy Sector (LUBW) (LUBW, 2021) and described in Section 2.2. In this step, different scenarios are created by varying land-use regulations. In parallel, hourly irradiance data in W/m² is simulated based on the logic implemented in the dynamic simulation environment INSEL (Schumacher, 2014). This logic is also applied in the rooftop PV workflow within SimStadt, a modular regional energy system modeling platform that allows assessing regional energy demands and renewable energy production potentials (Köhler et al., 2021; Nouvel et al., 2015) (Section 2.3). Lastly, the newly developed ground-mounted PV workflow applies geoinformatics and irradiance data to calculate the potential panel area achievable as well as the overall PV yield in GWh for each land polygon (Section 2.4). The workflow is then validated with yield data from three existing plants in Germany (Section 2.5) and used to simulate the potential yield for specific case study regions, which are described in Section 2.6. The results are then compared for the different restriction scenarios and contrasted with the respective electricity demands of the case study regions (Section 3).

2.1. Scenarios

Land use efficiency is becoming a more and more critical factor as wind, solar, and bioenergy are competing with agriculture and nature protection areas for land. The competition between PV and bioenergy has been discussed in particular in Calvert and Mabee (2015). A report by Wirth et al. showed that in Germany, photovoltaic plants are 52 times more efficient in terms of land use compared to bioenergy, as silage maize yields 19 MWh_{el}/ha while modern, south-facing ground-mounted PV in usual southern orientation generates about 980 MWh_{el}/ha. Wirth (2021, p. 39,43). Furthermore, with the advent of subsidy-free PV, land-use restrictions as imposed by the EEG (see Section 1) become less important. This study thus evaluates the current regulatory scheme in Germany and implements a range of land-use scenarios. The land categories eligible for ground-mounted PV according to EEG are summarized as follows (Bundesgesetzblatt, 2021, §§37,38):

- Areas along highways or railroads within 200 m of the outer edge of the paved roadway. A corridor located along the roadway or railway of at least 15 meters wide is kept clear.

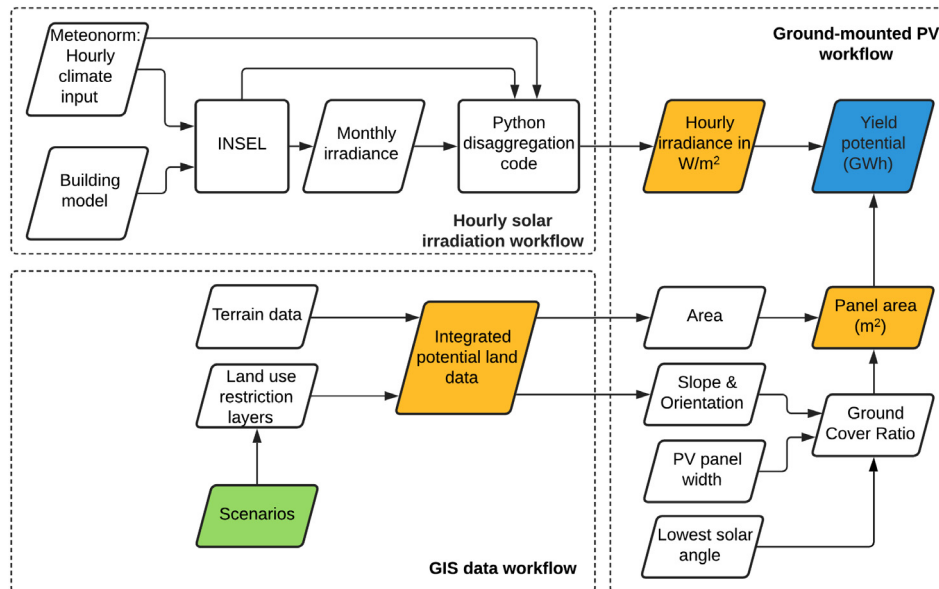


Fig. 1. Flowchart diagram of the method presented in this paper, including scenarios input (green), significant process values (yellow) and output (blue). (For interpretation of the references to color in this figure legend, the reader is referred to the web version of this article.)

- Conversion areas, i.e., areas which were formerly used for economic, traffic, housing or military purposes, sealed areas, designated commercial areas and other built facilities and whose previous use still has an effect (STMWI, 2021).
- Areas used as arable land and are located in a less-favored area (LFA) (Council Directive 86/465/EEC).
- Areas used as grassland and are located in a less-favored area (LFA) (Council Directive 86/465/EEC).
- Areas owned by the Federal Government or the Federal Agency for Real Estate Tasks (German 'BlmA'), i.e., an area of around 460.000 ha used for multiple purposes including housing, industrial, commercial, military, forestry and agricultural use (BlmA, 2021).

On the contrary, the Federation for the Environment and Nature Conservation Germany (German BUND) and the Nature Conservation Association Germany (German NABU) are appealing to ease the regulations placed by the EEG to accelerate the scale-up of renewable energies, pointing out that conventional monocultural agriculture has higher ecological impacts on land than ground-mounted PV (BUND and NABU, 2021).

This study thus investigates four scenarios, shown in Table 1, reflecting the regulations and trends of feasible lands for PV. Firstly, areas according to current EEG regulations are investigated. For simplification purposes, the first two categories will be combined as *Conversion areas* (CA) in the following work. The categories of arable land and grassland in LFAs are subject to an activation clause by each federal state, but only a few states have issued it so far. For this work, it is assumed that all federal states have given the clause to include these categories, in line with the methodology used by Kelm et al. Kelm et al. (2019, p. 29). These two categories are classified as scenario *Less-favored areas* (LFA). All scenarios do not include the last-mentioned category, as related data is not available at present. Additionally to data availability, Kelm et al. estimated an area of 3,400–6,800 ha as suitable for ground-mounted PV plants in this category, which equals 1.5–7.3% of the overall potential area calculated in Kelm et al. (2019, p. 22). Therefore, the areas falling in this category are assumed to be negligible in this study.

Scenario *Grassland* (GL) assesses the potential impact of subsidy-free ground-mounted PV. Grassland is a common type

Table 1

Scenario description.

Scenario	Abbreviation	Description
Conversion areas	CA	Conversion areas defined by EEG and 200 m-corridors along highways & railways
Less-favored areas	LFA	Grassland & arable land defined as agriculturally less productive
Grassland	GL	All grassland
Agri-Photovoltaic	APV	APV on all arable land

of land use chosen for subsidy-free PV in Germany due to its relatively low agricultural yield (BUND and NABU, 2021). The scenario thus considers all available grassland in the respective region. Lastly, *Agri-Photovoltaic* (APV) examines available arable land for APV applications. APV is a concept to realize food and electricity production on the same land, using various panel-mounting designs. Ground Cover Ratio (GCR) describes the ratio between the active PV panel area and the total ground surface area occupied by the installation. Regardless either tilted rows installed high above the ground or vertical installations of bifacial modules with high module row distances, a GCR of about one-third compared to conventional ground-mounted PV can be reached whilst the ground area can be used agriculturally (Trommsdorff et al., 2020, p. 28). In recent years, demonstration projects have been performed in multiple locations also in Germany (Schindele et al., 2020). The GCR of each polygon is divided by a factor of three for the yield calculation in the APV scenario.

All scenarios will be analyzed regarding their potential to cover regional electricity demands. The yearly electricity demands in all case studies are taken from statistical sources for the current case 7. Additionally, projected electricity demand in year 2045 is assumed by doubling the current electricity demand, as Wirth et al. indicated (Wirth and Bächle, 2021). Therefore, the demand coverage ratio in 2045 will always be half of the percentage in the current case. The estimated hourly demand in one case study region, Ludwigsburg, was calculated by downscaling available hourly demand data of the state of Baden-Wuerttemberg (Bundesnetzagentur, 2021). The downscaling metric is the yearly energy demand between Ludwigsburg county and of the whole

Table 2
Land use layers considered in the scenarios.

Scenario	Layers included	Comment
Conversion areas	Highway corridors	200 m buffer corridor
	Railway corridors	200 m buffer corridor
	Abandoned mining sites	
	Former military areas	
Less-favored areas	Abandoned industrial areas	
	LFA	Community list (86/465/EEC)
Grassland	Arable land & grassland	
Agri-Photovoltaic	GL	Grassland
	APV	Arable land

Table 3
Land use restriction layers.

Criteria	Layers included	Comment
Settlements	Residential, industrial and commercial areas; landfill; mining; areas of mixed use; areas of special functional character; sports, leisure and recreation area; cemeteries; settlement areas	
Airports	Air traffic operating areas	
Rail traffic	Railway tracks; rail traffic areas	15 m buffer
Roads	Main roads	15 m buffer
	Agricultural roads	5 m buffer
Water	All waterbodies	10 m buffer
Forest		10 m buffer
Flooding areas	Polder	
Protected areas	Water protection areas; nature protection areas; environmental protection areas; soil protection areas	

state. As more specific data was not available in the other two case study regions, the dataset from Baden-Wuerttemberg was also applied there to derive hourly demand values. Furthermore, any imbalance between production and demand must either be stored locally or exported, in most cases via medium voltage (MV) distribution lines ($20 \text{ kV} \leq \text{line voltage} \leq 110 \text{ kV}$). Data, i.e., the number of MV lines crossing the county's borders and their respective voltage levels is taken from (Eichhorn et al., 2018), with each line's transmission capacity calculated based on a method introduced in UW-Madison (2013).

2.2. Geoinformatics data modeling

To identify the location and topology of the areas defined by the scenarios described in Section 2.1, a GIS-based input data model is required. The method to generate the integrated potential land data model is derived from the criteria used by the Federal Environmental Institute Baden-Wuerttemberg (German LUBW) for their public energy atlas tool (LUBW, 2021). Firstly, different potential land layers are created for each scenario. Table 2 shows the land use layers used for the four scenarios.

For each scenario, the respective layers will be overlapped with all further layers prohibiting ground-mounted PV (Table 3). This includes settlements and infrastructure, water bodies, forests, flooding areas and protected areas.

The GIS-based approach to integrate, filter, and transform data is modeled and processed by the Feature Manipulation Engine (FME) software (Safe Software, 2021). Fig. 2 shows the overall FME workbench process used to create the map of point layer with the slope, aspect and land-use type information on each point.

The main GIS processes are :

1. Reading data sources

In this step (Fig. 2-1), multiple GIS data sources in vector and raster format are loaded into the FME workflow. The

GIS features from ATKIS Digital Landscape Model (DLM) (BKG, 2021) in Shapefile vector format loaded to the workflow contains the layers with land-use information, e.g., arable lands are expressed as polygons, while street networks are polylines. All polygons and vectors have attributes attached to be identified, i.e., ID, usage type, above/under-ground, width, etc. Also, the terrain surface point cloud from Digital terrain model of Germany with a resolution of 5 m (DGM5) (DGM5) (BKG, 2021) with a grid width of 5 meters in XYZ format is loaded to the workflow by Point Cloud XYZ Reader. Both feature and raster are geometric clipped to the area of interest described in Table 7.

2. Slope and aspect calculation

This step (Fig. 2-2) calculates slope and aspect map in raster from the DGM5 point cloud model. This point cloud is constructed with a Delaunay triangulation and then uniformly sampled to generate the digital elevation model (DEM) in raster format. The slope and aspect are calculated for each cell of a raster with the Eight neighbors Horn's algorithm which nearest points weighted more than diagonal neighbors and suitable to calculate the rough terrain. The resulting slope and aspect raster are then extracted as raster grid to determine suitable ground-mounted PV areas.

3. Identifying scenario areas

The restriction areas for ground-mounted PV filtered and extracted from the DLM geographical dataset (Fig. 2-3) using the spatial relationship filtering based on the rules from EEG as shown in Table 3. Then, the initial areas for all scenarios are derived 2-4 to 2-7 from the resulting restricted areas and DLM dataset based on scenario rules described in Table 2.

4. Filtering the point data for all scenarios

In this step (Fig. 2-4), the slope and aspect raster layer from step 2 are filtered by their spatial relations and intersected with each scenario area from step 3 and exported as point

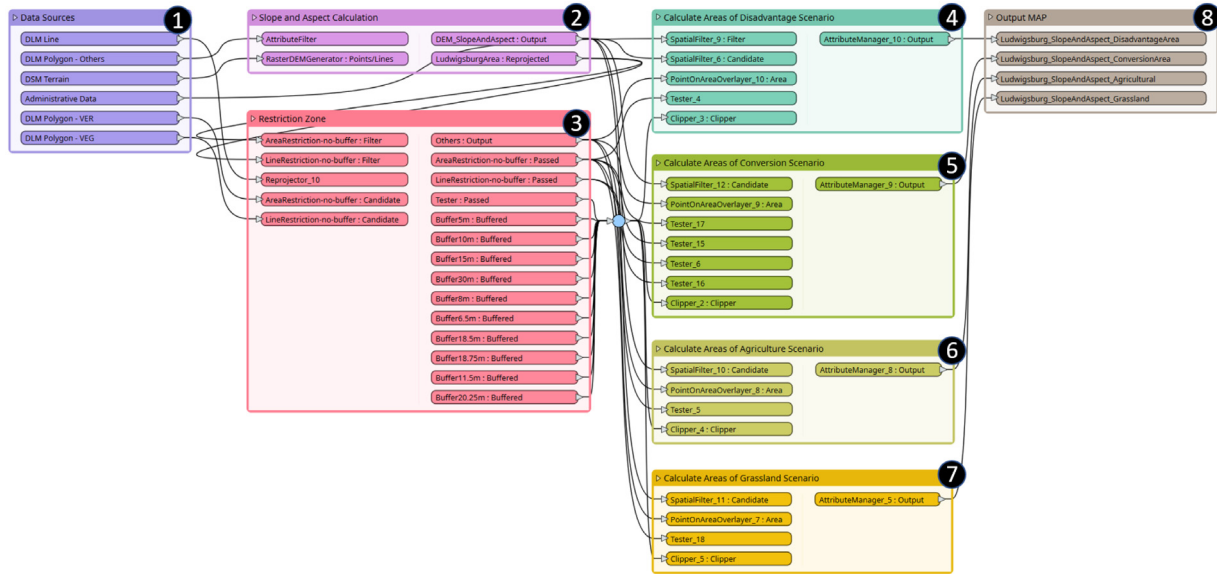


Fig. 2. The process diagram in FME workbench for identifying location and topology of each ground-mounted PV plant scenario.

feature dataset in rectangular grid layout with distance separation of 10 m. This data is then used as an input data for ground-mounted PV potential simulation in Section 2.4.

2.3. Hourly irradiance simulation

Local solar irradiance is a crucial metric for the assessment of PV potential. The accurate assessment of solar irradiance requires climate data, including horizontal and diffuse radiation and ambient temperatures. This data can be imported into the SimStadt platform through a weather processor from databases such as PVGIS (European Commission, 2021), INSEL (Schumacher, 2014), or by using Meteornorm weather files chosen by the user. Once climate data is available, the radiation processor within INSEL, coupled to SimStadt, computes the incoming irradiance on module surfaces based on their slope and orientation. This approach has already been applied to rooftop PV simulations. The rooftop PV potential simulation was validated and presented in Romero Rodríguez et al. (2017).

By integrating the same irradiance simulation logic for rooftop PV, the newly-established ground-mounted PV workflows share the same data accuracy and structure level. Furthermore, the newly-established method can thus simulate hourly yields if hourly climate data are available.

2.4. Ground-mounted PV potential simulation

The PV potential is the product of area and packing factor, which represents the total PV capacity in MW on a specific area in ha (Calvert and Mabee, 2015). The geoinformatics data process introduced in Section 2.2 creates a raster dataset that adds slope and orientation information by dividing the land use map into a grid of discrete 10 meters by 10 meters square cells. The PV potential simulation does not calculate the potential per raster cell, but per land-use polygon from the DLM, since (i) around 55% of the polygons have a size between 0.5 ha to 3.2 ha, while current ground-mounted PV plants in Germany usually have the size of 1.4 MW_{peak} on average, i.e., around 1.2 ha, aligning with the land field size (BNetzA, 2021), and (ii) land-use fields, represented by polygons, often have distinct owners. So, it is reasonable to assume that ground-mounted PV farms will be installed with the limits of one or more polygons. The raster cells which belong

to the same land fields are therefore grouped. The slope and orientation values of the land field are the mean values of all the grouped raster cells.

As mentioned in Section 1, a land polygon's slope and orientation are decisive factors for ground-mounted PV panel installation density, assuming an identical irradiation situation (Charabi et al., 2016). As a further limit, a slope ranging from 16° and 30° was considered poorly suitable for ground-mounted PV, while slopes larger than 30° are considered unfeasible (Perpiñá Castillo et al., 2016). Hence only polygons with a slope of less than 16° were considered. Furthermore, the utilization efficiency, i.e., the distance between each row, can vary with the land polygon's slope and orientation. Thereby, GCR evaluates the ground occupation. Project developers and operators prefer South-oriented ground-mounted PV due to the lowest levelized cost of electricity compared to tracking systems and east-west-oriented plants (Badelt et al., 2020, p. 10). The optimal distance between panel rows is defined by either the required sun hours (Siala and Stich, 2016) or sun angle (Aste and Del Pero, 2010) during the shortest day of the year to minimize self-shading effects over the year. In this paper, the row distance is defined so that no shading between rows occurs at 12.00 am on winter solstice (Aste and Del Pero, 2010).

The method applied in this paper simulates the optimal GCR based on the following assumptions: (i) PV modules are fixed and south-oriented with an angle of 20° to the horizontal axis regardless of actual slope, and orientation (ii) land fields with less than 16° are eligible for ground-mounted PV installation (iii) the row width is decided by the minimum solar height reached by the sun at 12.00 am on the winter solstice (iv) there is no space between panels in the same row. The layout of solar modules on an inclined terrain with a slope angle and orientation angle is shown in Fig. 3. The equations to calculate the GCR on a land field with slope and orientation are shown in Eqs. (1) and (2). In the APV scenario, the resulting GCR of each polygon is divided by a factor of three, as mentioned in Section 2.1.

$$x = \arctan(\cos\alpha \times \tan\beta), \tag{1}$$

$$GCR = \frac{1}{\frac{\sin\gamma - \cos\gamma \tan x}{\sin x + \cos x \tan \delta} + \frac{\cos \delta}{\cos x}}, \tag{2}$$

where:

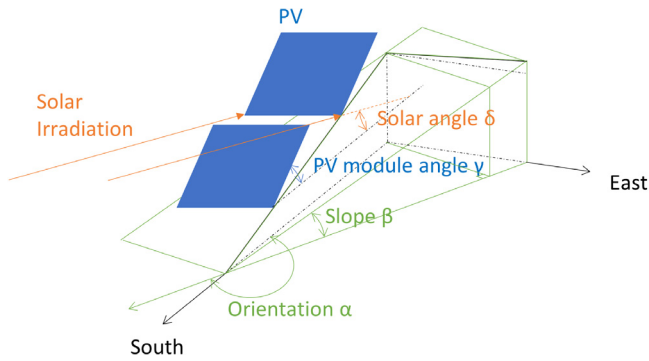


Fig. 3. Layout of solar modules on an inclined terrain. The terrain with its slope and orientation angle is shown in green. The due directions are in dash black. PV panels and its angle with horizontal surface are shown in blue. The solar angle and solar beam are shown in orange. (For interpretation of the references to color in this figure legend, the reader is referred to the web version of this article.)

- α the orientation angle, ranging from 0° (north facing) to 360° clockwise
- β the slope angle, ranging from 0° to 90°
- γ the module tilt with a default value of 20°
- δ the solar angle at 12.00 o'clock on winter solstice.

After the GCR is calculated by Eqs. (1) and (2), the calculation of the PV plant capacity in MW_p and the yearly electricity generation potential in MWh are derived according to Eqs. (3) and (4). For PV module efficiencies, an estimate of the statistical average efficiency 16% of installed plants with different established technologies, e.g., polysilicon and thin-film panels, has been applied. This value is however fully adjustable in the method to reflect further developments in module efficiencies or the use of a particular module type.

$$Capacity = Area \times GCR \times (1 - UL) \times MF \div 1000 \times \frac{MW}{m^2}, \quad (3)$$

$$Potential = Capacity \times SF \times Irradiance \times PR \div 1000 \times \frac{m^2 yr}{W}, \quad (4)$$

where:

- Capacity the nominal capacity of a PV plant in MW_{peak}
- Area the land field area in m^2
- GCR ground cover ratio: the ratio between PV panel area and land field area
- UL unusable area ratio: the area dedicated to access roads, converters, transformer buildings, fencing, potential ecological buffer zones and other infrastructure (Ong et al., 2013) with values between 5% to 10%
- MF PV module efficiency with a default value of 16%
- Potential the annual electricity yield of the PV plant in MWh
- SF shading factor produced by other panels with a default value of 98% according to the layout optimization method applied in this paper (Aste and Del Pero, 2010)
- Irradiance the accumulated sun radiant flux received by a surface per unit area per year in $Wh/(m^2 yr)$
- PR performance ratio: losses due to the conversion efficiency of the inverter, cabling losses, dust on the panels, and others. Electricity storage is considered

2.5. Validation

The newly developed method is validated by comparing the measured capacity and yield data from three existing ground-mounted PV plants in Germany, Zwiefaltendorf, Weddingstedt, and Wesertal, with the simulated results. These plants all featured parallel rows of south-facing modules and were installed between 2010 and 2017. Due to a lack of information on original module efficiency for Zwiefaltendorf and Weddingstedt, a default module efficiency of 14.5% from Wesertal is taken. Both module tilts of 20° and 30° are simulated. The results are presented in Tables 4–5.

The PV plant in Wesertal has the most detailed available plant parameters (Table 4). It was built in 2010 with a module tilt of 30° . Additionally, the GCR is 30% lower than the row width typically applied today of 20% due to higher module costs in 2010. This confirms the advancement in land-use efficiency of ground-mounted PV plants observed over the past decade (Kelm et al., 2019, p. 56). The PV plant area by simulation is around 4% less than the actual value, as the area is represented by rasters that do not have a smooth edge. The actual area and GCR (9.28 ha and 0.27 respectively) are used for the calibration instead of simulation values (8.9 ha and 0.38). The resulting deviation in capacity and yield are 0.3% and 4.8%, respectively. The remaining deviation factors of the solar irradiance and performance ratio cause the deviations. By only eliminating the error of GCR, the deviations of capacity and yield increase to 4% and 14% (the values in the brackets).

For the PV plant in Zwiefaltendorf (Table 5), the simulated area is 0.6% larger than the actual area. However, the simulated capacity and annual yield are 8% and 15%, respectively, lower than actual data. The PV plant was built in 2017 and presents the most current state of design of ground-mounted PV plant with higher module efficiency than the 14.5% assumed for Wesertal, which was built in 2010. Thus, by applying a higher module efficiency of 16% in Zwiefaltendorf the deviations of capacity and yield reduce to 2% and 4%, respectively.

Besides its location, only the installed capacity and annual yield are available for the PV plant in Weddingstedt (see Table 6). As module tilt is not available, simulations are run for both 20° and 30° . Based on default parameters, simulated installed capacity ranges between 2.7 MW_{peak} and 3.4 MW_{peak} , i.e., the actual installed capacity of 2.9 MW_{peak} lies well within that range. The actual annual yield is 2,645 MWh/a, also lying in the simulated range of 2,524 MWh/yr (tilt 30°) to 3,102 MWh/yr (tilt 20°).

The lack of data for two considered plants incurs high inaccuracy levels: module tilt, the GCR, the amount of unused land due to infrastructural or ecological measures influence, and module efficiency. These sources of deviation cause inaccuracy of capacity and yield of the individual plant. For the capacity calculation, a maximal deviation of 2% can be concluded. The yield calculation shows a maximal inaccuracy of 5%. In contrast, the plant in Zwiefaltendorf was built in 2017 and presents the most current design state of ground-mounted PV plants. As a result, the validation of the simulation method with this plant shows a deviation less than 4%, which confirms that the simulation described in Section 2.4 is designed according to modern plant layout standards. Moreover, the method intends to simulate the PV capacity and potential mostly on lands without existing PV plants. Using average up-to-date module tilt and efficiency seems to yield reliable and realistic results, based on the performed validation step.

2.6. Case study regions

Three case study regions (German 'Landkreise' or counties) are chosen for this study out of a total of 400 counties,

Table 4
Validation data plant Wesertal.

Parameter	Unit	Actual (EnBW)	Simulation	Calibration	Difference
Area	ha	9.28	8.9	8.9 (9.28)	4.1%
Module tilt	Degrees	30	30	30	0%
GCR	–	0.27	0.38	0.27	
Capacity	MW _{peak}	3.57	4.9	3.42 (3.58)	0.3% (4%)
Yield	MWh/yr	3,833	4,336	3,059 (3,649)	4.8% (14%)

Table 5
Validation data plant Zwiefaltendorf.

Parameter	Unit	Actual (EnBW)	Simulation	Calibration	Difference
Area	ha	7	7.04	7.04	0.6%
Module tilt	Degrees	n/a	20	n/a	n/a
Capacity	MW _{peak}	5.2	4.8	5.3	2%
Yield	MWh/yr	5,800	5,027	5,547	–4%

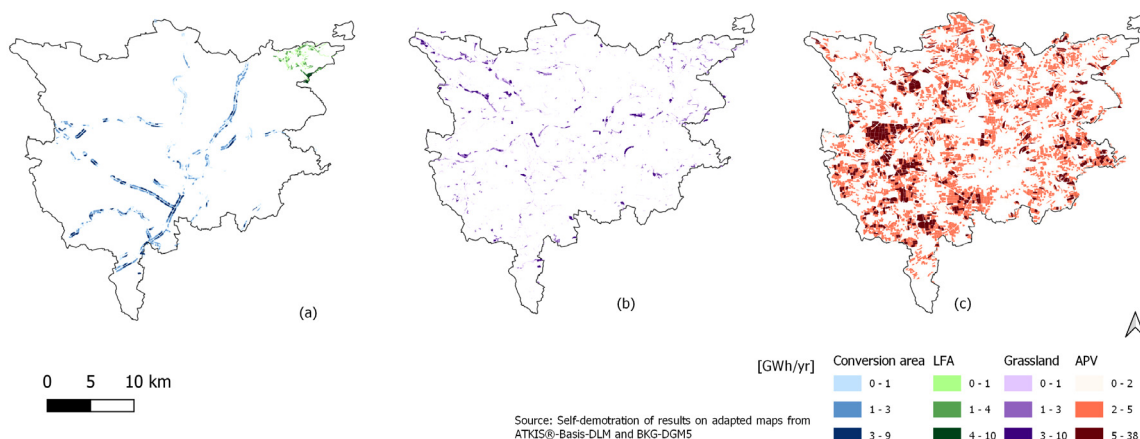


Fig. 4. Spatial distribution of potential areas in Ludwigsburg county. a) shows conversion areas (blue) and areas in less-favored land (green), b) shows grassland areas (purple) and c) shows agricultural areas (red). (For interpretation of the references to color in this figure legend, the reader is referred to the web version of this article.)

because, firstly, county-wide land use data are available; secondly, they differ concerning their land use structure; thirdly, they are located in different parts of Germany, with different climatic conditions. This allows a more holistic view of regional PV potentials and their national ramifications.

- (1) Sub-urban: Ludwigsburg, Baden-Wuerttemberg, Southern Germany
- (2) Forest dominant, semi-urban: Ilm-Kreis, Thuringia, Mid-Eastern Germany
- (3) Agriculture dominant: Dithmarschen, Schleswig-Holstein, Northern Germany

The choice of these counties thus reflects the diversity of Germany and to some extent more broadly typical northern and central European landscapes. Table 7 provides key characteristics for each county.

3. Results

3.1. Spatial distribution of ground-mounted PV potential

Fig. 4 shows a map of the areas suitable for ground-mounted PV according to the four scenarios in Ludwigsburg county. Restricted and unsuitable areas as outlined in Section 2.1 are excluded and shown in white. Only land polygons with at least 0.5 ha were considered to ensure a minimum economic feasibility per plant. The conversion areas and less-favored-areas scenarios indicating current EEG conditions are shown in Fig. 4-a). Conversion areas mainly are corridors parallel to railway tracks

Table 6
Validation data plant Weddingstedt.

Parameter	Unit	Actual (SMA Solar Technology AG, 2021)	Simulation
Capacity	MW _{peak}	2.9	2.7–3.4
Yield	MWh/yr	2,645	2,524–3,102

and highways. Areas in less-favored land appear only in one municipality in the north-eastern part of the county but can cover much larger land shares in other counties. The grassland scenario is shown in Fig. 4-b); grassland covers a similar amount of land as areas in Fig. 4-a). Furthermore, it is distributed equally across the county. In Fig. 4-c), all agricultural areas are illustrated.

Similar maps for Ilm-Kreis and Dithmarschen are shown in Appendices A and B. Generally, the amount of conversion areas correlates directly with the highway and railway network density, which is relatively constant across all counties. According to EEG guidelines, in Ilm-Kreis and Dithmarschen, more than half of the county area is defined as LFA. Ilm-Kreis has lower shares of grassland and agricultural landscapes. On the contrary, grasslands and agricultural lands is the dominate landscape in Dithmarschen, which provide high potential for PV expansion.

Table 8 shows the land area covered by each scenario, compared to the total area for all three counties. In Ludwigsburg, the areas promoted by current EEG regulations account for 3% of the county area. Grassland areas account for 2.8%, while the APV scenario covers around 40% of the county’s area and includes all arable land. For all three counties, conversion area make up 2.0% to 2.6% of the total land area. However, Dithmarschen and

Table 7
Relevant socio-economic, geographic and energetic data of the case study regions.

Parameter	Unit	Ludwigsburg	Ilm-Kreis	Dithmarschen
Area ^a	km ^b	687	805	1,428
Population Density ^a	pers./km ^b	794	132	93
Agricultural land cover rate ^b	%	55	47	76
Forest land cover rate ^b	%	18	45	4
Electricity demand ^{c,d,e}	GWh/yr	1,795	428	841

^aDESTATIS (2021).

^bFederal and state statistical offices (2021).

^cGrassl et al. (2015).

^dEUT (2013).

^eBottenbruch et al. (2013).

Table 8
The land area covered by ground-mounted PV under scenarios in three case study regions.

Region	Area	CA	LFA	GL	APV
Ludwigsburg	Absolute (ha)	1,818	276	1,927	28,380
	Relative (%)	2.6	0.4	2.8	41.3
Dithmarschen	Absolute (ha)	2,889	46,736	36,435	91,143
	Relative (%)	2.0	32.7	25.5	63.8
Ilm-Kreis	Absolute (ha)	2,105	28,894	8,566	23,236
	Relative (%)	2.6	35.9	10.6	28.9

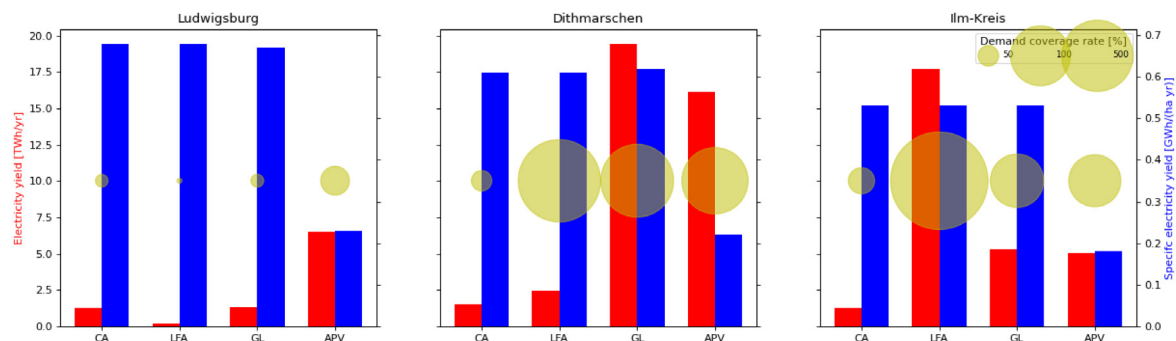


Fig. 5. Yearly aggregated electricity yield of four scenarios in three case study counties. Red bar: electricity yield in TW/yr; blue bar: specific yield in GWh/ha/yr; yellow bubble: coverage rate of the current demand. (For interpretation of the references to color in this figure legend, the reader is referred to the web version of this article.)

Ilm-Kreis have a larger share of LFA of 33% and 36% respectively, considered agriculturally less-productive due to its soil conditions. Lastly, Dithmarschen is the agriculture-dominant region of the three with grassland and agricultural land shares of 26% and 64%, respectively, compared with 11% and 29% in Ilm-Kreis.

3.2. Comparison of regional potential and demand

Fig. 5 shows the yearly potential yield of ground-mounted PV in all scenarios and counties and their statistical electricity demands. The numeric values are shown in Appendix C.

The specific yield in GWh/(ha yr) reflects local solar irradiance and GCR differences due to different latitudes and geometry. Ludwigsburg has the highest average specific yield (0.68 GWh/ha/yr), compared with 0.61 GWh/ha/yr in Dithmarschen and 0.53 GWh/ha/yr in Ilm-Kreis. Specific yields within a region do not differ much between scenarios, except for APV, with its lower GCR. In Ludwigsburg, while conversion areas and less-favored land areas can cover around 80% of current electricity demand, only 40% could be covered when related to 2045 projections. In Dithmarschen and Ilm-Kreis, installing ground-mounted PV plants on conversion areas alone can cover estimated 2020 electricity demand to 180% and 300%, respectively in principle, neglecting storage issues. A hypothetical electricity autarky can thus be achieved, also driven by the much lower demands

in Dithmarschen and Ilm-Kreis (840 GWh/yr and 430 GWh/yr, respectively) compared to 1800 GWh/yr in Ludwigsburg.

From an autarky perspective, Ludwigsburg would thus install PV plants beyond scenario conversion and LFA combined. PV plants on all grassland could generate 1300 GWh/a, covering up to 72% of 2020 demand. In Dithmarschen and Ilm-Kreis, installing PV on available grassland could cover demands more than sixfold.

Installing APV on all feasible agricultural land can supply 362% current and future demands in Ludwigsburg. The APV scenario enables the most prominent possible area utilization for ground-mounted PV among all scenarios, with theoretical yields ranging from 6500 GWh/yr in Ludwigsburg. In Dithmarschen, the theoretical PV yield on agricultural land with APV can reach up to 48,000 GWh/yr. Thus, the question should be what amount of land is required to theoretically cover demands if PV will be installed on those land parcels that are best suited. In Ludwigsburg, besides all conversion, LFA, and grasslands, an additional 373 GWh/yr of agricultural land, accounting for about 342 ha, is needed, accounting for 1.2% of all agricultural land area. Compared to the electricity demand projected for 2045, the demand gap of about 2,200 GWh can be covered by using 8.3% of agricultural area for PV. In the other two case study counties, installing ground-mounted PV on agricultural lands is not necessary to reach autarky from a yearly aggregated point of view. However, through expanding ground-mounted PV, Dithmarschen and Ilm-Kreis counties can become an electricity exporting region (2,900%

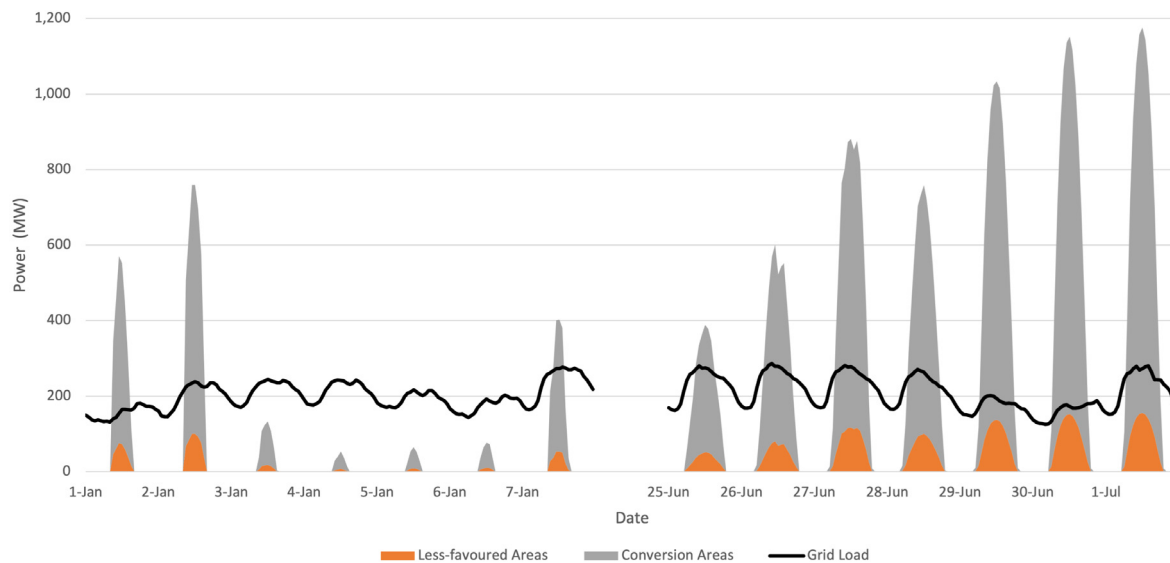


Fig. 6. Hourly profile of grid load and potential yield by ground-mounted PV plants in Ludwigsburg for a typical week in winter (left) and summer (right).

and 1,200%). But the hourly imbalance and grid transmission capacity need to be considered.

Fig. 6 illustrates the hourly ground-mounted PV production of scenarios CA and LFA and the estimated electricity demand in Ludwigsburg for a winter and summer week. The respective charts for IIm-Kreis and Dithmarschen can be found in appendix Appendices D and E. Given the general intermittency of PV power and the daily, weekly and seasonal fluctuations in electricity demand, hourly supply and demand balances can look very different from yearly coverage ratios. In winter, calculated PV yields for Ludwigsburg cannot cover demand even at its peak on mid-day. While mid-day PV generation exceeds demand by up to a factor of six in summer, it is still falling short of demand for 90% of hours of the week. The other two scenarios (GL and APV) cover more areas, increasing production during day times, while demand can still not be covered for 59% of the hours of the week.

To quantify this imbalance, temporal autarky and excess energy are defined: (i) the temporal autarky is the number of hours in a year in which PV at least covers local estimated electricity demand, (ii) the accumulated excess energy ratio is the ratio between accumulated hourly PV electricity production in excess of demand, related to total yearly PV electricity generation. Table 9 shows these factors for all three case study regions. By installing PV on all CA and LFA, temporal autarky values of 25% in Ludwigsburg, 39% in Dithmarschen, and 40% in IIm-Kreis are achieved, i.e., between 60% and 75% of the time locally produced PV electricity needs to be stored, exported or discarded. The yearly excess energy accumulated ratios in CA+LFA and GL scenario are between 52% and 56% in Ludwigsburg, i.e., local demand cannot consume around 680 GWh/yr generated at real-time. The rather low excess energy rate is caused by its high energy demand and comparatively low potentials for ground-mounted PV. In contrast, ground-mounted PV in Dithmarschen and IIm-Kreis generate high amounts of excess energy already in the scenarios representing current regulations, i.e., CA and LFA, with a surplus of 26 TWh and 19 TWh, respectively. Generally, adding more PV capacity by installing ground-mounted PV on more lands does not change the temporal autarky significantly but increases the amount of excess energy.

In the last step, the county's ability to export excess electricity is assessed by comparing the hourly excess PV production with the transmitting capacity of medium-voltage distribution lines, which is also shown in Table 9. In Ludwigsburg, due to

a high transmission capacity of 2,480 MW and comparatively small amounts of excess energy, all extra power can be exported in the scenario CA+LFA. Distribution lines in Dithmarschen and IIm-Kreis with capacities of 408 MW and 459 MW, respectively, do not allow the export of all excess energy even in scenarios CA+LFA.

4. Discussion

A newly established workflow that assesses ground-mounted PV potentials at the regional level with land-use polygon resolution was presented. Around 55% of the studied polygons range from 0.5 ha to 3.2 ha, which aligns on average with Germany's typical PV farm sizes. In contrast to previous studies, the proposed method considers site-specific terrain data and a detailed physical model for PV yield calculations. A validation process with three German PV plants showed the accuracy of the new method with reasonable deviations less than 4% on average. The workflow is then applied to evaluate the potentials for ground-mounted PV plants in German counties in different scenario settings.

Comparing the different scenarios shows that the sufficiency of current land-use regulations to cover regional electricity demands differs enormously depending on each county's geographical conditions, electricity demand, and land use structures. On a yearly basis, ground-mounted PV can contribute double-digit percentage shares to regional electricity demands in all three counties. Nevertheless, Ludwigsburg, a suburban county with a high population density, high electricity demands, and limited space for ground-mounted PV plants, using conversion areas and LFA, 3% of the land area, only covers 80% of 2020 electricity demand. This share drops to 40% using demand projections for 2045, potentially leading to a need to explore parts of the grassland area and install agri-photovoltaic systems if high shares of local production are a vital goal. GL scenario offers a potential covering 72% of the current electricity demand alone. Generally, installation of PV on 8% of all potential agricultural areas and thus on 3.3% of the county's total land area would meet 2045 demand. In contrast to these limited potentials, results for Dithmarschen and IIm-Kreis show high potentials and the ability for ground-mounted PV to cover regional demands on a yearly scale, with demand coverage ratios of more than 2,000% when compared to 2045 demand projections.

An hourly assessment shows that high amounts of excess energy supplied by PV at mid-day and the deficit at night lead to

Table 9
Analysis of hourly results: Autarky, Excess Energy and Transmission capacity under different scenarios.

Region	Energy balance	CA+ LFA	GL	APV
Ludwigsburg	Autarky (h/yr) ^a	2,186	2,069	3,138
	Autarky (%)	25	24	36
	Excess Energy (GWh/yr) ^a	794	678	5,750
	Excess Energy ratio (%)	56	52	88
	Transmission Capacity (MW) ^b		2,480	
	Transmission Overload time (%)	0	0	11
Dithmarschen	Autarky (h/yr) ^a	3,379	3,349	3,320
	Autarky (%)	39	38	38
	Excess Energy (GWh/yr) ^a	26,071	19,184	15,787
	Excess Energy ratio (%)	99	99	98
	Transmission Capacity (MW) ^b		408	
	Transmission Overload time (%)	35	34	34
Ilm-Kreis	Autarky (h/yr) ^a	3,495	3,352	3,342
	Autarky (%)	40	38	38
	Excess Energy (GWh/yr) ^a	18,801	5,128	4,884
	Excess Energy ratio (%)	99	96	96
	Transmission Capacity (MW) ^b		459	
	Transmission Overload time (%)	36	29	28

^aBundesnetzagentur (2021).

^bUW-Madison (2013) and Eichhorn et al. (2018).

hourly temporal autarky values between 25% and 40%. Increasing PV capacity by adding additional land for PV leads to an increase of excess energy only, but not temporal autarky ratios. Especially the counties with lower electricity demand and high amounts of available land, i.e., Dithmarschen and Ilm-Kreis reveal an excess energy ratio between 95% and 100% in all scenarios, which shows that solutions have to be found to store or export electricity. Ludwigsburg has tiny excess energy ratios and a high regional transmission line capacity, so an overload of transmission lines when exporting surplus energy produced by ground-mounted PV is not an issue. In contrast, Ilm-Kreis and Dithmarschen, representing regions with low population density, have a limited grid capacity to transport resulting excess energy in all scenarios, resulting in a share of around one-third of the year, where transmission lines are overloaded in all scenarios. These findings prove that apart from calculating overall yearly results, it is worthwhile to examine the potentials of renewable energy technologies in hourly resolution to evaluate imbalances and consider storage needs and transmission capacities. These results do not assume that 100% renewable energy systems will consist of more than one technology. However, due to the inherent intermittency of wind and solar installations, excess energy levels might be high.

The newly established method can be used in combination with other methods within the same simulation environment and that build on the same or very similar input data points. These allow, for example, to assess regional bioenergy potentials (Bao et al., 2020), housing electricity (Kohler, 2010), heating and cooling demands (Weiler et al., 2019) and thus enable to study regional energy systems in high spatial and temporal resolution or to understand the food–water–energy nexus (FWE) in regions by assessing bioenergy (Bao et al., 2020), food (Bao et al., 2021) and ground-mounted PV potentials whilst also considering local water demands for irrigation and in urban areas (Bao et al., 2020).

5. Conclusions

In many regions, the renewable transformation of energy systems towards will focus on a build-up of wind (onshore and offshore) and PV (rooftop and ground-mounted), with hydro, biomass and geothermal power often playing secondary roles. This study evaluates different land-use restriction scenarios by assessing ground-mounted PV potentials in high spatial–temporal detail and by comparing these with electricity demands on a

regional scale. Compared with similar approaches, the novelty of this study is twofold. First, it allows for a high spatial–temporal resolution (per land field), accuracy (geometry influences the yield) while maintaining scalability at least to the level of a county. Secondly, the method is integrated in a platform and data model that allows to assess, e.g., local biomass, food potentials or water, electricity and heating demands based on the same input data for an integrated energy system planning or analysis along the food–water–energy nexus. The method's high spatial resolution enables project developers and local governmental decision-makers to effectively identify potentials and restrictions not only in the whole region, but also for each targeted field. As a next step, integrating the assessment of ground-mounted PV with similar methods assessing local bioenergy and food potentials allows to quantify local land usage trade-offs, e.g. the loss of biomass potentials due to PV expansion and thus to develop optimal land-use scenarios within the food–water–energy framework. Therefore, on top of academics and projects developers with a focus on ground-mounted PV planning and approving, this work contributes to research fields that deal with land resources trade-off and food–water–energy nexus issues. Since the presented method focuses on one optimal GCR determination method, a possible next step would be the integration of further methods for the determination of PV row distances in ground-mounted PV plants.

Abbreviations

APV Agri-Photovoltaic

BUND Federation for Environment and Nature Conservation Germany (Germany)

DGM5 Digital terrain model of Germany with a resolution of 5 meters

DLM Digital Landscape Model

EEC European Economic Community

EEG Renewable Energy Sources Act (German)

EU European Union

FME Feature Manipulation Engine

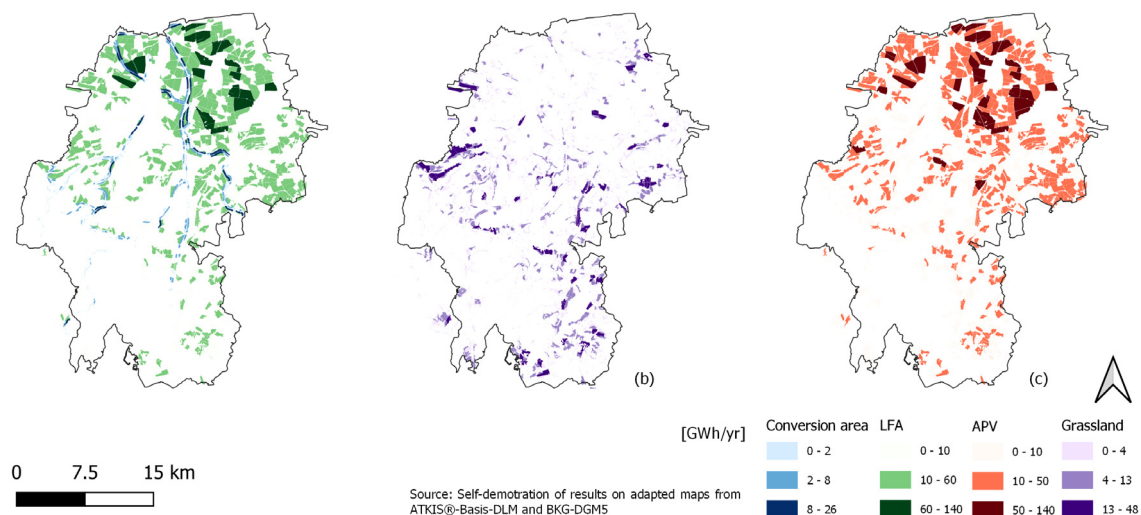


Fig. A.7. Spatial distribution of potential areas in Ilm-Kreis county. (a) shows conversion areas (blue) and areas in less-favored land (green), (b) shows grassland areas (purple) and (c) shows agricultural areas (red). (For interpretation of the references to color in this figure legend, the reader is referred to the web version of this article.)

FWE Food–Water–Energy

GCR Ground Cover Ratio

GIS Geographic Information System

LFA Less-favored Areas

LUBW Federal Environmental Institute Baden-Wuerttemberg (German)

MCA Multi Criteria Assessment

MV Medium voltage

NABU Nature Conservation Association Germany (German)

PV Photovoltaic

RE Renewable Energy

Code availability

SimStadt is an open-source simulation tool, which can be downloaded here (<https://simstadt.hft-stuttgart.de/>).

The python code of ground-mounted potential simulation is not available to the public.

CRedit authorship contribution statement

Keyu Bao: Resources, Conceptualization, Methodology, Software, Validation, Formal analysis, Investigation, Data curation, Writing – original draft, Writing – review & editing. **Louis Kalisch:** Methodology, Validation, Formal analysis, Investigation, Data curation, Writing – original draft, Writing – review & editing. **Thun-yathep Santhanavanich:** Methodology, Data curation, Writing – original draft, Writing – review & editing. **Daniela Thrän:** Writing – review & editing, Supervision. **Bastian Schröter:** Resources, Conceptualization, Writing – review & editing, Supervision.

Declaration of competing interest

The authors declare the following financial interests/personal relationships which may be considered as potential competing interests: Keyu Bao reports financial support was provided by Federal Ministry for Economy and Energy. Keyu Bao reports financial support was provided by European Union.

Funding

The work was developed within the structures of the Institute for Applied Research (IAF), HFT Stuttgart and was funded by the projects IN-SOURCE and EnSys-LE. IN-SOURCE is one of the projects of ERANET Sustainable Urbanisation Global Initiative (EN-SUGI) funded by European Union's Horizon 2020 research and innovation program under grant agreement No 730254 and other 19 funding agencies. The German IN-SOURCE subproject is funded by Federal Ministry of Education and Research (BMBF). EnSys-LE is funded by the German Federal Ministry for Economic Affairs and Climate Action (BMWi) under grant agreement No 03ET4061B. IAF provided the funding for publication.

Availability of data and material

Data is shown in supplementary data.

Appendix A

See Fig. A.7.

Appendix B

See Fig. B.8.

Appendix C

See Table C.10.

Appendix D

See Fig. D.9.

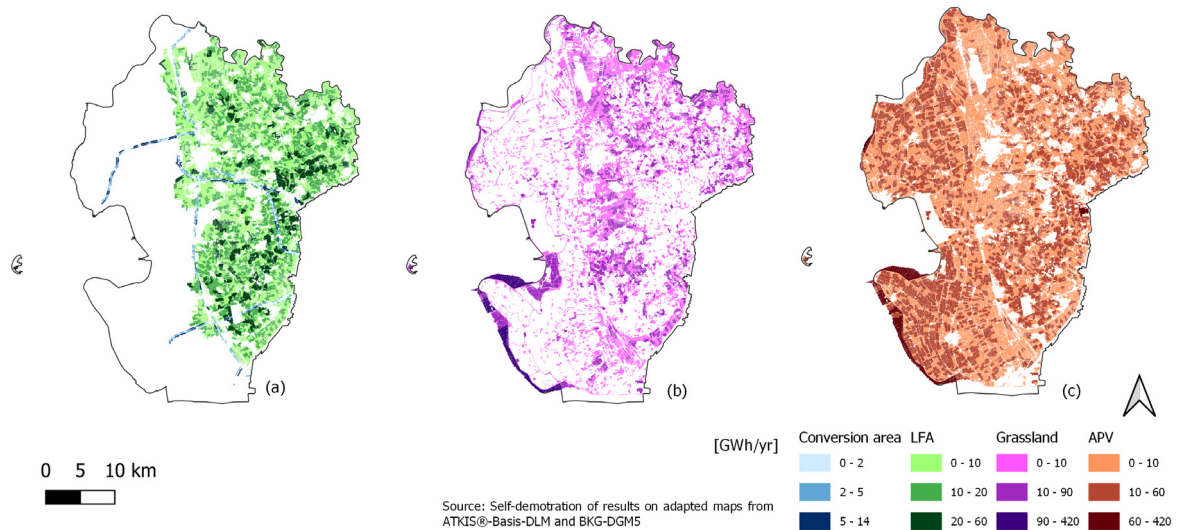


Fig. B.8. Spatial distribution of potential areas in Dithmarschen county. (a) shows conversion areas (blue) and areas in less-favored land (green), (b) shows grassland areas (purple) and (c) shows agricultural areas (red). (For interpretation of the references to color in this figure legend, the reader is referred to the web version of this article.)

Table C.10
Potential yields of ground-mounted PV according to the four scenarios.

Region	Yield	Conversion	LFA	Grassland	APV
Ludwigsburg	Absolute yield (GWh/yr)	1,235	187	1,295	6,503
	Specific yield (GWh/ha/yr)	0.68	0.68	0.67	0.23
	Demand Coverage (Current) (%)	69	10	72	362
	Demand Coverage (2045) (%)	34	5	36	181
Dithmarschen	Absolute yield (GWh/yr)	1,521	24,855	19,465	16,114
	Specific yield (GWh/ha/yr)	0.61	0.61	0.62	0.22
	Demand Coverage (Current) (%)	181	2,955	2,315	1,916
	Demand Coverage (2045) (%)	90	1,478	1,157	958
Ilm-Kreis	Absolute yield (GWh/yr)	1,282	17,692	5,322	5,074
	Specific yield (GWh/ha/yr)	0.53	0.53	0.53	0.18
	Demand Coverage (demand) (%)	300	4,134	1,244	1,185
	Demand Coverage (2045) (%)	150	2,067	621	593

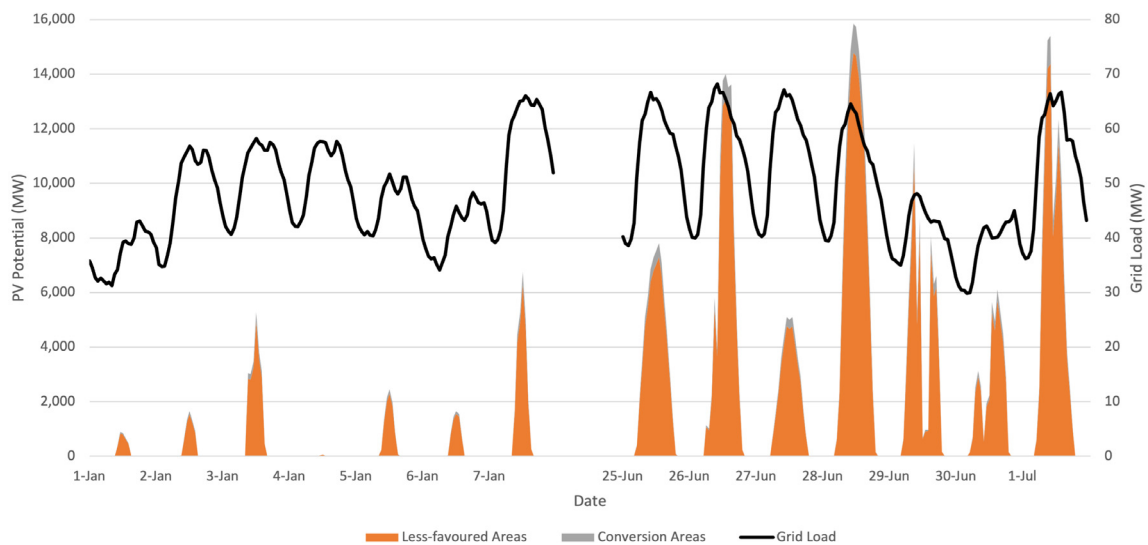


Fig. D.9. Hourly profile of grid load and potential yield by ground-mounted PV plants in Ilm-Kreis for an exemplary week in winter (left) and summer (right).

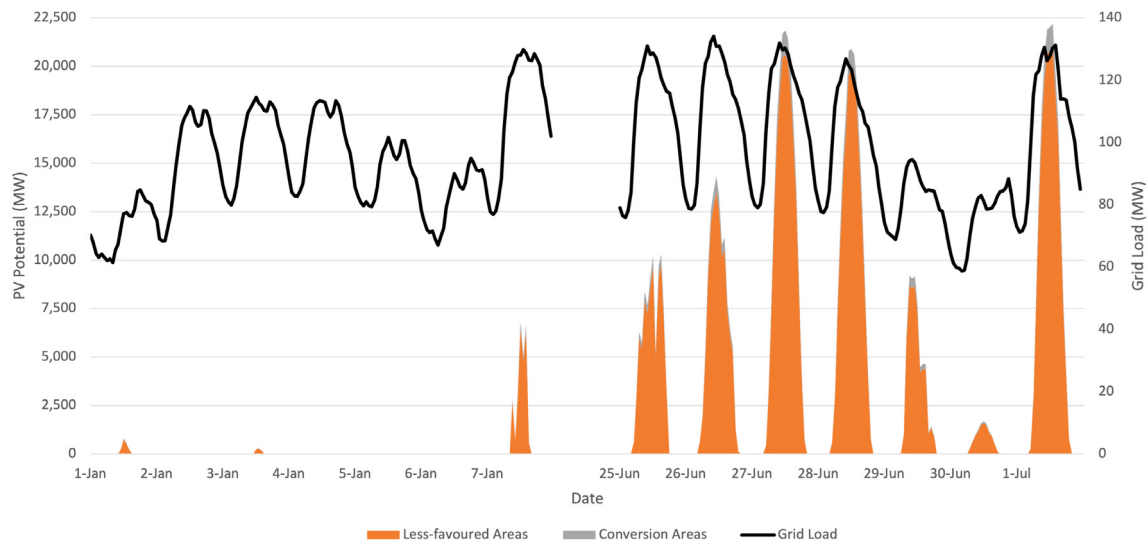


Fig. E.10. Hourly profile of grid load and potential yield by ground-mounted PV plants in Dithmarschen for an exemplary week in winter (left) and summer (right).

Appendix E

See Fig. E.10.

References

- Alanne, K., Saari, A., 2006. Distributed energy generation and sustainable development. *Renew. Sustain. Energy Rev.* 10 (6), 539–558. <http://dx.doi.org/10.1016/j.rser.2004.11.004>, <https://linkinghub.elsevier.com/retrieve/pii/S1364032105000043>.
- Aste, N., Del Pero, C., 2010. Technical and economic performance analysis of large-scale ground-mounted PV plants in Italian context. *Prog. Photovolt., Res. Appl.* 18 (5), 371–384. <http://dx.doi.org/10.1002/pip.984>, <https://onlinelibrary.wiley.com/doi/10.1002/pip.984>.
- Badelt, O., Niepelt, R., Wiehe, J., Matthies, S., Gewohn, T., Stratmann, M., et al., 2020. Integration von solarenergie in die niedersächsische energielandschaft (INSIDE). Hannover. <https://www.umwelt.uni-hannover.de/de/badelt/forschungsprojekte/forschungsprojekt-detailansicht-badelt/projects/integration-von-solarenergie-in-die-niedersaechsische-energielandschaft-inside/>.
- Bao, K., Padsala, R., Coors, V., Thrän, D., Schröter, B., 2020. A method for assessing regional bioenergy potentials based on GIS data and a dynamic yield simulation model. *Energies* 13 (24), 6488. <http://dx.doi.org/10.3390/en13246488>, <https://www.mdpi.com/1996-1073/13/24/6488>.
- Bao, K., Padsala, R., Coors, V., Thrän, D., Schröter, B., 2021. A GIS-based simulation method for regional food potential and demand. *Land* 10 (8), 880. <http://dx.doi.org/10.3390/land10080880>, <https://www.mdpi.com/2073-445X/10/8/880>.
- BImA, 2021. Daten und fakten. Federal Agency for Real Estate Tasks. <https://www.bundesimmobilien.de/daten-und-fakten-57e8b8690f78aac8>. (Accessed 22 September 2021).
- BKG, 2021. Digitale landschaftsmodelle. Bundesamt Für Kartographie Und Geodäsie. <https://gdz.bkg.bund.de/index.php/default/digitale-geodaten/digitale-landschaftsmodelle.html>. (Accessed 13 October 2021).
- BMVI, 2015. Räumlich differenzierte flächenpotentiale Für erneuerbare energien in deutschland. Federal Ministry of Transport and Digital Infrastructure, Berlin. https://www.bbsr.bund.de/BBSR/DE/veroeffentlichungen/ministerien/bmvi/bmvi-online/2015/BMVI_Online_08_15.html.
- BNetzA, 2021. Marktstammdatenregister: Erweiterte einheitenübersicht. Bundesnetzagentur. <https://www.marktstammdatenregister.de/MaStR/Einheit/Einheiten/ErweiterteOeffentlicheEinheitenuebersicht>. (Accessed 04 October 2021).
- Bottenbruch, R., Wamboldt, E., Winter, L., Pöhler, M., Wangelin, M., 2013. Integriertes klimaschutzkonzept Für den kreis dithmarschen. Tech. rep., p. 272.
- BUND, NABU, 2021. Positionspapier zur solarenergie von BUND und NABU. Tech. rep., <https://www.bund-bawue.de/service/publikationen/detail/publication/positionspapier-zur-solarenergie-von-bund-und-nabu/>.
- Bundesgesetzblatt, 2021. Erneuerbare-energien-gesetz vom 21. Juli 2014 (BGBl. I S. 1066), das zuletzt durch artikel 11 des gesetzes vom 16. Juli 2021 (BGBl. I S. 3026) geändert worden ist. EEG, https://www.gesetze-im-internet.de/eeg_2014/BjNR106610014.html.
- Bundesnetzagentur, S., 2021. Market data: Electricity consumption - transnetBW (DE). <https://www.smard.de/en/downloadcenter/download-market-data#!?downloadAttributes=%7B%22selectedCategory%22:2,%22selectedSubCategory%22:5,%22selectedRegion%22:%22TransnetBW%22,%22from%22:1546297200000,%22to%22:1577919599999,%22selectedFileType%22:%22XLS%22%7D>. (Accessed 19 October 2021).
- Calvert, K., Mabee, W., 2015. More solar farms or more bioenergy crops? Mapping and assessing potential land-use conflicts among renewable energy technologies in eastern ontario, Canada. *Appl. Geogr.* 56, 209–221. <http://dx.doi.org/10.1016/j.apgeog.2014.11.028>.
- Charabi, Y., Rhouma, M.B.H., Gastli, A., 2016. Siting of PV power plants on inclined terrains. *Int. J. Sustain. Energy* 35 (9), 834–843. <http://dx.doi.org/10.1080/14786451.2014.952298>, <http://www.tandfonline.com/doi/full/10.1080/14786451.2014.952298>.
- DESTATIS, 2021. Daten aus dem gemeindeverzeichnis: Kreisfreie städte und landkreise nach fläche, bevölkerung und bevölkerungsdichte am 31.12.2020. German Federal Statistical Office. <https://www.destatis.de/DE/Themen/Regionales/Gemeindeverzeichnis/Administrativ/04-kreise.html>. (Accessed 19 September 2021).
- Eichhorn, M., Thylmann, M., Peters, W., Kinast, P., Thrän, D., Bauschmann, M., et al., 2018. Spatial distribution of overhead power lines and underground cables in Germany in 2016. *Data* 3 (3), 34. <http://dx.doi.org/10.3390/data3030034>, <http://www.mdpi.com/2306-5729/3/3/34>.
- EnBW, Solar energy at EnBW. Sol. Energy <https://www.enbw.com/renewable-energy/solar/>. (Accessed 30 November 2021).
- European Commission, 2021. Photovoltaic geographical information system (PVGIS). European Commission (EC)- Joint Research Centre, Institute for Energy and Transport. <https://ec.europa.eu/jrc/en/pvgis>. (Accessed 30 September 2021).
- EUT, 2013. Klimaschutzprogramm ilm-kreis 2005–2015. Tech. rep., Energie- und Umweltpark Thüringen e.V., p. 96.
- Federal and state statistical offices, 2021. Regionaldatenbank deutschland: Bodenfläche nach art der tatsächlichen nutzung - kreise und kreisfreie städte (stichtag 31.12.2015). <https://www.regionalstatistik.de/generation/online?operation=abruftabelleBearbeiten&levelindex=1&levelid=1632081112969&auswahloperation=abruftabelleAuspraegungAuswaehlen&auswahlverzeichnis=ordnungsstruktur&auswahlziel=werteabruf&code=33111-01-01-4&auswahltext=&wertabruf=Werteabruf#abreadcrumb>. (Accessed 19 September 2021).
- Grassl, G., Blaich, C., Eicker, U., Coors, V., Bartke, N., Müller, M., et al., 2015. Landkreis ludwigsburg - integriertes klimaschutzkonzept. abschlussbericht band 1. Tech. rep.
- IEA, 2019. World energy outlook 2019. International Energy Agency, Paris. <https://www.iea.org/reports/world-energy-outlook-2019>.
- Kelm, T., Metzger, J., Fuchs, A.-L., Schicketanz, S., Günnewig, D., Thylmann, M., 2019. Untersuchung zur wirkung veränderter flächenrestriktionen Für pv-freiflächenanlagen. Tech. rep., p. 83.
- Kohler, S., 2010. Stochastic generation of household electricity load profiles in 15-minute resolution on building level for whole city quarters. entwicklung der wohnflächenversorgung in den städten und gemeinden baden-württembergs. Statistisches Monatsheft Baden-Württemberg.

- Köhler, S., Sihombing, R., Duminil, E., Coors, V., Schröter, B., 2021. A multi-scale, web-based application for strategic assessment of PV potentials in city quarters. In: Proceedings of the 10th international conference on smart cities and green ICT systems - SMARTGREENS. SciTePress, INSTICC, pp. 110–117. <http://dx.doi.org/10.5220/0010406201100117>.
- Kost, C., Shammugam, S., Fluri, V., Peper, D., Davoodi Memar, A., Schlegl, T., 2021. Stromgestehungskosten erneuerbare energien. Fraunhofer ISE, Freiburg, p. 46. https://publica.fraunhofer.de/eprints/urn_nbn_de_0011-n-6389438.pdf.
- LUBW, 2021. Potenzialanalyse - energieatlas BW. Landesanstalt Für Umwelt Baden-Württemberg, <https://www.energieatlas-bw.de/sonne/freiflachen/potenzialanalyse>. (Accessed 28 August 2021).
- Nouvel, R., Brassel, K.-H., Bruse, M., Duminil, E., Coors, V., Eicker, U., et al., 2015. SimStadt, a new workflow-driven urban energy simulation platform for CityGML city models. In: Proceedings of international conference CISBAT 2015. future buildings and districts. sustainability from nano to urban scale. Lausanne, LESO-PB, EPFL, pp. 889–894. <http://dx.doi.org/10.5075/EPFL-CISBAT2015-889-894>, <http://infoscience.epfl.ch/record/213437>.
- Ong, S., Campbell, C., Denholm, P., Margolis, R., Heath, G., 2013. Land-use requirements for solar power plants in the united states. Tech. rep. NREL/TP-6A20-56290, National Renewable Energy Laboratory (NREL), pp. NREL/TP-6A20-56290, 1086349. <http://dx.doi.org/10.2172/1086349>, <http://www.osti.gov/servlets/purl/1086349/>.
- Perpiña Castillo, C., Batista e Silva, F., Lavalle, C., 2016. An assessment of the regional potential for solar power generation in EU-28. Energy Policy 88, 86–99. <http://dx.doi.org/10.1016/j.enpol.2015.10.004>, <https://www.sciencedirect.com/science/article/pii/S0301421515301324>.
- Romero Rodríguez, L., Duminil, E., Sánchez Ramos, J., Eicker, U., 2017. Assessment of the photovoltaic potential at urban level based on 3D city models: A case study and new methodological approach. Sol. Energy 146, 264–275. <http://dx.doi.org/10.1016/j.solener.2017.02.043>, <https://www.sciencedirect.com/science/article/pii/S0038092X17301445>.
- Safe Software, 2021. FME - data integration platform. Safe Software. <https://www.safe.com/fme/>. (Accessed 13 October 2021).
- Schindele, S., Trommsdorff, M., Schlaak, A., Obergfell, T., Bopp, G., Reise, C., et al., 2020. Implementation of agrophotovoltaics: Techno-economic analysis of the price-performance ratio and its policy implications. Appl. Energy 265, 114737. <http://dx.doi.org/10.1016/j.apenergy.2020.114737>, <https://linkinghub.elsevier.com/retrieve/pii/S030626192030249X>.
- Schumacher, J., 2014. INSEL 8 - software zur simulation, Überwachung und visualisierung von energiesystemen. <https://www.insel.eu/de/>. (Accessed 30 September 2021).
- Siala, K., Stich, J., 2016. Estimation of the PV potential in ASEAN with a high spatial and temporal resolution. Renew. Energy 88, 445–456. <http://dx.doi.org/10.1016/j.renene.2015.11.061>, <https://www.sciencedirect.com/science/article/pii/S0960148115304778>.
- SMA Solar Technology AG, 2021. Freifläche weddingstedt jahresvergleich. SMA Sunny Portal. <https://www.sunnyportal.com/Templates/PublicPageOverview.aspx?plant=7426a0e0-dfeb-4448-af44-888236ddfdb2&splang=>. (Accessed 30 November 2021).
- SPD, Bündnis 90/Die Grünen, FDP, 2021. Koalitionsvertrag zwischen SPD, bündnis 90/DIE grünen und FDP. Sozialdemokratische Partei Deutschlands (SPD), <https://www.spd.de/koalitionsvertrag2021/>. (Accessed 13 December 2021).
- STMWI, 2021. Energie-atlas bayern - unser portal - lexikon - K - konversionsfläche. Bayerisches Staatsministerium Für Wirtschaft, Landesentwicklung Und Energie. <https://www.energieatlas.bayern.de/energieatlas/lexikon/k/konversionsflaeche.html>. (Accessed 21 September 2021).
- Trommsdorff, M., Gruber, S., Keinath, T., Hopf, M., Hermann, C., Schönberger, F., et al., 2020. Agrivoltaics: opportunities for agriculture and the energy transition - a guideline for Germany. Tech. rep., Fraunhofer ISE, p. 56. <https://www.ise.fraunhofer.de/content/dam/ise/en/documents/publications/studies/APV-Guideline.pdf>.
- UW-Madison, 2013. Estimating line-flow limits. Tech. rep., University of Wisconsin-Madison, p. 7. https://neos-guide.org/sites/default/files/line_flow_approximation.pdf.
- Weiler, V., Stave, J., Eicker, U., 2019. Renewable energy generation scenarios using 3D urban modeling tools—methodology for heat pump and co-generation systems with case study application †. Energies 12 (3), 403. <http://dx.doi.org/10.3390/en12030403>, <http://www.mdpi.com/1996-1073/12/3/403>.
- Wirth, H., 2021. Aktuelle fakten zur photovoltaik in deutschland. Tech. rep., Fraunhofer ISE, p. 96. <https://www.ise.fraunhofer.de/de/veroeffentlichungen/studien/aktuelle-fakten-zur-photovoltaik-in-deutschland.html>.
- Wirth, H., Bächle, S., 2021. Wie wir mit sonnenenergie einen wirtschaftsboom entfesseln und das klima schützen. Fraunhofer-Institut Für Solare Energiesysteme ISE, <https://www.ise.fraunhofer.de/de/presse-und-medien/presseinformationen/2021/wie-wir-mit-sonnenenergie-einen-wirtschaftsboom-entfesseln-und-das-klima-schuetzen.html>. (Accessed 15 September 2021).

Chapter 6

Land Resource Allocation between Biomass and Ground-Mounted PV under consideration of the Food-Water-Energy Nexus Framework at Regional Scale

Bao, K.; Thrän, D.; Schröter, B. . Submitted to Renewable Energy. 2022.

Submitted in Renewable Energy. 2022.

Land Resource Allocation between Biomass and Ground-Mounted PV under consideration of the Food-Water-Energy Nexus Framework at Regional Scale

Keyu Bao^{a,b,c,*}, Daniela Thrän^{b,c,d}, Bastian Schröter^a

^a*Center for Sustainable Energy Technology, Hochschule für Technik Stuttgart, Schellingstraße 24, 70174 Stuttgart, Germany*

^b*Department of Bioenergy, Helmholtz Center for Environmental Research, Torgauer Straße 116, 04247 Leipzig, Germany*

^c*Chair of Bioenergy System, Faculty of Economic Sciences, University of Leipzig, Grimmaische Straße 12, 04109 Leipzig, Germany*

^d*Unit Bioenergy System, DBFZ, Torgauer Straße 116, 04347 Leipzig, Germany*

Abstract

An economy's shift towards climate neutrality requires a massive expansion of renewable energy production. Next to wind, photovoltaic (PV) and biomass will be key renewable resources in many regions. A land-use change to PV thus increases local electricity production, but influences regional water and biomass availability. However, a regional quantitative guideline on biomass-PV tradeoff on all agricultural fields under food-water-energy (FWE) nexus thinking is still missing. This work presents a comprehensive bottom-up interdependency assessment between ground-mounted PV and biomass generation on a regional scale by integrating established independent methods with the same input at spatial field resolution. Their impacts on food and water availability are also quantified. Four scenarios were set up based on current policies and future trend emphasizing PV yield, feasibility, profit, or biomass, respectively. The assessment and scenarios are applied at three representative German counties with distinguished land-use structures and geometries as case studies. Scenario analysis shows that the optimal tech-

*Corresponding author

Email addresses: keyu.bao@hft-stuttgart.de (Keyu Bao),
daniela.thraen@ufz.de, thraen@wifa.uni-leipzig.de, daniela.thraen@dbfz.de
(Daniela Thrän), bastian.schroeter@hft-stuttgart.de (Bastian Schröter)

nical strategy among the proposed ones is to follow the individual market profit drive, which likely simultaneously is good for society, achieves high PV yields with limited biomass losses, and has more significant crop water saving effects.

Keywords:

Food-Water-Energy Nexus, Bottom-up simulation, Ground-mounted PV, Biomass, Land resources

1. Introduction

Water, energy, and food are essential resources for human development. In most world region, these three resources interact in synergetic or opposing ways. For example, the Food and Agriculture Organization of the United Nations (FAO) estimates that the global food production must be increased by 60% to meet the food demand requiring 40% more water and 50% more energy [1]. The basis of the Food-Water-Energy (FWE) Nexus is an attempt to balance different uses of ecosystem resources (energy, water, land, soil, and socio-economic factors).

In the German energy sector, 69 to 168 TWh of final energy, i.e., 15% to 20% of total final energy demand, is expected to be generated from photovoltaic (PV) by 2045 [2]. PV capacity is thus set to increase up to three-fold by 2045 compared to 2015 [2]. This amount of production capacity cannot be achieved by rooftop PV alone, but requires a strong expansion of ground-mounted PV plants. Ground-mounted PV plants consist of rows of PV panels installed on tilted frames, which are typically connected to the ground via metal foundations. In 2017, the share of ground-mounted PV plants had reached approximately 28% of the overall installed PV power nationally and is expected to be rising further due to their higher cost-efficiency compared to rooftop-PV [3, 4].

However, in the context of FWE nexus, ground-mounted PV plants have a high demand for land compared to conventional power plants and compete with other forms of land use, especially agriculture and bioenergy production [5]. To avoid conflicts between ground-mounted PV, other forms of land use, and ecological interests, the German government has outlined regulations in the National Renewable Energy Sources Act (German 'EEG'), that restricts the land areas eligible for ground-mounted PV plants benefiting from feed-in tariffs [5]. As subsidy-free PV plants become economically feasible,

these land-use restrictions in the current EEG and municipal council are becoming more and more obsolete [6]. Additionally, the Federation for the Environment and Nature Conservation Germany (German 'BUND') and the Nature Conservation Association Germany (German 'NABU') are appealing to ease the regulations placed by the EEG to accelerate the scale-up of renewable energies, pointing out that conventional mono-cultural agriculture has higher ecological impacts on land than ground-mounted PV [7]. Therefore, it is urgent to accelerate the transition process and understand the trade-offs between ground-mounted PV, biomass. and food.

To date, a few studies investigated the trade-offs between biomass and PV with the focus on agriculturally-eligible lands to avoid conflicts with food [8, 9]. Calvert et al. have evaluated the trade-off between solar PV and bioenergy crops on land that suits both technologies via Geographical Information System (GIS)-based siting, taking into account energy densities and each technology's ability to cover regional demands. PV and biomass yields are not simulated but chosen from several discrete statistical values [8]. Leirpoll et al. developed a method to compare the utilization of recently abandoned cropland on a global scale for bioenergy crops and ground-mounted PV. The study demonstrated a ten-fold higher land-use efficiency of ground-mounted PV. Yield potentials were calculated based on local irradiation data, but terrain data was not included. Instead, a static Ground Cover Ratio (GCR), of 0.33 was applied, i.e., the ratio between the active PV panel area and the total ground surface area occupied by the installation. Moreover, national regulations and regional environmental and socio-economic factors were not part of the study focus [9].

The amount of abandoned agricultural lands, however, is limited. Several studies [10, 11, 12] attempt to expand ground-mounted PV on agricultural lands by applying the concept of agro-photovoltaics (APV) to avoid conflicts with food again. APV combines biomass production and solar power production on the same land area, e.g. by installing PV panels vertically and allowing enough space for agricultural machines to be deployed between module rows. However, APV is in most cases still in a pilot phase and requires further research, e.g., impacts on crop growth and irrigation. Therefore, in this paper, APV is neglected due to its still continued technical variability and application uncertainty [11]. To solve the urgency of ground-mounted PV expansion on existing agricultural lands with a technically mature solution in the short-term future, a exclusive trade-off assessment between biomass/food and PV is still missing. The assessment should identify where

ground-mounted PV could be expanded in a region by causing as limited negative impacts as possible on biomass and water resources [13]. This challenge demands an integrated approach, considering economic, social, political, and environmental dimensions [14].

To address the food-water-energy related nexus issue, Hoff et al. introduced an initial guidance on how to solve the FWE nexus, including increasing efficiency, reducing trade-offs, building synergies, and improving governance across sectors [15]. For assessing the FWE inter-dependencies, two main approaches, i.e., bottom-up and top-down, are widely adopted [16]. The bottom-up approach quantifies the resource footprints of individual products or technologies, i.e., identifying how a specific technology contributes to the overall goal [17]. The bottom-up optimization approach does not necessarily guarantee a fine spatial resolution, but rather shows the linkages between elements [18, 19, 20, 21, 22, 23]. In contrast, the top-down approach starts from the “big picture” of sector performance by modeling the resource stocks and flows of the FWE systems in an economy and then breaks down the footprint, e.g., resource consumption, reduction potentials of individual sectors and end-uses.

The FWE framework has been used in various contexts at many spatial levels, e.g., resources at the global level [24], energy at the national level [25], and water management at the regional level [26], for management and planning. On agricultural fields, where ground-mounted PV is competing, the FWE framework has been adopted to optimize food security, water security and minimize carbon emissions. Besides the specific context, gaps persist with regards to tools and data availability. Firstly, there are no standalone methods and tools for implementing the nexus approach, i.e., existing methods used incompatible tools to generate results on FWE domains respectively [14]. Secondly, tools that can be replicated and/or adjusted to different sites and scales [27] and/or new case studies [28, 14, 29] are not available. Thirdly, utilization of robust data sets from multiple sources is still lacking [13].

To fill these research gaps, this paper integrates previously established workflows on ground-mounted PV potential [30] and biomass [31] potential in a same simulation platform using a shared input data including a map of land use, food production, soil, and temporal climate data and socio-economic factors with single-field resolution, which provides the scalability to any lower level of spatial detail, i.e., regional or national. Based on the two workflows mentioned above, this paper generates land-use trade-off scenarios addressing the land use transition trend in Germany based on current

political regulations. Compared to studies focusing on the national level, this regional-focused work thus helps local governments and municipalities in the decision-making process of finding a land use equilibrium between PV energy production and biomass by taking into account potential PV and bioenergy gains, amounts of saved irrigation, food loss, etc.

In this paper, field refers to the area of land which has a different use type, e.g., forest and arable land, or has boundaries, i.e., roads or water bodies, with surrounding areas. The term biomass refers to the plant-based material for energy use only. To simplify the language without specification PV refers to ground-mounted PV. Besides biomass and PV, onshore wind is another critical energy source contributing to the emission-free goal. However, due to relative smaller land footprint of onshore wind, as well as the scope of the paper, energy-use lands are limited to biomass and PV in this paper. The analysis on PV-biomass trade-off in this paper takes place in the suburban area covering with agricultural and grass lands, which are referred to as hinterland in the paper.

2. Materials and methods

2.1. Analysis approaches and information flow

Two elements are to be considered for any FWE nexus assessment: a) an understanding of the inter-dependencies between water, energy, and food systems in a given context, and b) the evaluation of performance of a technical or policy intervention in this given context [25]. Figure 1 shows the four steps and main items per step to address these two elements.

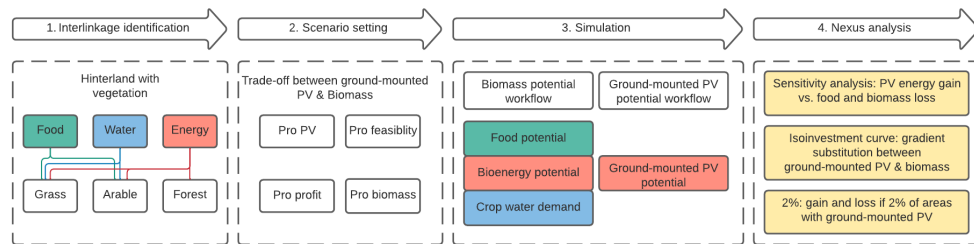


Figure 1: Nexus simulation and analysis used in this work. Blocks and lines with red background relate to energy topics; blue to water; green to food. The assessments are shown in yellow blocks.

- Qualitative and quantitative identification of the FWE inter-linkages (section 2.2): This paper focuses on trade-offs/synergies between ground-mounted PV and biomass production, as well as the impact on food potential and water consumption, i.e., the expansion of ground-mounted PV decreases the biomass/food production also the potential irrigation demand.
- Scenario setting (section 2.3): Based on the identified inter-linkages and political regulations, scenarios are set up.
- Application of the comprehensive FEW simulation tool (section 2.4). A regional energy workflow platform was extended with bottom-up FWE workflows on biomass and PV. Related data is collected and stored in a shared structured dataset.
- Assessment of trade-offs by indicators: Quantitative indicators are required to measure the trade-off. To evaluate the trade-off between PV and biomass both the technical potential, e.g., yield in tonnes per ha per year, and the economic benefits, e.g., profit from agricultural production, are considered (section 2.5).

2.2. Qualitative and quantitative identification of the inter-linkages

Flammini et al. suggested first to identify the most related FWE inter-linkages to research questions in terms of the sustainability of the ecosystem and human system at regional [25]. It is doubtful that all inter-linkages are addressed and integrated with one single simulation platform. Concerning the main research question of ground-mounted PV and biomass trade-off in this paper, table 1 shows the most crucial connections between energy, water, and food, that could be influenced by expanding PV on fields. The hinterland provides land area for plant-based use (biomass/food) and PV. Both trade-off and synergy can exist, e.g., (i) due to the exclusive biomass-PV trade-offs definition, the increase of land use for PV damages the biomass/food production, (ii) within the plant-base land use, if more land is used for biomass, less food production will be observed, (iii) positive synergy can be reached with potential crop water saving, where PV farms do not require water compared with crops. Regulations, that specified the boundary conditions within each inter-linkage, are explained below.

Table 1: Inter-linkages addressed in this paper concerning PV and biomass and their impacts on food, water, and energy production/consumption. The trade-off represented by '-', while synergy represented by '+'.

Interlinkage	Food	Water	Energy
Biomass and PV		+	-
Food production and PV	-	+	-
Food production and biomass	-		-

Regarding land use conflict between biomass/food and PV, the German Renewable Energy Sources Act (EEG) defined conversion areas (CA) and less-favored area (LFA) to restrict the growth of ground-mounted PV. Conversion areas are defined as (i) areas along highways or railroads within 200 m of the outer edge of the paved roadway. A corridor located along the high way or railway of at least 15 meters wide shall be kept clear. (ii) areas formerly for economic, traffic, housing, or military purposes, sealed areas, designated commercial areas, and other built facilities. Less-favored areas (LFA) are grass and arable land with low agricultural productivity (Council Directive 86/465/EEC). However, the German states of Bavaria and Baden-Württemberg cleared restrictions on ground-mounted PV expansion on LFA in 2017.

On agricultural land there is a trade-off between biomass and food crops. Energy crops usually have a disadvantage compared with crops with pure cost-revenue criteria [32]. In areas with adequate agricultural land per capita, the cultivation of energy crops is unlikely to affect food supply independence over the medium term. Additionally, with the Renewable Energy Directive 2018/2001 (RED II), adopted in December 2018, the EU is continuing the political framework for the use of renewable energy sources for the period from 2021 to 2030. Within that framework, first-generation bioethanol, i.e., ethanol sourced from dedicated crops, will be phased out until 2030 [33] and only secondary generation biomass, i.e., residues, and first-generation biogas from current maize cultivation, can be used for energy purposes. In this paper, the trade-off between food and energy crops only happens on the current energy maize field.

2.3. Scenario setting

Four scenarios are set up to address all relevant PV-biomass inter-linkages in table 1. The scenarios also respond to new policy measures and highlight

goals and trends with regards to different economic, social, and environmental issues. Table 2 summarizes all considered scenarios, where fields are prioritized accordingly for expanding PV.

Table 2: Scenarios at potential side.

Scenario	Description
Pro PV	The land fields with high PV potential are preferred for PV.
Pro feasibility	Ground-mounted PV plants are to be installed on fields with high technical (close to mid-voltage transmission lines) and political feasibility (CA and LFA).
Pro profit	The land fields with high payback ratio between PV and agricultural production are preferred.
Pro bioenergy	The maize fields for biogas are less favoured for PV, as well as fields with high bioenergy potential.

Scenario 'Pro PV' shows a land-use strategy focusing on maximizing electricity generation from PV. The land fields with the highest PV yield, i.e., usually south terrains, are prioritized to install PV first regardless of the land-use type and other restrictions.

Scenario 'Pro feasibility' considers the difficulties in installing plants in the mid-term future. The lands with the lowest implementation difficulty are conversion areas, followed by less-favored areas, grassland, and agricultural land, sequentially. Conversion areas have less difficulty comparing with LFA to get permission for PV expansion. Beyond conversion and LFA, in general, grassland is more favorable towards ground-mounted PV than other forms of agricultural land use, since (i) the agricultural revenue on grassland is lower than other agricultural land uses (see supplementary table S4), (ii) less food-energy conflict occurs on grasslands, and (iii) PV installations harm the biodiversity and yield production less significantly [34]. At the same time, the distance between PV plants and medium or high voltage power lines/cables is also considered.

Scenario 'Pro profit' maximizes the income for the landowners when making the decision for leasing their land for PV or keeping producing agriculturally. First it determines the leasing price in relation with PV potential, shown in supplementary figure S1. Then it calculates the agricultural profit

based on yields and crop types, shown in table S4 in supplementary data. The payback ratio between PV and food/biomass is then defined by dividing land leasing price and agricultural profit.

Scenario 'Pro bioenergy' prevents the loss of biomass, especially biogas from maize considering the regulation RED II. PV is superior to maize in terms of less non-renewable energy input, green house gas (GHG) emissions, acidification and eutrophication. However, currently, the key advantages of biogas are its lower price and its consistent availability without intermittence [35]. In this scenario, the conversion of energy maize fields to PV plants is avoided. The bioenergy potential from agricultural residues is not affected by RED II. Fields with high bioenergy potential are less favored to be transferred to PV.

2.4. Application of simulation workflows from an integrated platform

For assessing the various scenarios, the regional modeling platform SimStadt was chosen, which has been under constant development at HFT Stuttgart since 2012 [36]. SimStadt comprises a modular workflow management with each workflow serving a specific purpose, and with multiple workflows sharing the same input data. Although SimStadt originally focused on urban energy demands (heating [37] and electricity [38]), energy potentials (roof PV [39]), and GHG emissions from heating [40], new workflows with relevance to FWE issues have been developed recently, i.e., on regional biomass potentials [31], ground-mounted PV potentials, urban water demands [41], regional food potentials and demands [42], and green roofs [43].

Figure 2 shows the shared inputs and workflow steps in SimStadt. The shared basic input for the FWE workflow set is geographical data model in CityGML format [44]. The CityGML data model hosts 3D building objects and 2D land polygon objects. The two workflows used in this paper take only the 2D polygons objects on the hinterland with attributes, i.e., crop type distribution, topsoil texture distribution, terrain, and reference food potential. The geometric dataset has the description of each building with information on geometry, year of construction, usage, and land use field. The dataset ensures spatial fine resolution and accuracy without aggregation, as well as, the consistency of output data, i.e., output results link back to the same polygon/building via a unique ID. Detailed descriptions and sources of all input data can be found in Table S1 of supplementary data.

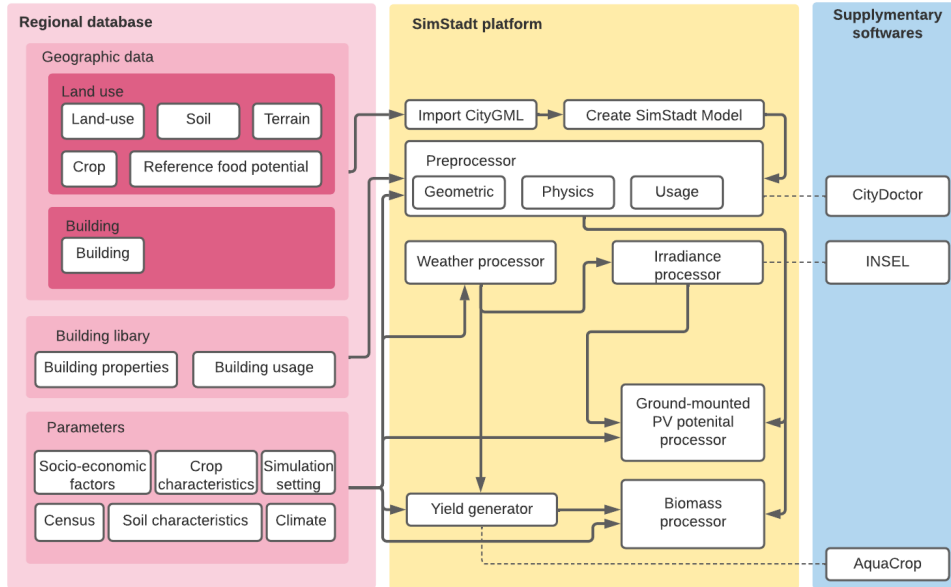


Figure 2: The information flow and main process elements of the FWE simulation platform. The input dataset is in red, the platform is in yellow, the supplementary software is in blue. The information flows from input to individual workflows are shown in solid line. The linkages between external supplementary softwares and SimStadt are shown in dash lines.

The raw CityGML data model needs to be imported to SimStadt by 'Import CityGML' step. Afterward, the step 'Create SimStadt Model' creates a readable data model. Another shared workflow step is 'Weather processor', which retrieves weather data, e.g., global irradiance, precipitation, temperature, etc., from external sources in Typical Meteorological Year 3 (TYM3) format for the geographical location. The processed input geographic and weather data are then passed on to various workflow steps.

Simulation of the trade-off/synergy between ground-mounted PV and biomass scenarios under FWE context requires workflows on (i) biomass and food: the biomass/food workflow calls the external dynamic yield simulation tool, AquaCrop, via 'Yield processor' to simulate accurate yield value based on information from weather processor and CityGML attributes. Then it further simulates the annual crop yield, transpiration/irrigation demand, bioenergy carrier potential, annual animal and vegetal products calorie po-

tential. (ii) the ground-mounted PV potential, that simulates the capacity and annual electricity yield. The irradiance values come from the existing step of 'Irradiance processor' generated by external simulation engine INSEL [45]. Detailed descriptions of workflows on biomass, food potential, and PV can be found in Appendix A.

2.5. Assessment of trade-off by indicators

The simulation via the workflows introduced in section 2.4, generates results for each land-use field with the parameters of PV electricity, biomass, and food potential. However, many results can not be used directly in the predefined scenarios, as they cannot convey the idea of the scenarios. For example, workflows do not have economics outputs to show the economic advantages of fields. Additionally, workflow direct outputs represents the real physical meaning, e.g., PV yield in MWh/ha, making it difficult to identify the strength of the indicator. Lastly, when combining indicators with different focuses, e.g., PV and economic benefit, the direct output from workflows need to be harmonized and translated into indicators with constant range, e.g., 0 to 1.

The indicators presented in table 3 translate the simulation results into numeric values that can be compared among land use fields for scenarios. In each scenario all fields are targeted with different indicator values. Fields with higher indicator values are prioritized to install PV. Each scenario employs one or more than one indicators: (i) scenario 'Pro PV' scenario: PV yield indicator, (ii) scenario 'Pro feasibility': grid access indicator and scenario-indicator, (iii) scenario 'Pro profit': an economic indicator . (iv) 'Pro biomass' scenario does not require additional indicator but directly reads the crop type and biomass yield.

Table 3: Assessment indicators, its target, and definition for land use decision making at FWE framework.

Indicator	Target	Definition
PV yield	The electricity generation efficiency of PV.	The GCR, i.e., PV panel area compared with total field area, range from 0 to 1. 1 means the full coverage of PV.
Economic	The investment payback comparison for land-owners	The ratio between the land leasing income for PV to the income of growing crops. The ratio then is divided by the maximal ratio over scenarios to make sure it is between 0 and 1.
Regulation	The difficulty of converting land for PV from agriculture	1: conversion area or non-vegetal area, 0.75: disadvantage area, 0.5: grassland, 0.25: agricultural arable area, 0: Non-eligible land for PV, i.e., forest, orchard and vineyard).
Grid access	The difficulty to connect PV with grid.	1: the polygon lies within 1 km radian of medium voltage grid (≥ 1 and < 72.5 kV). Otherwise 0.

3. Results

The key quantitative results of this analysis is the marginal change of PV, biomass, and water saving if a certain amount of agricultural area is converted to PV. This allows to create substitution curves, whose gradients yield information on the marginal rate of substitution between the two resources. Thus, the results mainly convey impacts of scenario, i.e., PV expansion strategy, on marginal changes and substitution rates.

Three case study regions (German 'Landkreise' or counties) are chosen for this study out of a total of 400 counties, because, firstly, county-wide land use

data are available; secondly, they differ concerning their land use structure; thirdly, they are located in different parts of Germany, with different climatic conditions. This allows a more holistic view of regional PV potentials and their national ramifications. The choice of these counties thus reflects the climatic and topographic diversity of Germany and to some extent more broadly typical northern and central European landscapes.

1. Sub-urban: Ludwigsburg, Baden-Wuerttemberg, Southern Germany
2. Forest dominant, semi-urban: Ilm-Kreis, Thuringia, Mid-Eastern Germany
3. Agriculture dominant: Dithmarschen, Schleswig-Holstein, Northern Germany

3.1. Sensitivity analysis

Figure 3 illustrates the change of marginal PV yield, avoided crop water demand, and biomass yield in county Ludwigsburg. The PV land cover ratio is the sensitivity variable shown in x-axis.

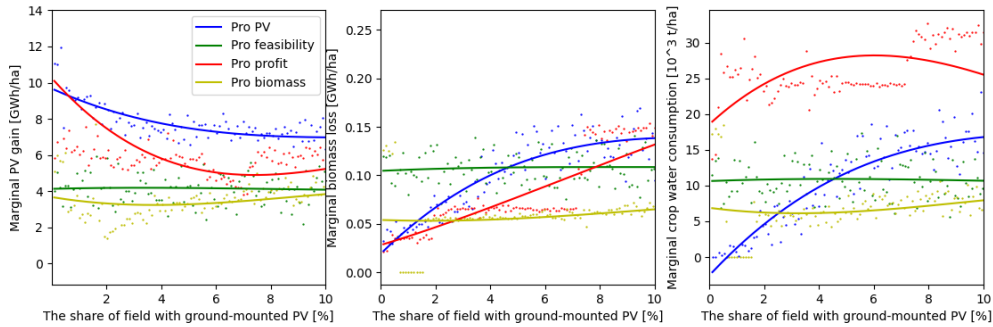


Figure 3: The marginal gain and loss of PV yield, biomass yield, crop water consumption in relation with the share of fields as PV farms in Ludwigsburg county. The percentage of fields for PV varies between 0% to 10% of the overall county area. Forth degree polynomial function is used as the fitting function.

The four scenarios in Ludwigsburg show distinguished trends of these parameters. In scenario 'Pro PV' (blue) around 12 GWh/ha of electricity can be generated if the first 0.1% of fields are converted into PV farms. The marginal PV yield decreases if more fields are included; the marginal PV yield gain is still above the 7 GWh/ha when PV covers 10% of county area. On the contrary, the marginal biomass yield loss increases from 0.03 GWh/ha to

0.15 GWh/ha, as the fields with high PV potential are usually not covered by crops, but vineyards and orchards, where energy biomass yields are low and water demand are not considered. When more arable fields are included, the marginal biomass yield loss and avoided water demand increase. The scenario 'Pro feasibility' (green) excludes the technical advantages of fields for PV, e.g., the conversion area and LFA do not necessarily cover those areas with high PV potentials, resulting in constant fitting curves. This scenario shows the average marginal gain/loss of PV yield (4.1 GWh/ha), biomass yield (0.11 GWh/ha), and crop water demand (1,100 t/ha).

The scenario 'Pro profit' (red) shares the similar trends as scenario 'Pro PV' with lower absolute marginal PV yield (7 GWh/ha), higher biomass loss margin (average 0.06 GWh/ha), and higher marginal water consumption (average 2,500 t/ha). As this scenario ensures land-owner's land-use income between land leasing income for PV and agricultural production, fields with above-average PV specific yield are usually included first. The exceptions happen on high-valuable agricultural lands, e.g., vineyard, where PV is excluded from. The above average marginal PV gain indicates that the 'Pro profit' scenario successfully secures high potential land for ground-mounted PV. At the same time lower marginal biomass loss and higher water consumption illustrate the scenario avoids the biomass loss in agricultural fields. Between 4% and 7% PV land cover ratios, where vineyards and fruit orchards are the major crop type, the marginal biomass yield and crop water consumption are almost constant at 0.05 GWh/ha and 2,400 t/yr. The 'Pro biomass' scenario has the lowest biomass loss of 0.05 GWh/ha and the lowest PV yield gain of 4 GWh/ha among all scenarios. An increasing trend is observed at marginal PV yield, biomass loss, and crop water consumption.

In terms of marginal PV gain, the other two case study regions, Ilm-Kreis (figure 4) and Dithmarschen (figure 5) show the similar pattern in terms of marginal PV gain (the most left sub-figure): the 'Pro PV' scenario has the highest marginal PV yield of 7 GWh/ha and 5.6 GWh/ha among all four scenarios. 'Pro profit' scenario has the second-highest marginal PV yield of 6 GWh/ha (Ilm-Kreis) and 5 GWh/ha (Dithmarschen). Scenario 'Pro feasibility' shows the indifferent average marginal PV yield of 2.6 GWh/ha and 4.4 GWh/ha. In Dithmarschen scenario 'Pro biomass' has the lowest average marginal PV yield of 2.3 GWh/yr. However, in Ilm-Kreis 'Pro biomass' scenario has a marginal PV yield of 3.4 GWh/ha, higher than the average. The slopes of the fitting curves of marginal PV gain regardless the scenarios in Ilm-Kreis and Dithmarschen are close to zero compared with Ludwigsburg,

i.e., in terms of PV marginal yield, the location is not critical due to the flat geometry.

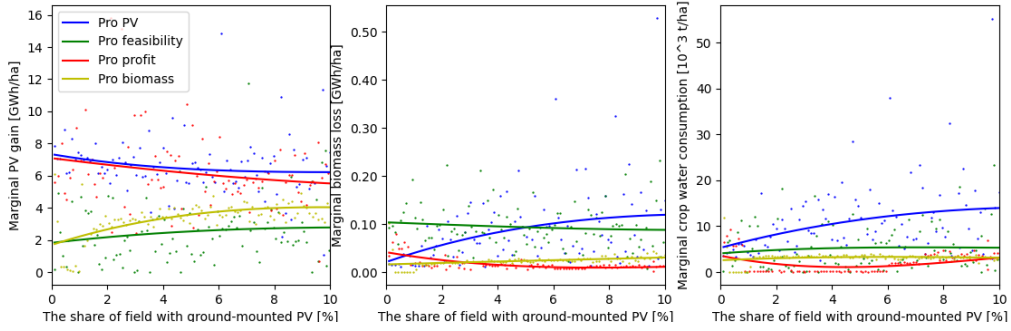


Figure 4: The marginal gain and loss of PV yield, biomass yield, crop water consumption in relation with the share of fields as PV farms in Ilm-Kreis.

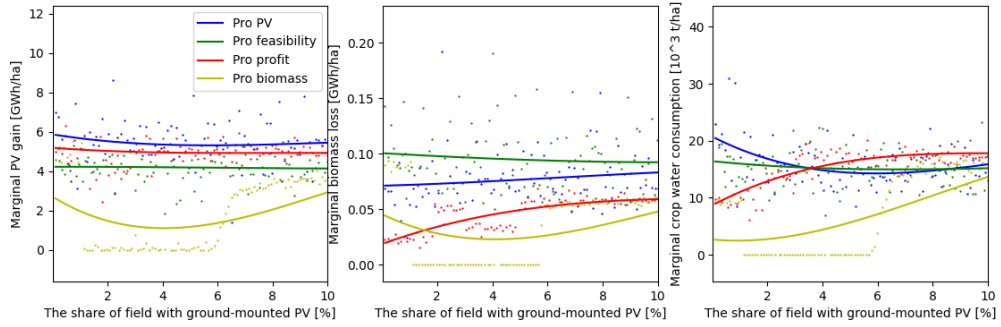


Figure 5: The marginal gain and loss of PV yield, biomass yield, crop water consumption in relation with the share of fields as PV farms in Dithmarschen.

In terms of marginal value for biomass potential saving (middle sub-figure), even though the magnitude of the values is relatively insignificant (up to 0.1 GWh/ha), any improvement of scenarios, even which maximizes the PV yield, reduces the biomass loss compared with the base scenario, 'Pro feasibility'. For example, scenario 'Pro feasibility' causes 30% more marginal biomass loss than scenario 'Pro PV' in Dithmarschen. While in Ilm-Kreis there is no clear advantage in terms of marginal biomass loss between scenario 'Pro PV' and 'Pro feasibility'. On the other side, the potential crop water saving potentials in Dithmarschen county are not distinguished from each other among scenarios, i.e., water saving argument is not valid

in Dithmarschen. Scenario 'Pro PV' in Ilm-Kreis county has the highest crop water saving potential (around $10,000 \text{ m}^3/\text{ha}$, doubled as scenario 'Pro feasibility') with comparable biomass loss.

3.2. Competition between biomass and PV

PV and biomass often compete with each other for land area due to their exclusive natures. Increasing 'production' from one technology would thus reduce the 'production' from the other. To evaluate the trade-offs the concept of isoinvestment curve, widely used in economic studies, is helpful. An isoinvestment curve is a function $z(x, y) = C$, that connects all points with the same total production C . In our context, C is the total energy production from PV and biomass on all fields. The figure 6 shows isoinvestment curves as functions of biomass abatement and PV increment, which are the two leading area-intensive energy technologies compared with onshore PV. The x-axis represents the PV yield divided by the total county area, and the y-axis is the biomass yield of the whole case study region divided by the total area. The gradient dy/dx of an isoinvestment curve $y(x)$ is the marginal rate of substitution between one GWh of increased PV yield and one GWh of biomass yield (Table 4). A higher gradient absolute value means an immense sacrifice of biomass yield when substituting an agricultural field with PV. Gradient value can give information on the appropriate combination of PV and biomass to achieve a particular share of fields for PV.

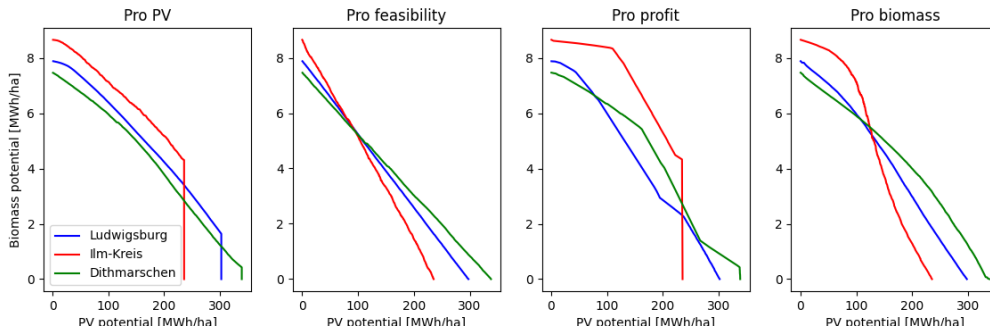


Figure 6: The isoinvestment curves between PV and biomass.

Table 4: The absolute substitution rate of dy/dx in $10^{-3} GWh_{Biomass}/GWh_{PV}$ between biomass and PV yield.

PV potential [TWh]		1	5	10	15	30	40
Pro PV	Ludwigsburg	10	23	29	29		
	Ilm-Kreis	15	27	21	28		
	Dithmarschen	16	17	17	25	37	31
Pro feasibility	Ludwigsburg	31	32	32	33		
	Ilm-Kreis	35	44	45	40		
	Dithmarschen	27	28	29	27	23	26
Pro profit	Ludwigsburg	11	31	41	21		
	Ilm-Kreis	03	02	36	48		
	Dithmarschen	10	12	13	15	53	19
Pro biomass	Ludwigsburg	17	23	34	42		
	Ilm-Kreis	07	14	89	57		
	Dithmarschen	17	16	17	19	27	39

Scenario 'Pro PV' has the highest marginal biomass loss in GWh/ha among all scenarios (figure 3,4,5). However, the higher gain of PV yield compensates the biomass loss, i.e., lower substitution rates. The gradients of scenario 'Pro PV' (first sub-figure of figure 6) are between 30% and 60% of the gradients in scenario 'Pro feasibility', i.e., every additional installed GWh PV following 'Pro PV' scenario can reduced is 40 to 70% less biomass loss compared with current scenario.

Scenario 'Pro feasibility' has constant substitution rates between biomass and PV for all counties, i.e., the loss of biomass of GWh/ha is indifferent if one more hectare of land is converted into PV following the current regulation. The absolute gradient values, however, vary between counties from 0.027 to 0.044 $GWh_{Biomass}/GWh_{PV}$. Ilm-Kreis has the highest gradient of 0.044 $GWh_{Biomass}/GWh_{PV}$ due to its relatively lower PV specific yield with similar marginal biomass loss of 0.1 GWh/ha among three counties.

The scenario 'Pro profit' and 'Pro biomass' successfully identify fields with low per-unit biomass potential loss when each GWh PV facility is built, especially in county Ilm-Kreis. This can be seen as the most flat curve in figure 6 as well as the lowest values in table 4.

3.3. 2% goal

The previous two sections discuss the prioritization of fields, this section intends to set a percentage of county area for energy, so that the total amount of energy generation from PV and biomass can be analyzed. Available land area plays the primary role in end supply amount of PV energy. In order to create the spatial conditions for the expansion of renewable energy, a minimum area target of 2 percent of the state's surface area for onshore wind plants and PV plants was agreed in the coalition agreement in the federal state Baden-Württemberg, Germany. The 2% goal is not bonding in other federal states but serves as a base metric. Still, the following demand values in figure 7 are based on the assumption that PV covers 2% of the county surface.

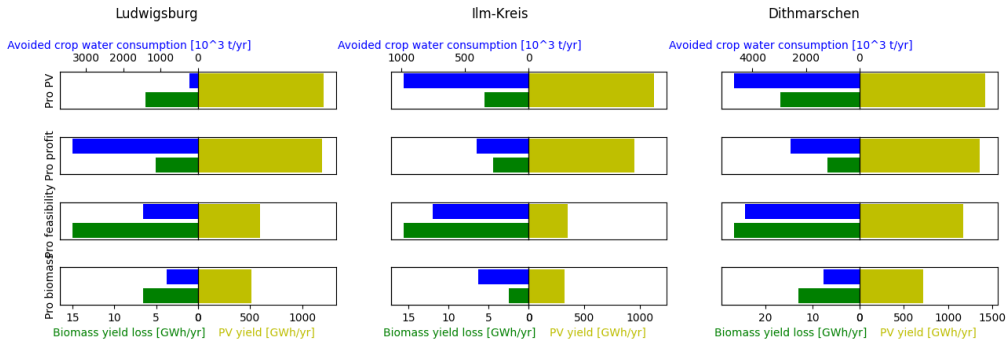


Figure 7: The PV yield gain, biomass yield loss and avoided crop water demand if 2% of the county surface is covered by PV.

Scenario 'Pro PV' maximizes the PV yield on limited areas, and would generate yearly PV yields of 1,200 GWh/yr (Ludwigsburg), 1,125 GWh/yr (Ilm-Kreis) and 1420 GWh/yr (Dithmarschen). Fields with a south-facing slope have higher PV yield, where vineyards usually are in Ludwigsburg. The water demand of vineyard is not included in crop demand simulation. Therefore, despite the high PV yield, the crop water demand is the lowest (2,300 t/yr). On the contrary, in other two counties by achieving highest PV generation, fields with high water demand will be replaced.

Scenario 'Pro profit', on the one hand, secures relatively high PV yields (up to 26% loss compared with the maximal yield), as it tends to install PV on grasslands. Grassland has the lowest agricultural revenue compared to other crop types and locates in areas with higher slopes, which are disadvan-

taged in massive agricultural production. On the contrary, steep fields can bring higher PV yields. Therefore, it minimizes the biomass loss and, at the same time, maximizes the PV gain by distributing PV on grasslands.

Scenario 'Pro feasibility' encourages PV plant on fields next to highways and railways, where the arable lands are. These fields have somewhat limited PV yield values from 29% to 80% of the maximal yield. The loss of biomass yield has the highest values (from 17 GWh/yr to 32 GWh/yr) among the three case studies scenarios.

Biomass loss is discussed intensively so far in this paper. Besides biomass for energy the more dominant role of hinterland is to provide food. Food security is not a relevant topic at the regional level, at least in Germany, as the required food variety can not be grown all locally. However, for regions that rely on the agricultural industry, the loss of food calorie potential by converting agricultural lands into PV farms is a factor in the decision-making process. The table 5 shows the average amount of food potential loss assuming 2% of county area with PV. Total food potential loss is expected on average 3,221 Mkcal/yr to 12,671 Mkcal/yr. By introducing RED II, the food loss is reduced by 26% to 43% by restricting energy crops. Higher loss is observed in Dithmarschen due to a higher share of arable land.

Table 5: Average food potential loss on 2% PV farm over four scenario. Climate in 2020 is taken and no irrigation applied.

<i>[Mkcal/yr]</i>	Luwgisburg	Ilm-Kreis	Dithmarschen
Food potential loss, status quo	7,243	5,632	12,671
Food potential loss, RED II	5,385	3,221	9,259

The avoided irrigation for crops can be an argument for promoting PV if a drier climate is expected to come. Both current and forecasted TMY3 climate file generated by Meteonorm were applied in the simulation. The table 6 shows the expected crop water consumption under the current climate and climate 2045 on the fields on which PV is expected to be installed. Crop transpiration, the water demand regardless of the irrigation, increase 2% in Ludwigsburg, 3% in Dithmarschen and dramatically 152% in Ilm-Kreis, as the rise of ambient temperature cause more transpiration for crops. However, the increase of crop water demand can be neglected if fields are rain-filled

without irrigation. The influence of irrigation is further simulated to keep the soil water content at 90% at all time. The irrigation demand increases by an average of 80% till 2045 in Ludwigsburg, oppositely, a decreasing trend of -63% and -77% in Ilm-Kreis and Dithmarschen. From the water supply point of view, more PV should be installed in Ludwigsburg, as converting fields into PV farms can increase the local sustainable energy production and relieve the irrigation pressure.

Table 6: Crop water demand and irrigation saving potential in year 2020 and 2045 if 2% of county surface is covered by PV over four scenarios.

[10 ³ t/yr]		LB	IK	DM
Rainwater potential	2020	50,082	48,461	112,955
	2045	49,189	47,415	119,952
	Difference	-2%	-2%	6%
Crop water demand	2020	219-838	397-983	1,352-4,681
	2045	225-930	1122-2,673	1,499-4,819
	Difference	2%	152%	3%
Irrigation	2020	38-91	1,018-3,345	0-1,961
	2045	70-117	368-1,394	0-475
	difference	80%	-63%	-77%

4. Discussion

This paper presents a trade-off analysis between biomass and PV considering various land use scenarios in Germany. The simulation results, i.e., PV yield, biomass yield, and water demand at single-field resolution in three case study regions, are standardized into indicators as ranking criteria for pre-defined scenarios. Due to higher irradiance in southern Germany the marginal PV gain can theoretically reach around 5 to 8 GWh/ha/yr PV yield. Around 2% of the county surface can even deliver PV yields of more than 8 GWh/ha, since Ludwigsburg is a mild hilly area and has higher solar irradiance than northern counties. However, 3.2% of the county area is vineyards, usually located on the slopes with high PV yield. It is arguable that vineyards can be removed and replaced with PV due to the highest economic revenue (4,000 €/ha/yr) of all crop types (table S4 in supplementary data) and cultural importance. Other two regions have lower marginal PV

yield gain around 5 GWh/ha/yr due to the weaker solar irradiance and flat geometry.

The geography of the counties also has an impact on technology allocation. In flat regions, i.e., Dithmarschen, the marginal PV yield (figure 5) or the total PV yield (figure 7) shows a PV yield deviation of around 50% among scenarios, compared with the highest deviation in Ilm-Kreis of 72%. It is more critical to evaluate the biomass yield loss if the PV yields are similar.

The cost of biomass loss is another debatable point. In general, by installing PV on up to 10% of the county surfaces, the average biomass loss is between 0.03 to 0.15 GWh/ha/yr. To be noticed, the biomass loss is the loss of agricultural residue waste for energy purposes except for biogas maize. For biogas maize the biomass is not only from residue, e.g., straw, but also from the fruits, e.g., corn, which have higher biomass amount. Therefore, the biomass energy density is relatively low than the PV gain (2.5 to 10 GWh/ha/yr). Focusing on land energy production trade-off, the substitution rate between biomass and PV shows the incremental gain of one resource at the cost of the other resource loss (figure 6). The lower the substitution rate indicates the fields have lower biomass loss per GWh when each more GWh PV is installed. However, scenario 'Pro biomass' has lower substitution rate, but it has also lower specific PV yield per ha. Therefore, scenario 'Pro biomass' does not bring sufficient PV generation.

The goal of this dissertation is to find a strategy, that locates ground-mounted PV on most PV-yield valuable land with low biomass loss and high crop water saving potential. Additionally, comparing biomass and PV alone, the absolute substitution rate should be low to avoid crucial biomass loss. Based on these criteria the most ideal scenario identified by this work is scenario 'Pro profit'. Scenario 'Pro profit' combines two main factors: field output of PV, and agriculture biomass loss. High land leasing price indicates the high PV yield, and low agriculture revenue indicates the low importance of the crop types. It is reasonable that less specific PV yield would be achieved compared with scenario 'Pro PV'. However, the loss is less than 26% compared with the technical maximal. Continuing current regulations (scenario 'Pro feasibility') obstructs high electricity production from PV, but also does not save biomass due to the imprecise and broad definition of LFA with low agricultural productivity.

Biomass can be utilized by a wide variety of combustion and gasification technologies producing heat, power, or fuels for transportation [46]. Figure

6 shows 30 folds more efficient PV than biomass in terms of specific energy output. The biomass mass yield loses 1.4% to 5.8% if 2% of the county area is PV. Energy crop becomes less significant if RED II is enforced, as only biogas maize will be allowed to grow and biogas maize only takes 7% of maize cultivation area [47]. The biogas maize fields can be easily avoided during PV expansion under 2% guideline.

5. Conclusion

This paper integrated previously established simulation workflows on biomass and ground-mounted PV potential with a shared geometrical data input on the same platform to simulate the trade-off between biomass and PV. The novel high-resolution outputs enable scenario analysis not at the aggregated level, but provide technical decision-making guidance at a single-field level for local authorities in any German case. The scenario analysis allows the question of which field should be preferred to convert to ground-mounted PV with optimal substitution of other resources to be answered, i.e., biomass, food, and water. The current inefficient ground-mounted PV policies should be improved with a systematic and more optimal PV allocation strategy under the FWE content. Future studies on integrating more technologies, e.g., onshore wind, roof PV, and demand, are relevant as they complete the energy system analysis circle.

6. Acknowledgement

The method is developed in Institute for Applied Research (IAF), HFT Stuttgart for projects IN-SOURCE. IN-SOURCE is funded by the European Union’s Horizon 2020 research and innovation program under grant agreement No 730254. The case studies and their DLM map data are funded by project EnSys-LE. EnSys-LE is funded by the German Federal Ministry for Economic Affairs and Climate Action (BMWi) under grant agreement No 03ET4061B. IAF provided the funding for publication. The authors would also like to thank Lisa Botero for the language support.

Appendix A. Simulation workflow of SimStadt

Appendix A.1. Biomass workflow

The assessment of energy biomass potentials from agriculture and forestry builds on an existing workflow, which has been introduced, validated and

applied in Germany, Austria and Réunion [31, 43, 48]. The biomass potential is calculated for each land use polygon/field.

To calculate the biomass yield based on local climate, soil characteristics, crop characteristics, land management pattern and irrigation pattern for most crops, a validated external crop yield and water simulation tool named AquaCrop, developed by the Food and Agriculture Organization of the United Nations [49], was integrated with SimStadt. The output of the step 'Yield generator' gives not only biomass yield but also the water demand during growing periods and irrigation requirement.

Given their deeper roots, most trees rely not only on irrigation and precipitation for water supply, but also on groundwater. Given the relative challenges in simulating dynamic yields for trees, static biomass yield values were used for orchards and forested areas in this study. The simulation methods for all sort of biomass included in this paper are shown in supplementary table S2. The types of the crop and soil that were included as inputs for AquaCrop are shown in table S3 and S4 in supplementary data.

After the yield of biomass in tonnes per year per hectare is identified, the technical bioenergy potential in the forms of energy carriers, i.e., biogas, bioethanol, vegetable oil and solid fuel, is calculated based on statistical valorization parameters, i.e., conversion efficiency, energy crop rate, low heating value, water content and, energy usage rate. The detailed bioenergy valorization calculation process is shown in text S1 in supplementary data, as well as in [49].

Appendix A.2. Food workflow

The 'Biomass processor' introduced in section Appendix A.1 was extended with the function of food potential simulation, which is introduced in [42]. After the biomass yield in weight is defined by 'Yield generator', the vegetal food potential is identified by multiplying variables, i.e., energy crop share, waste factor, nutritive factor. Pradhan et al. defined a reference raster food potential map indicating the relation in percentage between vegetal food potential and animal food potential linked by feed calorie. It is assumed that the percentage of vegetal potential used as animal feed is constant in each raster cell. Therefore, the animal food potential has a linear relation with vegetal food potential. The key calculation process and equations are shown in supplementary data text S3.

The regional food calorie demand is decided by population and consumption per capita. The current population is the aggregated sum of occupant

number in each building, which has been introduced in section ???. Population development forecast till 2045 is taken from statistical source. The per-capita food demand is simulated according to regional age structure, body weight, and food waste/storage rate. The temporal diet change, i.e., the consumption amount of vegetal and animal products, is regressed with Human development Index (HDI) (HDI). The calculation process of per-capita food demand is shown in supplementary text S4.

Appendix A.3. Ground-mounted PV workflows

Local solar irradiance is a crucial metric for the assessment of PV potential. The accurate assessment of solar irradiance requires climate data, including horizontal and diffuse radiation and ambient temperatures. This data can be imported into the SimStadt platform through a weather processor from databases such as PVGIS. Once climate data is available, the radiation processor within INSEL, coupled to SimStadt, computes the incoming irradiance on module surfaces based on their slope and orientation.

The PV potential is the product of area and packing factor, which represents the total PV capacity in MW on a specific area in ha. The eligible areas can be read from SimStadt model. A field polygon's slope and orientation are decisive factors for ground-mounted PV panel installation density, assuming an identical irradiation situation. As a further limit, a slope ranging from 16° and 30° was considered poorly suitable for ground-mounted PV, while slopes larger than 30° are considered unfeasible. Hence only polygons with a slope of less than 16° were considered. Furthermore, the utilization efficiency, i.e., the distance between each row, can vary with the land polygon's slope and orientation. Thereby, GCR evaluates the ground occupation. In this paper, the row distance is defined so that no shading between rows occurs at 12.00 o'clock on winter solstice. The detailed simulation process can be found in [30].

Abbreviations

APV Agrophotovoltaics

BUND Federation for the Environment and Nature Conservation Germany

CA Conversion area

CityGML City Geography Markup Language

EEG Renewable Energy Sources Act
FAO Food and Agriculture Organization of the United Nations
FWE Food-Water-Energy
GCR Ground cover ratio
GHG Green house gas
GIS Geographical Information System
HDI Human development Index
LFA Less-favoured area
NABU Nature Conservation Association Germany
PV Photovoltaic
RED II European Union
TYM3 Typical Meteorological Year 3

References

- [1] FAO, The future of food and agriculture: Alternative pathways to 2050, Rome, 2018.
- [2] T. Bründlinger, J. E. König, O. Frank, D. Gründig, C. Jugel, P. Kraft, O. Krieger, S. Mischinger, P. Prein, H. Seidl, et al., dena-leitstudie integrierte energiewende: Impulse für die gestaltung des energiesystems bis 2050, Deutsche Energie-Agentur GmbH (dena), ewi Energy Research & Scenarios gGmbH: Berlin/Köln, Germany (2018).
- [3] T. Kelm, J. Metzger, A.-L. Fuchs, S. Schicketanz, D. Günnewig, M. Thylmann, Untersuchung zur Wirkung veränderter Flächenrestriktionen für PV-Freiflächenanlagen, Tech. rep. (Jan. 2019).

- [4] C. Kost, S. Shammugam, V. Fluri, D. Peper, A. Davoodi Memar, T. Schlegl, Stromgestehungskosten Erneuerbare Energien, Tech. rep., Fraunhofer ISE, Freiburg, https://publica.fraunhofer.de/eprints/urn_nbn_de_0011-n-6389438.pdf (Jun. 2021).
- [5] BMVI, Räumlich differenzierte Flächenpotentiale für erneuerbare Energien in Deutschland, BMVI-Online-Publikation, Federal Ministry of Transport and Digital Infrastructure, Berlin, https://www.bbsr.bund.de/BBSR/DE/veroeffentlichungen/ministerien/bmvi/bmvi-online/2015/BMVI_Online_08_15.html (Aug. 2015).
- [6] H. Wirth, Aktuelle Fakten zur Photovoltaik in Deutschland, Tech. rep., Fraunhofer ISE, <https://www.ise.fraunhofer.de/veroeffentlichungen/studien/aktuelle-fakten-zur-photovoltaik-in-deutschland.html> (May 2021).
- [7] BUND, NABU, Positionspapier zur Solarenergie von BUND und NABU, Tech. rep., <https://www.bund-bawue.de/service/publikationen/detail/publication/positionspapier-zur-solarenergie-von-bund-und-nabu/> (Jul. 2021).
- [8] K. Calvert, W. Mabee, More solar farms or more bioenergy crops? mapping and assessing potential land-use conflicts among renewable energy technologies in eastern Ontario, Canada, *Applied Geography* 56 (2015) 209–221, cast. doi:10.1016/j.apgeog.2014.11.028.
- [9] M. E. Leirpoll, J. S. Næss, O. Cavalett, M. Dorber, X. Hu, F. Cherubini, Optimal combination of bioenergy and solar photovoltaic for renewable energy production on abandoned cropland, *Renewable Energy* 168 (2021) 45–56, <https://linkinghub.elsevier.com/retrieve/pii/S0960148120319236>. doi:10.1016/j.renene.2020.11.159.
- [10] D. Ketzer, N. Weinberger, C. Rösch, S. B. Seitz, Land use conflicts between biomass and power production – citizens’ participation in the technology development of agrophotovoltaics, *Journal of Responsible Innovation* 7 (2) (2020) 193–216. doi:10.1080/23299460.2019.1647085.
- [11] G. Barron-Gafford, A. Salazar, Phelps-Garcia, L. V., IV, L. Lopez, I. Barnett-Moreno, W. Cooke, M. S. Thompson, R. L. Minor, P. Murphy,

- M. Pavao-Zuckerman, J. Macknick, Co-locating agriculture and solar power renewables (agrivoltaics) to create a more sustainable food, energy, and water future, AGU Fall Meeting Abstracts 2019 (2019) B41B-01.
- [12] G. A. Barron-Gafford, M. A. Pavao-Zuckerman, R. L. Minor, L. F. Sutter, I. Barnett-Moreno, D. T. Blackett, M. Thompson, K. Dimond, A. K. Gerlak, G. P. Nabhan, J. E. Macknick, Agrivoltaics provide mutual benefits across the food-energy-water nexus in drylands, *Nature Sustainability* 2 (9) (2019) 848-855. doi:10.1038/s41893-019-0364-5.
URL <https://www.nature.com/articles/s41893-019-0364-5>
- [13] A. Purwanto, J. Sušnik, F. X. Suryadi, C. de Fraiture, Water-energy-food nexus: Critical review, practical applications, and prospects for future research, *Sustainability* 13 (4) (2021) 1919. doi:10.3390/su13041919.
URL <https://www.mdpi.com/2071-1050/13/4/1919/htm>
- [14] A. Endo, M. Yamada, Y. Miyashita, R. Sugimoto, A. Ishii, J. Nishijima, M. Fujii, T. Kato, H. Hamamoto, M. Kimura, T. Kumazawa, J. Qi, Dynamics of water-energy-food nexus methodology, methods, and tools, *Current Opinion in Environmental Science & Health* 13 (2020) 46-60. doi:10.1016/j.coesh.2019.10.004.
URL <https://www.sciencedirect.com/science/article/pii/S246858441930056X>
- [15] H. Hoff (Ed.), *Understanding the Nexus: Background paper for the Bonn2011 Nexus Conference*, Stockholm Environment Institute, 2011.
URL https://publications.pik-potsdam.de/pubman/faces/viewitemfullpage.jsp?itemid=item_17278_1&view=export
- [16] C. Böhringer, T. F. Rutherford, Combining bottom-up and top-down, *Energy Economics* 30 (2) (2008) 574-596. doi:10.1016/j.eneco.2007.03.004.
URL <https://www.sciencedirect.com/science/article/pii/S014098830700059X>
- [17] W. A. Hussien, F. A. Memon, D. A. Savic, An integrated model to evaluate water-energy-food nexus at a household scale, *Environmental Modelling Software* 93 (2017) 366-380.

doi:<https://doi.org/10.1016/j.envsoft.2017.03.034>.

URL <https://www.sciencedirect.com/science/article/pii/S1364815216306594>

- [18] Z. Chamas, M. Abou Najm, M. Al-Hindi, A. Yassine, R. Khat-tar, Sustainable resource optimization under water-energy-food-carbon nexus, *Journal of Cleaner Production* 278 (2021) 123894. doi:10.1016/j.jclepro.2020.123894.
URL <https://www.sciencedirect.com/science/article/pii/S0959652620339391>
- [19] Charalampos Avraam, Ying Zhang, Sriram Sankaranarayanan, Benjamin Zaitchik, Emma Moynihan, Prathibha Juturu, Roni Neff, Sauleh Siddiqui, Optimization-based systems modeling for the food-energy-water nexus, *Current Sustainable/Renewable Energy Reports* 8 (1) (2021) 4–16. doi:10.1007/s40518-020-00161-5.
URL <https://link.springer.com/article/10.1007/s40518-020-00161-5>
- [20] L. Ji, B. Zhang, G. Huang, Y. Lu, Multi-stage stochastic fuzzy random programming for food-water-energy nexus management under uncertainties, *Resources, Conservation and Recycling* 155 (2020) 104665. doi:10.1016/j.resconrec.2019.104665.
URL <https://www.sciencedirect.com/science/article/pii/S0921344919305713>
- [21] J. Liu, Y. Li, X. Li, Identifying optimal security management policy for water–energy–food nexus system under stochastic and fuzzy conditions, *Water* 12 (11) (2020) 3268. doi:10.3390/w12113268.
URL <https://www.mdpi.com/2073-4441/12/11/3268>
- [22] M. Li, V. P. Singh, Q. Fu, D. Liu, T. Li, Y. Zhou, Optimization of agricultural water–food–energy nexus in a random environment: an integrated modelling approach, *Stochastic Environmental Research and Risk Assessment* 35 (1) (2021) 3–19. doi:10.1007/s00477-019-01672-4.
URL <https://link.springer.com/article/10.1007/s00477-019-01672-4>

- [23] L. Wu, A. Elshorbagy, S. Pande, La Zhuo, Trade-offs and synergies in the water-energy-food nexus: The case of saskatchewan, canada, *Resources, Conservation and Recycling* 164 (2021) 105192. doi:10.1016/j.resconrec.2020.105192.
URL <https://www.sciencedirect.com/science/article/pii/S0921344920305097>
- [24] P. Andrews-Speed, R. Bleischwitz, T. Boersma, C. Johnson, G. Kemp, S. D. VanDeveer, The global resource nexus: The struggles for land, energy, food, water, and minerals.
- [25] A. Flammini, M. Puri, L. Pluschke, O. Dubois, Walking the nexus talk: assessing the water-energy-food nexus in the context of the sustainable energy for all initiative, *Environment and Natural Resources Management. Working Paper (FAO) eng no. 58* (2014).
URL <https://agris.fao.org/agris-search/search.do?recordID=XF2015001455>
- [26] E. Ramos, D. Kofinas, C. Papadopoulou, M. Papadopoulou, F. Gardumi, F. Brouwer, M. Fournier, E. Lluís, X. Domingo, L. Vamvakeridou-Lyroudia, D1.5: Framework for the assessment of the nexus.
URL www.sim4nexus.eu
- [27] L. Yung, E. Louder, L. A. Gallagher, K. Jones, C. Wyborn, How methods for navigating uncertainty connect science and policy at the water-energy-food nexus, *Frontiers in Environmental Science* 7 (2019) 37. doi:10.3389/fenvs.2019.00037.
URL <https://www.frontiersin.org/articles/10.3389/fenvs.2019.00037/full>
- [28] M. Kurian, The water-energy-food nexus: Trade-offs, thresholds and transdisciplinary approaches to sustainable development, *Environmental Science & Policy* 68 (2017) 97–106. doi:10.1016/j.envsci.2016.11.006.
URL <https://www.sciencedirect.com/science/article/pii/S1462901116305184>
- [29] M.-C. Hu, C. Fan, T. Huang, C.-F. Wang, Y.-H. Chen, Urban metabolic analysis of a food-water-energy system for sustainable resources management, *International Journal of Environmental Research and Public*

Health 16 (1) (2019) 90. doi:10.3390/ijerph16010090.
URL <https://www.mdpi.com/1660-4601/16/1/90/htm>

- [30] K. Bao, L. Kalish, T. Santhanavanich, D. Thraen, B. Schroeter, A bottom-up gis-based method for simulation of ground-mounted pv potentials at regional scale, submitted to Energy Reports, unpublished (2022).
- [31] K. Bao, R. Padsala, V. Coors, D. Thrän, B. Schröter, A method for assessing regional bioenergy potentials based on gis data and a dynamic yield simulation model, Energies 13 (24) (2020) 6488. doi:10.3390/en13246488.
- [32] B. Sliz-Szkliniarz, Assessment of the renewable energy-mix and land use trade-off at a regional level: A case study for the kujawsko-pomorskie voivodship, Land Use Policy 35 (2013) 257–270. doi:10.1016/j.landusepol.2013.05.018.
URL <https://www.sciencedirect.com/science/article/pii/S0264837713001105>
- [33] K. Meisel, M. Millinger, K. Naumann, F. Müller-Langer, S. Majer, D. Thrän, Future renewable fuel mixes in transport in germany under red ii and climate protection targets, Energies 13 (7) (2020) 1712. doi:10.3390/en13071712.
URL <https://www.mdpi.com/1996-1073/13/7/1712>
- [34] H. Blaydes, S. G. Potts, J. D. Whyatt, A. Armstrong, Opportunities to enhance pollinator biodiversity in solar parks, Renewable and Sustainable Energy Reviews 145 (2021) 111065. doi:10.1016/j.rser.2021.111065.
URL <https://www.sciencedirect.com/science/article/pii/S1364032121003531>
- [35] M. Graebig, S. Bringezu, R. Fenner, Comparative analysis of environmental impacts of maize-biogas and photovoltaics on a land use basis, Solar Energy 84 (7) (2010) 1255–1263. doi:10.1016/j.solener.2010.04.002.
URL <https://www.sciencedirect.com/science/article/pii/S0038092X10001489>

- [36] R. Nouvel, K.-H. Brassel, M. Bruse, E. Duminil, V. Coors, U. Eicker, Simstadt, a new workflow-driven urban energy simulation platform for citygml city models, Proceedings of International Conference CISBAT 2015 Future Buildings and Districts Sustainability from Nano to Urban Scale. No. CONF. LESO-PB, EPFL, 2015. (2015).
- [37] M. Zirak, V. Weiler, M. Hein, U. Eicker, Urban models enrichment for energy applications: Challenges in energy simulation using different data sources for building age information, *Energy* 190 (2020) 116292. doi:10.1016/j.energy.2019.116292.
URL <https://www.sciencedirect.com/science/article/pii/S0360544219319875>
- [38] S. Köhler, M. Betz, U. Eicker (Eds.), Stochastic Generation of Household Electricity Load Profiles in 15-minute Resolution on Building Level for Whole City Quarters, 2019.
- [39] L. Rodríguez, E. Duminil, J. Sánchez Ramos, U. Eicker, Assessment of the photovoltaic potential at urban level based on 3d city models: A case study and new methodological approach, *Solar Energy* 146 (2017) 264–275. doi:10.1016/j.solener.2017.02.043.
URL <https://www.sciencedirect.com/science/article/pii/S0038092X17301445>
- [40] V. Weiler, H. Harter, U. Eicker, Life cycle assessment of buildings and city quarters comparing demolition and reconstruction with refurbishment, *Energy and Buildings* 134 (2017) 319–328. doi:10.1016/j.enbuild.2016.11.004.
URL <https://www.sciencedirect.com/science/article/pii/S0378778816314141>
- [41] K. Bao, R. Padsala, D. Thrän, B. Schröter, Urban water demand simulation in residential and non-residential buildings based on a citygml data model, *ISPRS International Journal of Geo-Information* 9 (11) (2020) 642. doi:10.3390/ijgi9110642.
- [42] K. Bao, R. Padsala, V. Coors, D. Thrän, B. Schröter, A gis-based simulation method for regional food potential and demand, *Land* 10 (8) (2021) 880. doi:10.3390/land10080880.
URL <https://www.mdpi.com/2073-445X/10/8/880>

- [43] K. Bao, D. Thrän, B. Schröter, Simulation and analysis of urban green roofs with photovoltaic in the framework of water-energy nexus, *CITIES 20.50 – Creating Habitats for the 3rd Millennium: Smart – Sustainable – Climate Neutral*. Proceedings of REAL CORP 2021, 26th International Conference on Urban Development, Regional Planning and Information Society (2021) 671–680doi:10.48494/REALCORP2021.3030.
URL <https://repository.corp.at/796/>
- [44] Open Geospatial Consortium, Citygml (10/04/2021 14:11:02).
URL <https://www.ogc.org/standards/citygml>
- [45] Doppelintegral GmbH, Insel (2018).
URL https://www.insel.eu/en/home_en.html
- [46] V. Dornburg, A. P. Faaij, Efficiency and economy of wood-fired biomass energy systems in relation to scale regarding heat and power generation using combustion and gasification technologies, *Biomass and Bioenergy* 21 (2) (2001) 91–108. doi:10.1016/S0961-9534(01)00030-7.
URL <https://www.sciencedirect.com/science/article/pii/S0961953401000307>
- [47] FNR, Bioenergy in germany: Facts and figures 2020.
- [48] K. Bao, L.-M. Bieber, S. Kürpick, M. H. Radanielina, R. Padsala, D. Thrän, B. Schröter, Bottom-up assessment of local agriculture, forestry and urban waste potentials towards energy autonomy of isolated regions: Example of réunion, *Energy for Sustainable Development* 66 (2022) 125–139. doi:10.1016/j.esd.2021.12.002.
URL <https://www.sciencedirect.com/science/article/pii/S0973082621001460>
- [49] Food and Agriculture Organization of the United Nations, Introducing aquacrop.
URL <http://www.fao.org/3/a-i6321e.pdf>

Chapter 7

GIS-Based Assessment of Regional Biomass Potentials at the Example of Two Counties in Germany

Bao, K.; Padsala, R.; Coors, V.; Thrän, D.; Schröter, B.

Proceedings of 28th European Biomass Conference and Exhibition. 2020, pp 77-85. DOI: 10.5071/28thEUBCE2020-1CV.4.15

GIS-BASED ASSESSMENT OF REGIONAL BIOMASS POTENTIALS AT THE EXAMPLE OF TWO COUNTIES IN GERMANY

Keyu Bao¹, Rushikesh Padsala², Volker Coors², Daniela Thrän³ and Bastian Schröter¹

¹ Center of Sustainable Energy Technology, Hochschule für Technik Stuttgart, Schellingstraße 24, D-70174 Stuttgart (keyu.bao, bastian.schroeter)@hft-stuttgart.de

² Center for Geodesy and Geoinformatics, Hochschule für Technik Stuttgart, Schellingstraße 24, D-70174 Stuttgart (rushikesh.padsala, volker.coors)@hft-stuttgart.de

³ Department of Bioenergy, Helmholtz Center for Environmental Research, Torgauer Straße 116, D-04347 Leipzig daniela.thraen@ufz.de

ABSTRACT: The assessment of theoretical and technical biomass potential from different types of natural land cover is an integral part of simulation tools that aim to assess local multi-energy systems. This work introduces a new workflow which evaluates the local biomass potential from various sources, its transformation to different forms of biofuel and their thermal and electrical energy potentials, based on GIS-based land use data, satellite map on local crop types, and crop-specific energy yields from literature. One of the workflow's two test cases is the county of Ludwigsburg in the south of Germany, where the annual technical local biomass potential was calculated to be close to 700 GWh, or 8% of total electricity and heating demand (based on 2018 demand data) – compared to an actual contribution of biomass to the local energy mix of about 2% (2012). The second test case is the northern German county of Dithmarschen, where local technical biomass is about 2248 GWh, or 19% of electricity and heating demand according to our simulation. Under current utilization situation bioenergy potentials are not completely in use and can contribute to local energy concept. This new workflow will further complement an existing local energy system simulation platform that has so far focused on urban energy demands and potentials.

Keywords: Potential, Geographical information system (GIS), biofuel

1 INTRODUCTION

Although the metabolism of industrial societies strongly relies on minerals and fossilized biomass, annually harvested biomass from live vegetation contributes about 10% to primary energy use in the European Union [1]. Biomass can be derived from different resources, e.g. agricultural land or forest, and transferred into different forms of biofuel, e.g. biogas and solid fuel. Given a trend towards a decentralization of energy systems, it is important to assess regional biomass potential and to understand the possible variables which might influence this potential.

Two different approaches for biomass potential assessments can be distinguished: demand-driven and resource-focused. Demand-driven assessments analyse the economic competitiveness of biomass-based electricity, heat and/or biofuels, or estimate the amount of biomass required to meet exogenous targets on, e.g. renewable energy or emission reduction targets. Resource-focused assessments take the form of inventories of potential bioenergy sources, with an evaluation of possibilities to utilize the sources for energy purposes. [2] The workflow presented in the following applies the second approach, as this paper intends to have an overall picture of the possible bioenergy resources in the region.

Biomass (1) is often used in decentral and local energy systems, (2) can contribute to wind and solar as a flexible energy carrier, (3) is converted into different energy carriers. So, to use the available biomass potential most efficient, adequate information for local and regional decision maker are necessary. Specifically, it adds biomass as a further renewable energy source (RES) to an existing energy simulation environment, which is based on geoinformatics data. The goal is to allow (local) decision makers to make informed choices regarding the potentials and trade-offs between different RES on a strategic level – it thus needs to be reasonably accurate in the context of local energy systems and build upon a similar data structure as the methods already implemented, such as

assessments of rooftop PV potentials [3] or heat demand of city quarters [4]. Understanding local biomass potentials helps local governments and planning authorities to assess the benefits and limits of biomass to achieve national or self-imposed emission or renewable energy targets.

2 SCIENTIFIC INNOVATION AND RELEVANCE

In contrast to the approach presented here, the biomass potential assessment which have been undertaken typically either focus on specific types of land use or biomass, e.g. forests [5], or yield highly aggregated results [6], since their focus lies on providing data on a national or supranational level.

For the first, e.g., D. Lauka et al. introduced a model which is able to assess the low-quality biomass resource potential, but without taking biogas or bioethanol potentials into account [7], while the technical potential for power production from forest biomass was assessed in [5]. For the second, biomass potentials and various scenario on a national level are evaluated for example in [6].

Methods based on geographic information systems (GIS) are widely applied to assess biomass potentials [8–11]. They typically overlay various layers of data (forest, agriculture, urban, slope, road etc.) in order to locate area with biomass potentials. However only the statistical crop distribution was applied to aggregated feasible lands because the lack of crop distribution maps. Those methods are limited in their degree of accuracy and simplicity.

To the authors' knowledge, there is a lack of models that combine biomass potential assessments with other RES sources, most importantly solar photovoltaics and wind, on regional level in one aggregated modelling environment. However, such an approach is of great benefit if the goal is to assess local synergies, potential conflicts, economic merit orders or summed potentials of RES sources. The workflow introduced here extends an existing local energy system simulation platform that can

assess heat and power demands from residential areas [12] as well as rooftop photovoltaic potentials [13] on a single-building level. The objective of the new workflow is not to provide the most accurate assessment of regional bioenergy potentials with detailed and customized data in a specific area, but rather to have a generic method to evaluate potentials of any region with decent accuracy, and contrast these potentials to similar efforts for other RES, and heat and power demand assessments.

3 METHODS AND MATERIALS

3.1 Input data

The main input data for the new workflow consists of Digital Landscape Model (DLM) data given by Germany's Official Real Property Cadastre Information System (ALKIS). ALKIS was developed by the Working Group of the Surveying Authorities of the sixteen states of Germany (AdV). The DLM map consists of several object type, including building, water body, vegetation, transportation etc. Since the land area dedicated to transportation purposes is stored as line and buffer width in the DLM map, it can overlap with the vegetation layer, and the shared part of the vegetation layer needs to be cut out in order to avoid its inflation. The data structure of the vegetation land use type of ALKIS is essentially determined by the XML exchange format, and information on ID, land use, area, boundary coordinates and other important attributes, e.g. land use type, of every polygon are included. Instead of raster data with a given resolution, polygons represent the boundary with higher accuracy based on the topographic map with a resolution of 1:25 000.

DLM data accurately indicate the boundary and land use of each polygon. However, the specific crop type growing on polygons that are classified as agricultural land is missing. To fill this gap, the DLM data was combined with satellite data on crop types from [14]. There, Griffiths et al. derive a map of crop types and land cover from satellite data, and compare their results to available agricultural reference data from three (German) states as well as to the results of a national agricultural census. The resulting raster map captures the crop type distribution across Germany at 30m resolution and achieves 81% overall accuracy for 12 classes in the three states for which reference data was available. The mapping performance for most classes was highest for the 10-day composites and many classes are discriminated with class specific accuracies >80%. For several crops, such as cereals, maize and rapeseed, their mapped acreages compare very well with the official census data with average differences between mapped and census area of 11%, 2% and 3%, respectively. Other classes (grapevine and forest classes) perform slightly less well, likely because the available reference data does not fully capture the variability of these classes across Germany. The land use and crop types differentiated in that study are: Grassland, winter cereals, maize, winter rapeseed, spring cereals, sugar beet, potato, grapevine, deciduous mix forest, coniferous forest, built-up, water.

Conflicts between maps from different sources are common, since they were derived with different methods and are based on different sources. For example, land classified as vineyard in the DLM data is typically classified as built-up area in the satellite map. Generally, DLM data has a high level of accuracy and reliability in

terms of overall land use type, e.g. farming land, vineyard, or built-up area, when compared with satellite data, e.g. from Google Maps. Therefore, the polygons from this source served as the basic unit when merging both sources. In the case of a conflict regarding overall land use, the information of DLM data is taken. The crop information from satellite data [14] is then attached to each DLM polygon as an additional attribute. In case multiple crop types from the satellite data exist on the same polygon from the DLM map, which for agricultural land mostly refers to individual fields, the land use type with the largest area is assigned to this polygon. Only for farming fields the DLM map should be attached with additional agricultural crop type information from the satellite data. Figure 1 shows the original DLM and satellite data and the superimposed data at the example of the city of Marbach, Ludwigsburg county in the south-western state of Baden-Württemberg

To use the combined map data within the structure of our existing modelling environment, it is transformed into the open CityGML data format [15,16].

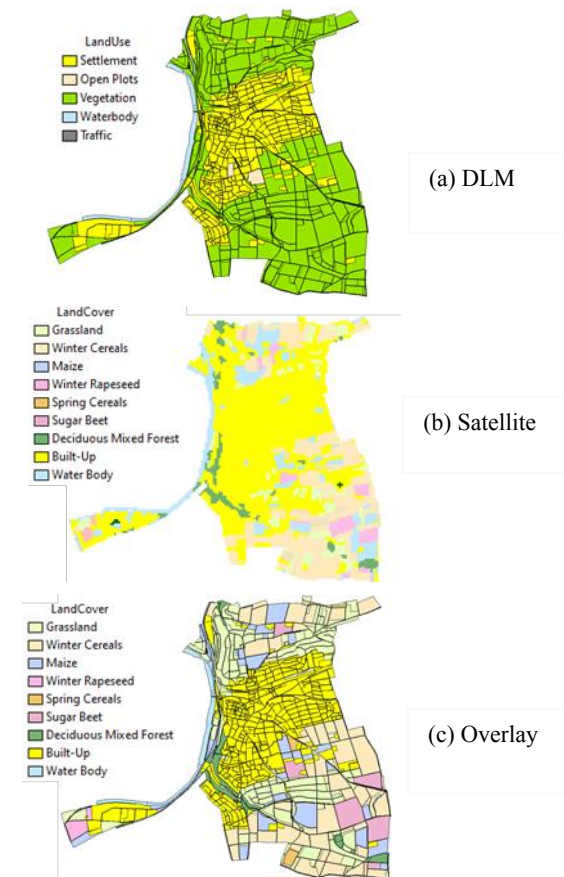


Figure 1: Input maps (a) DLM map in polygons with land use; (b) Satellite map in raster with crop type; (c) Integrated map

The accuracy of the thus created GML data set was validated by comparison with statistical data for Ludwigsburg county. The county's total land area, classified into the main forms of land use, is compared with the total land area from the state's 2018 land use report [17]. As table 2 shows, the total area dedicated to agriculture and forest differs by only 3.2%, and farming area by less than 7%. Grassland and garden areas, however, yield larger deviation between two sources, with

the possible reasons being (i) that the DLM dataset only counts polygons with areas of more than one hectare, with smaller fields not included in the dataset in the first place, (ii) that the DLM dataset contains more categories than the state land use report. For instance, orchard meadows, tree nurseries and fruit plantations are part of the created GML map, but not the land use report. Since orchard meadow could be regarded as describing grassland with fruit trees, combining both categories yield a sum (8,210 ha) that is closer to the grass land area from the land use report (7,967 ha). Similarly, adding nurseries and fruit plantations to the garden category reduces this difference.

Table I: Comparison of the summed value of land area from SimStadt and the summed statistic number (Source: [17])

Land use	Quantity	DLM	Difference
	[ha]	[ha]	[%]
Agriculture	37,704	36,493	3.2
of which Farming	26,990	25,150	6.8
Grass	7,967	3,417	57.1
Garden	549	234	57.4
Orchard meadow	-	4,793	-
Tree nursery	-	137	-
Fruit plantation	-	467	-
Vineyard	2,198	2,292	4.3
Brown land	0	0	0.0
Forest	12,362	11,997	3.0

Table II: Biomass potential yield factors of most relevant types of vegetation in Germany. Unit: GJ/(ha a)

Crop Type	The theoretical energy potential [1,4,5,7,14]	The technical potential					
		Biomethane [1,3,5,6,8]	Bioethanol [1]	Solid fuel [1]	Vegetable oil [8]	Residue as solid fuel [10,11]	Energy wood yield [12,13]
Cereals	205	133	93	205		76	
Maize	229	158		229		80	
Grass	263	143		202		114	
Sugar Beet	248	220	148	248		97	
Orchard meadow						37	
Rapeseed	147		46	147	55	80	
Short Rotation Coppice	205	137	83	205			
Forest	2,452						
coniferous	2,010					28	49
deciduous	2,919					28	22
deciduous and coniferous trees	2,452					28	39
Fruit plantation						90	
Spreading fruit stacker						37	
Grove	142			142		28	
Vineyard						15	

Source: [1,4,11] Flaig, Holger, and Hans Mohr, eds. *Energie aus Biomasse*, p. 609,189,274; [2,8,14]: Faustzahlen für die Landwirtschaft, p. 913,938,21; [3]: The whole plant; [5] Biogas density = 1,15 kg/m³, biogas calorific value = 23 MJ/m³; [6] Methane yield=265L/kgTM, Flaig, Holger, and Hans Mohr, eds. *Energie aus Biomasse*, p. 228; [7] Heat value of sugar beet, silphy, orchard meadow are not give, average value 17.8 MJ/kg taken; [9] Zimmer Y., *Competitiveness of rapeseed, soybeans and palm oil*, 2016, p. 86; [10] E. Ludger, etc., *Leitfaden Feste Biobrennstoffe*, Fachbericht der Fachagentur Nachhaltige Rohstoffe e. V. (FNR), 2014, p. 4.; [12] Third National Forest Inventory <https://bwi.info/> [14] H. Dietmar, etc., *Empfohlene Umrechnungsfaktoren für Energieholzsortimente bei Holz- bzw. Energiebilanzberechnungen*, 2009.

3.2 Assessment method for biomass potential

In the case of biomass or bioenergy potentials, a distinction can be made between theoretical, technical, economic, exploitable and sustainable potentials. In this paper only the theoretical and the technical potential are applied.

The theoretical potential describes the potential that exists in a given region within a certain time period of physically usable energy supply (e.g. the energy stored in the entire plant mass). It is determined by physical limits and marks the upper limit of bioenergy's theoretically realizable contribution to energy supply. Because of insurmountable technical, ecological, economic and administrative barriers, this potential can generally only be tapped to a very limited extent. It therefore has no practical relevance for assessing the actual usability of the biomass. [18]

The technical potential describes that part of the theoretical potential that can be used, taking into account the given technical restrictions (e.g. salvage rate, storage losses, conversion losses). In addition, existing structural and ecological restrictions as well as other legal requirements and possible social restrictions are taken into account, as they also represent barriers to the use of bioenergy, similar to technically induced restrictions. [18] By processing of the feedstock (pelletising, pyrolysis, methanisation, etc.) the theoretical potential is converted to technical potential.

The bioenergy potentials are calculated based on the

energetic yield (e.g., in GJ) per hectare and year, of the relevant and most widely spread crops in Germany, summarized in Tab. II. The following sub-chapters introduce the method to calculate the theoretical and technical energy yield.

3.2.1 Theoretical Energy Potential

The primary energy potential here refers to the theoretical biomass potential of a certain vegetation land use type, regardless of the further conversion process to biofuel carriers. The primary energy content of a certain form of biomass can be described by its heating value multiplied by its dry mass production yield. The water content in the fuel has a strong influence on the energy content or the calorific value. The heating calorific value of solid fuels - in relation to dry matter - is negligible and lies roughly between 16.5 and 19 MJ/kg dry mass (DM) [18]. In contrast, dry mass production yields differs by crop type. Therefore, the yield of crop production without water in solid form is desired for primary energy potential calculation.

The energetic use of orchard meadow, fruit plantation and spreading fruit stacker is only realized, if the clearing of older fruit or vine plantation, or if plant diseases have occurred. Therefore, only the felled down and unnecessary part of the wood are taken as residue solid fuel. And in primary energy calculation orchard meadow, fruit plantation and spreading fruit stacker are not considered.

$$P_{primary} = Y_{vegetation} \cdot H_u$$

$P_{primary}$ is the primary energy potential of a specific land field in GJ/ha·a. $Y_{vegetation}$ is the dry matter production yield of a specific vegetation type in t/ (ha·a). H_u is the calorific value in gigajoules per tonne [GJ/t_{utro}].

3.2.2 Theoretical and Technical Potential of Wood

Wood is used for material and energy purposes. Material users include primarily the sawmill industry, the wood-based materials industry and the pulp and paper industry. Since the early 2000s, the share of wood used energetically increased to 25.6% in 2016 in Germany [19]. Energetic use cases of wood include private wood heating systems and biomass combustion plants. Solid wood is round timber with a minimum diameter of over 7 cm. Waste wood and landscape conservation material can also be used to generate energy. [20] For the energy wood methodology, however, only solid forest wood is considered.

$$P_{energy\ wood} = A_{forest} \cdot E_{fm} \cdot n_{f,energy} \cdot n_{f,cf} \cdot p \cdot H_u$$

Where $P_{energy\ wood}$ is the forest fuel potential in gigajoules per year [GJ/a]. A_{forest} stands for the area of the individual forest type (broad-leaf, coniferous forest, the mix of both) in hectares [ha]. E_{fm} is the harvest cubic metres per hectare per year [m^3 /ha/a]. One harvest cubic metre of wood is equivalent to one cubic metre of solid wood stored without gaps in the stratification. $n_{f,cf}$ is the harvest share. $n_{f,energy}$ is the share of energetic use. p is the conversion factor for firewood [t_{utro}/m^3]. H_u is the calorific value in gigajoules per tonne [GJ/t_{utro}].

The theoretical energy potential of forest is based on E_{fm} of the total inventory of forest, which means the energy potential by cutting down all the trees, while the sustainable potential is based on the actual harvest amount [18].

3.2.3 Technical Potential of Biogas from Energy Crops

Biogas can be produced from energy crops, grass and orchard meadow which are all part of agricultural land use. Since grassland and orchards are shown as separate areas in the basic DLM, their energy potential is calculated separately. The energy potentials are combined into a total energy potential from biogas.

$$P_{biogas, GL/OM} = \sum A_i \cdot E_{crop,i} \cdot TS_i \cdot oTS_i \cdot E_{CH_4,i} \cdot n_{energy,i} \cdot H_{u,i}$$

Where $P_{biogas, GL/OM}$ is the annual biogas fuel potential [GJ/a]. i is the crop types. A_i is the area of the crop that can be as the source of biogas production in hectares [ha], E_{crop} is the crop harvest yield of fresh mass of each crops [$kg/ha \cdot a$], TS and oTS are its dry mass rate and organic dry mass rate, and $E_{CH_4,i}$ is its methane yield [$l/kg\ oTS$]. $n_{energy,i}$ is the share of actual energetic use per crop, and H_u is the calorific value of methane in gigajoules per tonne [GJ/l CH_4].

3.2.4 Technical Potential of Vegetable Oil from Energy Crops

The most important oil plant in Germany is rapeseed. More than half of Germany's rapeseed area is used to grow winter rapeseed for technical and energy purposes. It is mainly used to produce biodiesel and biofuels.

$$P_{VO} = \sum A_{Rapeseed} \cdot n_{energy} \cdot E_{PO}$$

Where P_{VO} is the fuel potential from rapeseed cultivation for vegetable oil production [GJ/a]. $A_{Rapeseed}$ is the area of rapeseed cultivation in hectares [ha], n_{energy} is the share of energetic use, and E_{PO} is the energy yield of vegetable oil production from rapeseed [GJ/ha/a].

3.2.5 Technical Potential of Bioethanol from Energy Crops

Ethanol is produced by the fermentation of sugars contained in plants. Plants containing sugar, starch and cellulose such as wheat, rye, corn, triticale, sugar beet, sugar cane and straw are suitable for this. Energetically used bioethanol is cultivated in Germany in the form of sugar beet, grain maize and cereals (wheat and rye).

$$P_{ethanol} = \sum A_{ethanol} \cdot n_{energy} \cdot E_{ethanol} \cdot H_u$$

Where $P_{ethanol}$ is the fuel potential from energy crops for ethanol production [GJ/a], $A_{ethanol}$ is the area of the area of bioethanol production crops (sugar beet, grain maize and cereals), and n_{energy} the share of energetic use. $E_{ethanol}$ is the ethanol production yield from energy crop [$l/ha/a$]. H_u is the calorific value of ethanol [GJ/l].

3.2.6 Technical Potential of Solid Fuel from Energy Crop

Solid fuels from agriculture come from the cultivation of Miscanthus or from short rotational plantations (SRP). Miscanthus, also known as giant Chinese reed, is grown in Germany on an area of approx. 4,500 ha grown for various material and energetic [21]. SRP are artificially established and systematically treated energy wood plantations. The cultivation concentrates on aspects relevant to energy sources. This means that usually fast-growing tree species with very short rotation periods (under 10 years) such as poplar or willow. [18] Theoretically all the crop can be used as solid fuel, therefore the energy potential of solid fuel is equal to primary energy potential.

3.2.7 Technical Potential of Solid Fuel from Residues and Waste

Residues from agriculture and forestry are an important source of bioenergy. In the residue methodology, only primary residues from land and forestry, without taking the residue of wood processing industry, e.g. furniture production, into consideration. These are residual forest wood, residual grain straw, leaf mass of the sugar beet and landscape conservation wood from orchard stakes, orchard meadows, orchards and wooded areas.

Within residues, which are typically used as solid fuels, it can be differentiated between cereal straw, forest residues and tree cuttings from orchards and meadows, orchards and wooded areas. The calculation of its biomass potential follows

$$P_{waste,solid\ fuel} = \sum A \cdot E_{waste} \cdot n_{energy} \cdot H_u$$

Where $P_{waste,solid\ fuel}$ is the fuel potential of residues as solid fuels in gigajoules per year in GJ/a, A is the area of individual object types in ha, E_{waste} is the residue yield of individual areas in kilograms per hectare times year $\frac{kg}{ha \cdot a}$, n_{energy} is the percentage of energy usage, and H_u is the heat value in gigajoule per kilogram.

3.3 Simulation Environment & Interface

As described earlier, the assessment of biomass potentials shall be included in an existing modelling environment in order to compare different RES potentials and contrast these with energy demands in a given region. The modelling environment SimStadt developed at HFT

Stuttgart allows to date to assess local energy demands (electricity, cooling and heat) and renewable energy potentials (photovoltaic) on a single-building level using 3D city models (in the CityGML format [16]). SimStadt provides a modular workflow management for various, primarily energetic system analysis purposes. Each workflow serves a specific purpose, e.g. heating demand of buildings or photovoltaic potential, while certain modules are shared between workflows, e.g. importing data or data pre-processing.

For the to-be-established workflow on regional biomass potentials, most of the predefined modules are not applicable due to the fact that the input data is land use polygons instead of building geometries, the exception being the import module that can read CityGML files regardless of the type of objects (building or land use polygon).

A new module, 'BiomassProcessor', was thus created, which processes all land use polygons. Lastly, the calculated biomass potential in the forms of theoretical potentials, technical potentials and end energy is calculated, stored and exported to a CSV file. Users can modify parameters, such as the annual forest energy use rate, the share of energy crop such as corn and rapeseed that are actually used for energetic purposes, or the grass land energy usage rate. More specific parameters, including the conversion pathways to different biofuel forms per relevant crop is enabled by importing an XML configuration file.

Table III: Typical scenario parameters

Parameter	Value	Explanation
Conifer harvest rate	4.5% (Martin et al. 2001, pp. 162–163)	The percentage in volume of conifer which is harvested annually out of all conifer trees under the current situation
Deciduous trees harvest rate	3.0% (Martin et al. 2001, pp. 162–163)	The percentage in volume of deciduous trees which is harvested out of all deciduous trees under the current situation
Forest energy usage rate	25.6% ((FNR) 2018)	The percentage in volume of solid forest wood with diameter over 7 cm which is used for energy purpose
Energy crop rate	14.0% ((FNR) 2019)	The percentage in area of farming land for energy crop cultivation out of all farming land. Since no data source gives the end product of crop (for energy or for food) of each land field, in this simulation, we assume for each land field 14% of area is used for energy purpose.
Residue energy usage rate	62.0% (Nitsch et al. 2012, p. 83)	The percentage in energy of residue by-products which are used for energetic purpose

Table IV: Scenario parameters

Scenario variant	Scenario Name	Explanation
1	Base case	Values of Tab III and Table V applied (Martin et al. 2001, p. 163)
2	100% forest harvesting	Extreme case: all available forest will be harvested within one year, i.e. scenarios reflects the theoretical bioenergy content of wood.
3	0% forest harvesting	No energetic use of timber
4	Energy crop 0%	The mentioned share of energy crops (cereal, sugar beet rapeseed, maize) is used for energy crop production (vs. food)
5	Energy crop 50%	
6	Energy crop 100%	
7	Biogas preferred	If an energy crop can be a source for a certain biofuel carrier (see Table V), all of it will be used to this end. If the crop cannot be used for the production of this biofuel carrier, it would follow the same default biofuel based on the distribution in Tab. V.
8	Bioethanol preferred	
9	Vegetable oil preferred	
10	Solid fuel preferred	
11	Residue energy use rate 0%	The mentioned share of residues from all forms of land use are used for energetic purposes.
12	Residue energy use rate 50%	
13	Residue energy use rate 100%	

3.4 Approach to data validation

A validation of the described workflow based on a comparison of the calculated annual biomass potentials on a sub-national and sub-state level with actual biomass usage levels is inherently limited, since information on in-/exports of biomass as primary or secondary energy carriers is typically limited, and technical potentials are rarely fully exploited for a variety of reasons. On the national level, few studies have determined the biomass potential at national level in long term scenarios [22–24]. Therefore, a validation needs to focus on comparing with the average energy yield density on national level. The biomass has the typical annual energy yield of 18 to 56 MWh/ha in Germany under the constraints of ecological limit and of energy use [22]. This range is compared with the simulation results of technical potential.

3.5 Scenarios setting

For each of the two case studies (see next section), 13 scenarios were defined to quantify the influence of different forest and residue usage rates, land area dedicated to energy crops, and a priority on different forms of biofuels produced from the available biomass resources. Tab. III shows the values applied in the base case scenario, while Tab. IV gives an overview of all scenarios and Tab. V shows the default biofuel production distribution among energy crops. In all scenarios, the parameters not explicitly mentioned in Tab. 3 remain the same as in the base case scenario.

Table V: Biofuel distribution from energy crop. Source: FNR [25]

	Biofuel	Bioethanol	Vegetable	Oil
Solid fuel				
Cereal	56%	44%	0%	0%
Maize	98%	2%	0%	0%
SRC	97%	0%	0%	3%
Sugar beet	42%	58%	0%	0%
Rapeseed	0%	0%	100%	0%
Grass	99%	0%	0%	1%

3.6 Test cases

The new workflow was tested in two German counties with different land coverages and population densities. The county of Ludwigsburg is located in the centre of Baden-Württemberg, in Germany's south-western corner. It covers an area of 687 km², with a population of about 550,000 inhabitants, spread across 39 municipalities. 55 % of the county's land area is agricultural land, and 18% forest [26]. In 2013, it has set itself a goal of reducing greenhouse gas emissions by 90 percent until 2050 through increased energy efficiency and increasing the share renewable energy sources, e.g., through using biomass for local heat and power generation [27].

The county's total end energy consumption (electricity, heating, gasoline, diesel) in 2012 was 8,355 GWh (more recent data are not available). As these data points are eight years old, the numbers were extrapolated to 2018 (latest available) based on data for end energy demand in Baden-Württemberg (BW) state, which increased from 387 TWh in 2012 to 394 TWh in 2018 [28]. By scaling the total end energy consumption of year 2012 with the development of energy consumption in BW, the end energy consumption in county Ludwigsburg has the value of 8506 GWh.

The county of Dithmarschen in the state of Schleswig-

Holstein is bordering the North Sea. Its population of 133,000 is spread over an area of 1,428 km², with 78 % of the county's land area being agricultural land, and 3% forest [29]. Thus, Ludwigsburg represents a typical suburban county in Germany's hilly south, whereas Dithmarschen is a more rural county in Germany's north with generally less forest cover. However, both counties use a sizeable share of their land for agriculture and should thus have meaningful bioenergy potentials.

The county Dithmarschen in 2005 consumed around 1,624 GWh electricity and 10,098 GWh heat [30]. More detailed data of other end energy forms or secondary energy demand value are not available. Similar to the county Ludwigsburg, the more up-to-date data is not available. The similar linear scaling method with German energy consumption data as the reference is also applied here. The end energy consumption was 2536 TWh in 2005 and 2499 TWh in 2018 [31].

4 RESULTS

4.1 Case study Ludwigsburg

The theoretical energy potential from biomass according to our simulation in Ludwigsburg is 6,417 GWh. Fig. 2 gives the secondary energy potentials for the 13 scenarios described in the previous section in the forms of energy wood, bioethanol potential, biogas potential, vegetable oil potential, solid fuel potential and residue solid fuel.

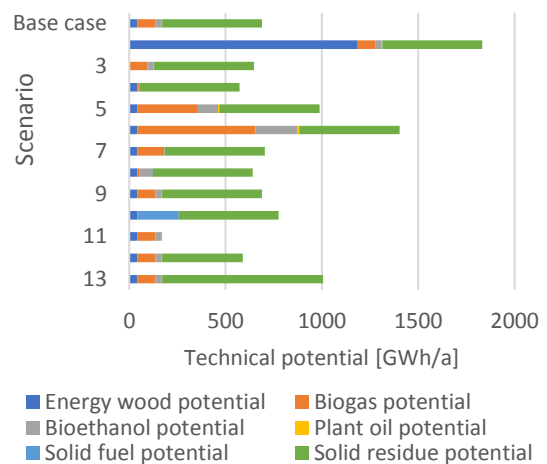


Figure 2: Input maps (a) DLM map in polygons with land use; (b) Satellite map in raster with crop type; (c) Integrated map

The base scenario gives an annual technical potential of 689 GWh, or 8% of total energy demand (based on 2018 demand data). This compares to an actual biomass share of 2% of total energy demand (in 2012) [27], which, however, must not be covered exclusively from local sources.

Scenarios 2 and 3 show the impact of using forest on biomass potential. The total energetic potentials of wood in LB amounts to 1,185 GWh. Since forest covers 18% of the total area of the whole county and only limited amount of forest can be harvested under forest growth rate due to regulation, biomass potential from forest has limited room to be increased. The ecological sustainable biomass potential from forest is 42 GWh/a.

Scenario 4 to 6 show the area of energy crop as a

variable to biomass potential. If all the available agriculture land is converted to the land for energy crop without food production, the biomass potential would be tripled from 573 GWh to 1403 GWh.

Scenario 7 to 10 indicate that there is no big difference of the total energy amount when the biomass is converted to different secondary energy forms. The bioethanol-first scenario has the lowest total secondary energy yield with 641 GWh, with a bioethanol potential of 67 GWh, compared to 31 GWh in the base case, while the solid fuel preferred scenario (#10) has the highest total secondary energy yield (776 GWh), since the conversion process from primary energy potential to solid fuel has the lowest losses.

Scenario 11 to 13 shows the importance of utilizing residue by-products. When residue from forest and agriculture land is not recycled, the total secondary energy potential is only 170 GWh/a, compared to 1,007 GWh/a when all residue is used for energy production.

Fig. 3 shows a biomass primary energy density map for the base case scenario for Ludwigsburg country. Vineyard and fruit plantation, shown in red, have the lowest potential density as only residue by-products are utilized as energy source. The grove and agriculture area are mostly yellow and green indicating the middle value of potential since only 14% of the production of the polygons are energy crop under this scenario. The potential of forest is relatively higher than the potential of agricultural land. Thus, the northern, eastern and southernmost parts of the county, which have a high forest coverage ratio, show high biomass potential densities. Urban areas, railway and streets are shown in white, assuming no relevant amounts of biomass potential in the context of this study (even though some studies have assessed urban biomass potentials, e.g. [32])

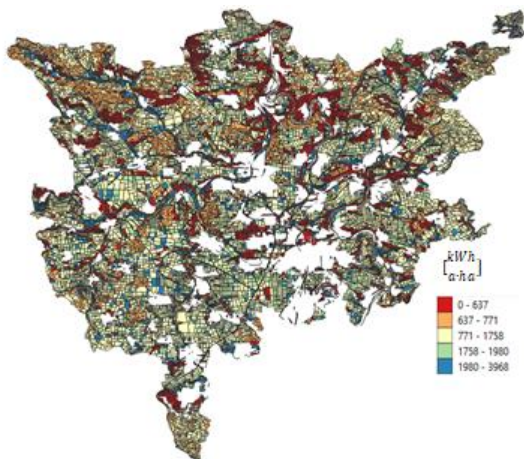


Figure 3: Technical biomass potential density map in county Ludwigsburg

Afterwards, the results were again combined with CityGML to visualise them on the web framework CesiumJS by using 3D Tiles. In Fig. 4, a small area of county Ludwigsburg, Marbach, was visualized with 3D buildings and satellite map. The red area represents area with very long biomass density, either with buildings, roads or water bodies. Each polygon has homogeneous density over all area because a polygon is assumed to be covered by one type of crop. Except for red build-up area, road and river, the only vegetation cover land type is

farming land in this map. Different colours represent different biomass potential brought by different crop types.

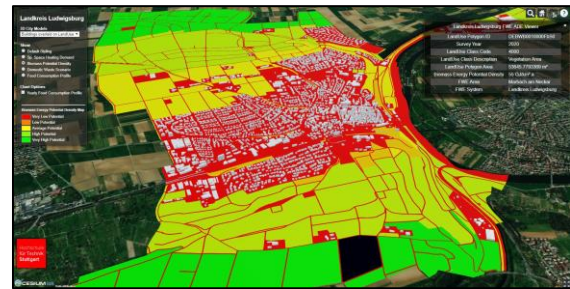


Figure 4: Visualisation of the Marbach's biomass potential using its CityGML LandUse model (Source: HFT Stuttgart)

4.2 Case study Dithmarschen

The base scenario gives an annual technical potential of 2248 GWh, or 19% of total electricity and heating demand (based on 2018 demand data). In the base case the technical potential in biofuel energy wood potential of 23 GWh, biogas potential of 329 GWh, bioethanol potential in 59 GWh, plant oil potential in 5 GWh and solid fuel in 3 GWh.

The trend of total secondary biomass potential in Dithmarschen (shown in Fig. 5) is identical with Ludwigsburg: By either harvesting more forest (Scenario 2), increasing the share of agricultural crops for energy uses (Scenario 6), more direct burning by using solid fuel (Scenario 10), or increasing the residue by-product energy utilization rate (Scenario 13) the total secondary energy potential can be increased. To be noticed by increasing forest harvesting rate from 0% to 100% only increase the total secondary potential from 2248 GWh/a to 2794 GWh/a since there is limited forest regions in Dithmarschen. Since comparing with forest, agriculture plays an important role in Dithmarschen. There are adequate agricultural regions can potentially serve as the producer for energetic biomass. Even though by direct burning biomass can result in slightly higher the total secondary energy potential, as it avoids conversion losses comparing with biogas, bioethanol and vegetable oil, the share for specific secondary energy forms should be suit the end energy demand in the region. A more efficient use of by-product, e.g. straw, can greatly increase the potential biomass amount. By cycling residue 100% only for energy purpose, the technical total secondary energy potential can reach 98 GWh/a from 65 GWh/a in base case.

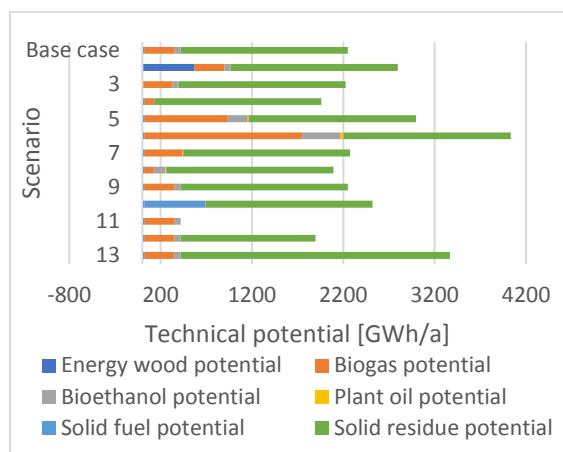


Figure 5: Secondary energy potential from biomass over 13 scenarios in Dithmarschen

5 CONCLUSION AND DISCUSSION

The newly established biomass workflow provides a reasonable result of primary and secondary biomass potential with high resolution applying to any region in Germany. At the same time for a county the calculation time is less than one minute in a PC. The workflow also enables users to modify various parameters to generate customized scenarios. The interdependency and nexus between energy, water and food will be studied with one generic data source and by the same tool. The new workflow can now be used in interactions with the urban energy demand workflow as well as the roof PV potential analysis workflow to design regional energy supply-demand balances which help local governments to make strategic decision with regards to regional energy systems, autarchy rates etc. More researches can be performed on important boundary conditions for securing, or optimizing, the assessed biomass potentials in the long term in the context of climate change, such as local water availabilities.

Even though PV has higher energy yield per area between 100 and 130 kWh/m² comparing with biomass of 2 to 6 kWh/m². Compared to the technical biomass potential of 689 GWh/a, local PV potentials in county Ludwigsburg add to 330 GWh/a of field-based and 13.9 GWh/a of field-based [27]. This could bring by the limited available land area in this county for PV installation.

County Dithmarschen has higher biomass self-sufficiency rate of 19% comparing with the county Ludwigsburg of 8%, even though Dithmarschen has higher demand for heating because of the cold weather. The possible reason behind it is that Dithmarschen has a larger agriculture area which has higher energetic biomass potential than forest. Even though forest contains a higher amount of primary energy, however in terms of technical available energy, only a limited amount of secondary energy can be extracted from forest.

Although this method gives biofuel potential in various forms, it has integrated additional material flow analysis connecting with biofuel. For example, with higher utilization and conversion rate of bioethanol, biodiesel and biogas also produce by-products, additional material can be reduced. Another limitation of this method is that it assumes a constant percentage of land products is used for energy for all land field. For the whole region the

assumption doesn't add error to aggregated number. However, the end use purpose for each land products is different from each other.

6 REFERENCES

- [1] Brief on biomass for energy in the European Union, [Publications Office of the European Union], [Luxembourg], 2019.
- [2] G. Berndes, M. Hoogwijk, R. van den Broek, The contribution of biomass in the future global energy supply: a review of 17 studies, *Biomass and Bioenergy* 25 (2003) 1–28.
- [3] A. Mittelstädt, S. Köhler, R. Sihombing, E. Duminil, V. Coors, U. Eicker et al. (Eds.), *A Multi-Scale, Web-based Interface for Strategic Planning of low-carbon City Quarters*, 2019.
- [4] Using 3D CityGML Models for Building Simulation Applications at District Level - IEEE Conference Publication, [June 09, 2020].
- [5] S. Bouchard, M. Landry, Y. Gagnon, Methodology for the large scale assessment of the technical power potential of forest biomass: Application to the province of New Brunswick, Canada, *Biomass and Bioenergy* 54 (2013) 1–17.
- [6] K. Ericsson, L.J. Nilsson, Assessment of the potential biomass supply in Europe using a resource-focused approach, *Biomass and Bioenergy* 30 (2006) 1–15.
- [7] D. Lauka, A. Barisa, D. Blumberga, Assessment of the availability and utilization potential of low-quality biomass in Latvia, *Energy Procedia* 147 (2018) 518–524.
- [8] M. Haase, C. Rösch, D. Ketzer, GIS-based assessment of sustainable crop residue potentials in European regions, *Biomass and Bioenergy* 86 (2016) 156–171.
- [9] D.F. Lozano-García, J.E. Santibañez-Aguilar, F.J. Lozano, A. Flores-Tlacuahuac, GIS-based modeling of residual biomass availability for energy and production in Mexico, *Renewable and Sustainable Energy Reviews* 120 (2020) 109610.
- [10] L. Quinta-Nova, P. Fernandez, N. Pedro, GIS-Based Suitability Model for Assessment of Forest Biomass Energy Potential in a Region of Portugal, *IOP Conf. Ser.: Earth Environ. Sci.* 95 (2017) 42059.
- [11] D. Voivontas, D. Assimacopoulos, E.G. Koukios, Assessment of biomass potential for power production: a GIS based method, *Biomass and Bioenergy* 20 (2001) 101–112.
- [12] V.C. Rushikesh Padsala, *Conceptualizing, Managing and Developing: A Web Based 3D City Information Model for Urban Energy Demand Simulation*, UDMV (2015).
- [13] L.R. Rodríguez, E. Duminil, J.S. Ramos, U. Eicker, Assessment of the photovoltaic potential at urban level based on 3D city models: A case study and new methodological approach, *Solar Energy* 146 (2017) 264–275.
- [14] P. Griffiths, C. Nendel, P. Hostert, Intra-annual reflectance composites from Sentinel-2 and Landsat for national-scale crop and land cover mapping, *Remote Sensing of Environment* 220 (2019) 135–151.
- [15] T.H. Kolbe, G. Gröger, L. Plümer, CityGML: Interoperable Access to 3D City Models, in: E.M. Fendel, P. van Oosterom, S. Zlatanova (Eds.), Geo-

- information for Disaster Management, 1. Aufl., Springer-Verlag, s.l., 2005, pp. 883–899.
- [16] R. Nouvel, K.-H. Brassel, M. Bruse, E. Duminil, V. Coors, U. Eicker, SimStadt, a new workflow-driven urban energy simulation platform for CityGML city models, Proceedings of International Conference CISBAT 2015 Future Buildings and Districts Sustainability from Nano to Urban Scale. No. CONF. LESO-PB, EPFL 2015.
- [17] Statistisches Bundesamt, Forstwirtschaftliche Bodennutzung - Holzeinschlagsstatistik, https://www.destatis.de/DE/Themen/Branchen-Unternehmen/Landwirtschaft-Forstwirtschaft-Fischerei/Wald-Holz/Publikationen/Downloads-Wald-und-Holz/holzeinschlag-2030331187004.pdf?__blob=publicationFile.
- [18] K. Martin, H. Hans, H. Hermann, Energie aus Biomasse: Grundlagen, Techniken und Verfahren, Springer Verlag, Germany, 2001.
- [19] Fachagentur Nachwachsende Rohstoffe e. V. (FNR), Rohstoffmonitoring Holz: Erwartungen und Möglichkeiten (2018).
- [20] J. MÜHLENHOFF, Reststoffe für Bioenergie nutzen–Potenziale, Mobilisierung und Umweltbilanz, Renew's Spezial, Ausgabe 64 (2013).
- [21] Fachagentur Nachwachsende Rohstoffe e. V. (FNR), Miscanthus, <https://pflanzen.fnr.de/energiepflanzen/pflanzen/miscanthus/>.
- [22] J. Nitsch, T. Pregger, T. Naegler, D. Heide, D. Luca de Tena, F. Trieb et al., Langfristszenarien und Strategien für den Ausbau der erneuerbaren Energien in Deutschland bei Berücksichtigung der Entwicklung in Europa und global, 2012.
- [23] P. AG, Öko-Institut, Modell Deutschland. Klimaschutz bis 2050: Vom Ziel her denken.
- [24] J. Nitsch, W. Krewitt, M. Nast, P. Viebahn, S. Gärtner, M. Pehnt et al., Ökologisch optimierter Ausbau der Nutzung erneuerbarer Energie in Deutschland, 2004.
- [25] Fachagentur Nachwachsende Rohstoffe e. V. (FNR), Anbau und Verwendung nachwachsender Rohstoffe in Deutschland (2019).
- [26] Statistisches Bundesamt, Anbauflächen, Hektarerträge und Erntemengen ausgewählter Anbaukulturen im Zeitvergleich: Hektarerträge ausgewählter Anbaukulturen im Zeitvergleich, <https://www.destatis.de/DE/Themen/Branchen-Unternehmen/Landwirtschaft-Forstwirtschaft-Fischerei/Feldfruechte-Gruenland/Tabellen/listefeldfruechte-zeitreihe.html>.
- [27] Landratsamt Ludwigsburg, Klimaschutzkonzept Ludwigsburg Kurzbericht (2015).
- [28] Statistisches Landesamt Baden-Württemberg, Struktur und Entwicklung des Energieverbrauchs nach Verbrauchsart und Verbrauchergruppen, [June 24, 2020], <https://www.statistik-bw.de/Energie/Energiebilanz/LRt1002.jsp>.
- [29] E. Ulich, A. Geruhn, H. Demmer, K. Frank, Regionalprofil 2006 des Kreises Dithmarschen: einschließlich Stärken- und Schwächen-Analyse.
- [30] Fachdienst technische Aufgaben des Kreises Dithmarschen, Energiebereich Kreis Dithmarschen 2005.
- [31] Endenergieverbrauch in Deutschland bis 2018 | Statista, [May 26, 2020], <https://de.statista.com/statistik/daten/studie/251538/mfrage/endenergieverbrauch-in-deutschland/>.
- [32] D.R. Grafius, S. Hall, N. McHugh, J.L. Edmondson, How much heat can we grow in our cities? Modelling UK urban biofuel production potential, GCB Bioenergy, 12(1), 118-132, GCB Bioenergy 12 (2019) 118–132.

Chapter 8

Urbane Energiesysteme und Ressourceneffizienz – ENsource

Bao, K.; Schröter, B. SimStadt.

Coors, V. Eds.; Fraunhofer Verlag: Stuttgart, 2021; pp 15-21.

BW-Forschungsverbund ENsource
Volker Coors (Hrsg.)

Urbane Energiesysteme und Ressourceneffizienz – ENsource

Stuttgart
am 1. März 2021

FRAUNHOFER VERLAG

Kontaktadresse:

Hochschule für Technik Stuttgart
Zentrum für Urbane Energiesysteme und Ressourceneffizienz (ENsource)
Schellingstr. 24, 70174 Stuttgart
Postfach 101452, 70013 Stuttgart
Telefon 0711 / 8926-0
info@hft-stuttgart.de
www.hft-stuttgart.de

Projekt ENsource:

Telefon 0711/8926-2708
ensource@hft-stuttgart.de
Volker.Coors@hft-stuttgart.de
www.ensource.de

DOI: <https://doi.org/10.24406/ise-n-621593>



Dieses Werk ist lizenziert unter einer Creative Commons Namensnennung 4.0 International Lizenz:
<https://creativecommons.org/licenses/by/4.0/legalcode.de>

Satz:
Späth Mediendesign GmbH, Birenbach

© Fraunhofer Verlag, 2021
Nobelstraße 12
70569 Stuttgart
verlag@fraunhofer.de
www.verlag.fraunhofer.de

als rechtlich nicht selbständige Einheit der

Fraunhofer-Gesellschaft zur Förderung
der angewandten Forschung e.V.
Hansastraße 27c
80686 München
www.fraunhofer.de

Inhaltsverzeichnis

Vorwort	7
Einführung.....	9
ENsource-Tools und ENsource-Services	13
1 SimStadt	15
2 Klimaneutrale kommunale Energiesysteme mit dem Modell KomMod optimieren	21
3 Dynamische Energieversorgungsanalyse	27
4 Bedarfsgerechte Steuerung von KWK-Anlagen und Wärmepumpen .	33
5 Übergeordnete Betriebsführung von Kälteanlagen.....	41
6 Quartierssteuerung – kooperatives Energiemanagement im Quartier	48
7 Mehrstufige Koordination von dezentralen Anlagensteuerungen im Quartier	55
8 Power-to-X-Prozesse als Energiespeicher und für eine nachhaltigere Mobilität und Industrie	62
9 Bioabfall-Energieertrag-Prognosemodell (BEP).....	70
10 Wirtschaftlichkeitsanalyse einer Power-to-Gas-Anlage bzw. einer Biogasanlage.....	77
11 Geschäftsmodellkonfigurator	82
12 Vergleichende Bewertung des Ressourcenaufwands urbaner Energiesysteme (ENsource-MöK).....	89
13 Berücksichtigung des Ressourcenaufwands bei der Energiesystemoptimierung	96
14 Serviceangebot	103
Fallstudien und Services durch Kopplung der Tools	109
A Fallstudie Rainau	111
B Fallstudie Mainau	119

C	Fallstudie Schwieberdingen	126
D	Fallstudie Mannheim	136
E	Fallstudie Stuttgart	145
	Zusammenfassung und Übertragbarkeit.....	153
	Literaturverzeichnis	155
	Glossar	165
	Abkürzungen.....	174
	Autoren	177
	Stichwortverzeichnis	180

Aus Gründen der besseren Lesbarkeit wird auf die gleichzeitige Verwendung der Sprachformen männlich, weiblich und divers (m/w/d) verzichtet. Sämtliche Personenbezeichnungen gelten gleichermaßen für alle Geschlechter.



In der aktuellen EU-Förderperiode (2014–2020) fördert das Ministerium für Wissenschaft, Forschung und Kunst das Zentrum ENsource mit 1,25 Mio € aus Landesmitteln und 1,25 Mio € aus Mitteln des Europäischen Fonds für regionale Entwicklung (EFRE).

1 SimStadt

Keyu Bao, Bastian Schröter

In Zeiten von Klimawandel, immer günstigerem Strom aus dezentralen und erneuerbaren Quellen sowie neuen Mobilitätskonzepten müssen Stadtquartiere und urbane Regionen neu gedacht werden. Tools, die bereits früh im Planungsprozess Transparenz über Strom- und Wärmeerzeugungspotenziale oder lokale Verbräuche schaffen, können diesen Prozess in Summe effizienter gestalten. SimStadt ist der Name einer Simulationsumgebung und in seiner jetzigen Ausbaustufe in der Lage, auf Basis von gängigen und in der Regel verfügbaren Daten, insbesondere 3D-Gebäudemodellen, verschiedenste energiebezogene Simulationen auf Basis dieser Daten durchzuführen – von Simulationen des Heizwärmebedarfs über Photovoltaik-Potenzialstudien bis hin zur Simulation von Gebäudesanierungs- und Versorgungsszenarien mit Erneuerbaren Energien.

SimStadt wurde im Rahmen von zwei Projekten (SimStadt und SimStadt 2.0) seit 2013 unter Federführung der HFT Stuttgart entwickelt und validiert¹. Im Rahmen von ENsource wurde SimStadt auf verschiedene Fallstudien angewandt.

1.1 Ein knapper Überblick zu SimStadt²

SimStadt arbeitet unter Einbindung der ebenfalls an der HFT Stuttgart maßgeblich weiterentwickelten Simulationsumgebung INSEL 8.2³. Bild 2 gibt einen Überblick über die verwendeten Datenquellen und die in die Umgebung eingebundenen Anwendungen: Durch die Generierung von 3D-CityGML-Gebäudemodellen aus LIDAR-Daten (vgl. Bonczak et al. 2019) und deren möglicher Anreicherung mit Gebäudeattributen, z. B. aus städtischen Quellen oder einer EnergyADE⁴ (vgl. Nouvel et al. 2017), können bestehende Umgebungen wie Gebäude, Straßen und Landschaften dargestellt werden, während Neubauquartiere auf Basis von CAD-Programmen wie z. B. SketchUp generiert werden können. Gebäudemodelle können dabei in fünf verschiedenen Detaillierungsgraden (auf Englisch: Level Of Detail, LOD) existieren (vgl. Bild 3), wobei mindestens LOD 2 mit seinen detaillierteren Informationen über Gebäudehöhen und Dachformen für energetische Simulationen notwendig ist.

¹ Das SimStadt 2.0-Projekt wird unter dem Förderkennzeichen 03ET1459A vom Bundesministerium für Wirtschaft und Energie (BMWi) gefördert.

² Kapitel 1.1. und 1.3. basieren auf dem Artikel von Weiler et al. (2019).

³ <https://insel.eu/de/>

⁴ Die CityGML Energy ADE erweitert den CityGML-Standard um Merkmale und Eigenschaften, die zur Durchführung einer Energiesimulation und zur Speicherung der entsprechenden Ergebnisse notwendig sind.

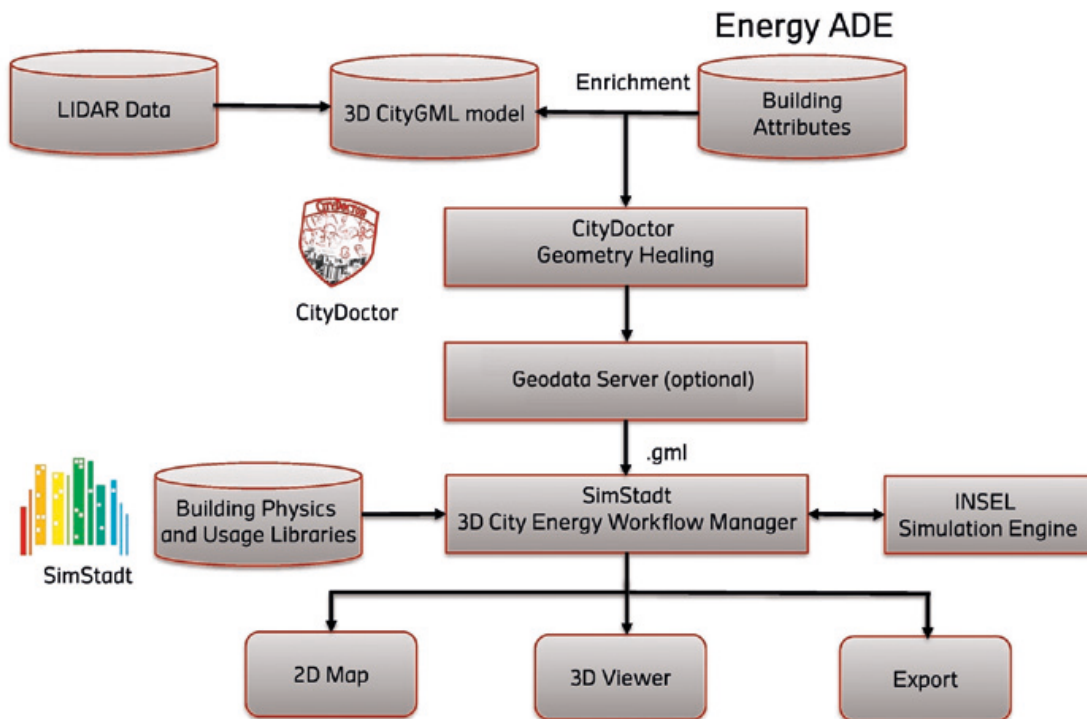


Bild 2 SimStadt-Simulationsumgebung mit Datenquellen

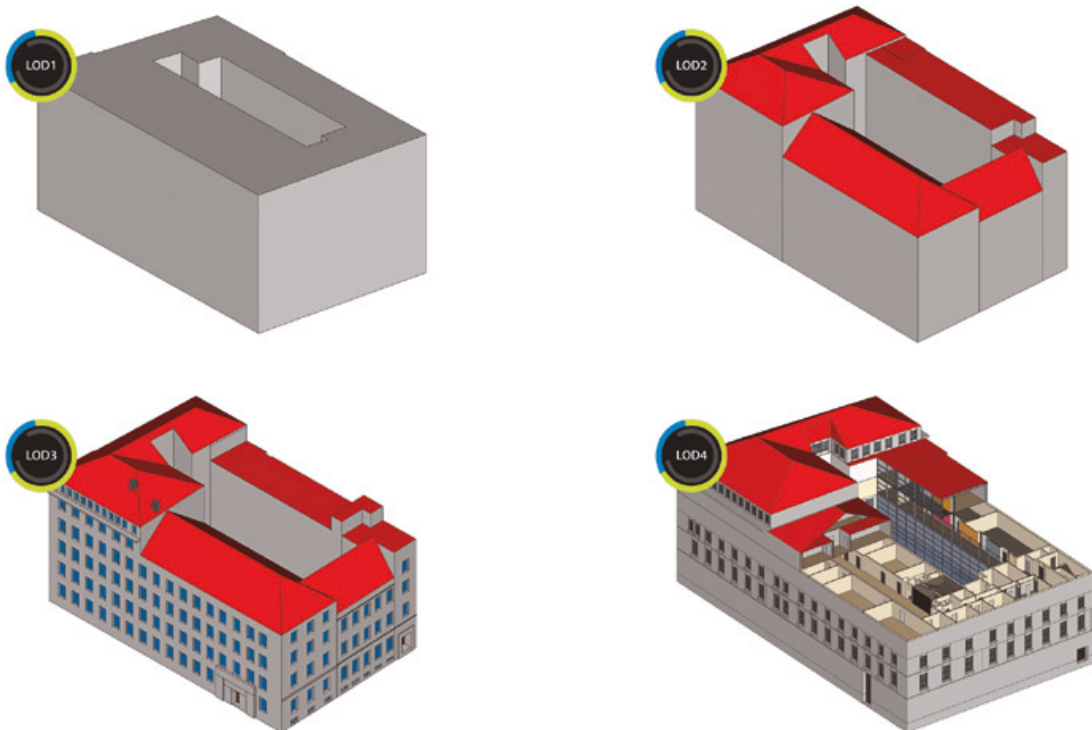


Bild 3 Visualisierung von LOD1 bis LOD4 im CityGML-Format

Das CityGML-Modell wird vor der eigentlichen Verwendung in SimStadt durch das Tool **CityDoctor** qualitätsgeprüft, wobei mögliche geometrische Fehler wie z. B. offene Polygone, die ein Gebäude nicht umfänglich »abschließen«, behoben werden.

SimStadt verfügt über eine grafische Benutzeroberfläche (GUI) und verarbeitet in verschiedenen Schritten das CityGML-Modell sowie Datenpunkte aus einer bauphysikalischen Bibliothek sowie Wetterdaten, wobei die Geometrie jedes einzelnen Gebäudes in der CityGML-Datei mit den verschiedenen Bibliotheken verknüpft wird.

Die **bauphysikalische Bibliothek** basiert auf der vom deutschen Institut Wohnen und Umwelt (IWU) (vgl. Loga et al. 2015) entwickelten Typologie, die Gebäude nach Typ und Baujahr klassifiziert. Für jeden Gebäudetyp und jede Bauperiode existiert ein Gebäudearchetyp mit spezifischen Wand-, Dach- und Fenstereigenschaften. Diese Eigenschaften werden auf die tatsächliche Gebäudegeometrie angewendet, und SimStadt berechnet dann für jedes Gebäude Wärmedurchgangskoeffizienten (U-Werte). Über die Gebäudearchetypen hinaus sind in der bauphysikalischen Bibliothek verschiedene Sanierungsoptionen hinterlegt, die eine Berechnung von »Was-wäre-wenn«-Sanierungsszenarien erlauben.

Weiterhin wird eine sogenannte **Nutzungsbibliothek** angewandt. Diese enthält Informationen auf Basis verschiedener (deutscher) Normen und Standards, womit Informationen, insbesondere zu Heizsollwerttemperaturen, Belegungsplänen und internen Gewinnen, d. h. die von Geräten und Bewohnern im Gebäudeinneren erzeugte Wärme, je nach Gebäudenutzungsart (Wohnen, Büro, Einzelhandel usw.), den einzelnen Gebäuden im 3D-Modell zugeordnet werden können.

Als letzter Baustein erlaubt die Simulationsumgebung **INSEL** die Programmierung von energietechnischen Anlagen in intuitiv-graphischer Weise, wobei einzelne Komponenten wie PV-Module oder Heizkessel durch Blockdiagramme repräsentiert und untereinander verbunden werden.

Die Ergebnisse der SimStadt-Simulationen können in 2D und 3D (vgl. Weiler et al. 2019) visualisiert werden und Detailergebnisse per *.csv-Datei exportiert werden.

1.2 Dienstleistungen und Anwender von SimStadt

SimStadt erlaubt auf Basis von wenigen Inputdaten, verschiedene Bedarfs- und Potenzialanalysen im Bereich Energie und Wasser durchzuführen, die für verschiedene Nutzergruppen relevant sind. Einen Überblick bietet Tabelle 1.

Tabelle 1 Anwendungsfälle von SimStadt für verschiedene Nutzergruppen

	Heizwärmebedarfsanalyse von Wohngebäuden/-quartieren, Sanierungsszenarien	Strombedarfsanalyse für Wohngebäude/-quartiere	Umweltverträglichkeitsprüfung, ggf. inklusive Sanierungsstrategie	PV-Potenzial- und Kostenanalyse in Stadtquartieren	Wärmeversorgungsoptionen von Stadtquartieren	Fern- und Nahwärmenetzdimensionierung für Stadtquartiere	Wasserbedarf von Wohngebäuden/-quartieren
Stadtwerk	x	x		x	x	x	x
Regionalverbände	x	x	x	x	x	x	x
(Energie-)Berater	x			x	x		
Kommunale Entscheider/ Ämter	x		x	x	x	x	x
Stadt-/Regionalplaner	x	x	x	x	x	x	x
(Bau-)Ingenieur-/Planungsbüro	x		x	x	x	x	x
Investoren				x	x		
Forscher	x	x	x	x	x	x	x

1.3 Input und Output, Funktionalität

Die für die verschiedenen in Tabelle 2 erwähnten Analyseoptionen benötigten Eingangsdaten unterscheiden sich leicht. Für viele Analysen genügt bereits ein um Gebäudenutzungsart und Baujahr angereichertes 3D-CityGML-Modell (siehe Kapitel 1.1), welches in Deutschland für Bestandsgebäude flächendeckend verfügbar ist.

Tabelle 2 Die Verbindung zwischen Analyseoption, Eingangsdaten und Ergebnissen

Analyseoption	Eingangsdaten	Ergebnis
Heizwärmebedarf von Wohngebäuden/-quartieren, Sanierungsszenarien	3D-Stadtmodell (City GML), Gebäudenutzungsart (inkl. Keller- und Dachflächennutzung), Baujahr. Im Falle von Strom- und Wasserbedarfsanalyse zudem Zensusdaten der Statistischen Ämter des Bundes und der Länder (liegen für Deutschland vor)	Stündlicher und monatlicher Wärmebedarf (pro Gebäude sowie für das Gesamtquartier), ggf. vor und nach Sanierung
Strombedarfsanalyse für Wohngebäude/-quartiere		Stündlicher und monatlicher Strombedarf (pro Gebäude sowie für das Gesamtquartier)
Umweltverträglichkeitsprüfung , ggf. inklusive Sanierungsstrategie		Primärenergiebedarf und CO ₂ -Emission (pro Gebäude sowie für das Gesamtquartier)
PV-Potenzial- und Kostenanalyse in Stadtquartieren		PV-Potenzial (in kWp) je Gebäude, bei Bedarf inkl. Fassaden-PV, monatliches und stündliches Stromerzeugungspotenzial (in kWh) je Gebäude
Wärmeversorgungsoptionen von Stadtquartieren		Kosten, Dimensionierung und stundengenauer Einsatzplan für ausgewählte zentrale und dezentrale Wärmeversorgungsszenarien (z. B. Blockheizkraftwerk (BHKW) mit Gaskessel, Wärmepumpen je Gebäude))
Fern- und Nahwärmenetz- dimensionierung für Stadtquartiere		(Grob-)Dimensionierung des Wärmenetzes (Länge und Durchmesser der Rohre, Durchfluss je Zeitintervall bei verschiedenen Temperaturniveaus)
Wasserbedarf von Wohngebäuden/-quartieren		Jährlicher Trinkwasserbedarf (pro Gebäude sowie für das Gesamtquartier)

Die wichtigsten Analyseoptionen werden im Folgenden knapp erläutert.

1.3.1 Wärmebedarfsanalyse vor und nach Sanierung

SimStadt berechnet den Wärmebedarf eines Gebäudeensembles als monatliche Energiebilanz nach DIN 18599. Hierbei werden auf Basis der Informationen in den bauphysikalischen und nutzungsbezogenen Bibliotheken Wärmedurchgangskoeffizienten je Gebäude nach Gebäudetyp und -alter ermittelt. Die Monatswerte können in Abhängigkeit von Außentemperatur und gewünschter Raumtemperatur in Stundenwerte überführt werden (nach Norm VDI 4710).

Zudem kann angenommen werden, dass einzelne Komponenten (Dach, Fenster, Fassade) einzelner Gebäude oder ganzer Ensembles energetisch ertüchtigt werden, und dann kann ermittelt werden, welchen Einfluss dies auf die Wärmebedarfe hat. Eine Kostenanalyse der Sanierungsvarianten ist (excelbasiert) im Nachgang der SimStadt-Berechnungen möglich.

1.3.2 Photovoltaik-Potenzialanalyse

Die installierbare PV-Leistung sowie die hieraus unter Einbezug lokaler Wetter- und Strahlungsdaten erzeugbare stündliche Strommenge kann ebenso ermittelt werden. Hierbei berechnet SimStadt auf Basis des 3D-City-GML-Modells Neigung und Azimut jeder Dachfläche und damit die Sonneneinstrahlung auf diese Fläche, wobei verschiedene Strahlungsmodelle angewendet werden können. Durch eine individuelle Parametrisierung können Größen wie Mindestfläche und jährliche Mindesteinstrahlung sowie das Verhältnis von Modulfläche zu Dachfläche oder die Installationskosten je kWp angepasst werden. Neben der erzeugbaren Strommenge können somit für jedes Dach die Stromgestehungskosten sowie die Amortisationszeit der Investition dargestellt werden (vgl. Mittelstädt et al. 2019).

1.3.3 Strom- und Wasserbedarfsanalyse

Auf Basis einer Kombination von Zensusdaten⁵, die von Statistischen Ämtern des Bundes und der Länder bezogen werden, und dem 3D-Gebäudemodell kann in einem ersten Schritt errechnet werden, wie viele Wohneinheiten und Personen sich (statistisch) in einem Gebäude aufhalten. Dies erlaubt im zweiten Schritt, je Wohneinheit bzw. Gebäude stundenscharfe Strombedarfsprofile (vgl. Köhler et al. 2019) oder jahresgenaue Trinkwasserbedarfe (vgl. Bao et al. 2020) zu ermitteln. Hierbei weichen insbesondere die erzeugten Strombedarfsprofile von gängigen und gemittelten Standardlastprofilen ab und erlauben so beispielsweise, realitätsnah Situationen mit Bedarfsspitzen zu untersuchen.

1.3.4 Wärmeversorgungsoptionen von Stadtquartieren

Auf Basis einer vorangehenden Heizbedarfsermittlung (mit oder ohne Sanierung) sowie einer eventuell notwendigen Netzdimensionierung können verschiedene Wärmeversorgungsoptionen modelliert werden. Hierfür werden maßgeschneiderte Lösungen unter Einbezug bestehender INSEL-Modelle (bspw. Quartiersversorgung mittels BHKW + Spitzenlastkessel) aufgesetzt. Ergebnisse dieser Analyseoption sind die benötigten Dimensionen der einzelnen Komponenten sowie stundenscharfe Einsatzpläne für ein Beispieljahr. Im Nachgang können zudem wesentliche Kostenparameter verschiedener Optionen verglichen werden.

⁵ <https://www.zensus2011.de/>

Chapter 9

Stakeholder-supported Research on the Food-Water-Energy Nexus with three International Case Studies

Pietzsch, U.; Bao, K.; Padsala, R.; Gebetsroither-Geringer, E.; Smetschka, B.; Raven, J.; Coors, V.

Proceedings of REAL CORP 2021, 26th International Conference on Urban Development, Regional Planning and Information Society. 2021, pp. 1225-1231. ISSN 2521-3938

Stakeholder-supported Research on the Food-Water-Energy Nexus with three International Case Studies

Ursula Pietzsch, Keyu Bao, Rushikesh Padsala, Ernst Gebetsroither-Geringer, Barbara Smetschka, Jeffrey Raven, Volker Coors

(M.A. Ursula Pietzsch, Hochschule für Technik Stuttgart, ursula.pietzsch@hft-stuttgart.de)

(M.Sc. Keyu Bao, Hochschule für Technik Stuttgart, keyu.bao@hft-stuttgart.de)

(M.Tech. Rushikesh Padsala, Hochschule für Technik Stuttgart, rushikesh.padsala@hft-stuttgart.de)

(Dr. Ernst Gebetsroither-Geringer, AIT Austrian Institute of Technology, Digital Resilient Cities; Vienna, AT, ernst.gebetsroither@ait.ac.at)

(Dr. Barbara Smetschka, BOKU, Institute of Social Ecology; Vienna, AT, barbara.smetschka@boku.ac.at)

(M StJeffrey Raven, FAIA, New York Institute of Technology, USA, jraven@nyit.edu)

(Dr. Volker Coors, Hochschule für Technik Stuttgart, volker.coors@hft-stuttgart.de)

1 ABSTRACT

The projected increasing population in cities and metropolitan regions results in higher demands of resources, i.e., food, water, and energy (FAO 2018), that are essential for human well-being, poverty reduction, and sustainable development (Hülsmann and Ardakanian 2018). There are clear interactions between water, food, and energy that may result in synergies or trade-offs between different sectors or interest groups. To address the issue, the international project IN-SOURCE models and analyses the Food-Water-Energy Nexus (FWE Nexus) in three case study regions of Germany, Austria and the United States of America. Due to the complexity of the nexus issue, stakeholders have been involved actively in the research process, whose valuable output would strongly support the decision-making processes. This paper gives an overview of the methods, case studies, and stakeholder involvement of the whole project. With the novel methods, stakeholder-oriented process, and case studies' representativity, IN-SOURCE serves as a benchmark for future FWE researches.

Keywords: Urban Simulation Platform, CityGML, Stakeholder Engagement, Food Water Energy Nexus, Planning Tools

2 INTRODUCTION

Cities and metropolitan regions are deemed to face major urban management challenges in the future: 55 percent of the world's population already lives in urban areas, and according to a United Nations report (United Nations, Department of Economic and Social Affairs, Population Division 2019), it will be more than two-thirds by 2050. Such a high population density in a limited space requires even better planning of public infrastructure services, especially the secure and stable supply of food, water and energy. However, the growth of cities also opens up synergetic opportunities. With the expansion and reconstruction of sustainable infrastructures, cities can take comparatively large energy-efficient transformation steps to fulfil their climate protection goals.

In this context, the international project "INtegrated analysis and modelling for the management of Sustainable urban food, water, and energy resOURCES" (IN-SOURCE) is aimed to model and analyse the Food-Water-Energy Nexus (FWE Nexus) in three case study regions of Germany, Austria and the United States of America. A common goal is to develop tools that support sustainable FWE strategies in collaboration with local stakeholders. The main focus is a shared open urban data and modelling framework, integrating 3D visualisation tools to assess FWE nexus impacts and support decision-making processes quantitatively.

The proposed modelling framework is based on the Open Geospatial Consortium (OGC) standardised open data model of CityGML and a newly proposed CityGML FWE Application Domain Extension (FWE ADE)¹ (Padsala et al., 2021). To date, this model, by finding its interfaces to urban simulation platforms such as UD_InfraSim² and SimStadt³, can simulate energy, water and food potentials in decentralised supply infrastructures under boundary conditions such as climate change, population growth, and land use change in the timeframe to 2050 (Padsala et al., 2021). Nexus relations and further development of the FWE ADE to extend its support to the open source 3D City Database (3DCityDB) are currently being worked upon.

¹ <https://transfer.hft-stuttgart.de/pages/in-source/in-source/FWEADE/>

² <https://www.ait.ac.at/en/research-topics/digital-resilient-cities/projects/ud-infrasim>

³ <https://www.hft-stuttgart.de/forschung/projekte/aktuell/simstadt-20>

Additionally, environmental footprint indicators are being analysed for food supply and demand (Kaufmann et al., 2021) and wastewater treatment plant (WWTP) analyses, for which the FWE data model integration is currently being investigated.

To facilitate public authorities' engagement, co-creative stakeholder processes are aimed to configure alternative urban and regional scenarios for integrated carbon-neutral and sustainable infrastructure. The goal is to understand the interlinkages between food, water and energy demand and analyse the feasibility of a decentralised and increasingly autonomous FWE supply. This encompasses efficient wastewater treatment with sewage sludge to energy projects, treated effluent reuse for irrigation in agriculture or a high regional food production ratio including food, green and forest waste to energy concepts. Prototype solutions will be analysed for their scalability and transferability to other cities and regions.

This paper tries to 1) consolidate major outcomes and lessons learnt during the development of the FWE urban data and modelling framework and discuss 2) results derived from the past co-creative stakeholder processes in the three international case study regions of Germany, Austria and the United States of America for larger public awareness and scientific community reach.

The IN-SOURCE project (May/June 2018 – September 2021) is part of the Sustainable Urbanisation Global Initiative (SUGI), established by the Belmont Forum and the Joint Programming Initiative Urban Europe. The project is funded by the EU Horizon 2020 programme and national funders, the Federal Ministry of Education and Research in Germany, the Federal Ministry for Climate Action, Environment, Energy, Mobility, Innovation and Technology in Austria and the National Science Foundation in the USA.

3 SHARED MODELING FRAMEWORK

3.1 Nexus relations

The workflows for food, water and energy production potentials and demand have now been elaborated. Recently, the team has been working on local food security and the sustainable food system, adding the food component to the existing energy-water simulation platform and thus finalising it. Food demand, productive potential and self-sufficiency can be analysed in the context of the food-water-energy nexus at community, sub-regional and regional levels. Currently, the nexus interrelations are being explored, which is intrinsically important for estimating future needs and potentials under changing boundary conditions. Lastly, visualisations of different FWE nexus related scenarios shall give decision support to stakeholders.

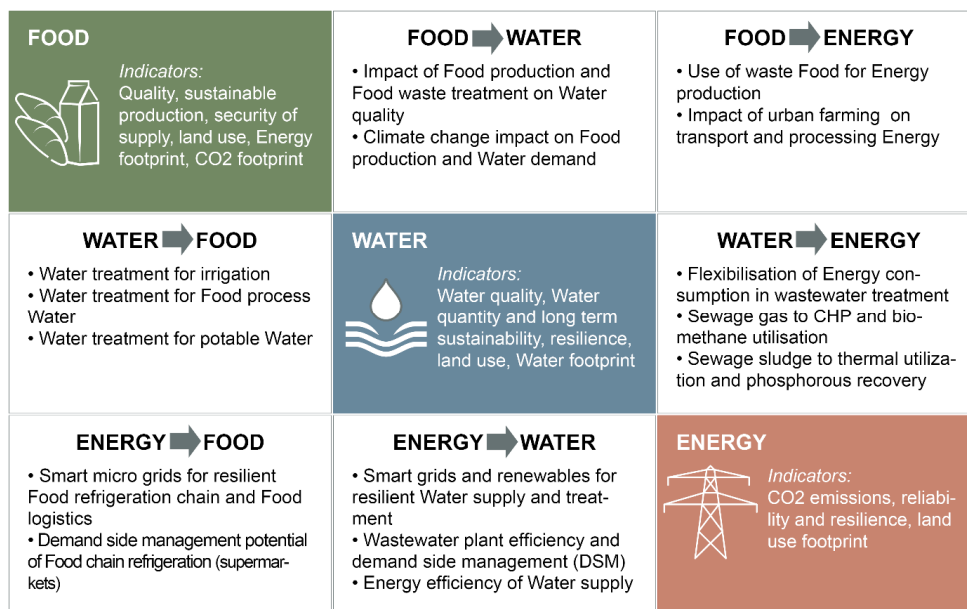


Fig. 1: The main indicators and FWE nexus questions addressed in IN-SOURCE (source: HFT Stuttgart)

3.2 Shared data model: developing a CityGML based Food-Water-Energy ADE

The development of the shared modelling framework is based on a 3D CityGML model depicting the county of Ludwigsburg in Germany, one of the three case study regions. The HFT research team set it up to model

FWE related scenarios, develop measures and work with the regional government to speed up implementing sustainable infrastructure for the whole region with 39 communities.

IN-SOURCE aims to model the impact of land use change and renewable energy transition on urban infrastructure using 3D city models. The CityGML data model was extended for the food and water using CityGML's extension mechanism of the application domain extension (ADE). All national teams intensively worked on the definition of parameters according to their respective case study regions. The CityGML FWE ADE acted as a standard data exchange platform for connecting domain specific tools to simulate FWE related scenarios. For example, to calculate biomass potential using SimStadt for a land use scenario simulated using UD_InfraSim based on Vienna's future population growth, climatic conditions and city development plan or simulating building stock energy demand using SimStadt for the neighbourhood development scenarios from the Gowanus case study of New York modelled initially using Rhinoceros3D (Padsala et al., 2020).

3.3 Simulation tools covering aspects of the FWE nexus

3.3.1 SimStadt: A comprehensive bottom-up tool to simulate potentials and demands of FWE nexus

Depending on the defined nexus relations, corresponding tools were applied and further developed to solve the nexus issue. To the author's knowledge, an assessment of biomass potentials along with other energetic potential and demand at the regional level based on a consistent set of geographical input has not been performed yet. The research question of this work will be: What are the local biomass resource potentials, their dependency on other resources, mainly water, their conflicts with other usages, i.e., food, competition with other energy technologies, i.e., wind and open land PV, and their contribution to renewable energy supply at the regional level?

To address this gap, work has been done to introduce a new workflow in SimStadt, the regional energy simulation platform developed at HFT Stuttgart (Nouvel et al., 2015). It evaluates the local biomass potential and irrigation demand on arable and forestry lands and its transformation to different forms of secondary energy, i.e., solid fuels, biogas, or bioethanol, based on geographical inputs. Based on the intermediate results of the above-mentioned biomass workflow, each land use field's vegetal and animal feed potentials are simulated (Bao et al. 2020a).

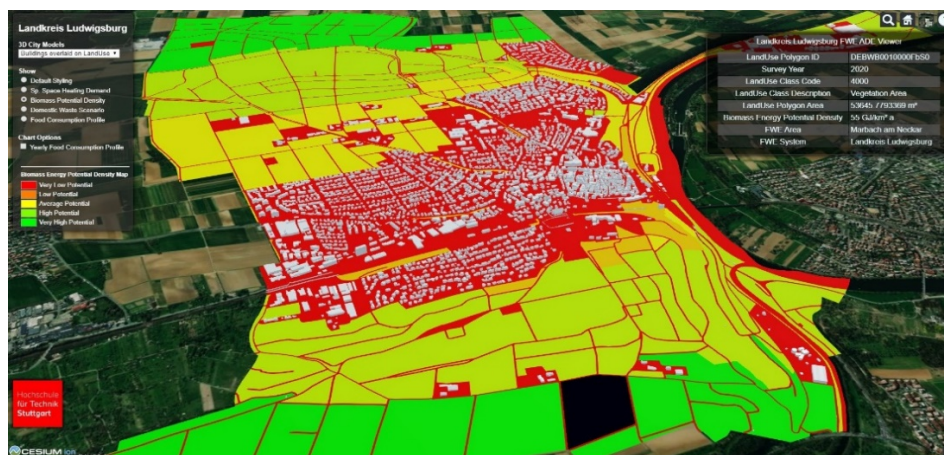


Fig.2: Biomass potential visualisation of Marbach, County of Ludwigsburg, Germany using CityGML 3D City Models (source: HFT Stuttgart, Bao/Padsala)

Since urban areas are the main consumers of resources, urban food⁴ and water demand workflows (Bao et al. 2020b) were developed in SimStadt, including socio-economic factors, i.e., income, age, human development index, etc. While biomass in urban areas might not provide substantial amounts of bioenergy to local consumers, the example of green roof with PV modules is used to assess exemplarily the energetic impact and economic feasibility of urban biomass on the roof PV yield and heating demand (Weiler et al.

⁴ Not published yet.

2019), which are simulated by existing and well-validated workflows in SimStadt, using the same geoinformatics input data.⁵

3.3.2 FWE Land Use Simulator: A tool to simulate urban growth induced land use change and impacts to Food, Water and Energy

The FWE Land Use Simulator was built using UD_InfraSim. This simulation platform enables urban planners to estimate the impact of urban development, urban growth, infrastructure costs, for example, for road and water networks, in relation to changes in land use (growth patterns) in the urban region (Gebetsroither-Geringer et al., 2015). It is built upon earlier 'urban development simulation tools' (Gebetsroither-Geringer and Loibl, 2007; Gebetsroither, 2009; Gebetsroither and Loibl, 2014). Within the IN-SOURCE project, the simulation platform was used, adapted and extended to build the FWE Land Use Simulator. This FWE Land Use Simulator enables, e.g., to explore the impact of urban growth scenarios on arable land and biomass production, the water demand and roughly estimate the renewable energy production potential from rooftop PV production.

3.3.3 HANPP and eHANPP environmental footprint indicator: visualisation of urban food production and global impacts of food consumption

We quantify urban land use intensities using HANPP (Human Appropriation of Net Primary Production) as environmental footprint indicator. HANPP measures the depth of human interventions into the biological productivity of ecosystems. Human appropriation of NPP occurs through land cover/use change (e.g., from forest to cropland, HANPP_{luc}) which alters ecological patterns and processes and through agricultural and forestry harvest, where biomass is removed from ecosystems (HANPP_{harv}). In IN-SOURCE HANPP was calculated for the city of Vienna and its food demand. The interactive website called “HANPP Explorer” shows a visualization of the urban food production and the global impacts of food consumption as well as the simulated impacts of dietary changes (Kaufmann et al., 2021).

4 THE CASE STUDY REGIONS

4.1 Low-density metropolitan region: County of Ludwigsburg

The administrative district of Ludwigsburg – County of Ludwigsburg – is a Southern German region of 687 square kilometres with 39 small to medium-sized cities. 540.000 inhabitants (786 per square kilometre) live in that district. The county stands for a growing metropolitan region adjacent to the Baden-Württemberg state capital of Stuttgart, including agricultural land.

The county governance seeks to speed up implementation of sustainable infrastructure such as maximum renewable supply, efficient wastewater treatment with sewage sludge to energy projects, treated effluent reuse for irrigation in agriculture, or a high regional food production ratio including food, green and forest waste to energy concepts. IN-SOURCE took up the ambitious climate protection plan of the county to support its implementation and demonstrate synergies in the food-water-energy sector. For this purpose, the potential of sustainable energies that can be used locally was analysed, e.g. the county-wide biomass utilisation potential, taking into account a good energy-food balance. In the area of wastewater, waste2power plays a role. By switching to CHP, the self-supply of electricity in waste water treatment plants can be increased to over 90%.

Further potentials lie in co-digestion and the decoupling of upgraded biogas as biomethane. In Ludwigsburg County, agricultural food production (still) plays a role and can cover the local food demand to a certain extent. Increased direct marketing and water reuse for irrigation in agriculture are other relevant topics.

4.2 Medium-density urban area: Vienna

Vienna represents a rapidly growing European capital with currently just under 2 million inhabitants. The city is pursuing an urban development plan (STEP), a climate protection plan and a smart city initiative. Urban planning faces the challenge of creating infrastructure and housing in a sustainable manner while maintaining a high quality of life. Economic and population growth induce changes in land use as well as

⁵ The workflows of roof PV potential and heating/electricity demand are developed in the project SimStadt 2.0 (03ET1459A) funded by BMWi.

energy, water and food consumption; in this context, the city government has a strong planning and regulatory role regarding water and energy supply and was therefore included in the stakeholder process. There are still a number of farms within the city limits, and initiatives to promote urban and vertical farming and food production are emerging and gaining public attention, therefore we invited stakeholders from NGOs as well.

The city of Vienna is a medium dense European city, where also a 3D CityGML model is available that was already in use for energy-related analyses (Skarbal et al., 2017). Within IN-SOURCE, the CityGML model, together with the CityGML FWE ADE and the FWE Land Use simulator, will analyse the consequences of land use change for biomass generation rooftop PV potential climate change adaptation and population growth (Padsala et al., 2021). Urban food production and biomass potentials (HANPP) and current food demand are analysed as well as global, international and national impacts of changes in dietary patterns (eHANPP) (Kaufmann et al., 2021).

4.3 High density urban area: New York City/Gowanus

The expanding and very dense city of New York faces challenges of a limited capacity urban infrastructure, particularly the electricity grid, and increasing needs to provide a resilient infrastructure for water and food supply. New York committed itself to reduce GHG emissions by 80% by 2050. This should be reached by transforming the energy system into a sustainable energy system with a reduced carbon footprint.

In New York, the district of Gowanus/Brooklyn was examined. The common data model based on the CityGML standard was used for modelling as in the European case studies.

Urban transformative change requires substantial changes in the supply system and affects the FWE system widely. Gowanus is to be restructured in a climate-neutral manner and is an example of a very densely populated urban district. The current industrial district will be rezoned to a combined residential and industrial area, increasing population. Due to the lack of arable land in the densely built area to grow food within the city, land cultivation will be limited, and the focus lies on the import of food and urban agriculture. In order to reduce the carbon footprint, NYC is investing in more efficient public transportation systems, other means of electric vehicles (scooters, bikes), ride sharing and vision zero NYC (safe streets for pedestrians). Efforts on improving the energy efficiency of large electricity consumers (subway systems, wastewater treatment plants, etc.) have been taken by the city.

5 STAKEHOLDER ENGAGEMENT

An important goal of the IN-SOURCE project was the involvement of stakeholders throughout the process. This meant first and foremost identifying the relevant stakeholders in each case study region, for example, administration/municipality representatives, urban planners, energy and water utilities, food producers and logistics companies, supermarket associations, food promoters, citizens and NGOs. A stakeholder mapping table was produced in order to get an overview. In addition, potential contact persons were evaluated in terms of their professional affiliation with the respective nexus elements and their possible influence on the project.



Fig.3: US and international experts at a cross-sectoral workshop held in December 2019 at the Center for Architecture in New York

A joint workshop design for all three case study regions, as initially foreseen, soon turned out to be not practicable. Each national team had to find a suitable form of co-operation. In the New York Gowanus district, a participation process was already initiated and mainly involved citizens, architects and urban planners (the Net Zero Neighborhoods project and Gowanus by Design, (<http://gowanusbydesign.org/>)). Another stakeholder co-creation process running in parallel focused on optimising wastewater treatment plants throughout the city and involved, among others, NYC Agencies and the Mayor's Office.

In Vienna, a stakeholder process was started with identifying relevant stakeholders from the city administration and planning offices, civil society organisations and NGOs. These were invited to a series of three half-day workshops (Smetschka 2020). The Vienna team developed a Causal Loop Diagram to discuss the FWE nexus and stimulating co-operation. After elaborating a set of challenges and visions, key factors were identified, and available data analysed. Scenarios for sustainable urban development addressing food, water and energy production and demand were developed in the second workshop. In the final third workshop, results from modelling, visualisations of these results and the tools employed during the research will be presented, and their usability for city administration will be evaluated.

In the German case study, stakeholder engagement suffered from the Covid pandemic. However, several consultation meetings were held to exchange mutual knowledge in wastewater treatment to enable the modelling of a wastewater treatment plant to identify flexibilities for the grid-serving operation of the power grid. In addition, virtual meetings are still planned to initiate stakeholder engagement in the County of Ludwigsburg, focusing on co-identifying and co-producing knowledge on varied elements of the urban FWE systems, which scenario simulations can now support.

Thus, in each local case study, stakeholders cooperate in developing a vision of how urban space and infrastructures should be designed, how FWE synergies can be optimised, renewables can best be integrated, and how population growth, land use changes and climate change challenges can be envisaged for future developments. Strategies and goals can be defined by converting these considerations into scenarios with key performance indicators (KPI), such as CO₂ emissions.

6 CONCLUSION

IN-SOURCE managed to develop a shared urban simulation toolbox and a single shared data framework for all three case study regions, which has a good replication potential for other cities and regions. Furthermore, the transferability of the shared urban modelling framework has been proved.

The stakeholder involvement helped to consider common urban and technological challenges in the three very different case studies. A joint workshop design was not feasible given the different stakeholder groups involved. However, a network of individuals with diverse professional backgrounds has been established, their visions and strategic planning skills pooled. With IN-SOURCE, an interesting learning process for stakeholders and researchers has begun.

7 REFERENCES

- Bao, K.; Padsala, R.; Coors, V.; Thrän, D.; Schröter, B. (2020a): A Method for Assessing Regional Bioenergy Potentials Based on GIS Data and a Dynamic Yield Simulation Model. In *Energies* 13 (24), p. 6488. DOI: 10.3390/en13246488.
- Bao, K.; Padsala, R.; Thrän, D.; Schröter, B. (2020b): Urban Water Demand Simulation in Residential and Non-Residential Buildings Based on a CityGML Data Model. In *IJGI* 9 (11), p. 642. DOI: 10.3390/ijgi9110642.
- FAO (2018): *The future of food and agriculture: Alternative pathways to 2050*. Rome.
- Hülsmann, S.; Ardakanian, R. (Eds.) (2018): *Managing Water, Soil and Waste Resources to Achieve Sustainable Development Goals. Monitoring and Implementation of Integrated Resources Management*. Cham: Springer International Publishing. Available online at <http://search.ebscohost.com/login.aspx?direct=true&scope=site&db=nlebk&AN=1792738>.
- Gebetsroither-Geringer, E.; and Loibl, W. (2015): *Urban Development and Infrastructure Cost Modelling for Managing Urban Growth in Latin American Cities*. https://www.corp.at/archive/CORP2015_120.pdf.
- Gebetsroither-Geringer, E.; Loibl, W. (2007): GIS-Based Water Resource Management of the Dead Sea Region – Integrating GIS, System Dynamics and Agent Based Modelling. In: Zeil, Peter; Kienberger, Stefan (eds.): *Geoinformation for Development: Bridging the Divide through Partnerships*. pp. 26-32, Heidelberg: Wichmann.
- Gebetsroither-Geringer, E. (2009): *Combining Multi-Agent Systems Modelling and System Dynamics Modelling in Theory and Practice*. Alpen-Adria Universität Klagenfurt: Fakultät für Technische Wissenschaften, p. 166, Klagenfurt.
- Gebetsroither-Geringer, E.; Loibl, W. (2014): *Urban Development Simulator: An interactive decision support tool for urban planners enabling citizen's participation*. RealCORP 2014. Proceedings, 749-756, Vienna.
- Kaufmann, L.; Smetschka, B.; Matej, S.; Erb, K.; Kozłowska, A.; Gebetsroither-Geringer, E (2021): *Urban land use and food supply: the example of Vienna*. RealCORP 2021. Proceedings, Vienna (Forthcoming).

- Nouvel, R.; Brassel, K.-H.; Bruse, M.; Duminil, E.; Coors, V.; Eicker, U. (2015): SimStadt, a new workflow-driven urban energy simulation platform for CityGML city models. In Proceedings of International Conference CISBAT 2015 Future Buildings and Districts Sustainability from Nano to Urban Scale. No. CONF. LESO-PB, EPFL.
- Padsala, R.; Fink, T.; Peters-Anders, J.; Gebetsroither-Geringer, E.; Coors, V. (2020). From Urban Design to Energy Simulation – a Data Conversion Process Bridging the Gap Between Two Domains. RealCORP 2020. Proceedings, Germany.
- Padsala, R.; Gebetsroither-Geringer, E.; Peters-Anders, J.; Coors, V. (2021): INCEPTION OF HARMONISING DATA SILOS AND URBAN SIMULATION TOOLS USING 3D CITY MODELS FOR SUSTAINABLE MANAGEMENT OF THE URBAN FOODWATER AND ENERGY RESOURCES. 6th International Conference on Smart Data and Smart Cities, Stuttgart, Germany (Forthcoming).
- Padsala, R.; Gebetsroither-Geringer, E.; Bao, K.; Coors, V. (2021): The Application of CityGML Food Water Energy ADE to Estimate the Biomass Potential for a Land Use Scenario. RealCORP 2021. Proceedings, Vienna (Forthcoming).
- Skarbal, B.; Peters-Anders, J.; Faizan Malik, A.; Agugiaro, G. (2017): HOW TO PINPOINT ENERGY-INEFFICIENT BUILDINGS? AN APPROACH BASED ON THE 3D CITY MODEL OF VIENNA, ISPRS Ann. Photogramm. Remote Sens. Spatial Inf. Sci., IV-4/W3, 71–78, <https://doi.org/10.5194/isprs-annals-IV-4-W3-71-2017>.
- Smetschka, B.; Gaube, V. (2020): Co-creating formalised models: Participatory modelling as method and process in transdisciplinary research and its impact potentials. Environ. Sci. Policy 103, 4149. <https://doi.org/10.1016/j.envsci.2019.10.005>.
- United Nations, Department of Economic and Social Affairs, Population Division (2019): World Urbanization Prospects: Final Report. The 2018 Revision. ST/ESA/SER.A/420. United Nations. New York.
- Weiler, V.; Stave, J.; Eicker, U. (2019): Renewable Energy Generation Scenarios Using 3D Urban Modeling Tools—Methodology for Heat Pump and Co-Generation Systems with Case Study Application. In Energies 12 (3), p. 403. DOI: 10.3390/en12030403.

Chapter 10

The Application of CityGML Food Water Energy ADE to Estimate the Biomass Potential for a Land Use Scenario

Padsala, R.; Gebetsroither-Geringer, E.; Bao, K.; Coors, V.

Proceedings of REAL CORP 2021, 26th International Conference on Urban Development, Regional Planning and Information Society. 2021, pp. 851-861. ISSN 2521-3938

The Application of CityGML Food Water Energy ADE to Estimate the Biomass Potential for a Land Use Scenario

Rushikesh Padsala, Ernst Gebetsroither-Geringer, Keyu Bao, Volker Coors

(M.Tech. Rushikesh Padsala, Hochschule für Technik Stuttgart, rushikesh.padsala@hft-stuttgart.de)

(M.Tech. Rushikesh Padsala, Concordia University Montreal, rushikesh.padsala@mail.concordia.ca)

(Dr. Ernst Gebetsroither-Geringer, AIT Austrian Institute of Technology GmbH, ernst.gebetsroither@ait.ac.at)

(M.Sc. Keyu Bao, Hochschule für Technik Stuttgart, keyu.bao@hft-stuttgart.de)

(Prof. Dr. Volker Coors, Hochschule für Technik Stuttgart, volker.coors@hft-stuttgart.de)

1 ABSTRACT

Cities are undergoing rapid urbanisation throughout the globe. A common challenge amongst them is to provide food, water, and energy (FWE) supplies under sustainable and economically productive conditions. As a result, new tools and techniques must be developed to support domain experts and decision-makers to understand, simulate and visualise the nexus impact on the sustainable supply of the FWE resources. A critical part of such a development process is to eliminate data silos and move towards an integrated FWE based data model, which can then be used to connect domain-specific urban simulation tools to simulate FWE nexus scenarios based on changes in landuse, population, and climatic conditions. This paper demonstrates the CityGML FWE Application Domain Extension (ADE) application as a central data exchange format to connect different urban simulation tools. First, it gives an insight into the ongoing development of the FWE ADE to the standardised open city information data model of CityGML. Secondly, it demonstrates the role of the CityGML FWE ADE in exchanging datasets between a FWE based landuse simulator built with UD_InfraSim and an urban energy simulator SimStadt to estimate the biomass potential for a landuse scenario of Vienna based on its future population and climatic changes.

Keywords: Data Modelling, 3D City Modelling, Food Water Energy ADE, CityGML, Food Water Energy Nexus

2 INTRODUCTION

Food, water, and energy (FWE) are critical for human survival. In the 21st century, cities across the globe are pressing for natural resources more than ever before. They are undergoing rapid urbanisation, and together with population growth and climate change, they are continuously challenged to provide FWE resources under healthy, sustainable and economically productive conditions. To help face such a challenge, solutions should not be proposed in their silos, as these three domains interact with each other. For example, according to an estimate¹ from the United Nations, by 2050, the world population will increase by 2 billion, entailing the global food production increase by 60%, which will require 40% more water and 50% more energy.² Such an increase in food production will demand more significant land, water, energy, or their combination. A critical challenge here would be finding a balance between the supply and demand of such critical urban infrastructures. Understanding and finding solutions within the individual domain silos of food, water, energy, land management, climate change would no longer be helpful. Thus new tools and techniques that can support domain experts and decision-makers to understand, analyse, and visualise the entire urban infrastructural system as a whole must be developed and prioritised.

The past decade has shown a rapid rise in the use of information and communication technology in sustainable urban development. Computer science and geo-informatics experts from both public and private sectors have developed many open and proprietary geospatial tools (e.g. ArcGIS, QGIS, ERDAS Imagine, GRASS GIS, and others), which provided new digital methods for city planning and decision making. Conventionally, a two-dimensional method of analysing the built environment has now been upgraded to three dimensions by developing the digital twins of cities. While geospatial tools and techniques allow users to generate and analyse geo-datasets, various urban simulation tools have also been developed to use geo-datasets to simulate different present and future built environment scenarios. With such a hand in hand development between geospatial technology and urban simulators, a commonly adopted and standardised city information model to store and exchange datasets related to different built environment objects (e.g. buildings, roads, vegetation, landuse, water bodies and others) became crucial for data interoperability

¹ <https://population.un.org/wpp/>

² <http://www.fao.org/news/story/en/item/275009/icode/>

between tools, domain experts and decision-makers. In 2008, the Open Geospatial Consortium (OGC) standardised and released an open city information data model called CityGML. CityGML is a commonly adopted standardised open city information data model, which has been used in more than 100 cities³ publicly or privately. Moreover, it offers flexibility to extend its original data model with domain-specific objects and attributes. Therefore, it shows promising signs for developing a CityGML based Food Water Energy Application Domain Extension (FWE ADE). The development process of the FWE ADE has been led by an international group of domain experts from the food, water, energy, urban design and geoinformatics domains as a part of IN-SOURCE (INtegrated analysis and modelling for the management of sustainable urban FEW Res-SOURCES) project (2018-2021). An integrated urban data model can become a vital software infrastructure for the planning, operation, and maintenance of present and future cities (Eicker et al. 2020). FWE ADE will not only allow FWE related data storage and exchange across different bottom-up or top-down urban simulation tools since it provides a data frame from building stocks to the regional level. But, it will also allow the domain experts and decision-makers to visualise the integrated FWE datasets driven by population, land use and climate change.

With this background, first in section 3, CityGML and its extension mechanism in developing the FWE ADE is explained in detail. Later as an example concept in section 4, the role of CityGML FWE ADE to connect the FWE land use simulator based on UD_InfraSim with an urban energy simulator SimStadt to estimate the biomass potential for a land use scenario in Vienna is documented. Having such a data exchange setup can allow connecting domain specific simulation tools to simulate FWE resources based on changed population, land use and climatic conditions.

3 SHARED DATA MODEL: CITYGML AND FWE ADE

3.1 CityGML and its Extension Mechanisms

CityGML is an XML-based open city information data model standardised by OGC in 2008. The encoding standard documentation⁴ for its last release, version 2.0, is available from the OGC website. The CityGML standard document uses Unified Modelling Language (UML) diagram and its XML schema definition (XSD) to describe data models, which explains how to model virtual 3D city models, also called CityObject, such as buildings, vegetations, land use, roads, bridges, tunnels, street furniture and water bodies in terms of their geometry, topology, semantics and appearance in five different Level of Details (LoD). For example, a building in CityGML can be represented as a 2D building footprint in LoD0, an extruded building block model in LoD1, while LoD2 includes additional roof geometries. Moreover, LoD3, in addition to LoD2, includes building openings, e.g. doors and windows, while LoD4, in addition to LoD3, also includes building interiors. Different use cases have shown the usefulness of CityGML globally with the development of various CityGML based tools and workflow pipelines. For example, its use in city planning (Agugiaro et al., 2020), disaster mapping (Kilsedar et al., 2019), urban energy demand (Padsala et al., 2020), urban water demand (Bao et al., 2020) and many such urban modelling and simulation related use cases.

CityGML is a domain independent city information data model. Hence it does not contain domain specific objects and attributes. However, CityGML offers two official ways to extend its original data model 1) generics and 2) a formalised mechanism to develop domain specific extensions called Application Domain Extension (ADE). Generics, which can also be called “CityGML extension during the run time”, is the easiest way to extend the original data model of CityGML. Using generics, users can add an arbitrary number of extra attributes, known as genericAttribute, to any CityObject without preparing a new data model or its application schema. Users can also define a new CityObject known as genericCityObjects, which can have arbitrary geometries with genericAttribute for its every LoD. Both genericAttribute and genericCityObjects are given an XML namespace of “gen” to differentiate themselves from the original XML namespace of CityObjects. XML namespaces are a set of unique element names which prevents conflicts between elements of the same name. For example, Bao et al. (2020a), in their biomass workflow of SimStadt, extended the CityGML CityObject of LandUse by adding land use area, soil type, crop type as some of the many other generic attributes for its later use in estimating biomass and its derived bio-energy for the counties of Ludwigsburg, Dithmarschen and Ilm-Kreis in Germany. Figure 1 shows a typical

³ <https://3d.bk.tudelft.nl/opendata/opencities/>

⁴ <https://www.ogc.org/standards/citygml>

workflow of adding genericAttributes or genericCityObjects using Feature Manipulation Engine (FME)⁵ to extend CityGML. FME is a commercial extract, transform and load (ETL) tool commonly used for data conversion, integration and manipulation.

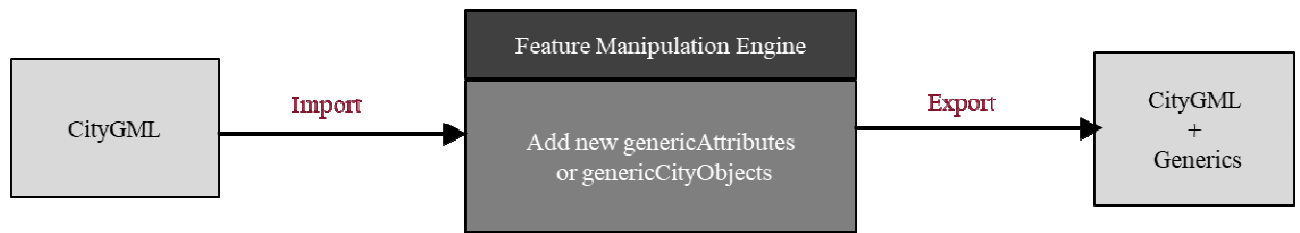


Fig. 1: A typical workflow to extend CityGML with generics using FME

On the other hand, application Domain Extension, or ADE, is a formalised way to extend the CityGML data model for a specific domain. Like generics, ADE is also an extension mechanism to CityGML for introducing domain-specific objects and attributes, which is often the case as specific applications require specific objects, attributes, and relationships that are not available in the original data model of CityGML. However, unlike generics, which 1) does not change the original CityGML XML schema, 2) have the same XML namespace and 3) can be specified at run time, ADEs 1) can change the original CityGML XML schema with domain specific new objects, attributes and relationships, 2) must have ADE specific unique XML namespaces to allow using multiple ADEs and prevent conflicts amongst the same CityGML document and 3) must be specified using UML diagrams or XSD. Such advantages over generics allow domain experts to adopt ADEs as a commonly adopted data model to support specific domains and applications. Though initially, using XSD as the only way to model ADEs was described in the CityGML encoding standard, van den Brink et al. (2012), in their article and later, OGC in their CityGML best practise document (OGC, 2014), described modelling an ADE using UML diagrams. Since then, a commonly adopted process to implement an ADE includes 1) Using software such as Enterprise Architect⁶ (EA) to create a UML diagram to represent a data model 2) converting UML diagram to XSD either using EA's inbuilt XSD converter or open source tool such as ShapeChange⁷ and 3) validate the ADE injected CityGML document against the original XSD of CityGML using tools such as FME validator, val3dity⁸, CityDoctor⁹. Validation will make sure that it satisfies the CityGML's standardised specifications and definitions set by the OGC. Figure 2 explains a typical ADE implementation workflow using FME.

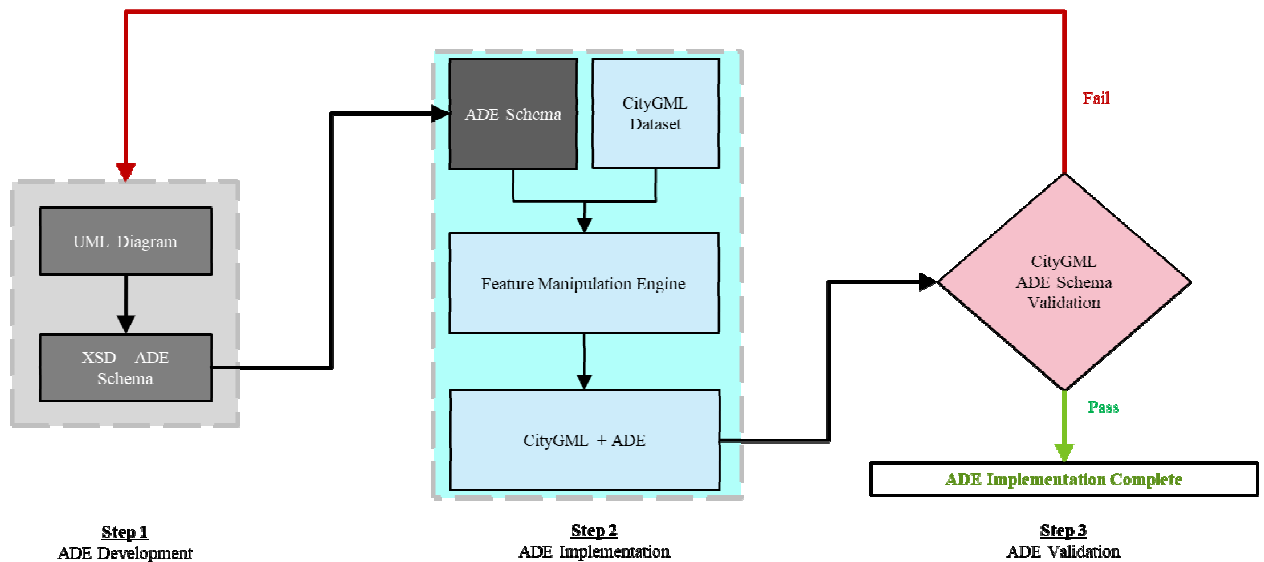


Fig. 2: A typical workflow to extend CityGML with ADE using FME

⁵ <https://www.safe.com/>

⁶ <https://sparxsystems.com/>

⁷ <https://shapechange.net/>

⁸ <https://github.com/tudelft3d/val3dity>

⁹ <https://projekt.beuth-hochschule.de/citydoctor2/>

Because with ADEs, a formalised domain specific objects, attributes, and relationships can be modelled, it is commonly used amongst the domain experts to store and exchange their datasets amongst different tools and simulation workflows. Biljecki et al. (2018) found that until 2018, around 44 ADEs supported a wide range of domains and applications. Some of the regularly used ADEs are Energy ADE (Agugiario, 2018) and its use in building stock energy demand simulations (Geiger et al., 2019; Rossknecht and Airaksinen, 2020), Utility Network ADE (Becker et al., 2011) and its use in modelling below ground utility networks (Duijin et al., 2018; Fossatti et al., 2020), Noise ADE (Groger et al., 2012) and its use in noise mapping (Czerwinski et al., 2006; Kumar et al. 2017) and Dynamizer ADE (Chaturvedi et al., 2015) to store time dependent variables in CityGML (Chaturvedi et al., 2019; Chatzinikolaou et al., 2020). However, despite different ADEs supporting different individual domains, a single integrated data model supporting multiple domains such as food, water, and energy, that can be used for FWE nexus related simulations is still missing. Hence, as one of the IN-SOURCE project outcomes, a new FWE ADE is under constant development. Its first version extending the CityGML version 2.0 was recently made available using the project's GitLab page.¹⁰

3.2 The CityGML Food Water Energy ADE

In its current version, the FWE ADE is divided into four modules, each representing a spatial level 1) FWEBuilding, 2) FWELanduse, 3) FWEArea, and 4) FWESystem. FWEBuilding targets building stock level and extends the original CityGML CityObject of Buildings with FWE related parameters. FWELanduse targets land use polygons representing land use (e.g. residential, commercial, vegetation) and extends the original CityGML CityObject of LandUse with FWE related parameters. Finally, FWEArea and FWESystem are introduced as two new CityObjects with multi-surface geometry in the CityGML data model to store FWE related parameters at administrative boundaries. A multi-surface geometry is a two dimensional geometry collection of surfaces representing a feature boundary. Using multi-surface geometries, FWEArea represents zonal or municipality boundaries, FWESystem represents city or regional level boundary. Two main reasons behind dividing FWE ADE into these four modules are 1) to cover different spatial level of any study area as shown in figure 3 and 2) to introduce FWE parameters specific to a spatial level that might not be available on other spatial levels.

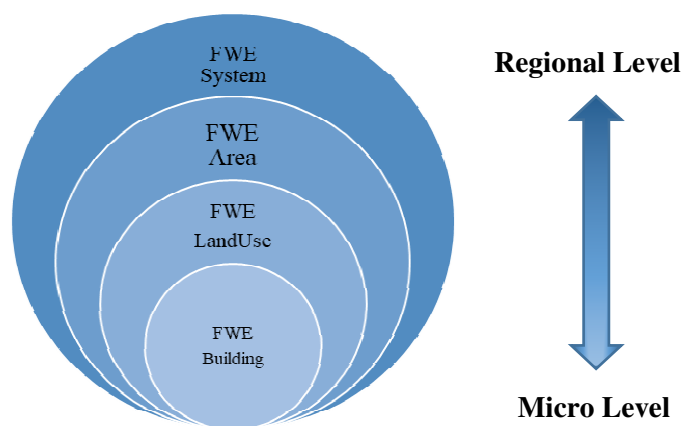


Fig. 3: A conceptual diagram showing the FWE ADE at different spatial levels

The complete documentation of FWE ADE, UML diagrams and its XSD schemas are available through the project's GitLab page as referenced before. In the context of this paper, because the biomass workflow of SimStadt using the CityGML CityObject of LandUse as its input, the FWELanduse module is explained further.

As mentioned before, the FWELanduse module is an extension to the CityGML CityObject of LandUse. CityGML LandUse is defined as a multi-surface geometry describing areas of land dedicated to a specific use. To indicate land use attributes, class, function, and use are already part of the CityGML LandUse data model. While the class attribute is used to classify land use objects, like settlement area, vegetation, water body etc., the attribute function defines the nature of the land use object, e.g. residential, commercial, institutional etc. The attribute use can be used for more detailed classification such as single-family houses, multi-family houses, hospitals, schools, etc. As an extension to the CityGML LandUse data model, FWE

¹⁰ <https://transfer.hft-stuttgart.de/gitlab/in-source/fwe-ade>

related parameters such as population, survey year, land use area, crop type, soil type, irrigation demand, transpiration loss, biomass primary energy potential are introduced as a part of new FWELanduse objects for CityGML LandUse CityObject. These new parameters, along with the CityGML LandUse geometry, are required as an input to the SimStadt's biomass workflow.

4 FWE ADE APPLICATION: BIOMASSPOTENTIAL FOR A LAND USE CHANGE SCENARIO

In the following section, as an example concept showcasing the role of FWE ADE in connecting two different urban simulator tools to achieve a data flow amongst them is explained in detail. A high level workflow of the data exchange setup between UD_InfraSim and SimStadt via FWE ADE capsulated inside 3DCityDB is shown in figure 4.

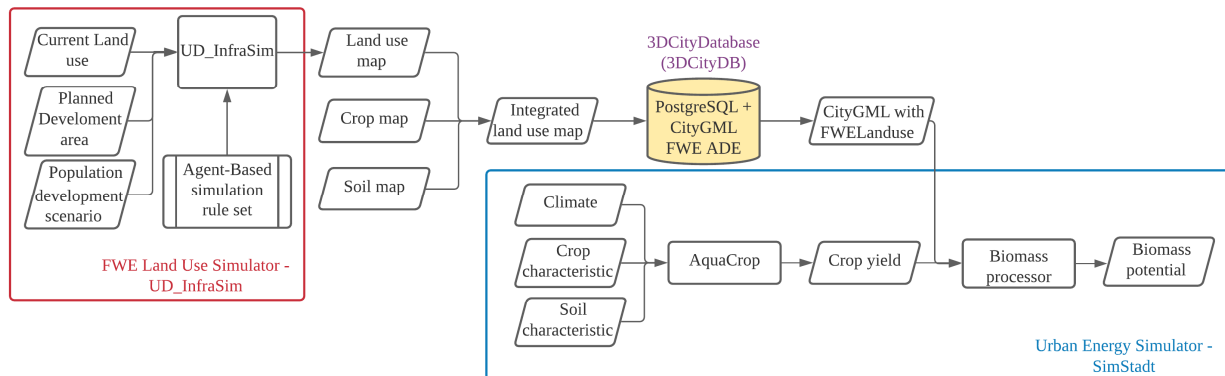


Fig. 4: Workflow Diagram

4.1 UD_InfraSim and its FWE Land Use Simulator

The UD_InfraSim is a simulation platform that enables urban planners to estimate the impact of infrastructure costs, for example, for road and water networks, in relation to changes in land uses (growth patterns) in the urban region¹¹ (Gebetsroither-Geringer et al., 2015). It is built upon earlier 'urban development simulation tools' (Gebetsroither-Geringer and Loibl, 2007; Gebetsroither, 2009; Gebetsroither and Loibl, 2014). Within the IN-SOURCEproject, the simulation platform was used, adapted and extended to build the FWE Land Use Simulator¹².

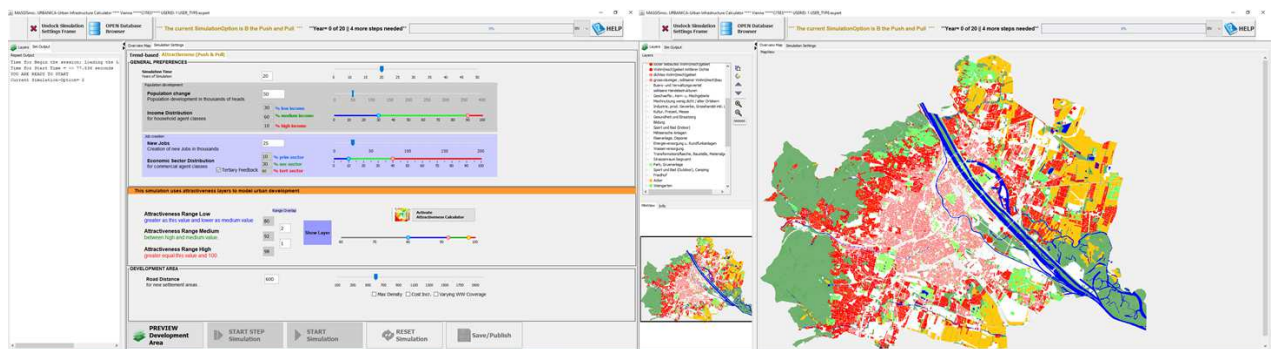


Fig. 6: Screenshot of the FWE Land Use Simulator

Different data sources have been used for the case study in Vienna. For example, open government data regarding the current land use in Vienna and remote sensing data for crop type classification to derive the spatial crop distribution for different crop types (Vuolo et al., 2018). For the biomass calculation with Aqua Crop, the soil type was needed, which was gained from BFW.¹³ Using the FWELand Use Simulator, the current and a scenario for future land use were simulated. For the future land use scenario, an additional population of 150,000 new inhabitants in Vienna was assumed. The scenario also uses information about the future development plan of Vienna to estimate the loss of arable land due to new settlements and the

¹¹ <https://www.ait.ac.at/en/research-topics/digital-resilient-cities/projects/ud-infrasim>

¹² <https://drc.ait.ac.at/sites/insource/fwe-land-use-simulator/>

¹³ digital soil map, the 1km raster data set is open source and can be downloaded here <https://bodenkarte.at/>

corresponding loss of biomass. This assumed population increase is lower than the official prognosis show¹⁴, but as it is assumed that the growth concentrates on the already planned new development areas in Vienna, it is reasonable. The chosen scenario frameconditions depict just one possible city development pathway. However, in the context of this paper, it is not necessary to derive the most likely development scenario as the goal of the paper is to demonstrate the concept of connecting different domain specific tools using CityGML FWE ADE. As a final output from the UD_InfraSim based FWE land use simulator, an integrated map showing the land use scenario merged with crop type, and soil type dataset is produced in the shapefile data format. Using FME, shapefile is converted to the CityGML LandUse dataset, which is then imported to 3DCityDB.

4.2 3DCityDB and its connection to FWE ADE

3D City Database or 3DCityDB is an open source software to store, manage, analyse and visualise CityGML datasets (Yao et al., 2018). It is built on top of spatial relational database management system Oracle Spatial/Locator or PostgreSQL with PostGIS. For the present work, 3DCityDB with PostgreSQL is used. It consists of SQL scripts that comply with the CityGML standards to generate required database tables, functions, procedures and views that allow users to store, manage and query CityGML datasets in PostgreSQL. For easy operation of 3DCityDB, a free importer/Exporter tool for 3DCityDB is also distributed as a part of the 3DCityDB package. Importer/Export tool is available in both graphical user interface and command line interface version. Apart from allowing users to import, manage, query and export CityGML datasets, the tool also allows users to export their CityGML datasets to other data formats such as KML, COLLADA and glTF, which are some of the commonly used data formats to visualise 3D city models on the web using digital globes. The complete list of its functionalities, along with its source code and documentation, is available on their GitHub¹⁵ page. An important feature of the tool used in the present work is its ADE manager plugin. Using the ADE manager plugin, new database tables related to the FWELanduse module of the FWE ADE and its required operational SQL syntax, also called Data Definition Language (DDL) statements, could be generated automatically. The DDL statements are required to define the data structure and modify the datasets inside PostgreSQL. By default, 3DCityDB does not allow importing and exporting CityGML datasets enriched with ADEs. Hence, two custom FWE ADE based java modules, 1) citygml4j and 2) ADE specific importer-exporter extension for 3DCityDB, are in development. While citygml4j will be used by the Importer/Exporter tool to parse and write ADE specific CityGML datasets, the ADE specific importer-exporter extension will be used to read and write datasets to ADE tables in the PostgreSQL/3DCityDB. An example implementation to develop such ADE specific importer/exporters to 3DCityDB is available on its GitHub¹⁶ page. Figure 7 shows a typical workflow for importing, managing and exporting FWE ADE enriched CityGML datasets in 3DCityDB.

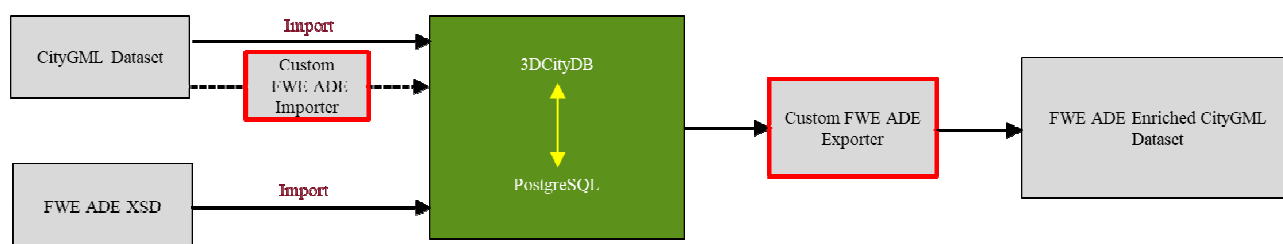


Fig. 7: 3DCityDB's FWE ADE Importer/Exporter workflow

After importing the CityGML LandUse scenario map from UD_InfraSim to 3DCityDB, an internal mapping of the required FWE parameters of land use polygon area, crop type, soil type was made between the imported CityGML LandUse datasets converted from the UD_InfraSim's integrated land use map and the FWELanduse ADE schema using SQL scripts in PostgreSQL. With this, the imported CityGML land use data is made to comply with the FWE ADE's module of FWELanduse and exported as an FWE ADE enriched CityGML LandUse dataset. This dataset is then used as an input to SimStadt's biomass workflow.

¹⁴ <https://www.wien.gv.at/statistik/bevoelkerung/tabellen/bev-2048.html>

¹⁵ <https://github.com/3dcitydb>

¹⁶ <https://github.com/3dcitydb/extension-test-ade>

4.3 SimStadt and its BiomassWorkflow

The assessment of energetic biomass potentials from agriculture is based on an existing biomass workflow that has been introduced before in section 3.1, validated, and applied at the example of three German counties as case studies. The workflow was reconfigured from accepting inputs using genericAttributes to complying with the FWE ADE schema. The workflow is now compatible with and transferable to other regions, as long as (i) land use information was provided under FWE ADE schemain CityGML format, (ii) information on new land use/crop types is available and is added to an existing SimStadt's XML library and (iii) the new crop/soil types are described and written in standard inputs crop/soil files for the yield simulation software AquaCrop (Raes, 2016). The workflow is part of a versatile regional energy system modelling environment, SimStadt¹⁷, that aims to compare different renewable energy resource potentials and contrasts these with local energetic demands in a given region. SimStadt, which is under constant development at HfT Stuttgart since 2012 (Nouvel et al., 2015), comprises modular workflow management, with each workflow serving a specific purpose. To date, it can assess building-related demands (cooling and heating (Weiler et al., 2019), residential electricity (Kohler et al., 2010), water (Bao et al., 2020b) and renewable energy potentials (rooftop photovoltaics (RomeroRodriguez et al., 2017) and biomass (Bao et al., 2020c) on a single-building or single-field level using 3D city models or digital landscape models in the CityGML format.

For the biomass workflow, a key input is the FWE ADE's FWELanduse enrichedCityGMLLandUse object having multi-surface geometries. Besides geometric and attribute data from the FWE ADE, meteorological data of Vienna's current climate, i.e. the average over the past 10 years, and forecasted climate data in 2040 in TMY3¹⁸ format, was provided by Meteonorm¹⁹.

To calculate the biomass yield based on local climate, soil characteristics, land management pattern, and irrigation pattern for most crops, a validated external crop yield and water simulation tool named AquaCrop, developed by the Food and Agriculture Organization of the United Nations (FAO, 2018) was integrated with SimStadt. The key characteristics of the crop and soil files that were generated as inputs for AquaCrop were collected based on statistical literature values (KTBL, 2018). The specific yields in fresh mass (t_{FM}/ha/yr) of selected key crop types under average climate between 2000 and 2010 were validated with the statistical yield in 2015 and 2016 from the Vienna Agriculture Report (Wiener Landwirtschaftsbericht, 2017). The specific yield resulting from biomass workflow is based on the dry mass of the above-ground biomass. To compare with the fresh yield from the Vienna Agriculture Report, the harvest rate and water content (KTBL, 2018) were applied to convert the dry mass to fresh mass. The validation result is shown in table 1.

Crop type	Specific yield in t _{FM} /ha/yr		Area in ha	
	Simulation	Statistic	Simulation	Statistic
Maize	7.0	6.8 - 8.4	293	121 - 138
Potato	28.1	43.4 - 26.5	84	66 - 88
Soybean	3.1	1.5 - 2.2	132	54 - 81
Sugar beet	48.9	65.1 - 76.7	254	219 - 230
Sunflower	3.1	2.5 - 2.8	189	11 - 21
Wheat	5.8	4.9 - 4.4	2776	2172 - 2200

Table 1: Areas and specific yields of selected crops from simulation and literature.

Table 1 shows that the area allocation of potato and sugarbeet aligns with the statistical values. However, for sunflower that occupied less than 0.4 % of the agricultural area, the difference of area between simulation and statistic can be up to 17 times, as a part of the polygons were either overlooked or misplaced due to the limitation of the method of satellite image recognition (Vuolo et al., 2018). For the main crop type, i.e., wheat, the deviation is less than 10 %. At the aspect of specific yield, the error of the input map was isolated; only the accuracy of the biomass workflow was shown. According to table 1, the yields of most crops fall within the range from the statistic, except for sugar beet and wheat. The crop map did not differentiate the

¹⁷ <https://simstadt.hft-stuttgart.de/de/index.jsp>

¹⁸ <https://www.nrel.gov/docs/fy08osti/43156.pdf>

¹⁹ <https://meteonorm.com/>

subtypes of wheat; therefore, winter cereal was applied to represent the family. The statistical yield of winter cereal was 5.5 to 6.3 tFM/ha/yr compared with the simulation result of 5.8 tFM/ha/yr, verifying the yield simulation result. As for sugar beet, the deviation might be brought by the inaccurate crop characters input for AquaCrop. Therefore, the standard sugar beet growing characteristic combined with the typical growing period in Vienna was applied, which might bring the yield difference.

4.4 Application Results

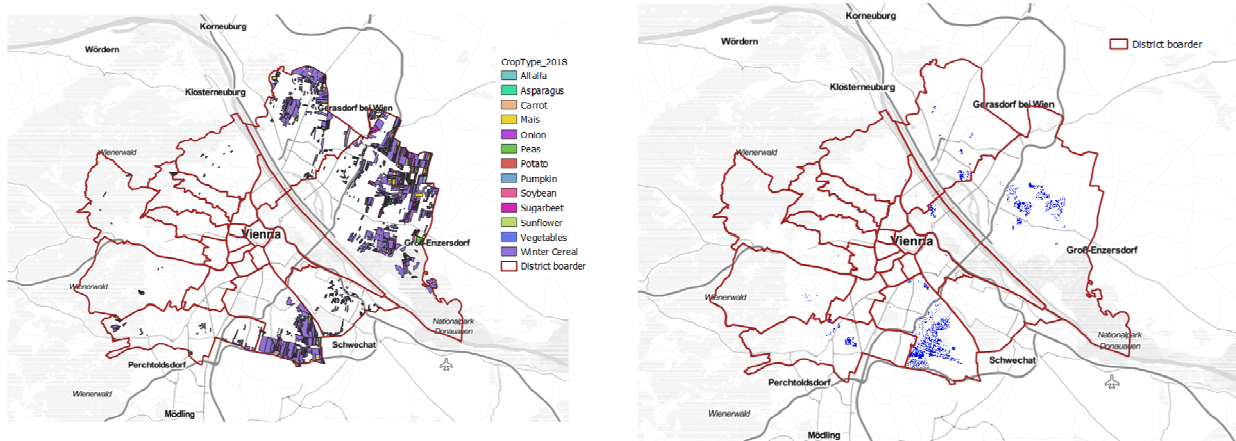


Fig. 8: Crop map 2018 depicted from remote sensing (left image) and a future settlement scenario 2038 (right image)

Figure 8 shows the crop distribution map gained from remote sensing on the left side and a population growth scenario within the next 20 years on the right side. The images show that, especially in the south and northeast of Vienna, arable land and thus crop biomass production is affected. In this scenario, the destruction of arable land is not extreme because many of the planned new development areas already are not anymore used for agriculture, and it was assumed that the population density for new settlements is relatively high.

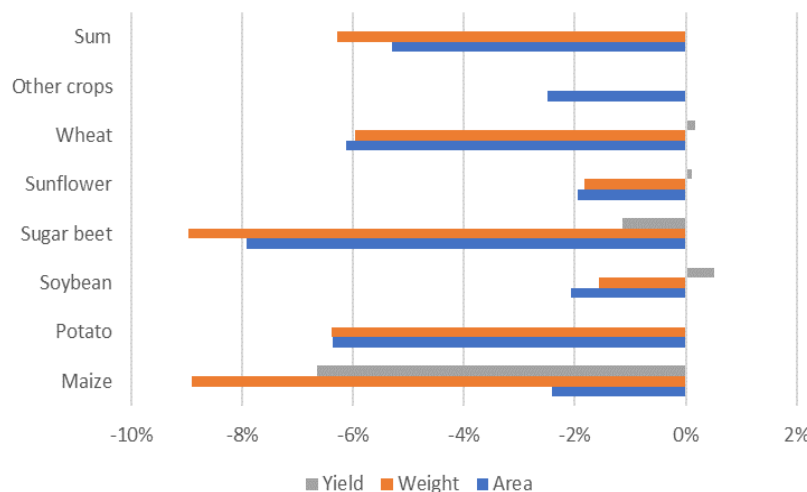


Fig. 9: Percentage change of area, weight, and yield of selected crops in the current scenario and 2038 scenario.

Figure 9 shows the development of the agricultural area, the amount of biomass produced, and the specific yield of several crop types. Climate difference, i.e., the annual average temperature dropped from 11.8 °C to 11.6 °C, and precipitation increased from 608 mm/yr to 618 mm/yr, influenced specific yields to various extents depending on the crop types. Maize acted most negatively to the climate change with a yield drop of 6.7 % following by sugar beet with -1.2%. For other crops, i.e., potato, soybean, sunflower, and wheat, the yield increase by 0.5 %. In the term of the total agricultural area according to the scenario setting of the FWE land use simulator, there would be 2.1% to 7.9 % less land for crop growing in 2038 comparing with the current case (2018). The most significant area decreases were estimated for sugarbeet (7.9 %) and wheat (6.1 %). Even though few crops would be more productive, i.e., up to 0.5 %, under the 2040 climate, combined

with the more significant drop of the agricultural areas, the total biomass weight was estimated to drop from 1.6 % to 9 % varying from crop types.

5 CONCLUSION

This paper introduces the concept of data exchange between two simulation tools in two domains using a shared FWE ADE extended from the standardised open city information data model of CityGML. Unlike the generic extension method of CityGML, which cannot have a formal data structure or schema, a full ADE can be formally specified, has a well-defined data structure, and its realisation can be validated against its schema, which is not possible with generic attributes and objects. Translating the use of ADE in a complicated real life application involving several domain specific tools, an ADE can provide a well structured data framework to store and exchange datasets between different tools. Moreover, CityGML being a city information model and ADE being its domain specific extension mechanism was proved to be very helpful in translating integrated urban infrastructural systems such as the FWE nexus domain to an object oriented data model. Such an integrated data model provides data interoperability between different urban simulation tools in the FWE nexus domains and helps develop simulation workflows that can analyse the entire urban infrastructural system as a whole and not just in their silos.

In terms of spatial and temporal detail levels, FWE ADE defined data at different spatial levels, i.e., building stocks, land field, community, or region, and additionally introduced time as a variable, i.e., the value of an attribute in a specific year. In the context of this paper, due to the fine spatial resolution down to land use polygons, bottom-up simulation tools can directly take geographical inputs or store outputs at the corresponding level achieving a high level of data accuracy and detail. For example, with such information, a trade-off between an open-field PV system and food production can be determined according to the potential simulation results. The top-down analysis method can also find inputs through the FWE ADE, i.e., by aggregating the values of land field polygons in the study region and store output at the regional level. The temporal variable enables the FWE ADE to present the changes in attributes over a certain period, i.e., the yield change in 10 years due to climate change.

Within the application of linking two tools addressing different issues within the FWE nexus, the proposed FWE ADE also proved its usefulness. UD_InfraSim simulated the land use change, i.e., the expansion of residential area at the expense of arable lands. A workflow from SimStadt simulated the biomass potential of arable lands. The accuracy of the final results was defined by several factors, including the quality of the crop distribution map, the crop rotation, and the yield simulation tool. The nature of seasonal and annual agriculture rotation makes it difficult to estimate the exact crop distribution. Regardless, the decentralised crop map (with a resolution of 5 m) and soil distribution map (with a resolution of 200 m) served as the input of FWE ADE, later applied in the FWE Land Use Simulator and the bottom-up biomass workflow in SimStadt. The geographical resolution in the presented application is 25 meters. As already mentioned above, the elaborated scenario is just one possible scenario of how Vienna can develop based on “forecasted” frame conditions, i.e., government policies, forecasted population growth and climate change. The established connection can be used to easily calculate other development scenarios. It enables urban planners and sustainability experts to compare future land use scenarios and evaluate its effect on the biomass potential to find scenarios with less reduction in the region’s biomass production. Furthermore, it supports spatial energy planning to estimate the renewable bioenergy production potential in the region to increase the local share of renewable energy supply.

6 ACKNOWLEDGEMENTS

This paper is part of the IN-SOURCE (INtegrated analysis and modelling for the management of sustainable urban FEW Res-SOURCES) project. The IN-SOURCE project is funded from the European Union’s Horizon 2020 research and innovation program under grant agreement No 730254. We want to give our acknowledgements to the JPI Urban Europe, the Belmont Forum, the Federal Ministry of Education and Research – BMBF Germany and the Federal Ministry Republic of Austria Climate Action, Environment, Energy, Mobility, Innovation and Technology (BMK) for their financial support to the project IN-SOURCE. We would also like to thank our international IN-SOURCE project partners from the USA, New York Institute of Technology (NYIT), the City University of New York (CUNY) and Prof. Dr. Ursula Eicker from Concordia University, Montreal, Canada, for their continued help and support. We would also like to

acknowledge Matthias Betz and Dr. Preston Francisco Rodrigues from Hochschule für Technik Stuttgart for knowledge sharing and the first development of FWE ADE specific citygml4j. A special thanks to Dr. Claus Nagel and Dr. Zhihang Yao from Virtual City Systems GmbH, Berlin for conducting a hands-on workshop on the development of ADE specific importer-exporter extension for 3DCityDB.

7 REFERENCES

- Agugiaro, G., Benner, J., Cipriano, P. et al.: The Energy Application Domain Extension for CityGML: enhancing interoperability for urban energy simulations. *Open geospatial data, softw. stand.* 3, 2. <https://doi.org/10.1186/s40965-018-0042-y>, 2018.
- Agugiaro, G., García G., Francisco G., and Cavallo, R.: The City of Tomorrow from... the Data of Today. *International Journal of Geo-Information*, 9. <https://doi.org/10.3390/ijgi9090554>, 2020.
- Bao, K., Padsala, R., Coors, V., Thrän, D., and Schröter, B.: GIS-Based Assessment of Regional Biomass Potentials at the Example of Two Counties In Germany. <https://doi.org/10.5071/28thEUBCE2020-1CV.4.15>, 2020.
- Bao, K., Padsala, R., Coors, V., Thrän, D., and Schröter, B.: A Method for Assessing Regional Bioenergy Potentials Based on GIS Data and a Dynamic Yield Simulation Model. *Energies*. 13. <https://doi.org/10.3390/en13246488>, 2020.
- Bao, K., Padsala, R., Thrän, D., Schröter, B.: Urban Water Demand Simulation in Residential and Non-Residential Buildings Based on a CityGML Data Model. *ISPRS Int. J. Geo-Inf.*, 9, 642. <https://doi.org/10.3390/ijgi9110642>, 2020.
- Becker, T., Nagel, C. & Kolbe, T.H.: Integrated 3D Modeling of Multi-utility Networks and Their Interdependencies for Critical Infrastructure Analysis. <https://mediatum.ub.tum.de/doc/1145740/1145740.pdf>, 2011.
- Biljecki, F., Kumar, K., and Nagel, C.: CityGML Application Domain Extension (ADE): overview of developments. *Open Geospatial Data, Software and Standards*. 3. 13. <https://doi.org/10.1186/s40965-018-0055-6>, 2018.
- Chaturvedi, K. and T. H. Kolbe.: Dynamizers - Modeling and Implementing Dynamic Properties for Semantic 3D City Models. *Eurographics Workshop on Urban Data Modelling and Visualisation Workshop*. <https://dx.doi.org/10.2312/udmv.20151348>, 2015.
- Chaturvedi, K., Yao, Z., and Kolbe, T.: INTEGRATED MANAGEMENT AND VISUALISATION OF STATIC AND DYNAMIC PROPERTIES OF SEMANTIC 3D CITY MODELS. *ISPRS - International Archives of the Photogrammetry, Remote Sensing and Spatial Information Sciences*. XLII-4/W17. 7-14. <https://doi.org/10.5194/isprs-archives-XLII-4-W17-7-2019>, 2019.
- Chatzinikolaou, E., Pispidikis, I., and Dimopoulou, E.: A SEMANTICALLY ENRICHED AND WEB-BASED 3D ENERGY MODEL VISUALISATION AND RETRIEVAL FOR SMART BUILDING IMPLEMENTATION USING CITYGML AND DYNAMIZER ADE, *ISPRS Ann. Photogramm. Remote Sens. Spatial Inf. Sci.*, VI-4/W1-2020, 53–60. <https://doi.org/10.5194/isprs-annals-VI-4-W1-2020-53-2020>, 2020.
- Czerwinski, A., Kolbe, T. H., Plumer, L. and Stocker-Meier, E.: Interoperability and accuracy requirements for EU environmental noise mapping. In: H. Kremers and V. Tikunov (eds), *International Conference on GIS and Sustainable Development (InterCarto – InterGIS 12)*, Berlin, Germany, pp. 182–194. <https://api.semanticscholar.org/CorpusID:2222165>, 2006.
- den Duijn, X., Agugiaro, G., and Zlatanova, S.: MODELLING BELOW- AND ABOVE-GROUND UTILITY NETWORK FEATURES WITH THE CITYGML UTILITY NETWORK ADE: EXPERIENCES FROM ROTTERDAM, *ISPRS Ann. Photogramm. Remote Sens. Spatial Inf. Sci.*, IV-4/W7, 43–50. <https://doi.org/10.5194/isprs-annals-IV-4-W7-43-2018>, 2018.
- Eicker, U., Weiler, V., Schumacher, J., Braun, R.: On the design of an urban data and modeling platform and its application to urban district analyses. *Energy and Buildings*. <https://doi.org/10.1016/j.enbuild.2020.109954>, 2020.
- Fossatti, F., Agugiaro, G., Olde Scholtenhuis, L., Doree, A.: Data modeling for operation and maintenance of utility networks: Implementation and testing. *ISPRS Annals of Photogrammetry, Remote Sensing and Spatial Information Sciences*, 6 (4/W1), 69-76. <https://doi.org/10.5194/isprs-annals-VI-4-W1-2020-69-2020>, 2020.
- FAO: AquaCrop Reference Manual. <http://www.fao.org/publications/card/en/c/BR244E/>, 2018.
- FAO: AquaCrop Training Handbook. <https://www.fao.org/aquacrop/software/aquacropstandardwindowsprogramme/en/>, 2018.
- Gebetsroither-Geringer, E., and Loibl, W.: Urban Development and Infrastructure Cost Modelling for Managing Urban Growth in Latin American Cities. https://www.corp.at/archive/CORP2015_120.pdf, 2015.
- Gebetsroither-Geringer, E., Loibl, W.: GIS-Based Water Resource Management of the Dead Sea Region – Integrating GIS, System Dynamics and Agent Based Modelling. In: Zeil, Peter; Kienberger, Stefan (eds.): *Geoinformation for Development: Bridging the Divide through Partnerships*. pp. 26-32, Heidelberg: Wichmann, 2007.
- Gebetsroither-Geringer, E.: Combining Multi-Agent Systems Modelling and System Dynamics Modelling in Theory and Practice. *Alpen-Adria Universität Klagenfurt: Fakultät für Technische Wissenschaften*, p. 166, Klagenfurt, 2009.
- Gebetsroither-Geringer, E., Loibl, W.: Urban Development Simulator: An interactive decision support tool for urban planners enabling citizen's participation. *RealCORP 2014. Proceedings*, 749-756, Vienna, 2014.
- Groger, G., Kolbe, T. H., Nagel, C. and Hafele, K.-H.: OGC City Geography Markup Language (CityGML) Encoding Standard version 2.0.0. https://portal.ogc.org/files/?artifact_id=47842, 2012.
- Geiger, A., Joachim, B., Häfele, K., Hagenmeyer, V.: Building Energy Simulations at Urban Scale Based on Standardized Data Models Using a Transparent Enrichment Process. 3202-3208. <https://doi.org/10.26868/25222708.2019.210250>, 2019.
- Kilsedar, C., Fissore, F., Pirrotti, F. and Brovelli, M. EXTRACTION AND VISUALISATION OF 3D BUILDING MODELS IN URBAN AREAS FOR FLOOD SIMULATION. XLII-2/W11. 669-673. <https://doi.org/10.5194/isprs-archives-XLII-2-W11-669-2019>, 2019.
- Kumar, K., Ledoux, H., Commandeur, T. J. F., and Stoter, J. E.: MODELLING URBAN NOISE IN CITYGML ADE: CASE OF THE NETHERLANDS, *ISPRS Ann. Photogramm. Remote Sens. Spatial Inf. Sci.*, IV-4/W5, 73–81. <https://doi.org/10.5194/isprs-annals-IV-4-W5-73-2017>, 2017.
- Köhler, S., Betz, M., Eicker, U.: Stochastic generation of household electricity load profiles in 15-minute resolution on building level for whole city quarters. *Energy Challenges for the Next Decade*, 16th IAEE European Conference, August 25-28, 2019. *International Association for Energy Economics*. <https://api.semanticscholar.org/CorpusID:211053294>, 2019.
- KTBL: General figures for agriculture. <https://www.ktbl.de/shop/produktkatalog/19523>, 2018.

- Nouvel, R., BRASSEL, K., BRUSE, M., Duminil, E., Coors, V., Eicker, U and Robinson, D.: SimStadt, a new workflow-driven urban energy simulation platform for CityGML city models. CISBAT 2015, EPFL, Lausanne, September 9-11th. <https://doi.org/10.5075/epfl-cisbat2015-889-894>, 2015.
- OGC.: Modeling an application domain extension of CityGML in UML (OGC Best Practice). OGC, Best Practice OGC 12-066. Open Geospatial Consortium. https://portal.ogc.org/files/?artifact_id=49000, 2014.
- Padsala, R., Theresa, F., Peters-Anders, J., Gebetsroither-Geringer, E., Coors, V.: From Urban Design to Energy Simulation – a Data Conversion Process Bridging the Gap Between Two Domains. Real CORP 2020. <https://doi.org/10.48494/REALCORP2020.1054>, 2020.
- Rossknecht, M. and Airaksinen, E.: Concept and Evaluation of Heating Demand Prediction Based on 3D City Models and the CityGML Energy ADE–Case Study Helsinki. ISPRS Int. J. Geo-Inf. 2020, 9, 602. <https://doi.org/10.3390/ijgi9100602>, 2020.
- Romero Rodriguez, L., Duminil, E., Jose Sanchez, R. and Eicker, U.: Assessment of the photovoltaic potential at urban level based on 3D city models: A case study and new methodological approach. Solar Energy. 146. 264-275. <https://doi.org/10.1016/j.solener.2017.02.043>, 2017.
- Weiler, V., Stave, J. and Eicker, U.: Renewable Energy Generation Scenarios Using 3D Urban Modeling Tools–Methodology for Heat Pump and Co-Generation Systems with Case Study Application †. Energies, 12, 403. <https://doi.org/10.3390/en12030403>, 2019.
- Yao, Z., Nagel, C., Kunde, F. et al.: 3DCityDB - a 3D geodatabase solution for the management, analysis, and visualisation of semantic 3D city models based on CityGML. Open geospatial data, softw. stand. 3, 5. <https://doi.org/10.1186/s40965-018-0046-7>, 2018.

Chapter 11

Bottom-Up Assessment of Local Agriculture, Forestry and Urban Waste Potentials Towards Energy Autonomy of Isolated Regions: Example of La Réunion

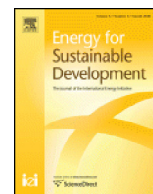
Bao, K.; Bieber, L.; Kürpick, S.; Radanielina, M.H.; Padsala, R.; Thrän, D.; Schröter, B.

Energy for Sustainable Development 2022, 66, 125. DOI: [10.1016/j.esd.2021.12.002](https://doi.org/10.1016/j.esd.2021.12.002)



Contents lists available at ScienceDirect

Energy for Sustainable Development



Bottom-up assessment of local agriculture, forestry and urban waste potentials towards energy autonomy of isolated regions: Example of Réunion☆



Keyu Bao ^{a,1,*}, Lisa-Marie Bieber ^{a,1}, Sandra Kürpick ^{a,1}, Mamy Harimisa Radanielina ^b, Rushikesh Padsala ^c, Daniela Thrän ^{d,e,f}, Bastian Schröter ^a

^a Center for Sustainable Energy Technology, Hochschule für Technik Stuttgart, Schellingstraße 24, 70174 Stuttgart, Germany

^b PIMENT Laboratory, University of La Réunion, 117 Rue Du General Ailleret, 97430 Le Tampon, Reunion

^c Center for Geodesy and Geoinformatics, Hochschule für Technik Stuttgart, Schellingstraße 24, 70174 Stuttgart, Germany

^d Department of Bioenergy, Helmholtz Center for Environmental Research, Torgauer Straße 116, 04247 Leipzig, Germany

^e Chair of Bioenergy System, Faculty of Economic Sciences, University of Leipzig, Grimmaische Straße 12, 04109 Leipzig, Germany

^f Unit Bioenergy System, German Biomass Research Center (DBFZ), Torgauer Straße 116, 04347 Leipzig, Germany

ARTICLE INFO

Article history:

Received 4 August 2021

Revised 17 September 2021

Accepted 2 December 2021

Available online 15 December 2021

Keywords:

Biomass potential simulation

Urban waste recycling

Sustainable energy system

Energy autonomy

ABSTRACT

This work assesses the role of biomass and municipal solid waste in isolated energy systems. For this, La Réunion, a French overseas territory in the Indian Ocean with a population of about 850,000, serves as a case study. Methodically, the study assesses technical biomass-based potentials based on an island-wide digital landscape model, detailed information on land use, soil, and climate, and a dynamic yield simulation tool, while technical waste-based energy potentials are calculated from local data. In total, 9 crops, 11 waste streams, and forested areas are considered. The potential contribution of biomass and waste to the energy system is studied in three scenarios. In all, unsustainable outcomes are avoided by valorizing only crop residues and applying sustainable harvesting rates to forests. Depending on the scenario, biomass or waste based energy could cover between 19% and 22% of 2019 electricity demand compared to an actual value of 6% (2019). Furthermore, prioritizing the production of secondary energy carriers allows to meet 8% of 2019 energy demand in the transport sector. These results are in good accordance with previous studies and scenarios on Réunion's energy transition. Given its bottom-up approach based on standard geoinformatic data, the proposed method is in principle transferable to other isolated regions, also in developing countries. A first, high-level assessment of four comparable island (states) shows that in three cases similar contributions of biomass and waste as in Réunion can be expected. As a next step, the purely technical assessment shall be complemented by economic considerations.

© 2021 The Authors. Published by Elsevier Inc. on behalf of International Energy Initiative. This is an open access article under the CC BY-NC-ND license (<http://creativecommons.org/licenses/by-nc-nd/4.0/>).

Introduction

Given their isolated location and clear boundary conditions, the sustainable development of oceanic islands is closely related to locally

☆ The work was funded by German Academic Exchange Service (DAAD) for B.S. short term lectureship stay (#91790676) at the University of La Réunion. The biomass simulation workflow was developed in the context of the INSOURCE project, funded by the European Union's Horizon 2020 research and innovation program under grant agreement No 730254.

* Corresponding author.

E-mail addresses: keyu.bao@hft-stuttgart.de (K. Bao),

lisa-marie.bieber@student-hfr.de (L.-M. Bieber), sandra.kuerpick@student-hfr.de

(S. Kürpick), mamy.radanielina@univ-reunion.fr (M.H. Radanielina),

rushikesh.padsala@hft-stuttgart.de (R. Padsala), daniela.thraen@ufz.de,

thraen@wifa.uni-leipzig.de, daniela.thraen@dbfz.de (D. Thrän),

bastian.schroeter@hft-stuttgart.de (B. Schröter).

¹ These three authors contribute equally to this paper.

available sources of renewable energy. In terms of energy supply, most islands in the European Union and other parts of the world depend on imports, mainly fossil fuels (Chen et al., 2007). The island of La Réunion (subsequently referred to as Réunion), a French overseas territory in the southern Indian Ocean, is no exception: in 2019, 87% of total primary energy demand was imported as fossil fuels, namely oil, diesel, coal (Réunion Island Energy Observatory, 2018).

Nevertheless, Réunion adopted a strategy for sustainable development in 2011 that aimed to achieve a 50% share of renewable energy (RE) in the electricity generation mix by 2020, to reduce the import volume of fossil fuels for the transport sector by 10% until 2020, and to move towards 100% local renewable electricity generation by 2030 (French Ministry of Ecological Transition, n.d.). Over the last decade, decision makers on Réunion have thus supported a range of renewable energy projects that intend to transform the island into a hub for new energy technologies. These projects, however, also highlighted the technological

<https://doi.org/10.1016/j.esd.2021.12.002>

0973-0826/© 2021 The Authors. Published by Elsevier Inc. on behalf of International Energy Initiative. This is an open access article under the CC BY-NC-ND license (<http://creativecommons.org/licenses/by-nc-nd/4.0/>).

and social risks associated with innovation and the possible lack of local returns. So, while the island had managed to attract innovative actors, well-proven technologies such as hydroelectricity, biomass, and solar power are currently driving renewable energy supply on the island, but are as yet not fully exploited (Sawatzky & Albrecht, 2017).

Globally, biomass satisfies 19% of total energy demand (Gielen et al., 2019). In developing countries, a high share of cooking and heating is based on biomass especially from woody fraction (Dasappa, 2011), although this trend declines as income increases (IEA, n.d.). As biomass is considered a renewable energy carrier, its conversion into electrical power, process heat and transportation fuels are well established today (O'Connor et al., 2021; Li et al., 2017). However, the limited availability of biomass in most regions and the lack of local guidelines have been highlighted as a constraint to energy development policies (Maltsoglou et al., 2015; Owen et al., 2013). On top of biomass, municipal solid waste (MSW) is another important source for local energy (Breeze, 2017; Grosso et al., 2010; Kumar & Samadder, 2017; Pichtel, 2005), with waste to energy (WtE) conversion technologies ranging from the well-proven (incineration) to novel approaches (plasma gasification) (Arena, 2012). However, a generally high moisture content of MSW and low budgets for MSW management mean that landfilling is still the dominant form of MSW treatment especially in developing countries (Ngoc & Schnitzer, 2009; Tun & Juchelková, 2018; Tun & Juchelkova, 2019).

To design sustainable energy systems in particular for isolated regions, it is important to understand local potentials and the available processes and technologies for exploiting these in detail. A range of studies investigated the technical feasibility of reaching high shares of renewable energy in isolated islands (Drouineau et al., 2015; Kalinci et al., 2015; Maïzi et al., 2018; Praene et al., 2012; Ricci et al., n.d.; Selosse et al., 2018; Biscaglia et al., 2019). For instance, (Kalinci et al., 2015) studied the role of hydrogen production and storage in a stand-alone hybrid energy system for a Turkish island. The proposed system included the renewable technologies of wind, photovoltaic (PV), and hydrogen without biomass and shows that local hydrogen production provides a storable and versatile energy vector. In contrast, (Chary et al., 2018) examined the import of biomass for energy production in comparison to the utilization of local resources using the example of Guadeloupe. For Réunion, (Praene et al., 2012) assessed the current local renewable resources utilization, as well as electricity demands based on statistical data, and discussed options and barriers to further development of renewable energy. Given its statistical approach, however, it did not include scenario analysis or forecasts. (Ricci et al., n.d.; Selosse et al., 2018) adopted a bottom-up optimization model called TIMES-Reunion to assess the local energy system in detail, including a mix of current and future technologies. The model was driven by an electricity demand as an input and aims to find the optimized energy technology mix to minimize the total discounted cost of the energy system until 2030. It computed a total net present value of the stream of the total annual cost. The total annual cost included investment and dismantling costs, annual fixed and variable operation and maintenance costs, and costs incurred for imports and for domestic resource production (Ricci et al., n.d.). Several scenarios, including 100% renewable energy in power generation by 2030, limiting intermittent energy sources, i.e., the share of PV and wind power, were studied. Given the small size of energy systems in isolated territories such as Réunion, large-scale integration of intermittent renewable energy sources such as wind and photovoltaics raises technical issues and may lower the reliability of power supply, at least in the absence of large-scale storage options (Drouineau et al., 2015; Haller et al., 2012; Golušin et al., 2013). Similar to (Ricci et al., n.d.; Selosse et al., 2018), (Drouineau et al., 2015; Maïzi et al., 2018) simulated the electricity supply-consumption system using TIMES, but increased the model's temporal resolution from yearly to seasonal, and one day into eight-hour slices, so that the reliability of the electricity system can be studied in higher detail. The study also included electric cars on the demand side. However, both (Biscaglia et al., 2019) did not consider urban waste as a

potential energy source, aggregated biomass as one single source based on data from (Praene et al., 2012), and focused on the electricity sector only.

The goal of this work is to assess the role that biomass from agriculture and forestry and MSW can play in an isolated energy system in a bottom-up approach. Its novelty stems from two facts: first, a high level of spatial resolution. For biomass potentials, this included information on land coverage and soil characteristics on a single-field level for agricultural areas, and information on national park boundaries and topographic characteristics for forested areas. The study focuses on residues and agricultural wastes only, i.e., does not compete with food production except for hypothetical scenarios. Second, given the use of publicly available geoinformatic data, the proposed method is scalable and transferable as long as relevant information is available or can be generated, e.g., from satellite images. Thus, energy potentials from biomass and waste can be assessed for comparable regions without necessarily resorting to potentially unreliable statistical data. The study covers the electricity sector, but also investigates the role biomass and waste can play in substitution of primary energy. It thus aims to contribute to the ongoing discussion on how isolated regions can best be supplied with energy in a renewables-only world (Kaldellis et al., 2012; Kaldellis et al., 2009; Petrakopoulou et al., 2016). More specifically, as replacing coal with imported biomass on Réunion is discussed (LesEchos, 2020), this study provides answers to what extent local resources can replace fossil fuels without compromising food security. This paper focuses on the maximal technical potential feasibility analysis rather than economic feasibility, which should be addressed in the future studies. Extending the concept of isolated regions to isolated parts on the mainland in terms of energy system, this study is also valuable for developing countries, since biomass and MSW are often available at low cost in many regions (Rago et al., 2018).

An overview of the considered biomass and waste sources, conversion process and secondary and final energy carriers is given in Section 0. The assessment of the technical potential of biomass is given in Section 0, while the energy potentials of urban waste are introduced in Section 0, followed by a description of the current energy infrastructure on Réunion in Section 0. Subsequently, three scenarios are introduced to study the impact of different allocation strategies on the energy system (Section 0). Results are shown in Section 0, and discussed in Section 0.

Materials and methods

Energy flow

This paper focuses on the local energy potential analysis of biomass and MSW, the two most accessible and adequate resources in developing regions. The general process including the inputs, tools and outputs is shown in Fig. 1. In a first step, the study assesses the technical potential of agricultural and forestry biomass and MSW, i.e., it reflects on the potential that can be realized under existing technical and legal restrictions (Thrän & Pfeiffer, 2015). The local technical biomass potential was simulated by SimStadt and AquaCrop based on geoinformatic data and other user-defined data inputs. While MSW potential data was collected from local report (ADEME, 2019). Details on the derivation of the biomass and waste streams are provided in Sections 0 and 0 respectively. A total of 23 various streams were identified and are depicted in Fig. 2. The technical energy potential serves as the base for further potential calculations, i.e., of secondary energy carriers or electricity, which depend on the chosen valorization paths. It is to be noted, that in this paper the above-mentioned energy streams were theoretical energy flows exploring the maximal local biomass and MSW potential, not necessarily practically or commercially viable. It was assumed that 100% of the agricultural waste is available for valorization (see Section 0). In terms of MSW, the used values from (ADEME, 2019) is the actually collected MSW amount.

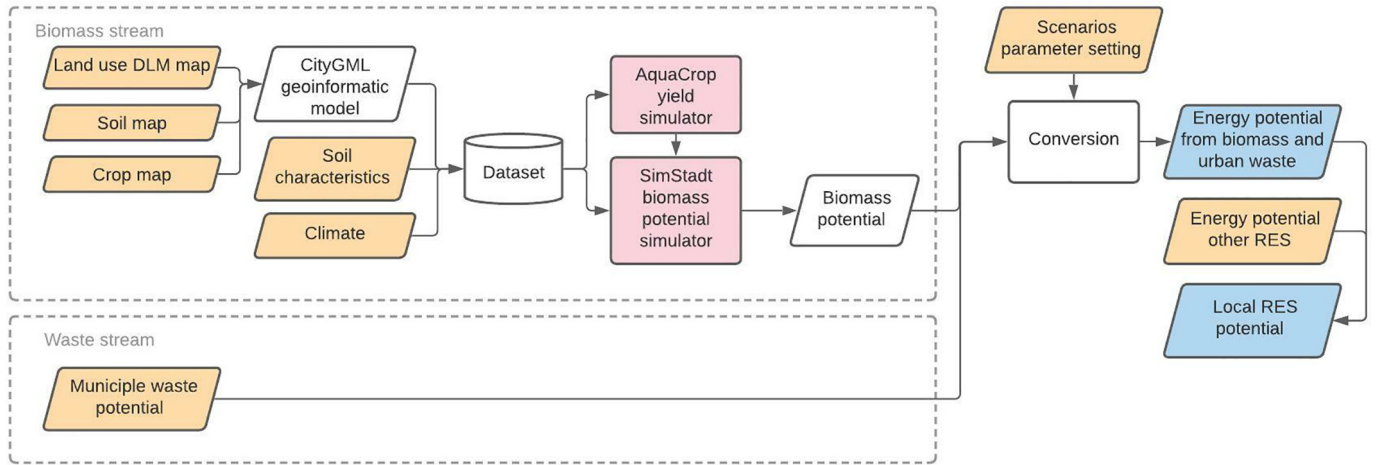


Fig. 1. Illustration of the information flow and methodology including the inputs (yellow), processing tools (red) and outputs (blue). The inputs can be replaced to adopt different local situations.

In line with the Waste Frame Directive (WFD) of the European Union (Communication department of the European Commission, n. d.), material recovery (recycling) has priority over the energy recovery of MSW streams. For non-recyclable streams, multiple conversion techniques exist in order to generate secondary energy carriers or usable energy in line with the WFD. This study focuses on incineration, gasification, and anaerobic digestion (AD). These conversion methods are considered as well-established treatment options for biomass and MSW (Arafat et al., 2015; Breeze, 2017; Kumar & Samadder, 2017; Kumar et al., 2019). All three are either already used on Réunion or will be implemented within the next three years (Assemblée Plénière, 2020). Fig. 2 shows these WtE technologies; valorization pathways that are considered in this study are represented by continuous lines, while dashed lines represent possible, yet discarded options. The selection of considered pathways is oriented on current practice.

The most common WtE technology is incineration (Kumar & Samadder, 2017). Taking all thermodynamic and electric losses into

account, electricity generation from incineration has a process efficiency of about 22% (Arafat & Jijakli, 2013). This low efficiency is countered by the advantage that in general all non-toxic streams with a water content of less than 50% can be incinerated unsorted (Arafat & Jijakli, 2013; McKendry, 2002). Therefore, in this paper only those with less than 50% water content can be included in incineration process, i.e., the paper, MSW streams and all biomass streams with high lignin content, e.g. coconut, mango, citrus, forestry and sugarcane bagasse.

Gasification is a thermal process that converts carbonic substances into syngas. For this, a MSW stream is exposed to high-temperatures of over 700 °C, with limited supply of oxygen (Kumar & Samadder, 2017). The produced syngas is composed of usable gases for energy, e.g., hydrogen, carbon monoxide and methane, and carbon dioxide and nitrogen (Ptasinski, 2008). The composition of gases depends on process parameters, e.g., temperature and pressure, and the feedstock. The overall energy conversion efficiency lies between 50% and 70% (Pio et al., 2017; Robinson et al., 2017; Zhang et al., 2011), whereby

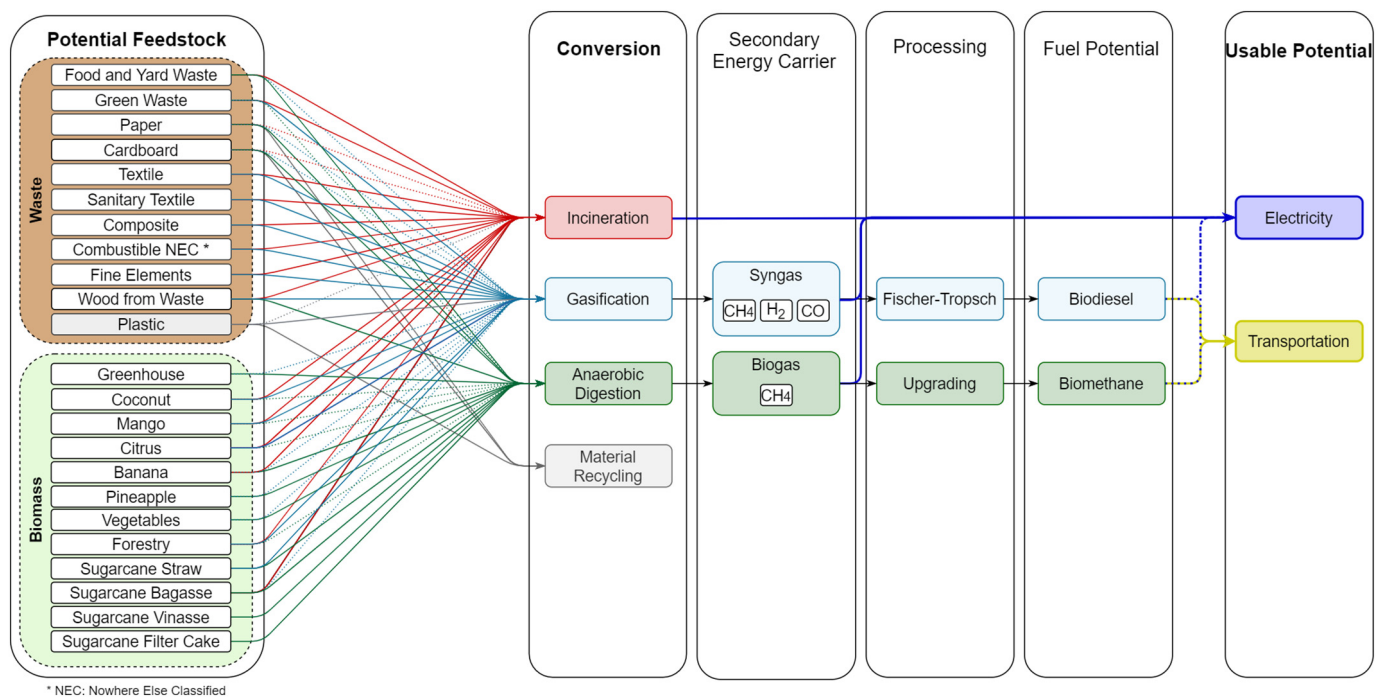


Fig. 2. Illustration of the considered valorization options per biomass and MSW stream.

the energy needed for driving the process is already considered. The syngas can either be combusted for electricity generation or processed further, with one option being the Fischer-Tropsch synthesis to generate biodiesel (Hu et al., 2012; Molino et al., 2016).

In this study, only biomass streams with high lignin content were considered for gasification, as this option was regarded as the most efficient method for converting lignin cellulosis (Widjaya et al., 2018). Furthermore, this study considered MSW streams for gasification (Arena, 2012; Breeze, 2017).

Anaerobic digestion is particularly suitable for organic substances with a high moisture content. The feedstock is fermented in a complex microbial process in the absence of oxygen, producing a gas consisting mainly of methane (Bridgwater, 2006). Other components are carbon dioxide, water vapour, ammonia, and hydrogen sulphide. The quality of the biogas depends on the substrate, as well as process parameters such as biodigester temperature (Kumar & Samadder, 2017). It can be directly used for electricity generation through combustion in gas turbines or upgraded to natural gas quality. The energy needed for upgrading the biogas to biomethane can either be taken from external sources or generated by combusting some of the biogas for electricity generation, whereby the required overall energy input depends on various factors like the specific AD process, feedstock or biogas composition. All in all, about 8% of the generated electricity is necessary for driving the process, e.g., electric components of control, monitoring, etc. (Pöschl et al., 2010). Part of the generated heat is used in the AD process control, and for sterilization of feedstock, if required (Pöschl et al., 2010). In this paper, due to the warm climate of Réunion, the generated heat by CHP was not considered to be reused in the process.

According to the WFD, digesting paper and cardboard can be classified as material recovery (Communication department of the European Commission, n.d.). In this study, non-woody biomass streams, as well as all sugarcane residue and digestible MSW streams were considered suitable for anaerobic digestion.

The usable energy potential was obtained by selecting a valorization path for each stream and taking the corresponding efficiencies into account. The choices of biomass and MSW streams to various conversion paths, i.e., incineration, gasification and anaerobic digestion, were defined according to users' settings (Fig. 1). These settings formed the different scenarios. This potential indicated the amount of energy that is available as electricity or for transportation and can thus substitute energy from fossil fuels.

Technical biomass potential

The assessment of energy biomass potentials from agriculture and forestry builds on an existing workflow, which has been introduced, validated and applied at the example of three German counties as case studies (Bao et al., 2020a). The workflow is compatible with and transferable to other regions, as long as (i) land use information and (ii) information on new land use/crop types is available and is added to an existing XML library, and (iii) the new crop/soil types are described and written in standard inputs crop/soil files for the yield simulation software *AquaCrop* (Raes et al., n.d.). The workflow is part of a versatile regional energy system modelling environment, SimStadt, that aims to compare different renewable energy resources potentials and contrasts these with local energy demands in a given region. SimStadt, that is under constant development at HFT Stuttgart since 2012 (Nouvel et al., 2015), comprises a modular workflow management, with each workflow serving a specific purpose. To date, it can assess building-related demands (cooling and heating (Weiler et al., 2019), residential electricity (Köhler, 2010), water (Bao et al., 2020b)) and renewable energy potentials (rooftop photovoltaics (Romero Rodríguez et al., 2017) and biomass (Bao et al., 2020a)) on a single-building or single-field level using 3D city models or digital landscape models in the CityGML format (Nouvel et al., 2015). CityGML is an open standardised data

model and exchange format to store digital 3D models of cities and landscapes (Fendel et al., 2005).

For the biomass workflow, a key input thus is the data model with land use objects polygons in CityGML format. For Réunion, a 2017 land use map was provided by the French Agricultural Research Centre for International Development (CIRAD) (CIRAD, 2019a). The map contains 35 different land use types, including urban coverages (built surfaces, roads and PV panels), water surfaces, natural surfaces (rock and beach) and agricultural areas, themselves differentiated by crop types. A condensed version of the data is shown in Fig. 3. The map has a resolution of 1.5 m and with a precision for users of 80%, which indicates the probability that an object which has been classified in a class is indeed the class in reality (CIRAD, 2019b). As plant-soil relationships in the surface soil layer affect crop productivity (Wyland et al., 1996), information on local soil type should be considered to obtain accurate biomass yield simulation results. The morpho-pedological soil map of Réunion from 1989 is taken from CIRAD (1989). The land use map and soil map were subsequently merged and converted into CityGML format. The list of related land use and soil types can be found in Tables S1 and S3. Furthermore, meteorological data of Réunion's current climate, i.e., the average over the past 10 years, and forecasted climate data until 2050 in TMY3 format was provided by Meteotest (Meteotest, 2021). More detailed information on SimStadt tool can be found in the supplementary data Text S1.

To calculate the biomass yield based on local climate, soil characteristics, land management pattern and irrigation pattern for most crops, a validated external crop yield and water simulation tool named *AquaCrop*, developed by the Food and Agriculture Organization of the United Nations (FAO, 2020), was integrated with SimStadt. The key characteristics of the crop and soil files that were generated as inputs for *AquaCrop* are shown in Tables S2 and S3. Given their deeper roots, most trees rely not only on irrigation and precipitation for water supply, but also on groundwater. Given the relative challenges in simulating dynamic yields for trees, static biomass yield values were used for orchards and forested areas in this study. The simulation methods for all sort of biomass included in this paper are shown in Table 1. Where possible, simulated biomass yields were validated with literature values and are summarized in Table S5 in the supplementary data. More detailed information, e.g., access link, on *AquaCrop* tool can be found in the supplementary data Text S2.

For the technical potential, only those parts of the biomass that are not used for food provision were considered (Assemblée Plénière, 2020). For vegetables, potato, pineapple and vegetables from greenhouse, this means leafy residues from harvest are considered as an energy usable stream. The total biomass yield is multiplied with the share of waste from harvest and cultivation according to literature (see Table S4). According to the studies (Björnsson & Prade, 2021) and (Zeller et al., n.d.), around 50% to 70% residues of crops on arable land should be kept on land fields to maintain the land fertility and serve as mulch to reduce the water demand. However, the studies investigated cereal in Germany. Due to different climate, crops and soil, the numbers cannot be directly applied to Réunion. Also, the main valorization path chosen for harvest residues is AD. The residue of AD, biogas slurry, is widely known to serve as fertilizer for soil and harvest quality (Nkoa, 2014; Tang et al., 2019; Yu et al., 2010). Thus, it was assumed that 100% of the agricultural waste could be collected and valorized. While wooden fractions, similar to yard waste, were considered usable for valorization (including citrus, mango and coconut plantations as well as forests). An overview of the biomass sources can be found in Table 1. The energy potential of forestry plantation, which excludes the forestry protection areas, only includes the wood residue without those for material use.

Sugarcane, the most important and widely-grown crop on Réunion (Morel et al., 2014) must be considered separately, since substantial waste streams that can be valorized are generated during its processing into sugar and rum. Usable residues to consider include straw (harvest

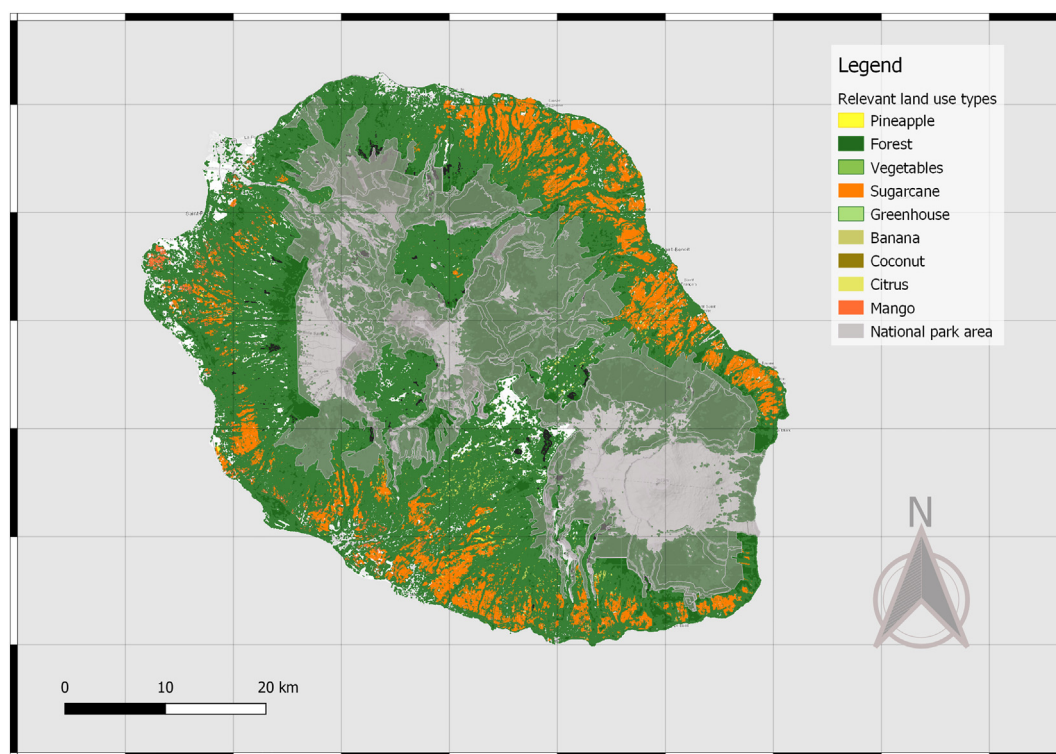


Fig. 3. Map of Réunion with relevant land use types (provided by CIRAD (2019a)) enriched with information on national park areas (provided by peigeo (2014)).

residue (Carvalho et al., 2017)), bagasse (milling residue (Pattra et al., 2008)), and vinasse and filter cake (from sugar and rum production (Hoarau et al., 2018; Ochoa George et al., 2010a)). Vinasse makes up less than 1% of the sugarcane harvest (Hoarau et al., 2018) and is already valorized for energy use on Réunion by AD (Praene et al., 2012). Thus, vinasse was not considered further for the calculations in this study.

Filter cake, the residue from cane juice filtration, is considered difficult in terms of energy utilization. A calculation of its technical potential was not possible (Ochoa George et al., 2010b). However, the biogas yielded from its digestion was considered in the derivation of the usable potential.

Having identified the technical feedstock potential, i.e., the weight-based potential, for each biomass stream, the technical biomass potential was derived by reducing the quantity of each stream by its water content and multiplying it with its lower heating value (LHV) (Thrän & Pfeiffer, 2015).

Technical energy potential from MSW

Municipal solid waste includes residential, commercial, institutional, industrial and municipal sources (Pichtel, 2005). According to

(Communication department of the European Commission, n.d.), MSW is waste from households and waste with similar composition. In terms of physical properties and composition, MSW is generally very heterogeneous (ADEME, 2019; Lebon et al., 2020).

On Réunion, residual waste from households is collected alongside green waste by a door-to-door collection service (Lebon et al., 2020). In addition, bulky waste and dry recyclable waste (paper, cardboard, metal, glass and plastic) is collected. The second source of MSW next to households is waste from economic activity (WEA), collected in five streams: paper and cardboard, wooden fraction, plastics, metals, and glass. In addition, biodegradable waste, residues, and others, like construction debris or old tyres, are collected (ADEME, 2019).

In current practice, dry recyclable MSW is sorted locally and sent for recycling to Indonesia and China (paper and cardboard), Malaysia (metal), India and Hong Kong (plastic), as well as South Africa (glass). The remaining MSW is landfilled, not valorized (Lebon et al., 2020). The locations of the two landfill sites are shown in Fig. 5.

The underlying data of the technical MSW potential in this study was obtained from a characterization campaign by the French National Agency for Ecological Transition (ADEME) in 2017. The campaign investigated MSW streams on Réunion in terms of quantity, composition, and

Table 1
Simulation method of selected crops and forested areas in Réunion.

Crop type	Usable part for energy generation	Simulation method
Sugarcane	Bagasse and straw	AquaCrop
Other vegetable crops (including watermelon and aubergine)	All biomass except harvested part	AquaCrop
Potato	All biomass except harvested part	AquaCrop
Pineapple	All biomass except harvested part	AquaCrop
Greenhouse or shaded crops (including tomato, carrot, cabbage and lettuce)	All biomass except harvested part	AquaCrop
Citrus orchards	Woody branches and leaves	Static
Mango orchard	Woody branches and leaves	Static
Coconut tree plantation	Shell/endocarp, which is the inner part that surrounds the flesh of the coconut	Static
Banana	MSW including all the banana tree excluding fruits and roots	Static
Forestry plantation	Wood residue during harvest in none-forestry production area	Static

their LHV (ADEME, 2019). For the calculation of the technical potential, all streams from households and economic activity as classified by ADEME were clustered as shown in Fig. 2. Streams such as metal and glass that cannot be valorized for energy use were not considered for the technical potential (Breeze, 2017). Plastic is known to have a high calorific value and to be suitable for both incineration and gasification (Arafat & Jijakli, 2013). However, in accordance with the WFD, it is supposed to be recycled and is thus not listed in the technical potential (Communication department of the European Commission, n.d.).

The total amount of annual MSW per capita of 508 kg (ADEME, 2019) on Réunion is typical for a high income country (Hoorneweg & Bhada-Tata, n.d.). As the data was provided by a specialized national institution (ADEME), it is a reliable source. The amount of MSW per capita includes all waste that is collected on the island. It is possible that there is additional waste that is illegally disposed. However, due to the French legislation, this is not very likely and is thus dismissed. It has to be noted that other studies on waste on Réunion, e.g., (Agorah Reunion, n.d.) determined numbers that are 19% higher. This discrepancies are mainly due to minor differences in considered streams. Since the data derived from ADEME waste characterization report corresponds to the MSW that is available for further utilization, the report serves well as the basis of this study.

The composition of the clustered streams is shown in Table 2. The LHVs and moisture contents were derived as the weighted average of the original streams in the ADEME report (ADEME, 2019). Only streams of relevance to the technical potential are listed. The technical energy potential from MSW was determined by multiplying the amount of MSW allocated to each stream with the corresponding LHV (Thrän & Pfeiffer, 2015).

Energy demand and supply on Réunion

As mentioned in Section 0, Réunion is facing challenges with regards to its energy infrastructure (Assemblée Plénière, 2020; EDF, n.d.; Horizon Reunion, 2020). The current energy consumption amount and structure, and the current infrastructure are the basic information for further studies. Therefore, the information was collected from official reports and previous studies shown in this section. In 2019, fossil fuels accounted for 87% of primary energy consumption and 69% of electricity generation, as shown in Fig. 4. As Réunion has no fossil fuel reserves, all fossil fuels are imported. In 2019, 52% of fossil fuels were used for transportation, 43% were converted to electricity, and 5% were used in agriculture and industry (Horizon Reunion, 2020). 66% of energy demand in transportation is attributable to road traffic, with the remaining 34% divided between air and water transportation. Of the vehicles in road traffic, 75% are diesel-powered and 25% are powered by petrol (Horizon Reunion, 2019). The amount of electricity-powered vehicles

Table 2
Composition of considered MSW streams.

MSW stream	Content
Food waste	In particular uneaten food, kitchen scraps or commercial cooking waste
Yard waste	Green cuttings from garden
Green waste	Plant residues, mainly from urban landscaping on public ground
Paper	All types of paper waste, but excluding cardboard (separate category)
Cardboard	Mostly flat and corrugated cardboard packaging
Composite	Packaging from composite materials and small electronic devices
Textile	All types of textiles
Sanitary textile	Hygienic fraction, soiled paper fraction
Combustible	Combustible Waste that is nowhere else classified
NEC	
Fine elements	Elements under a diameter of 20 mm
Wood from Waste	Wooden fraction from WEA waste, e.g., pallets

is rising fast, but to date still negligible. As another possible interim solution is running certain types of vehicles on natural gas (Assemblée Plénière, 2020).

In terms of electricity, 3045 GWh were generated on Réunion in 2019, with 31% from renewable energy sources. Coal accounted for the largest proportion of the electricity mix (36% and 1089 GWh), with other fossil fuels accounting for 1007 GWh (Horizon Reunion, 2020). As Fig. 4 shows, the sources for energy from biomass are bagasse (240 GWh), bioethanol and biogas (cumulative 22 GWh). Adding PV, hydro and wind energy, renewable energy sources (RES) made up for 950 GWh in 2019 (Horizon Reunion, 2020). MSW, however, does not yet play a role in the energy system.

Fig. 5 shows key facilities of the energy and MSW infrastructure on Réunion. Two co-firing plants, namely Le Gol and Bois Rouge, incinerate coal and sugarcane bagasse. With a cumulative installed capacity of 210 MW, they valorized 1116 GWh of primary energy in the form of bagasse and 4175 GWh of coal in 2019 (Horizon Reunion, 2019). Both cofiring plants are expected to be transformed to solely incinerating biomass until 2030, which is planned to be mostly imported (LesEchos, 2020). To meet the goal, by 2023 most of the biomass will be imported. The energy autonomy goal will only be reach by 2030, i.e., all the biomass source for CHP should have a local origin (LesEchos, 2020). Furthermore, two combustion turbines of 80 MW installed capacity in La Baie convert heavy oil into electricity (Horizon Reunion, 2020). The Port Est thermal diesel power plant has an installed capacity of 211 MW. It is mainly used for balancing consumption peaks or volatile production of RES (EDF, n.d.). Its turbine can be reworked to be powered with natural gas (EDF Réunion, 2016b). The combustion turbine TAC Sud runs on bioethanol (80%) and diesel (20%) and has an installed capacity of 41 MW (Gauthier & Neuvy, 2019). Lastly, three biogas plants exist on the island, two of them located in direct vicinity to the island's landfills (EDF, n.d.). They normally digest vinasse, sewage sludge, or capture landfill gas (Lebon et al., 2020; Praene et al., 2012) and have a cumulative capacity of 4.4 MW (Horizon Reunion, 2020).

Setting of scenarios

Three main scenarios were developed in order to investigate the role biomass and urban waste can play in the island's energy supply. The key differentiating factor between the scenarios are the valorization paths of the various MSW streams. Table 3 provides an overview of the scenarios.

In scenario 1, the **Base Case scenario**, the current infrastructure as described in the previous section was considered as a constraining factor. The goal is to show what amount of electricity can be generated with the existing energy infrastructure, and to provide a basis for comparison to the other scenarios. Since no capacities exist for gasification or AD of biomass and MSW today, the complete feedstock potential is used for incineration, as far as suitable according to Section 0.

Scenario 2 (**Electricity Enhancement**) maximizes electricity generation without infrastructural constraints. Thus, AD and gasification are considered for streams if electricity production can be optimized compared to scenario 1. Biogas and syngas are directly combusted in turbines in order to generate electricity.

In a third approach, the potential contribution of local energy sources beyond the electricity sector is investigated. In the **Energy Carrier Enhancement scenario**, gaseous energy carriers are not combusted for electricity generation, but further processed. Valorization paths were chosen to maximize biogas and syngas generation, with biogas being processed to biomethane, and syngas to biodiesel. These fuels can substitute fossil fuels in the transportation sector, either directly as biodiesel or biomethane as a natural gas substitute. The latter could also substitute butane currently used for cooking in households, or in industry. Even though electrification of passenger cars is more efficient, e-fuels can play a role in reducing emissions from heavy-duty vehicles such as tractors or lorries (Ueckerdt et al., 2021). Maximizing the

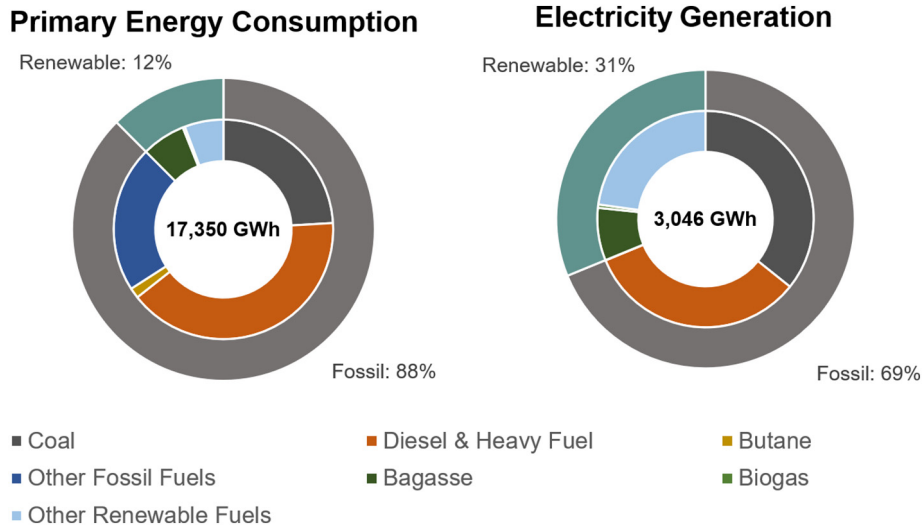


Fig. 4. Split of primary energy consumption and electricity generation on Réunion, 2019. Other fossil fuels include petrol, jet fuel and waste oil, other renewables bioethanol, solar, wind and hydro energy (provided by *Horizon Reunion, 2020*).

production of natural gas might also be important from an electricity sector standpoint, as biomethane could substitute natural gas in the Port Est power plant and perform grid balancing tasks. Given its small system size, a sufficiently large, reliable source of balancing power will be necessary on Réunion going forward to ensure reliability of supply, as discussed in [Section 0](#).

In extensions of scenarios 2 and 3, electricity and secondary energy generation was maximized regardless of competing uses. Plastic, not

considered due to its recyclability, has a high calorific value and can contribute to decreasing fossil fuel imports ([ADEME, 2019](#)). Additionally, all of sugarcane, i.e., not only residues, i.e., bagasse and straw, from harvest and processing, were considered for energy valorization in these sub-scenarios, as sugarcane is by far the most important local agricultural crop and its energy valorization well proven and widespread. The energy potential whole sugarcane plant is derived by multiplying the dry mass weight of sugarcane and low heating value.

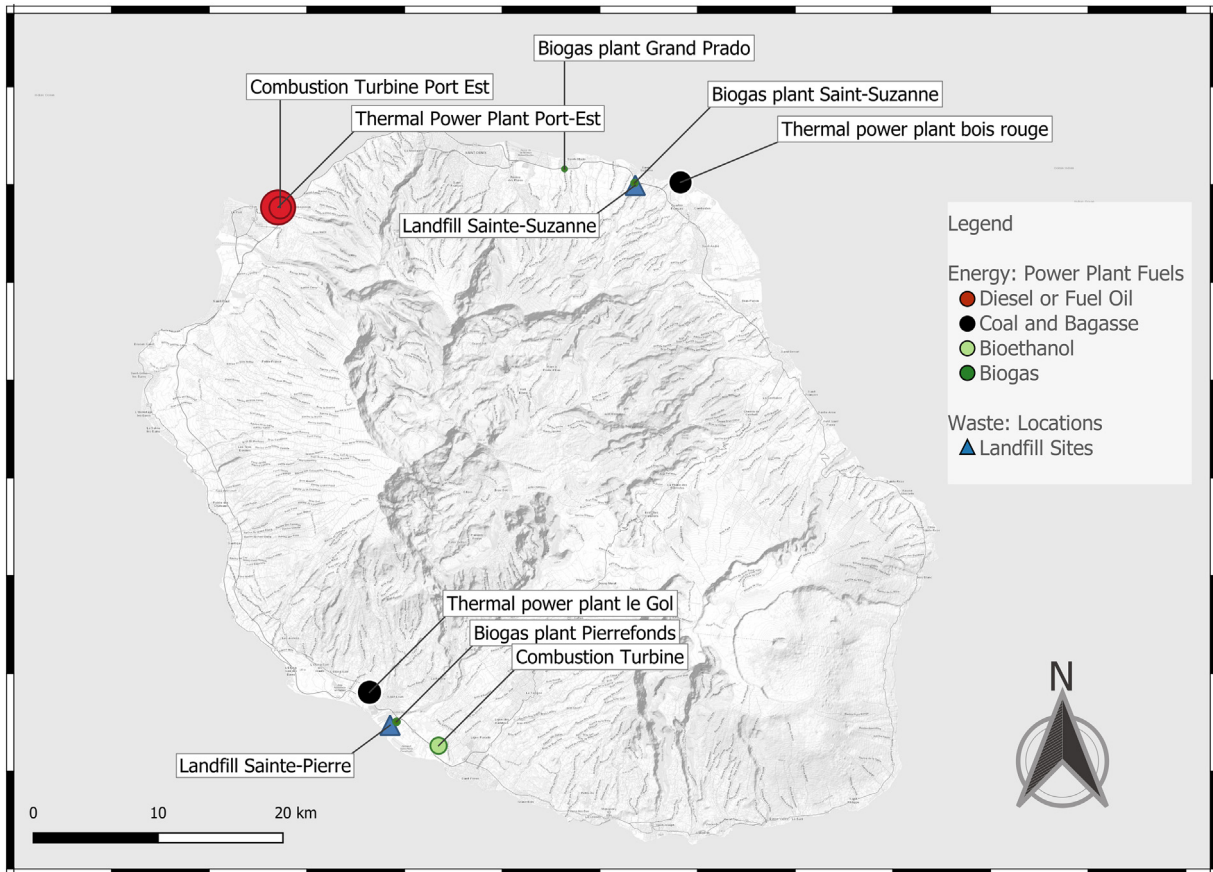


Fig. 5. Energy and MSW infrastructure on Réunion: locations of major power plants. Bubble sizes reflect installed capacities ([EDF, n.d.](#); [EDF Réunion, 2016a](#); [EDF Réunion, 2020](#)).

Table 3
Overview and summary of the investigated scenarios.

Scenario	Description
1 Base Case	Energy valorization of biomass and MSW as far as possible given existing infrastructure.
2 Electricity Enhancement	Energy valorization of biomass and MSW without infrastructural limitations in order to maximize electricity generation.
2.1 Beyond restrictions	Electricity Enhancement scenario, but including the energy valorization of all sugarcane and plastic waste.
3 Energy Carrier Enhancement	Valorization of biomass and MSW in order to maximize gaseous energy carriers.
3.1 Beyond restrictions	Energy Carrier Enhancement scenario, but including the valorization of all of sugarcane and plastic waste.

Results

Technical energy potential

Based on the described approaches and limitations, the technical energy potential from biomass residues and MSW on Réunion had the amount up to 3552 GWh, with biomass contributing 3040 GWh/yr or 85% of the total, and MSW contributing 513 GWh/yr or 14%. Table 4 lists the technical energy potential in GWh/yr and feedstock potentials in 1000 t/yr for all considered streams. By 2023, the co-firing powering plants will only burn biomass, mostly with imported biomass. Only by 2030 the biomass would come from local resources (LesEchos, 2020). According to (Assemblée Plénière, 2020), except for bagasse, around 100,000 t non-agricultural local biomass, i.e., green waste, forest waste and package, can be provided feasibly for the power plant by 2030. This amount is the biomass potential with economic and technical feasibility in the short term. Based on our simulation, the above-mentioned non-agricultural biomass had the total technical feed-stock potential of 244,000 t regardless the economic feasibility. The difference between feasible potential and technical potential also shows the room of increasing local biomass supply share.

Sugarcane is the crop and considered stream with the highest energetic potential. It covered n 58% of the agricultural and forested area, and its residues accounted for 45% of technical biomass potential. Another major potential source for local biomass was waste from banana and mango plantations and from forestry, accounting for further 40% of the technical energy potential from biomass. The most promising MSW stream in terms of energy use was the combustible fraction, that

Table 4
Technical energy and feedstock potential from MSW and biomass on Réunion.

Stream	Feedstock	Technical
	Potential (1000 t/yr)	Potential GWh/yr
Food waste	43	44
Yard waste	13	20
Green waste	77	53
Paper	28	55
Carton	28	56
Composite	14	40
Textile	8	14
Sanitary textile	31	15
Combustible NEC	48	163
Fine elements	41	49
Wood from waste	1	4
MSW potential	332	513
Banana (waste)	226	471
Citrus (waste)	19	40
Mango (waste)	194	403
Coconut (waste)	<1	<1
Forest (waste)	142	536
Pineapple (waste)	2	1
Vegetables (waste)	6	4
Sugarcane straw	282	401
Greenhouse (waste)	1	1
Sugarcane bagasse	553	1183
Sugarcane filter cake	70	n.d.
Potentials from biomass	1425	3040
Sums	1806	3552

could not be classified elsewhere (Combustible NEC), which made up about 5% of the total technical potential. As this was a very heterogeneous stream, made up of for example of shoes, leather, and wooden packaging (ADEME, 2019), it was also unlikely to be recycled.

Base Case scenario

In accordance with the valorization paths of the Base Case scenario described in Section 0, the whole energy usable feedstock was incinerated. This yields a potential electricity generation of 668,757 GWh/yr/a, i.e., 2225% of 2019 generation, as shown in Fig. 6. As outlined in Section 0, recyclable MSW streams, i.e., paper, carton and plastic, were not valorized for energy use energetically. Since sugarcane bagasse is the only considered stream that is already valorized today, the above-mentioned calculated results (260 GWh/yr) were compared with the real electricity production from bagasse in 2019, which amounted to 240 GWh (Horizon Reunion, 2020), i.e., a deviation of less than 10%. This further validated the results of this research.

Electricity Enhancement scenario

In order to maximize electricity generation from biomass and MSW, the identified MSW and biomass streams were allocated to the most energy efficient valorization pathways, ignoring infrastructural constraints. The resulting assignments of the various streams are shown in Fig. 7. By this, 776 GWh/yr can be generated, i.e., a 16% increase compared to the Base Case scenario. For example, electricity generation from digestion instead of incineration of sugarcane bagasse yielded 324 GWh/yr, an increase of 47% compared to the previous scenario. This matched the result of (Kiatkittipong et al., 2009), who investigated the electricity generation of bagasse by incineration and digestion. The improvement results in an increased the share of bagasse in the electricity mix from 8% to 11%. In this scenario, paper and cardboard were valorized to energy through anaerobic digestion, adding about 40 GWh/yr of electricity generation potential. Other biomass waste, wood from waste, yard waste and waste from greenhouse plantation were digested. For filter cake no technical potential could be determined. However, its biogas yield was included in the electricity generated from digestion. Woody biomass, including waste from coconut plantations, could be best valorized through gasification. The cumulative usable potential of these streams equaled 252 GWh/yr.

The electricity generation potential could hypothetically be increased further by energy valorizing all of sugarcane. Incineration of the entire sugarcane harvest alone provided 40% of the island's electricity generation in 2019. Including all other streams, 57%, or 1728 GWh of electricity could be produced annually. This almost doubled the values in the Electricity Enhancement scenario. Additionally, gasification of plastic waste added another 42 GWh/yr of electricity generation potential resulting in an overall electricity generation potential of 1770 GWh, or 58% of 2019 total generation.

Energy Carrier Enhancement scenario

The Energy Carrier Enhancement scenario focused on maximizing energy carrier yields. Valorization of biomass and municipal waste streams along the pathways yielding the highest secondary energy

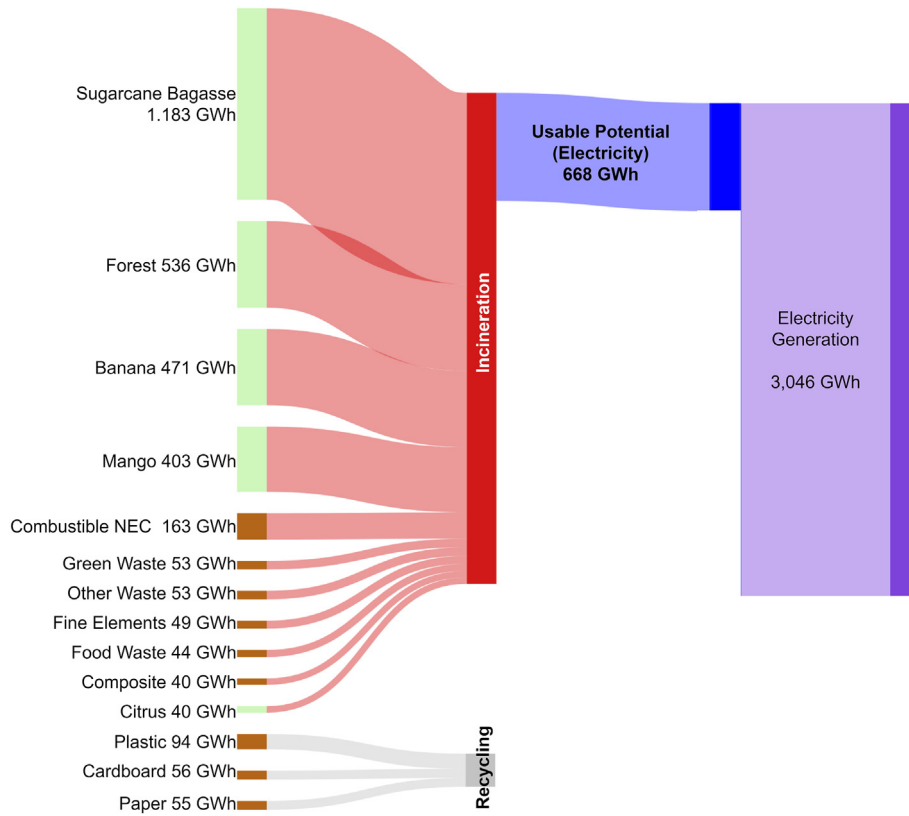


Fig. 6. Illustration of valorization pathways in the Base Case scenario. All energy usable streams were incinerated for electricity generation, yielding 668 GWh/yr. Wood from waste, yard waste, sanitary textiles and textiles are summarized in other MSW. Other biomass waste includes wastes from vegetables, pineapple, greenhouses, and coconut plantations.

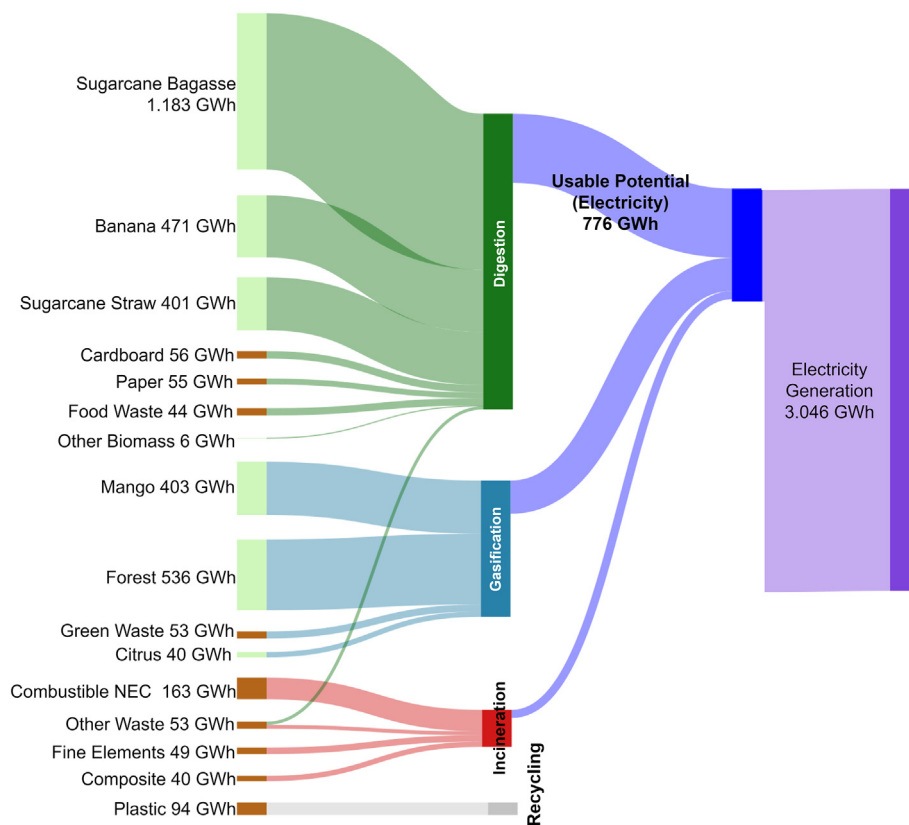


Fig. 7. Illustration of the energy flow in the Electricity Enhancement scenario. For each stream, the valorization method that yields in the highest usable potential was applied.

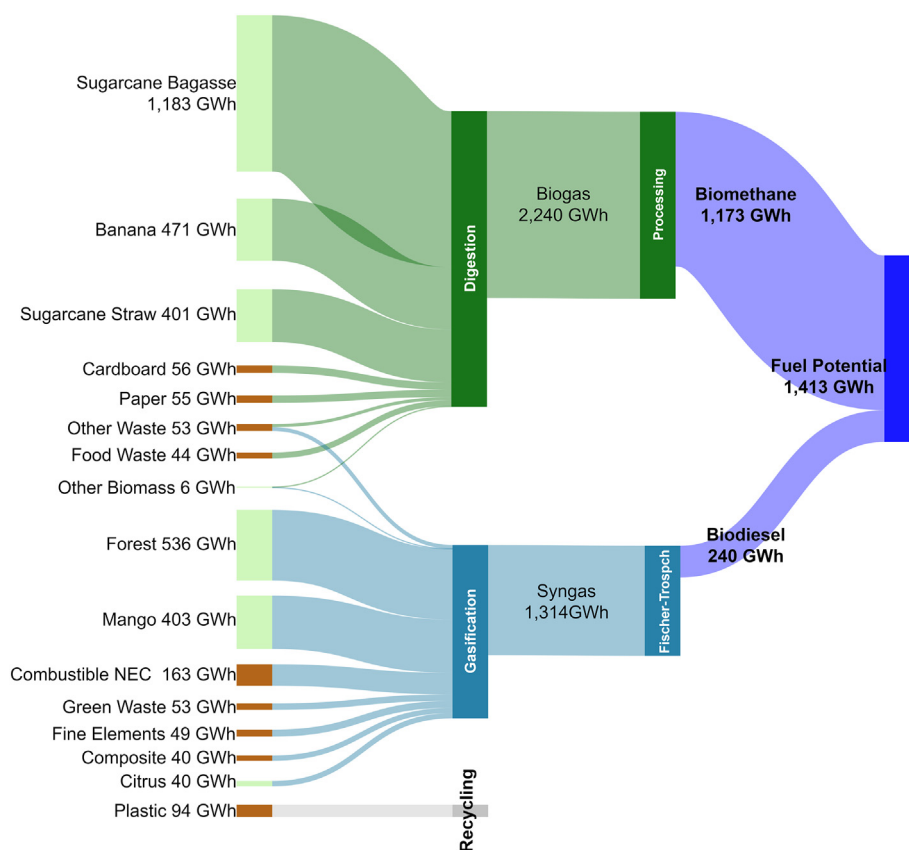


Fig. 8. Illustration of the energy flows in the Energy Carrier Enhancement scenario. The streams are valorized in the way that yields the highest energy carrier potential: wood from waste, yard waste, waste from vegetable, pineapple and greenhouse plantations was digested. Filter cake was treated as in the scenario 2. Sanitary textiles, textiles and waste from coconut plantation were used for gasification. Biogas generated from digestion was processed to biomethane, the syngas generated from gasification was used for producing biodiesel via Fischer-Tropsch synthesis.

carrier potential led to a total annual potential of 1400 GWh, or 8% of total primary energy demand in 2019. Of these, 1173 GWh were in the form of biomethane, and 227 GWh in the form of biodiesel. Fig. 8 shows the valorization paths for each stream, and the resulting fuel potential.

Again, this potential could be enhanced hypothetically by valorizing the entire sugarcane harvest and plastic waste. In order to maximize yields in this scenario, sugarcane was digested and plastic waste was used for gasification. The resulting fuel potential amounted to 3129 GWh, with 2900 GWh/yr in the form of biomethane and 239 GWh/yr of biodiesel.

Discussion

Pathways towards energy autonomy

The presented scenarios show a significant amount of unexploited energy from biomass and MSW exists on Réunion, even if infrastructural constraints were taken into consideration: in the Base Case scenario, an additional 22% of the 2019 electricity generation could be met from biomass and MSW streams, increasing the share of renewable energy sources in the electricity generation mix from 31% to 45% based on 2019 data. If all additional electricity generation replaced imported coal, annual greenhouse gas (GHG) emissions dropped by about 618,000 t, or 14% of the island's 2019 GHG emissions (Horizon Reunion, 2020). Leaving infrastructural limitations behind, the electricity generated in Electricity Enhancement scenario replaced 22% of electricity from imported fossil fuels, increasing the share of renewable energy in the electricity generation mix to 49. In this scenario, GHG emissions were reduced by 21% compared to 2019 levels, assuming that coal is replaced as a priority.

Agricultural waste and byproducts from sugarcane processing made up 3040 GWh of the available technical potential of 3646 GWh annually. Both the missing infrastructure for collecting the waste and competing uses like on-field composting for soil quality were dismissed. Whether the produced biogas slurry is sufficient for soil fertilization was not considered, as the focus of this study is a theoretical potential analysis. Also the economic feasibility of developing infrastructure for each stream would need to be decided upon on a case by case basis, depending on available potentials and collection cost. In contrast, the considered urban solid waste streams are collected to date. Incineration of these in already existing power plants, that are moreover located close to existing landfill sites (see Fig. 5), are favorable from an environmental standpoint and would require minor adjustments to collection practices, logistics and power plants (Cucchiella et al., 2017). It furthermore shows that waste incineration is economically viable in most cases (Massarutto, 2015).

In scenario 2, i.e., maximized electricity generation without infrastructural constraints, substantial investments in AD and gasification infrastructure needed to be made. According to (Assemblée Plénière, 2020), ten AD plants with a cumulative capacity of 7 MW were planned to be built until 2030, plus four gasification sites with a cumulative capacity of less than 1 MW. Running at 8000 full load hours, these plants produced 64 GWh of secondary energy carriers annually, 2% of 2019 electricity demand. In contrast, 25% of electricity is generated by AD and gasification in scenario 2, implying a tenfold increase in planned AD and gasification capacities. Also regarding the federal goals, the planned AD and gasification projects are not sufficient. (Assemblée Plénière, 2020) While AD is a proven technology, gasification has not been applied on a large scale in tropical climates yet (Ockwell et al., 2008). Infrastructural adjustments might thus pose a big hurdle to

unlocking the additional 170 GWh/yr of biomass and MSW resources. This study, however, focuses on a theoretical potential. Future studies on the technical and economic feasibility are essential.

To compare these values, (Biscaglia et al., 2019) is one of the previous works that investigates optimal energy mixes for Réunion to achieve 100% of renewable electricity generation. It applied a time horizon until 2030, and also considered grid-related, organisational and economic implications of such a transition. The study assessed biomass and MSW streams comparable to the approach presented here, but in an infrastructure-oriented, statistical top-down approach, compared with the bottom-up methodology presented here. Despite these differences, potentials for biomass-based electricity as presented in scenarios 1 and 2 of our work (757 GWh and 926 GWh, respectively) aligns with the 1000 GWh presented in Biscaglia et al. (2019).

To better illustrate the role of biomass and MSW in a future energy system, 2030 potentials for solar PV, wind onshore, hydro and geothermal power from two scenarios in (Biscaglia et al., 2019) (“BAU (business as usual)”, sometime also referred as Tendency in (Biscaglia et al., 2019), a base case following the current trend of energy systems, and “Autonomy”, a case aiming at energy autonomy in electricity and transport) were combined with our results. Fig. 9 shows electricity demand for 2030 and the contributions of the other RES in 2030 as expected in (Biscaglia et al., 2019), and the contributions from biomass and MSW for scenarios 1 and 2. Electricity generated from PV, wind onshore, hydro and geothermal is around 3400 GWh in “Autonomy”, comparing with 2100 GWh in “BAUTendency”. Electricity demands are 3550 GWh and 4050 GWh in “BAU” and “Autonomy” respectively. In the “BAU” scenario, biomass and MSW potentials from scenarios 1 and 2 are not sufficient to satisfy electricity demand, similar to the overall results from (Biscaglia et al., 2019), where the remaining gap would be filled by imported biomass. An alternative option would be to use sugarcane beyond its residues and/or plastic waste for energy production; the Electricity Enhancement scenario beyond restrictions would allow one to close the gap in both the “BAU” and “Autonomy” scenario. It, however, introduces food-energy conflicts in the case of sugarcane and/or contradict priority for recycling in the case of plastic waste. In the

“Autonomy” scenario, where the installed capacity of other RES is 60% more than “BAU”, combined with biomass and MSW potential in any scenario, energy autonomy can be achieved.

For full energy autonomy, other sectors such as transportation and cooking must be included. In scenario 3 (Energy Carrier Enhancement scenario), the potential for producing biomethane and biodiesel locally by processing biogas and syngas was investigated. Local biomethane potentials could satisfy 100% of demand for cooking (266 GWh in Fig. 4). Subtracting that amount leaves 77% of local biomethane potentials for transportation sector. Fig. 10 shows the fuel potential of the Energy Carrier Enhancement scenario both with and without the valorization of all sugarcane for energy purposes and plastic waste, as well as the transportation fuel demands according to the “BAU” and “Autonomy” scenarios from (Biscaglia et al., 2019). By generating biodiesel from gasification and subsequent Fischer-Tropsch synthesis of local biomass and MSW, up to 6% of 2019 diesel demand of 3981 GWh could be substituted. However, biomethane can substitute neither petrol nor diesel directly and would thus require the introduction of a vehicle fleet fueled by this energy carrier. Given current development pathways, this seems unrealistic for passenger cars (accounting for 66% of the transportation sector’s energy demand), but can be an option for larger vehicles such as lorries, tractors ships or ships that are more difficult to electrify. Using again (Biscaglia et al., 2019) as a reference, biodiesel and biomethane potentials as calculated in Energy Carrier Enhancement scenario could in principle meet 72% and 83% of energy demand in transportation in the “BAU” and “Autonomy” scenarios, respectively. Here the “BAUTendency” scenario assumed a share of 25% for electric vehicles among all road transporters on the island in 2030, while “Autonomy” scenario assumed a share of 100%. One further use case for biomethane is in stabilizing energy systems with high shares of intermittent renewable energy sources, namely wind and solar PV (Drouineau et al., 2015; Maïzi et al., 2018).

As mentioned in Section 0 Réunion set a sustainable development strategy in 2011 to make sure that by 2023 the CHP will only be fueled by biomass, and the energy autonomy goal will only be reach by 2030, i.e., all the biomass source for CHP should have a local origin

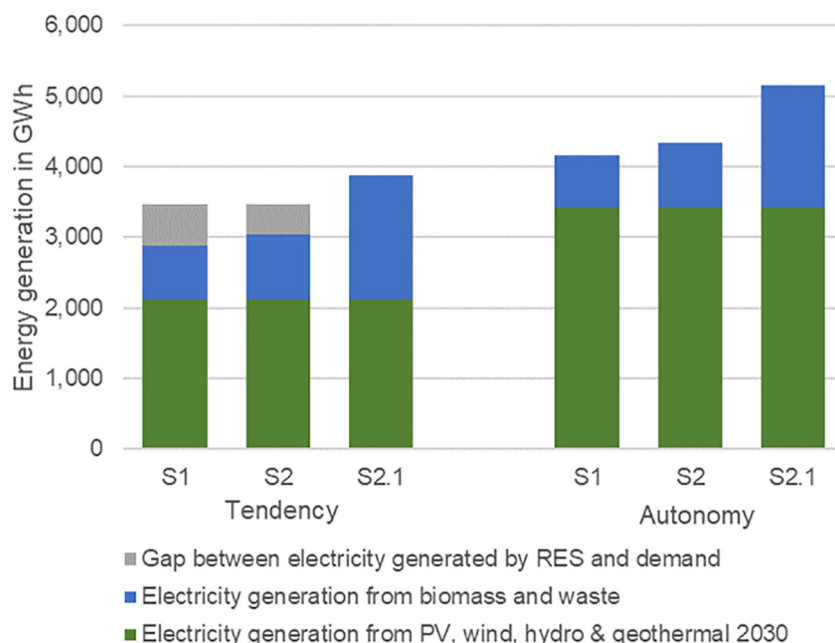


Fig. 9. Share of (i) biomass and MSW electricity potential (green) from scenarios 1, 2, and 2.1, and (ii) other RES including PV, wind, hydro and geothermal (blue) in year 2030 according to (Biscaglia et al., 2019). The share of other RES (blue) varies between “BAU” (left group) and “autonomy” (right group) scenarios, defined in (Biscaglia et al., 2019). If there is a gap between electricity production from RES and consumption, the gap is shown in gray.

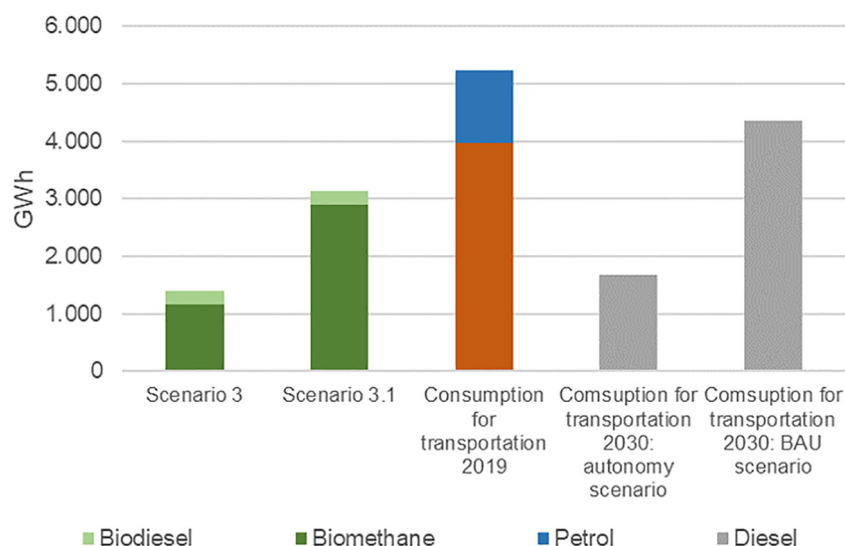


Fig. 10. Fuel potentials of Energy Carrier Enhancement scenario and Energy Carrier Enhancement scenario beyond restrictions with the fuel demand in transportation sector in year 2019 and 2030. The transportation fuel demands in 2030 were calculated based on the current fuel demand (Horizon Reunion, 2020) and forecasted development of electrical vehicles (Biscaglia et al., 2019).

(LesEchos, 2020; French Ministry of Ecological Transition, n.d.). However between 2023 and 2030 a large amount of biomass need to be imported to reach the sustainable goal, even though according to our analysis that there is sufficient local biomass resources. As the next step the economic and technical feasibility in collecting and valorizing local biomass potential.

Transferability of results to other oceanic island regions

The described method of a bottom-up simulation of the local biomass potentials and urban solid waste potential assessment from a detailed MSW characterization study has been proven useful for Réunion. Among other reasons, the island was chosen because of very good data availability compared to similar regions.

Table 5 compares biomass and MSW-related indicators of Réunion to those of Mauritius, Seychelles, Guadeloupe, and Martinique, four oceanic islands of similar size and climate. Sources for all values can be found in Table S8.

Of the four islands, Mauritius is closest to Réunion in terms of location, size, population, electricity demands and agricultural land use: its total amount of MSW differs by less than 5%, its sugarcane harvest exceeds the one on Réunion by about 30%, and the non-protected forested area is ten times higher, albeit on a small base (Government of Mauritius, 2020; Ministry of Agro Industry and Food Security, n.d.; Nundlall, n.d.). It can thus be assumed that overall biomass and MSW potentials and their contribution Mauritius' energy system will be of the same order as for Réunion. A similar result is expected for Guadeloupe: with a population and electricity generation about half the size if Réunion, its MSW production is almost 150% of Réunion's value. In relation to electricity generation and population, the amount of harvested sugarcane is in the same order as on Réunion, while the available forested area is larger.

Table 5

Relevant energy, biomass and MSW parameters for comparable oceanic islands.

	Réunion	Seychelles	Guadeloupe	Martinique	Mauritius
Electricity production (GWh/yr)	3046	442	1596	758	3237
Energy dependency ratio (%)	88	95	94	93	84
MSW total (1000 t/yr)	424	48	603	181	438
Sugarcane harvest (1000 t/yr)	2012	–	774	208	3617
Other crops harvest (1000 t/yr)	2490	10	54	130	112
Non-protected forested area (km ²)	1054	303	499	16	310

Martinique, with a population very similar to Guadeloupe, has less than half Guadeloupe's sugarcane harvest nor a large forested area. Even though electricity generation is not even a quarter of Réunion's, Martinique's biomass potential is unlikely to make a significant contribution to its energy system. The Seychelles, being the smallest region in this list, with an electricity generation of only a fifth of Réunion's, a population eight times smaller and a negligible agricultural sector might gain a certain amount of energy from its forested areas and MSW streams. For energy autonomy, other technologies and approaches, most likely including a certain form of imports also in the future, will however need to be considered.

Conclusion

This study, investigated local biomass and MSW potentials at the example of Réunion, shows that biomass and MSW can substantially contribute to increasing the share of renewable resources in isolated energy systems. Especially in combination with the development of more intermittent renewable energy, a big step towards energy autonomy or climate neutrality can thus be achieved. The basis for a subsequent utilization of these potentials is the identification, quantification and prioritization of the relevant streams, which can be achieved by applying the methods proposed in this study. Prospectively, the proposed method can be applied to other isolated energy systems or developing regions where less data points are available and may thus contribute to progressing these towards energy autonomy or 100% renewable energy generation. For this, further investigation on the economic feasibility of MSW recycling, local agricultural potentials as well as the availability or generation of digital land use models is required. In a second step, larger but yet isolated and under-exploited regions in terms of energy system, e.g., Madagascar and developing states in Africa, should be

investigated with the proposed methods in order to design regional/national 100% renewable energy systems.

Acronyms

AD	Anaerobic digestion
ADEME	Agency for ecological transition
BAU	Business as usual
CIRAD	French Agricultural Research Centre for International Development
CHP	Combined heat and power plant
e.g.	Exempli gratia
GHG	Greenhouse gas
GWh	Gigawatt hours
i.e.	Id est
LHV	Lower heating value
MSW	Municipal solid waste
MWh	Megawatt hours
NEC	Nowhere else classified
PV	Photovoltaic
RE	Renewable energies
RES	Renewable energy sources
WEA	waste from economic activity
WFD	Waste Frame Directive
WtE	Waste to energy

Declaration of competing interest

The authors declare that they have no known competing financial interests or personal relationships that could have appeared to influence the work reported in this paper.

Acknowledgement

The authors thank Alexandre Fays, Reyhan Fessard and Hourmalla Thabiti for their valuable contributions in collecting biomass yields on La Réunion.

Appendix A. Supplementary data

Supplementary data to this article can be found online at <https://doi.org/10.1016/j.esd.2021.12.002>.

References

- ADEME (2019). Caractérisation des déchets sur l'île de la Réunion. URL www.ademe.fr/mediatheque.
- Agorah Reunion (d). Rapport annuel de l'ord: Édition 2019. URL http://agorah.com/upload/environnement/RapportAnnuel_ORD_2019.pdf.
- Arafat, H. A., & Jijakli, K. (2013). Modeling and comparative assessment of municipal solid waste gasification for energy production. *Waste Management (New York, N.Y.)*, 33(8), 1704–1713. <https://doi.org/10.1016/j.wasman.2013.04.008>.
- Arafat, H. A., Jijakli, K., & Ahsan, A. (2015). Environmental performance and energy recovery potential of five processes for municipal solid waste treatment. *Journal of Cleaner Production*, 105, 233–240. <https://doi.org/10.1016/j.jclepro.2013.11.071>.
- Arena, U. (2012). Process and technological aspects of municipal solid waste gasification. A review. *Waste Management (New York, N.Y.)*, 32(4), 625–639. <https://doi.org/10.1016/j.wasman.2011.09.025>.
- Assemblée Plénière (2020). La programmation pluriannuelle de l'énergie - vers un mix électrique la réunion 100% renouvelable des 2023. URL https://regionreunion.com/IMG/pdf/raa_novembre_2020-volume-1.pdf.
- Bao, K., Padsala, R., Coors, V., Thrän, D., & Schröter, B. (2020a). A method for assessing regional bioenergy potentials based on GIS data and a dynamic yield simulation model. *Energies*, 13(24), 6488. <https://doi.org/10.3390/en13246488>.
- Bao, K., Padsala, R., Thrän, D., & Schröter, B. (2020b). Urban water demand simulation in residential and non-residential buildings based on a citygm data model. *ISPRS International Journal of Geo-Information*, 9(11), 642. <https://doi.org/10.3390/ijgi9110642>.
- Biscaglia, S., Marchal, D., Parrouffe, J. -M., & Vizios, E. (2019). *Towards energy self-sufficiency in non interconnected zones*.
- Björnsson, L., & Prade, T. (2021). Sustainable cereal straw management: Use as feedstock for emerging biobased industries or cropland soil incorporation? *Waste and Biomass Valorization*, 12(10), 5649–5663. <https://doi.org/10.1007/s12649-021-01419-9>.
- Breeze, P. (2017). *Energy from waste*. London, United Kingdom: Elsevier Science & Technology URL <http://ebookcentral.proquest.com/lib/hs-rottenburg/detail.action?docID=5106105>.
- Bridgwater, T. (2006). Biomass for energy. *Journal of the Science of Food and Agriculture*, 86(12), 1755–1768. <https://doi.org/10.1002/jsfa.2605>.
- Carvalho, J. L. N., Nogueiro, R. C., Menandro, L. M. S., Bordonal, R. d. O., Borges, C. D., Cantarella, H., & Franco, H. C. J. (2017). Agronomic and environmental implications of sugarcane straw removal: A major review. *GCB Bioenergy*, 9(7), 1181–1195. <https://doi.org/10.1111/gcbb.12410>.
- Chary, Killian, Aubin, Joël, Guindé, Loïc, Sierra, Jorge, & Blazy, Jean-Marc (2018). Cultivating biomass locally or importing it? Ica of biomass provision scenarios for cleaner electricity production in a small tropical island. *Biomass and Bioenergy*, 110, 1–12. <https://doi.org/10.1016/j.biombioe.2018.01.009> URL <https://www.sciencedirect.com/science/article/pii/S0961953418300151>.
- Chen, F., Duic, N., Manuel Alves, L., & da Graça Carvalho, M. (2007). Renewislands—renewable energy solutions for islands. *Renewable and Sustainable Energy Reviews*, 11(8), 1888–1902. <https://doi.org/10.1016/j.rser.2005.12.009> URL <https://www.sciencedirect.com/science/article/pii/S1364032106000232>.
- CIRAD (1989). Soil map of réunion: Morphopedological map of reunion island drawn up in 1989. URL <https://sextant.ifremer.fr/eng/Data/Catalogue#/metadata/af4f9f72-01e5-4e12-90a9-86b157bfd12/formatters/xsl-view?root=divview=advancedheader=falselated>.
- CIRAD (2019a). Carte d'occupation du sol 2017 pléiades (niveau 3). URL https://aware.cirad.fr/layers/geonode:classified_017_leiades_ode3_v2.
- CIRAD (2019b). Complementary sheet to the carte d'occupation du sol 2017 pléiades. <https://aware.cirad.fr/documents/307>.
- Communication department of the European Commission (d). Directive 2008/98/EC of the European parliament and of the council of 19 november 2008 on waste and repealing certain. URL <https://eur-lex.europa.eu/legal-content/EN/ALL/?uri=CELEX:02008L0098-20180705>.
- Cucchiella, F., D'Adamo, I., & Gastaldi, M. (2017). Sustainable waste management: Waste to energy plant as an alternative to landfill. *Energy Conversion and Management*, 131, 18–31. <https://doi.org/10.1016/j.enconman.2016.11.012> URL <https://www.sciencedirect.com/science/article/pii/S019689041631007X>.
- Dasappa, S. (2011). Potential of biomass energy for electricity generation in sub-Saharan Africa. *Energy for Sustainable Development*, 15(3), 203–213. <https://doi.org/10.1016/j.esd.2011.07.006> URL <https://doi.org/10.1016/j.esd.2011.07.006>.
- Drouineau, M., Assoumou, E., Mazauric, V., & Maïzi, N. (2015). Increasing shares of intermittent sources in Réunion island: Impacts on the future reliability of power supply. *Renewable and Sustainable Energy Reviews*, 46, 120–128. <https://doi.org/10.1016/j.rser.2015.02.024> URL <https://www.sciencedirect.com/science/article/pii/S1364032115001124>.
- EDF (d). Bilan prévisionnel de l'équilibre offre/demande d'électricité à la réunion. URL https://reunion.edf.fr/sites/default/files/SEI/producteurs/reunion/edf_sei_bp2019_2020_reunion_v2.pdf.
- EDF Réunion (2016a). Environnement et sécurité. URL <https://reunion.edf.fr/la-centrale-de-port-est/environnement-et-securite>.
- EDF Réunion (2016b). Présentation. URL <https://reunion.edf.fr/la-centrale-de-port-est/presentation>.
- EDF Réunion (2020). Nos moyens de production électrique à la réunion. URL <https://reunion.edf.fr/edf-a-la-reunion/nos-installations-a-la-reunion/nos-moyens-de-production-electrique-a-la-reunion>.
- FAO (2020). *Introducción acuacrop*.
- Fendel, E. M., van Oosterom, P., & Zlatanova, S. (Eds.). (2005). *Geo-information for disaster management* (1st ed.). s.l.: Springer-Verlag.
- French Ministry of Ecological Transition (d). Réunion's regional climate, air and energy scheme (srcae) adopted - deal réunion (04/14/2021 08:37:18). URL <http://www.reunion.developpement-durable.gouv.fr/le-schema-regional-du-climat-de-l-air-et-de-l-a337.html>.
- Gauthier, J., & Neuvy, C. (2019). *Commissioning of the first peak-load combustion turbine fueled by sugarcane-based bioethanol in la réunion: Press release*. (25.02.2019).
- Gielen, D., Boshell, F., Saygin, D., Bazilian, M. D., Wagner, N., & Gorini, R. (2019). The role of renewable energy in the global energy transformation. *Energy Strategy Reviews*, 24, 38–50. <https://doi.org/10.1016/j.esr.2019.01.006> URL <https://www.sciencedirect.com/science/article/pii/S2211467X19300082>.
- Golušin, M., Munitlak Ivanović, O., & Redžepagić, S. (2013). Transition from traditional to sustainable energy development in the region of western balkans – Current level and requirements. *Applied Energy*, 101, 182–191. <https://doi.org/10.1016/j.apenergy.2012.06.008>. <https://www.sciencedirect.com/science/article/pii/S0306261912004503>.
- Government of Mauritius (2020). URL <https://npsc.govmu.org/Pages/National>.
- Grosso, M., Motta, A., & Rigamonti, L. (2010). Efficiency of energy recovery from waste incineration, in the light of the new waste framework directive. *Waste Management (New York, N.Y.)*, 30(7), 1238–1243. <https://doi.org/10.1016/j.wasman.2010.02.036>.
- Haller, M., Ludig, S., & Bauer, N. (2012). Bridging the scales: A conceptual model for coordinated expansion of renewable power generation, transmission and storage. *Renewable and Sustainable Energy Reviews*, 16(5), 2687–2695. <https://doi.org/10.1016/j.rser.2012.01.080> URL <https://www.sciencedirect.com/science/article/pii/S1364032112001128>.
- Hoarau, J., Caro, Y., Grondin, I., & Petit, T. (2018). Sugarcane vinasse processing: Toward a status shift from waste to valuable resource. A review. *Journal of Water Process Engineering*, 24(Supplement), 11–25. <https://doi.org/10.1016/j.jwpe.2018.05.003>.
- D. Hoorneweg, P. Bhada-Tata, What a waste? a global review of solid waste management. Horizon Reunion (2019). *Bilan énergétique de la Réunion: Les chiffres-clés*.

- Horizon Reunion (2020). *Bilan énergétique de la réunion: Edition 2020*.
- Hu, J., Yu, F., & Lu, Y. (2012). Application of Fischer–Tropsch synthesis in biomass to liquid conversion. *Catalysts*, 2(2), 303–326. <https://doi.org/10.3390/catal2020303>.
- IEA (d). Energy access outlook 2017: World energy outlook special report. URL https://iea.blob.core.windows.net/assets/9a67c2fc-b605-4994-8eb5-29a0ac219499/WEO2017SpecialReport_EnergyAccessOutlook.pdf.
- Kaldellis, J. K., Gkikaki, A., Kaldelli, E., & Kapsali, M. (2012). Investigating the energy autonomy of very small non-interconnected islands: A case study: Agathonisi, Greece. *Energy for Sustainable Development*, 16(4), 476–485. <https://doi.org/10.1016/j.esd.2012.08.002> URL <https://www.sciencedirect.com/science/article/pii/S097308261200052X>.
- Kaldellis, J. K., Zafirakis, D., Kaldelli, E. L., & Kavadias, K. (2009). Cost benefit analysis of a photovoltaic-energy storage electrification solution for remote islands. *Renewable Energy*, 34(5), 1299–1311. <https://doi.org/10.1016/j.renene.2008.09.014> URL <https://www.sciencedirect.com/science/article/pii/S0960148108003455>.
- Kalinci, Y., Hepbasli, A., & Dincer, I. (2015). Techno-economic analysis of a stand-alone hybrid renewable energy system with hydrogen production and storage options. *International Journal of Hydrogen Energy*, 40(24), 7652–7664. <https://doi.org/10.1016/j.ijhydene.2014.10.147> URL <https://www.sciencedirect.com/science/article/pii/S0360319914030730>.
- Kiatkittipong, W., Wongsuchoto, P., & Pavasant, P. (2009). Life cycle assessment of bagasse waste management options. *Waste management (New York, N.Y.)*, 29(5), 1628–1633. <https://doi.org/10.1016/j.wasman.2008.12.006>.
- Köhler, S. (2010). Stochastic generation of household electricity load profiles in 15-minute resolution on building level for whole city quarters. *entwicklung der wohnflächenversorgung in den städten und gemeinden baden-württemberg*, *Statistisches Monatsheft Baden-Württemberg*, 2010.
- Kumar, A., & Samadder, S. R. (2017). A review on technological options of waste to energy for effective management of municipal solid waste. *Waste Management (New York, N.Y.)*, 69, 407–422. <https://doi.org/10.1016/j.wasman.2017.08.046>.
- Kumar, S., Zhang, Zengqiang, Awasthi, Muhes Kumar, & Li, R. (2019). *Biological processing of solid waste*.
- Lebon, E., Madushele, N., & Adelard, L. (2020). Municipal solid wastes characterisation and waste management strategy evaluation in insular context: A case study in Reunion island. *Waste and Biomass Valorization*, 11(11), 6443–6453. <https://doi.org/10.1007/s12649-019-00860-1>.
- LesEchos (2020). La réunion : les centrales électriques passent à la biomasse. URL <https://www.lesechos.fr/pme-regions/outre-mer/la-reunion-les-centrales-electriques-passent-a-la-biomasse-1277228>.
- Li, M., Luo, N., & Lu, Y. (2017). Biomass energy technological paradigm (betp): Trends in this sector. *Sustainability*, 9(4), 567. <https://doi.org/10.3390/su9040567> URL <https://www.mdpi.com/2071-1050/9/4/567>.
- Maïzi, N., Mazauric, V., Assoumou, E., Bouckaert, S., Krakowski, V., Li, X., & Wang, P. (2018). Maximizing intermittency in 100% renewable and reliable power systems: a holistic approach applied to Reunion island in 2030. *Applied Energy*, 227, 332–341. <https://doi.org/10.1016/j.apenergy.2017.08.058> URL <https://www.sciencedirect.com/science/article/pii/S0360261917310747>.
- Maltsoglou, I., Kojakovic, A., Rincón, L. E., Felix, E., Branca, G., Valle, S., ... Thofern, H. (2015). Combining bioenergy and food security: an approach and rapid appraisal to guide bioenergy policy formulation. *Biomass and Bioenergy*, 79, 80–95. <https://doi.org/10.1016/j.biombioe.2015.02.007> URL <https://www.sciencedirect.com/science/article/pii/S0961953415000434>.
- Massarutto, A. (2015). Economic aspects of thermal treatment of solid waste in a sustainable waste management system. *Waste management (New York, N.Y.)*, 37, 45–57. <https://doi.org/10.1016/j.wasman.2014.08.024>.
- McKendry, P. (2002). Energy production from biomass (part 2): conversion technologies. *Bioresource Technology*, 83(1), 47–54. [https://doi.org/10.1016/S0960-8524\(01\)00119-5](https://doi.org/10.1016/S0960-8524(01)00119-5).
- Meteotest (2021). *Meteonorm*. URL <https://meteonorm.com/en/>.
- Ministry of Agro Industry and Food Security (d). Black river gorges national parc (17.05.2021). URL <http://pes.govmu.org/pes-sites/visiting-pes-sites/#-3>.
- Molino, A., Chianese, S., & Musmarra, D. (2016). Biomass gasification technology: the state of the art overview. *Journal of Energy Chemistry*, 25(1), 10–25. <https://doi.org/10.1016/j.jechem.2015.11.005>.
- Morel, J., Todoroff, P., Bégué, A., Bury, A., Martiné, J.-F., & Petit, M. (2014). Toward a satellite-based system of sugarcane yield estimation and forecasting in smallholder farming conditions: A case study on Reunion island. *Remote Sensing*, 6(7), 6620–6635. <https://doi.org/10.3390/rs6076620> URL <https://www.mdpi.com/2072-4292/6/7/6620>.
- Ngoc, U. N., & Schnitzer, H. (2009). Sustainable solutions for solid waste management in southeast asian countries. *Waste Management*, 29(6), 1982–1995. <https://doi.org/10.1016/j.wasman.2008.08.031> URL <https://www.sciencedirect.com/science/article/pii/S0956053X0800442X>.
- Nkoa, R. (2014). Agricultural benefits and environmental risks of soil fertilization with anaerobic digestates: a review. *Agronomy for Sustainable Development*, 34(2), 473–492. <https://doi.org/10.1007/s13593-013-0196-z>.
- Nouvel, R., Brassel, K.-H., Bruse, M., Duminiel, E., Coors, V., & Eicker, U. (2015). Simstadt, a new workflow-driven urban energy simulation platform for citygml city models. *Proceedings of International Conference CISBAT 2015 Future Buildings and Districts Sustainability from Nano to Urban Scale*. No. CONF. LESO-PB, EPFL, 2015.
- Nundlaul, V. (d). URL <https://npcs.govmu.org/Documents/NPCS>.
- Ochoa George, P. A., Eras, J. J. C., Gutierrez, A. S., Hens, L., & Vandecasteele, C. (2010). Residue from sugarcane juice filtration (filter cake): Energy use at the sugar factory. *Waste and Biomass Valorization*, 1(4), 407–413. <https://doi.org/10.1007/s12649-010-9046-2>.
- Ochoa George, Pedro A., Cabello Eras, Juan J., Gutierrez, Alexis Sagastume, Hens, Luc, & Vandecasteele, Carlo (2010). Residue from sugarcane juice filtration (filter cake): Energy use at the sugar factory. *Waste and Biomass Valorization*, 1(4), 407–413. <https://doi.org/10.1007/s12649-010-9046-2> URL <https://link.springer.com/article/10.1007/s12649-010-9046-2>.
- Ockwell, D. G., Watson, J., MacKerron, G., Pal, P., & Yamin, F. (2008). Key policy considerations for facilitating low carbon technology transfer to developing countries. *Energy Policy*, 36(11), 4104–4115. <https://doi.org/10.1016/j.enpol.2008.06.019> URL <https://www.sciencedirect.com/science/article/pii/S0301421508003091>.
- O'Connor, S., Ehimen, E., Pillai, S. C., Black, A., Tormey, D., & Bartlett, J. (2021). Biogas production from small-scale anaerobic digestion plants on European farms. *Renewable and Sustainable Energy Reviews*, 139, 110580. <https://doi.org/10.1016/j.rser.2020.110580> URL <https://www.sciencedirect.com/science/article/pii/S1364032120308649>.
- Owen, M., van der Plas, R., & Sepp, S. (2013). Can there be energy policy in Sub-Saharan Africa without biomass? *Energy for Sustainable Development*, 17(2), 146–152. <https://doi.org/10.1016/j.esd.2012.10.005> URL <https://doi.org/10.1016/j.esd.2012.10.005>.
- Patra, S., Sangyoka, S., Boonmee, M., & Reungsang, A. (2008). Bio-hydrogen production from the fermentation of sugarcane bagasse hydrolysate by *Clostridium butyricum*. *International Journal of Hydrogen Energy*, 33(19), 5256–5265. <https://doi.org/10.1016/j.ijhydene.2008.05.008>.
- peigeo (2014). *Vocations du coeur charte 2015*. URL <http://41.213.202.31:8080/geonetwork/srv/api/records/0268cca0-753b-41af-8949-cf3210965cf7>.
- Petrakopoulou, F., Robinson, A., & Loizidou, M. (2016). Simulation and evaluation of a hybrid concentrating-solar and wind power plant for energy autonomy on islands. *Renewable Energy*, 96, 863–871. <https://doi.org/10.1016/j.renene.2016.05.030> URL <https://www.sciencedirect.com/science/article/pii/S0960148116304414>.
- Pichtel, J. (2005). *Waste management practices*. CRC Press. <https://doi.org/10.1201/9781420037517>.
- Pio, D. T., Tarelho, L., & Matos, M. (2017). Characteristics of the gas produced during biomass direct gasification in an autothermal pilot-scale bubbling fluidized bed reactor. *Energy*, 120, 915–928. <https://doi.org/10.1016/j.energy.2016.11.145>.
- Pöschl, M., Ward, S., & Owende, P. (2010). Evaluation of energy efficiency of various biogas production and utilization pathways. *Applied Energy*, 87(11), 3305–3321. <https://doi.org/10.1016/j.apenergy.2010.05.011>.
- Praene, J. P., David, M., Sinama, F., Morau, D., & Marc, O. (2012). Renewable energy: Progressing towards a net zero energy island, the case of Reunion island. *Renewable and Sustainable Energy Reviews*, 16(1), 426–442. <https://doi.org/10.1016/j.rser.2011.08.007> URL <https://www.sciencedirect.com/science/article/pii/S1364032111004175>.
- Ptasinski, K. J. (2008). Thermodynamic efficiency of biomass gasification and biofuels conversion. *Biofuels, Bioproducts and Biorefining*, 2(3), 239–253. <https://doi.org/10.1002/bbb.65>.
- D. Raes, P. Steduto, C. T. Hsiao, E. Fereres, Reference manual, annexes – aquacrop, version 6.0 – 6.1.
- Rago, Y. P., Mohee, R., & Surroop, D. (2018). A review of thermochemical technologies for the conversion of waste biomass to biofuel and energy in developing countries. In W. Leal Filho, & D. Surroop (Eds.), *The Nexus: Energy, environment and climate change, green energy and technology* (pp. 127–143). Cham: Springer. <https://doi.org/10.1007/978-3-319-63612-28> URL <https://doi.org/10.1007/978-3-319-63612-2.8>.
- Reunion Island Energy Observatory (2018). *Energy balance Reunion island*.
- Ricci, O., Seloese, S., Garabedian, S., & Maïzi, N. (d). Réunion island's energy autonomy objective by 2030, EcoMod2014 (7069). URL <https://ideas.repec.org/p/ekd/006356/7069.html>.
- Robinson, T., Bronson, B., Gogolek, P., & Mehrani, P. (2017). Air-blown bubbling fluidized bed co-gasification of woody biomass and refuse derived fuel. *The Canadian Journal of Chemical Engineering*, 95(1), 55–61. <https://doi.org/10.1002/cjce.22641>.
- Romero Rodríguez, L., Duminiel, E., Sánchez Ramos, J., & Eicker, U. (2017). Assessment of the photovoltaic potential at urban level based on 3d city models: A case study and new methodological approach. *Solar Energy*, 146, 264–275. <https://doi.org/10.1016/j.solener.2017.02.043> URL <https://www.sciencedirect.com/science/article/pii/S0038092X17301445>.
- Sawatzky, M., & Albrecht, M. (2017). Translating eu renewable energy policy for insular energy systems: Reunion island's quest for energy autonomy. *Fennia - International Journal of Geography*, 195(2), 125–141. <https://doi.org/10.1143/fennia.60312> URL <https://fennia.journal.fi/article/view/60312>.
- Seloese, S., Garabedian, S., Ricci, O., & Maïzi, N. (2018). The renewable energy revolution of Reunion island. *Renewable and Sustainable Energy Reviews*, 89, 99–105. <https://doi.org/10.1016/j.rser.2018.03.013> URL <https://www.sciencedirect.com/science/article/pii/S136403211830114X>.
- Tang, Y., Wen, G., Li, P., Dai, C., & Han, J. (2019). Effects of biogas slurry application on crop production and soil properties in a rice-wheat rotation on coastal reclaimed farmland. *Water, Air, & Soil Pollution*, 230(3). <https://doi.org/10.1007/s11270-019-4102-4>.
- Thran, D., & Pfeiffer, D. (Eds.). (2015). *Methodenhandbuch: Stoffstromorientierte Bilanzierung der Klimagaseffekte* URL www.energetische-biomassenutzung.de.
- Tun, M. M., & Juchelková, D. (2018). *Journal of Material Cycles and Waste Management*, 20(3), 1397–1408. <https://doi.org/10.1007/s10163-017-0697-y> URL <https://link.springer.com/article/10.1007>.
- Tun, M. M., & Juchelkova, D. (2019). Drying methods for municipal solid waste quality improvement in the developed and developing countries: A review. *Environmental Engineering Research*, 24(4), 529–542. <https://doi.org/10.4491/eer.2018.327> URL <https://www.koreascience.or.kr/article/JAKO201909255110410.page>.
- Ueckerdt, Falko, Bauer, Christian, Dirnauichner, Alois, Everall, Jordan, Sacchi, Romain, & Luderer, Gunnar (2021). Potential and risks of hydrogen-based e-fuels in climate change mitigation. *Nature Climate Change*, 11(5), 384–393. <https://doi.org/10.1038/s41558-021-01032-7> URL <https://www.nature.com/articles/s41558-021-01032-7>.
- Weiler, V., Stave, J., & Eicker, U. (2019). Renewable energy generation scenarios using 3d urban modeling tools—Methodology for heat pump and co-generation systems with

- case study application †. *Energies*, 12(3), 403. <https://doi.org/10.3390/en12030403> URL <https://www.mdpi.com/1996-1073/12/3/403>.
- Widjaya, E. R., Chen, G., Bowtell, L., & Hills, C. (2018). Gasification of non-woody biomass: a literature review. *Renewable and Sustainable Energy Reviews*, 89, 184–193. <https://doi.org/10.1016/j.rser.2018.03.023>.
- Wyland, L. J., Jackson, L. E., Chaney, W. E., Klonsky, K., Koike, S. T., & Kimple, B. (1996). Winter cover crops in a vegetable cropping system: Impacts on nitrate leaching, soil water, crop yield, pests and management costs. *Agriculture, Ecosystems & Environment*, 59(1), 1–17. [https://doi.org/10.1016/0167-8809\(96\)01048-1](https://doi.org/10.1016/0167-8809(96)01048-1) URL <http://www.sciencedirect.com/science/article/pii/0167880996010481>.
- Yu, F. -B., Luo, X. -P., Song, C. -F., Zhang, M. -X., & Shan, S. -D. (2010). Concentrated biogas slurry enhanced soil fertility and tomato quality. *Acta Agriculturae Scandinavica, Section B - Plant Soil Science*, 60(3), 262–268. <https://doi.org/10.1080/09064710902893385>.
- Vanessa Zeller, Daniela Thrän, Martin Zeymer, Bernhard Bürzle, Philipp Adler, Jens Ponitka, Jan Postel, Franziska Müller-Langer, Stefan Rönsch, Arne Gröngroft, Claudia Kirsten, Nadja Weller, Marian Schenker, Harald Wedwitschka (DBFZ), Bernhard Wagner, Peter Deumelandt, Frank Reinicke (INL), Armin Vetter, Christian Weiser (TLL), Klaus Henneberg, Kirsten Wiegmann, Dbfz report nr. 13: Basisinformationen für eine nachhaltige Nutzung von landwirtschaftlichen Reststoffen zur Bioenergiebereitstellung.
- Zhang, Y., Li, B., Li, H., & Liu, H. (2011). Thermodynamic evaluation of biomass gasification with air in autothermal gasifiers. *Thermochimica Acta*, 519(1–2), 65–71. <https://doi.org/10.1016/j.tca.2011.03.005>.